Regulation of venous valve development and maintenance

Lyons, Oliver Timothy

Awarding institution:
King's College London

Regulation of venous valve development and maintenance

Oliver Lyons

Thesis submitted for the degree of
Doctor of Philosophy
2014

Academic Department of Vascular Surgery
Cardiovascular Division
School of Medicine
King's College London
St Thomas' Hospital

Statement of originality

The work contained in this thesis is my own original work, except where acknowledged in the text.

Acknowledgements

I would like to thank my supervisor Professor Alberto Smith for his continued support, advice and kindness throughout this study. I would also like to express my gratitude to Mr Bijan Modarai for his guidance in both my clinical and academic interests, and Professor Steve Jeffrey, Dr Saha Mansour and Mr Glen Brice for advice on the human genetics of lymphatic disorders.

I am indebted to Professor Taija Makinen, Professor Tanya Petrova and Professor Nigel Brown for their longstanding support of my studies; without their enthusiasm encouragement and generosity with advice and materials (including many murine lines), it would not have been possible to carry out this work. I am grateful to Professor Tom Kume for the Foxc2^{lx} mouse line.

I would like to thank Dr Eleni Bazigou for useful discussions, and acknowledge our collaborative work at the start of this project. In particular, Dr Bazigou's finding of expression of Prox1 in venous valves enabled much of the conditional genetic approach to this study.

I would like to thank Dr Gema Vizcay-Barrena for great assistance in scanning and transmission electron microscopy, and in particular in the development of methods to attempt to visualise venous valve gap junctions. I am grateful to Mr Steven Grover, Mr David Eastham, Dr Julia Humphries, Dr Kat Nuthall Miss Bushra Rais, Mr Paul Delaney, Dr Sandra Wood, Dr Celia Cope and Dr Ray Moss for advice and discussions, technical work with immunohistochemistry, western blotting and scanning electron microscopy.

I am indebted to Dr Soundrie Padayachee, Mr Adam Kuchta and Mr Andrew Arnold for their ultrasound assessment of human venous valves.

I would like to acknowledge assistance given by Dr Lukas Stanczuk and Dr Amelie Sabine in animal husbandry at Cancer Research UK and University of Lausanne (respectively), and Dr Sabine for advice and discussion of the project.

I would like to acknowledge the financial support of the Medical Research Council, British Heart Foundation, and National Institute of Health Research, without which this study would not have been possible.

Miss Emily Brown produced the original illustrations that were modified to create the schematic in Figure 17.

Finally I would like to thank my family for their love and support.

Abstract

Venous valve failure and associated venous hypertension is common in man, yet very little is known about the development and maintenance of venous valves. Existing therapies for valve failure most commonly involve removal or ablation of the vein in the superficial venous system. Little can be done to correct reflux in the deep veins.

Immunofluorescence and electron microscopy were used to visualise and quantify venous valves at different stages of development in an experimental mouse model. Several proteins previously thought to be specific markers for arterial or lymphatic endothelium were found in venous endothelia and venous valves. Constitutive and conditional loss of function genetic approaches revealed how an initially homogenous population of endothelial cells acquire distinct expression patterns and behaviours, but act co-ordinately to orchestrate valve formation. The expression of several factors, previously found to be required for cardiac and/or lymphatic valve formation, was also found to be important for venous valve formation, including connexins 37, 43 and 47, integrin-α9, ephrinB2, Foxc2, and NFAT-calcineurin. Mutations in VEGFR3, FOXC2, GJC2 and GJA1 were found to be associated with structural venous valve defects in man.

It has been postulated that fluid flows regulate lymphatic and venous valve development in vivo. A novel model of altered blood flow was developed, and used to show that normal blood flow is required for postnatal valve development.

These data enhance our understanding of the cellular mechanisms underlying human venous valve disease caused by mutations in VEGFR3, FOXC2, GJC2 and GJA1, and suggest novel candidate genes, such as Itga9 and GJA4 for human venous valve disease. Improved knowledge of the factors regulating venous valves could lead to new treatments for valve failure, or regenerative medicine approaches to venous reflux.

Table of Contents

Index of Figures

Index of Tables

Abbreviations

4OHT	Tamoxifen
Ab	Antibody
AU	Airy Unit
BD	or bid, twice daily
BSA	Bovine serum albumin
BCIP/NBT	5-bromo-4-chloro-3'-indolyphosphate p-toluidine salt, nitro-blue tetrazolium chloride
Bgal	β-galactosidase (enzyme encoded by LacZ)
CABG	Coronary artery bypass graft
Cre	Cre recombinase (enzyme derived from P1 bacteriophage)
CVI	Chronic venous insufficiency
DMSO	Dimethyl sulfoxide
DPX	Dibutyl pthalate, Xylene (mounting medium)
EMLA	Eutetic mixture of local anaesthetics
FFPE	Formalin fixed paraffin embedded (section)
FS	Frozen section
GJIC	Gap junction intercellular communication
GFP	Green fluorescent protein
HIER	Heat induced epitope retrieval
HRP	Horseradish peroxidase
HTA	Human Tissue Act
HUVEC	Human umbilical vein endothelial cell
ID	Identification
IVC	Inferior vena cava
IMS	Industrial methylated spirit
JLS	Jugular lymph sac
LacZ	Gene encoding β-galactosidase
LV	Lymphatic valve
lx/lx	gene flanked by loxP sites in both alleles
Mf1	Former name for Foxc1
Mfh1	Former name for Foxc2
MIP	Maximum intensity projection

NA	Numerical aperture
OCT	Optimal cutting temperature
P1	Murine post-natal day 1
PBS	Phosphate buffered saline
PCR	Polymerase chain reaction
PFA	Paraformaldehyde
RT	Room temperature
s/c	Subcutaneous
SEM	Scanning electron microscopy
SNP	Sequence nucleotide polymorphism
siRNA	Short interfering ribonucleic acid
TAE	Tris-acetate EDTA buffer
TEM	Transmission electron microscopy
Ti	Titanium
VEGFR2/3	Vascular endothelial growth factor receptors 2/3
VFC	Valve-forming cell(s)
VFR	Valve-forming region
VV	Venous valve(s)
W	Tungsten
WT	Wildtype
Xgal	5-bromo-4-chloro-indolyl-β-D-galactopyranoside (or BCIG)

Nomenclature

In accordance with the consensus for forkhead genes, species differences are indicated by the use of uppercase letters for human (e.g.FOXC2), a capital F for mouse (e.g. Foxc2). In accordance with convention, both gene and protein for vascular endothelial growth factors and their receptors are capitalised.

Key gene and protein names

Gene	Protein
EfnB2	EphrinB2
FOXC2 (Mfh1)	Forkhead box protein C2, Foxc2
Fn-EIIIA	FibronectinEIIIA, encoding EIIIA splice variant of fibronectin
GATA2	GATA-binding protein 2
Itga9	Integrinα9 or integrin-αRLC
LacZ	βgalactosidase
NFATc1 (NFAT2)	Nuclear factor of activated T cells c 1, NFATc1,
PPP3R1	Calcineurin B subunit isoform 1, CnB1
PROX1	Prox1
GJA1	Connexin 43
GJA4	Connexin 37
GJC2	Connexin 47
NRP1	Neuropilin1
NRP2	Neuropilin2
TnC	Tenascin C

1 GENERAL INTRODUCTION

1.1 The venous system

The primary function of the venous system is to return blood to the heart. It also plays a capacitance role and can accommodate large volumes of blood.[1] An effective venous return from the extremities requires the interaction of the heart, peripheral muscle pump in the leg, and competent venous valves (Figure 1).[1]

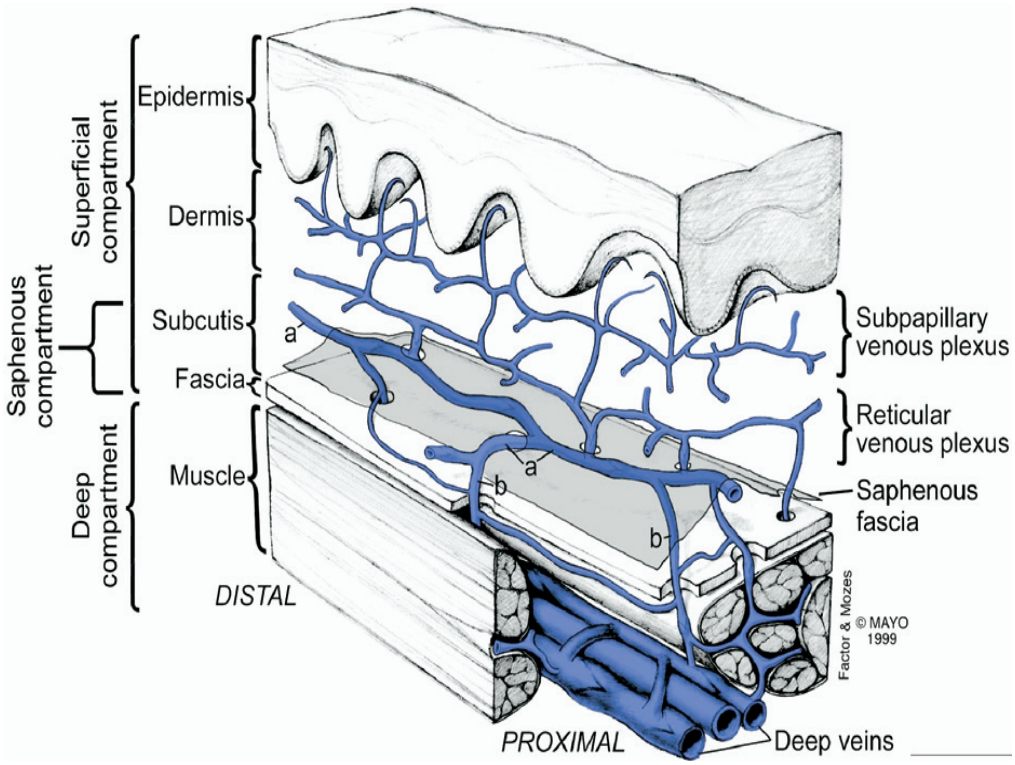

Figure 1 Deep and superficial veins of the lower limb[2]
The fascia covers the muscle and separates the deep and superficial compartments of the limb. Superficial veins (a) drain the skin via the subpapillary and reticular venous plexuses (in the dermis and subcutis) which drain into the deep veins via valved perforating veins (b). The great saphenous vein is invested by its own layer of fascia within the superficial compartment. Blood flow is from distal to proximal.

Compression of valved muscular veins forms a muscle pump (found in the foot, calf and thigh in the lower limb) and with the onset of walking the venous pressure at the ankle rapidly drops from around 100mmHg to a mean of 22mmHg within 7-12 steps. Whilst valves in the named veins are most

commonly discussed, the majority of valves are in fact found in veins less than 100μm in diameter.[1-3]

1.2 Ambulatory venous hypertension

Unlike the collecting lymphatics, veins themselves do not contract to produce a pumping action.[1, 4] In the lower limb the most important muscle pump is formed by the gastrocnemius and soleus muscles and their valved draining veins; muscular contraction generates pressures of around 200mmHg, driving blood in the high capacitance popliteal and femoral veins.[1] Repeated pumping lowers the distal venous pressure (Figure 2). The normal calf venous blood volume is approximately 100-150ml, of which a single contraction will eject 40-60%.[1] Without deep venous valves, blood oscillates between the calf and more proximal veins, and there is failure of the normal reduction in ankle venous pressure, termed 'ambulatory venous hypertension'.[1, 5]

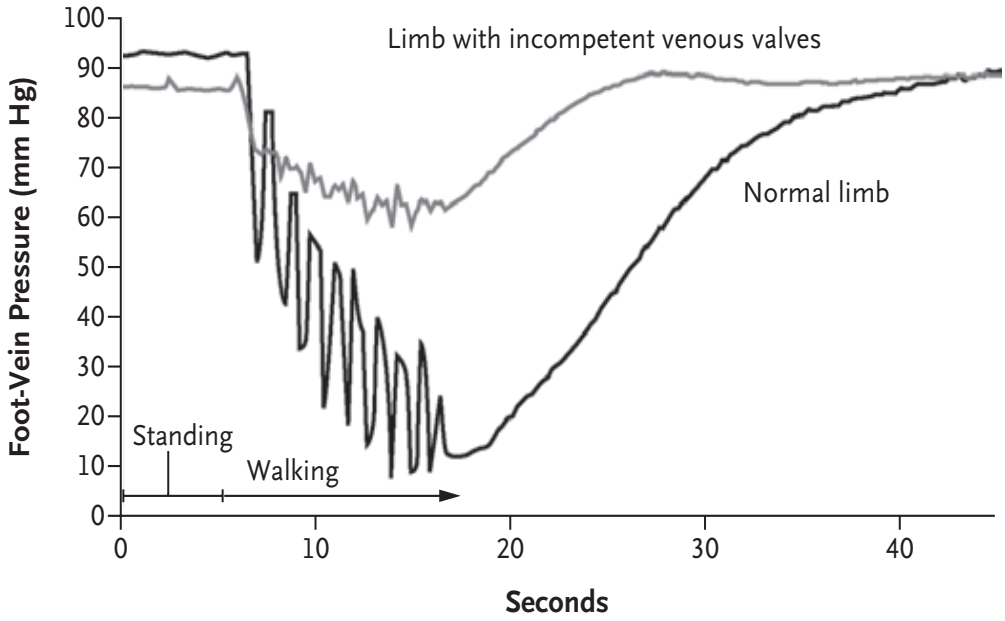

Figure 2 Foot-vein pressure changes on walking[5]
On standing, venous pressure in veins of the foot is approximately 90-100mm Hg. In a normal limb, activation of the calf muscle pump during walking results in a rapid fall in distal venous pressure and stopping walking is followed by a gradual return to the resting state. In a limb with incompetent VV, the calf pump fails to lower distal pressure (ambulatory venous hypertension) and recovery to the resting state is faster.[5]

This failure of the venous system to function normally results in persistently raised venous blood pressure in the lower limbs, termed ambulatory venous hypertension (Figure 2).[6] This leads to the associated skin and subcutaneous tissue changes of chronic venous insufficiency (CVI), but the mechanisms underlying this clinico-pathological relationship remain poorly understood.[1, 6] The features of CVI include pain, oedema, pigmentation, fibrosis, and ulceration.[1] The end stage, ulceration (Figure 3), is very difficult to treat; approximately 50% of ulcers require a year or more to heal, and they may recur after treatment.[6, 7] Long term management places a significant burden on western healthcare systems and is estimated to consume approximately 2% of the NHS budget.[1, 8, 9]

Figure 3 Chronic venous insufficiency with ulceration[5]
The photograph shows a chronic venous ulcer near the medial malleolus, with surrounding evidence of skin changes including pigmentation.[5]

1.2.1 Primary venous disease

CVI may be primary (genetic) or secondary. Primary CVI involves only venous reflux.[1] Duplex ultrasound studies have suggested that primary valvular incompetence (sometimes partially compensated for by an effective calf pump) is more common than previously thought, and it may underlie 20% of CVI.[1] Primary valvular agenesis is rare.[7] Venous reflux in association with rare cases of primary lymphoedema will be discussed in detail later in this chapter.

'Varicose' veins are abnormally dilated and tortuous superficial veins and are estimated to affect 5-30% of the Western population.[7, 8] It is not known whether varicose veins are caused by a primary failure of the venous valves, dilatation of the vein wall, or a combination of the two.[8, 9]

1.3 Secondary venous disease

Secondary disease typically involves a combination of reflux and obstruction.[1] The most common cause of secondary CVI is deep venous thrombosis (DVT). Other causes include trauma, surgical complications, and tumours.[10]

Recanalisation of the vein lumen after DVT is rarely complete, and residual thrombus is replaced by cribiform synechiae of endothelialised fibrous tissue that may cause obstruction to blood flow. In addition, valves may be damaged with resulting structural defects including leaflet adhesions, widening of the valve commissure, and shrinkage of the leaflets.[10, 11]

1.4 Treatment of chronic venous insufficiency

1.4.1 Non-operative therapy

The mainstay of therapy for CVI is graduated elastic compression stockings.[6, 7] This aims to counteract the venous hypertension, but is poorly tolerated by patients. Some studies have suggested a role for pharmacotherapy,

particularly micronized purified flavonoid fraction (Daflon), which can reduce symptoms of pain, heaviness and oedema in patients with venous reflux.[12]

1.4.2 Operative and interventional procedures

The most commonly performed procedures for superficial venous disease involve ablation of the great or short saphenous veins, using methods such as radiofrequency or laser ablation.[6, 7] These less invasive techniques have rapidly replaced open surgical disconnection of the sapheno-femoral junction and stripping of the vein.

Relief of deep venous CVI, which is most commonly secondary, may involve treatment directed at relief or obstruction, reflux, or both. Approximately 10%-30% of patients with severe CVI show significant abnormalities in venous outflow involving the iliac segments; in the past this has been treated surgically (for example by Palma bypass), but with the success of venous stenting this is now less commonly done.[7] Duplex studies show that reflux of deep veins is seen in around 40% of patients with chronic venous insufficiency and may be significant in 10-15%.[6, 7, 13]

Various procedures have been performed in an attempt to achieve long lasting resolution of valve failure in highly selected patient groups, but have been troubled by early thrombosis, poor patency and competency, and high patient morbidity.[6, 7, 14-18] Venous valvuloplasty provides only 59% competency and 63% ulcer-free recurrence at 30months.[7] Other procedures include transposition of vein containing functional valves (eg from the axillary or great saphenous vein) into the popliteal or femoral vein segments. Cryopreserved vein valve allografts have also been used.[7, 16, 17, 19]

1.5 The development and valves of the venous and lymphatic systems

1.5.1 Venous system

In man, primitive vascular channels first appear in the limb in the third week of gestation. Prior to this, only a capillary network is present, followed by the appearance of large plexiform structures. By the by the third week of gestation large channels develop including arteries and veins[1] Between 9 and 11 weeks the great saphenous vein wall is reported to consist only of endothelium, and is joined by irregular cells of tunica media from 12 to 16 weeks. From weeks 18 to 37, three distinct layers are seen.[20] The superficial veins of the lower limbs develop earlier than the deep veins.[21]

Intraluminal valves appear after the organisation of the veins. The first studies of the development of the venous valves were made in the 1920's by Kampmeier and La Fleur Birch in the United States.[22] They cut 20μm paraffin sections of decalcified human cadavers from 2.5months gestation onwards, and focused their search on the saphenous veins where the first venous valves begin to develop near the sapheno-femoral junction at 3.5 months, with a tendency for development to progress from proximal towards distal veins. Valves in the upper limb were found to develop earlier than those in the lower, where valve formation was found to be complete by the fifth month of gestation. An increase in the number of valves between 13 and 19weeks gestation is seen in the human foetal short saphenous veins with no further increase (on average) after 19weeks.[23] Similarly, the first valves appear at 13weeks in human foetal great saphenous veins.[20] Others have found the first venous valves appearing between 18 and 25weeks.[24]

Although there have been significant advances in our understanding of lymphatic valve (LV) development, there is little information describing the morphological processes responsible for VV development.[22, 25, 26] Kampmeier arbitrarily divided the development of the venous valves into five stages

(Figure 4).[22] Development began as two 'ridge-like' endothelial thickenings placed opposite to one another and 'more or less transversely to the long axis of the vessel' just distal the ostium of a tributary (stage 1). These ridges were thought to join to form a complete ring-shaped or circular ledge within the lumen of the vein. Almost synchronously with stage 1, the 'endothelial anlage' (valve leaflets) was seen to lengthen in the direction of flow by 'invasion of the subjacent mesenchyme', and the valve sinus became perceptible (stage 2). The key conformational changes to produce two near-parabolic lines of attachment of the leaflets (stage 3) were not clearly elucidated. Enlargement of the sinus and thickening of the free edges of the leaflets completed development by 5months gestation (stage 4). By term, the vein wall at the sinus was thinned by a reduction in the tunica media (stage 5). They found a large variability in the developmental stage of valves, even within segments of the same vein.

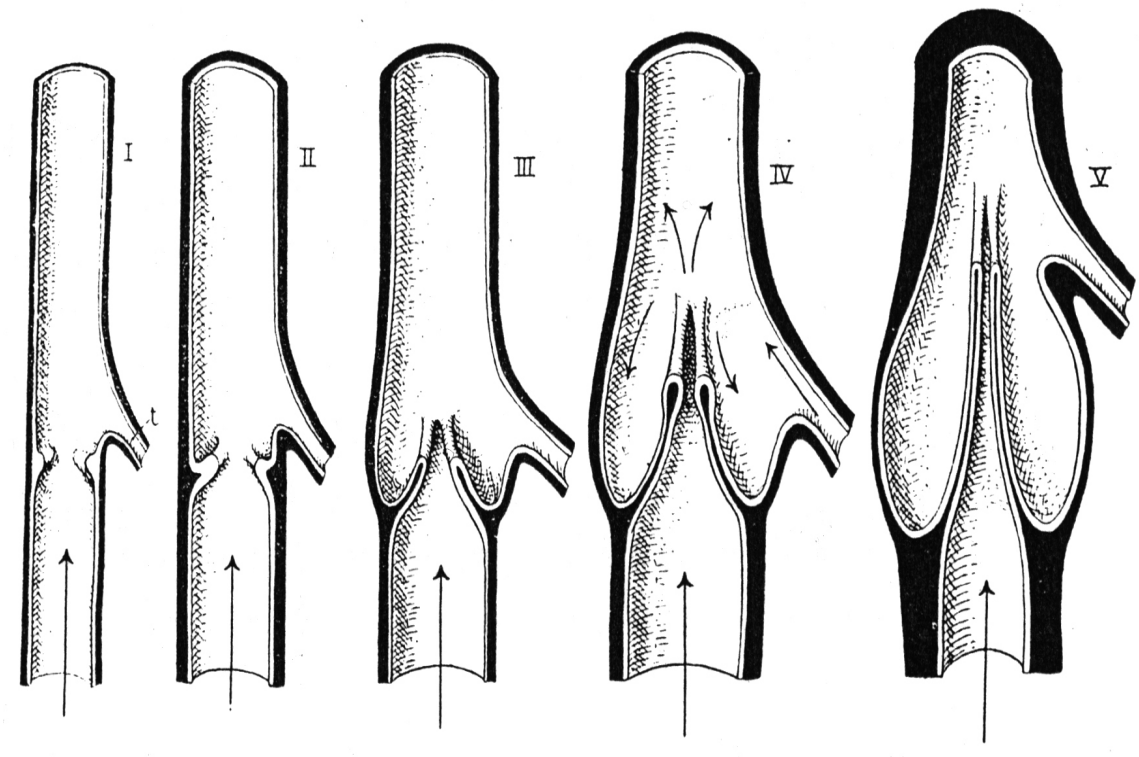

Figure 4 Stages in human venous valve development [22]
I. Ridge-like endothelial thickenings placed opposite to one another
II. Endothelial anlage (valve leaflets) lengthen in the direction of flow
III. Two near-parabolic lines of attachment of the leaflets
IV. Enlargement of the sinus and thickening of the free edges of the leaflets
V. Thinning of vein wall by reduction in the tunica media.
Arrows indicate the direction of flow

These developmental findings were confirmed by Otto Jager in 1926, who similarly reported 'progressive deepening of outgrowths from the inner layers of the vein wall, beginning near the tributary entries' in pig embryos[25] as reviewed in [15,18]. This process was thought to be influenced by the mechanical stimulus of blood flow.[11, 25, 26] There are some data describing the anatomical features of the formed venous valves in the rat (lower limb) and duckling (head veins), mouse (coronary veins), giraffe, ostrich and other animals.[27-33] However, there are no data describing the *development* of VV in an animal model and the precise morphological events resulting in this complex three dimensional VV structure are not clearly understood.[20]

1.5.2 Lymphatic system

Work in this thesis is based in the hypothesis that some molecular regulators are shared between the arterial, venous and lymphatic systems, and it is therefore necessary to examine the development of the lymphatic system. The lymphatic system originates by the sprouting of endothelial cells dorsally from the cardinal veins and superficial venous plexus as loosely adherent strings of cells.[34,35] In a restricted subset of venous endothelial cells, proteins including Sox18, Prox1, VEGFR3 are expressed, leading to differentiation of lymphatic endothelial cells that migrate away from the parent veins.[35-37] (Reviewed in [38]) These initial lymphatic endothelial cells (iLECS) subsequently coalesce to form lumenised paired dorsal peripheral longitudinal lymphatic vessels (PLLV) and ventral primordial thoracic ducts (pTD). The pTD's maintain strongly positive Prox1-expressing connections to the Cardinal Veins, and these sites are likely to form the first lymphovenous valves.[37] The lymphatic system develops from these initial condensates by further sprouting and migration to give a plexus of lymphatic vessels, followed by remodelling into a hierarchical system of capillaries and valved collecting vessels. These converge on the subclavian veins, where the thoracic duct and right thoracic duct empty into the venous system.[37,39,40]

There are similarities in the way that human venous and lymphatic valves develop. Human lymphatic valves (LV) develop earlier than venous (VV)

valves, with 3 processes of LV development described (the 3rd – describing valve formation in large lymphatic trunks – closely resembles the description of venous valve formation, Figure 5).[41]

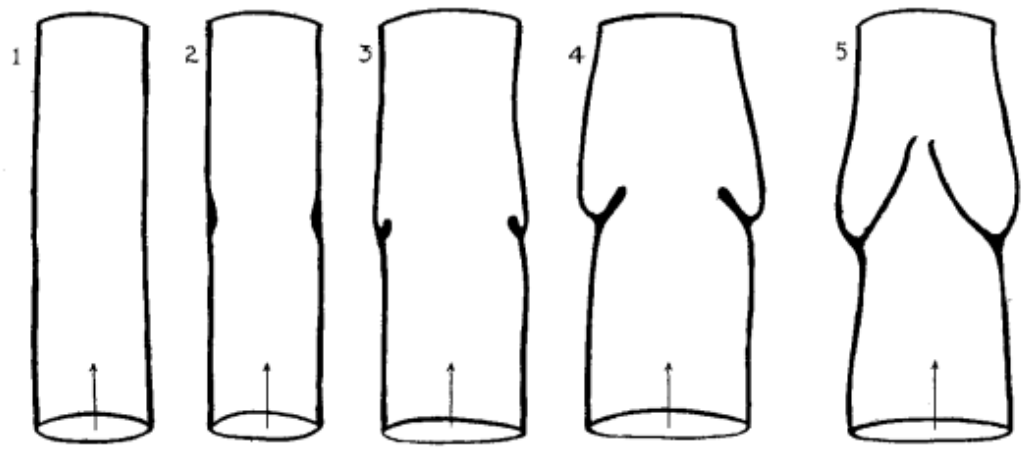

Figure 5 Lymphatic valve formation - Kampmeier 1928
Endothelial cell proliferation and 'invasion of the subjacent mesenchyme' causes the leaflets to elongate into the vessel, and paired sinuses are separated by the buttresses (commissures). Lymphatic valves are described as almost always being bicuspid.

More recently, lymphatic valve development has been analysed by confocal microscopy, primarily in the murine mesenteric lymphatics.[42-44] Four stages have now been defined in LV development (Figure 6).[42,45] At Stage 1, Prox1 expression is increased in a clustered subset of LEC's on one side of the vessel, typically near a branch point. Prox1^{hi} LECs are subsequently termed lymphatic valve-forming cells (LVC's). This is followed by circularisation of Prox1^{hi} LECs to form a ring-like domain of cells at Stage 2. Constriction alters the vessel morphology, and invagination of LVC's into the lumen with increased deposition of lamininα5 in the leaflet core produces the appearance of valve leaflets at Stage 3. Further undefined 'maturation' events occurs to produce a bicuspid valve at Stage 4 (Figure 6).[42] Similar findings have been reported by Levet et al.[45] Bazigou et al reported similar stages to 2-4, but did not comment on circularisation prior to stage 1.[43]

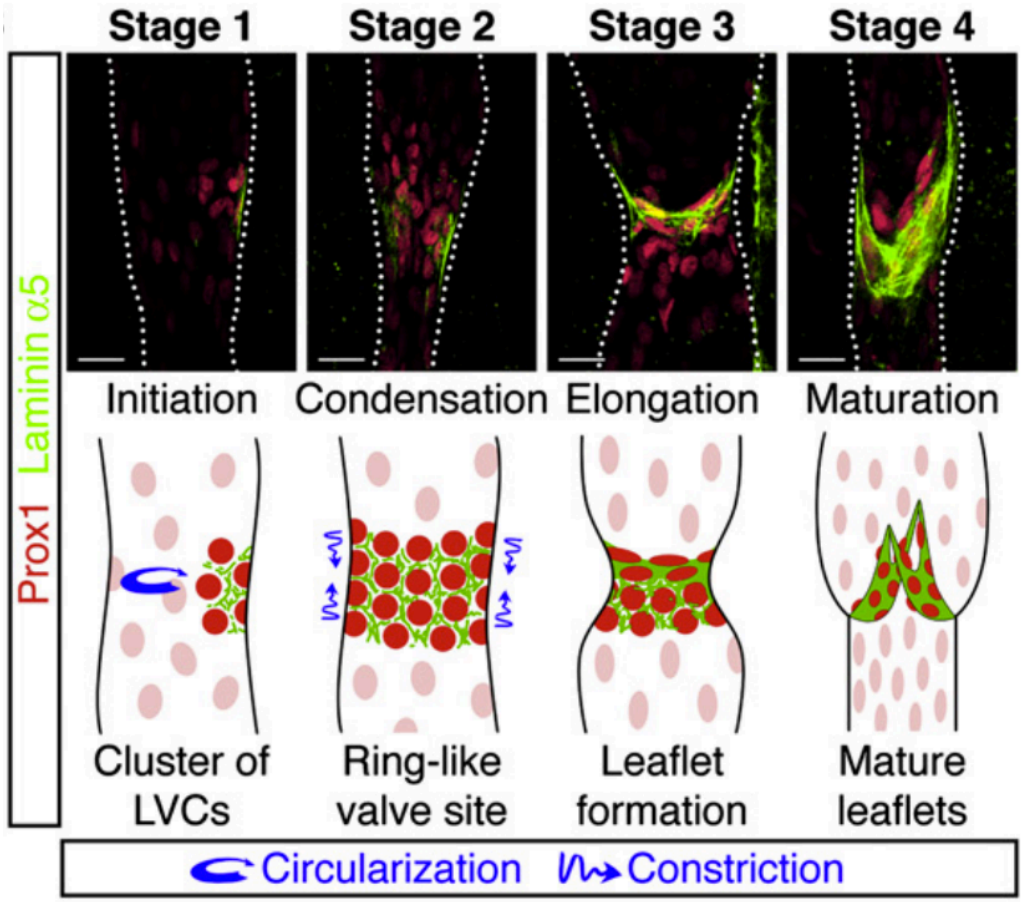

Figure 6 Lymphatic valve development - Sabine 2012[42]
Immunolocalisation of the nuclear transcription factor Prox1 is shown in red, and the extracellular matrix protein lamininα5 (expressed in the leaflet core) in green. Scale bar 20µm.
Stage 1 - Prox1 expression increased in clustered subset of LEC's, near a branch point.
Stage 2 - Circularisation of Prox1hi LECs to form a ring-like domain of cells
Stage 3 - Constriction alters the vessel morphology, and invagination of LVC's into the lumen with increased deposition of lamininα5 in the leaflet core.
Stage 4 - Undefined 'maturation' events produce a bicuspid valve

1.6 Primary lymphoedema and links with venous reflux

In man, lymphoedema may be primary (genetic) or secondary.[46] In some patients with primary lymphoedema, patients have been noted to show venous reflux, suggesting some shared molecular pathways controlling venous and lymphatic disease. Some clinical aspects of lymphoedema caused by mutations in FOXC2, VEGFR3, GJA1 and GJC2 will be discussed here, and their known roles in signalling during valve formation will be further discussed later in this chapter.

1.6.1 Lymphoedema Distichiasis

Mutations in FOXC2 cause lymphoedema distichiasis (LD) and show autosomal dominant inheritance with a high degree of penetrance. A variety of FOXC2 mutations have been described in LD, primarily frame shift mutations that truncate the protein, but all likely resulting in haploinsufficiency. LD is characterised by asymmetric bilateral lower limb swelling of pubertal onset and a double row of eyelashes (due to aberrant development of the meibomian glands).[47, 48,49] Additional features include congenital heart disease, ptosis, varicose veins, cleft palate, and spinal extradural cysts.[49] Lymphoscintigraphy shows a normal or increased number of hyperplastic lymphatics.[49] Patients with FOXC2 mutations (even those without lymphoedema) have reflux in their long saphenous vein, implicating a role for FOXC2 in venous valve development. [50]

1.6.2 Milroy's disease

Mutations in VEGFR3, cause Milroy's disease and show autosomal dominant inheritance with variable penetrance.[51,52,53] Mutations in VEGFC (encoding the major ligand for VEGFR3) have also been described in patients with a Milroy-like phenotype.[54,55] Patient's with Milroy's disease typically show bilateral oedema below the knee identified at birth, although oedema can also be detected by ultrasound in utero.[53] Injections of fluorescent tracer into the feet of Milroy's patients shows greatly reduced or absent filling of dermal initial lymphatics in the swollen foot, and is due to initial lymphatic hypoplasia and dysfunction.[48] Accordingly, lymphoscintigraphy is rarely possible in these patients due to a failure of tracer uptake.

1.6.3 Lymphoedema associated with GJA1 (encoding Cx43)

Mutations in GJA1, encoding Cx43, have previously been associated with oculodentodigital dysplasia (ODDD), characterised by soft tissue fusion of the digits, abnormal craniofacial bone development, small eyes and loss of tooth enamel.[56] Very recently, mutations the same gene were associated with

lymphoedema.[57] In the proband with lymphoedema, a venous duplex was normal other than showing 'mild incompetence' in one short saphenous vein. Cx43 is the most abundant and widely expressed connexin in the family, but it remains unclear how GJA1 mutations cause such a diverse range of pathologies.[56]

1.6.4 Lymphoedema associated with GJC2 (encoding Cx47)

Mutations in GJC2 (also known as GJA12), encoding Cx47, were recently described as a cause of primary 4-limb lymphoedema.[4,58] The first report of GJC2 lymphoedema noted sporadic venous insufficiency[4] and although a venous phenotype had not been systematically assessed, several patients who had venous duplex ultrasound assessments demonstrated reflux in their long saphenous veins, or had varicose veins.[58] This is surprising as the first study to show a role for GJC2 in lymphoedema was based in part on the finding that Cx47 is expressed in lymphatic and not blood endothelial cells.[4] It has been suggested that the predominance of lower limb lymphoedema may be as a result of excessive filtration secondary to venous hypertension.[58]

Mutations in GJC2 also cause Pelizaeus-Merzbacher-like disease (PMLD), a rare central nervous system hypomyelinating disorder.[59] These patients have not been described as affected by venous reflux or lymphoedema, nor have patients with GJC2 lymphoedema been noted to have neurological defects. It remains unclear how mutations in the same gene may produce two possibly distinct syndromes, especially since lymphoedema-associated mutations are distributed throughout the gene, and in one example the same mutation has been independently reported as being causative of both disorders.[4, 59, 60]

Notably, two mutations predicted to result in a null allele have been identified and produced no discernable clinical phenotype. This is analogous to the Cx47 heterozygous or homozygous deficient mouse, which has been reported to show no gross phenotype, and will be discussed further in this chapter.[4,61] These findings have led to the conclusion that the lymphatic phenotype in patients with GJC2 mutations is caused by a *functional* rather than *structural*

defect; likely improper coordination of lymphatic pumping as a result of altered gap junction intercellular communication.[4]

1.7 Molecular regulation and signalling in lymphatic and venous valve development

1.7.1 Integrinα9

The integrins are a family of heterodimeric transmembrane glycoproteins that associate with both extracellular and intracellular proteins to facilitate 'inside-out' and 'outside-in' signalling, and regulate cell-cell and cell-extracellular matrix (ECM) adhesion.[62] They are known to play essential roles in developmental and other processes where cells are required to interact with each other and their surrounding ECM. 18 alpha subunits and 8 beta subunits comprise the 24 known heterodimers in man.[63] Integrinα9, encoded by Itga9, was first discovered in 1993, with a widespread expression pattern that included veins.[63, 64] Itga9$^{-/-}$ pups were subsequently found to fail to survive beyond postnatal day 6-12, and die with lymphatic defects including severe bilateral chylothorax, but no obvious structural defects were observed in the analysed thoracic ducts.[65] Mutations in Itga9 have subsequently been identified in human foetal chylothorax.[66,67] Integrinα9 is only known to dimerise with β1 (other than in gametes) and has several known ligands, including ECM components such tenascin C, VCAM-1, the EIIIA splice variant of fibronectin, EMILIN1, and soluble growth factors VEGFA/C/D.[64,63, 65]

In lymphatics, integrins α5 and α6 are present at low levels throughout the vessels, whilst α9 is localised at high levels to the valves[43] Subsequent analysis of Itga9$^{-/-}$ mesenteric LV at P0 revealed a failure to develop beyond the ring stage (analogous to stage 1 in VV formation) associated with a failure to remodel the fibronectin-EIIIA expressed around the valve, and failure to form the matrix core of the valve leaflet.[43] Accordingly, Fn-EIIIA null mice also showed LV defects, but these were overcome by P21, suggesting possible redundancy in signalling through integrinα9. EMILIN$^{-/-}$ mice show a more complex lymphatic defect, involving the capillaries, valves, and accumulation of mural cells.[68] At P0 and P6 EMILIN1$^{-/-}$ mice show similar defects to double

EMILIN1$^{-/-}$;FnEIIIA$^{-/-}$ knockout mice, suggesting that EMILIN1 may be the more important α9 ligand. Whilst Fn-EIIIA is progressively downregulated postnatally, EMILIN1 persists and P21 EMILIN1$^{-/-}$ mice show persistent lymphatic defects. It remains possible that other parts of the lymphatic phenotype seen in Itga9$^{-/-}$ mice (e.g. chylothorax, which is not seen in FnEIIIA$^{-/-}$ or EMILIN1$^{-/-}$ mice) is due to further undescribed signalling roles. Interestingly Prox1 and integrinα9 are also expressed in cardiac valves, but a cardiac phenotype has not been identified to date.[69] Recently we showed that integrinα9 is expressed in developing VV, and is required for VV development and maintenance.[44] (Appendix 13)

1.7.2 Eph-ephrin signalling

The Eph receptors are the largest family of receptor tyrosine kinases found in man, and are bound by two subclasses of ligand – ephrinAs and ephrinBs. Whilst the A-subclass proteins are tethered to the membrane by a glycosylphosphatidylinositol anchor, the ephrinBs are transmembrane proteins with a short cytoplasmic region.[70] As both ligand and receptor are membrane bound, signalling requires cell-cell contact. Several functions have been attributed to Eph/ephrin signalling, including in early vascular development, formation of tissue borders, axon guidance, cell migration and in synaptic plasticity. [70,71,72]

Following binding of clustered ligand, Eph receptors oligomerise and autophosphorylate leading to the association of adaptor proteins and ongoing signalling into the cell ('forward signalling') including cytoskeletal effects, which may be mediated by actin-binding proteins such as Abl and Arg. In neurons, activation of Eph receptors activates Rho, and inhibits Cdc42 and Rac (Rho family GTPases), leading to a shift in actin cytoskeletal dynamics towards increased contraction and reduced extension. Activation of Eph receptors by contacting a cell expressing the appropriate ephrin can therefore lead to repulsion away from the ephrin-expressing cell and the establishment of tissue boundaries. These mechanisms appear to be cell and context specific, as ephrin-Eph interactions may also mediate attractive forces.[70,72]

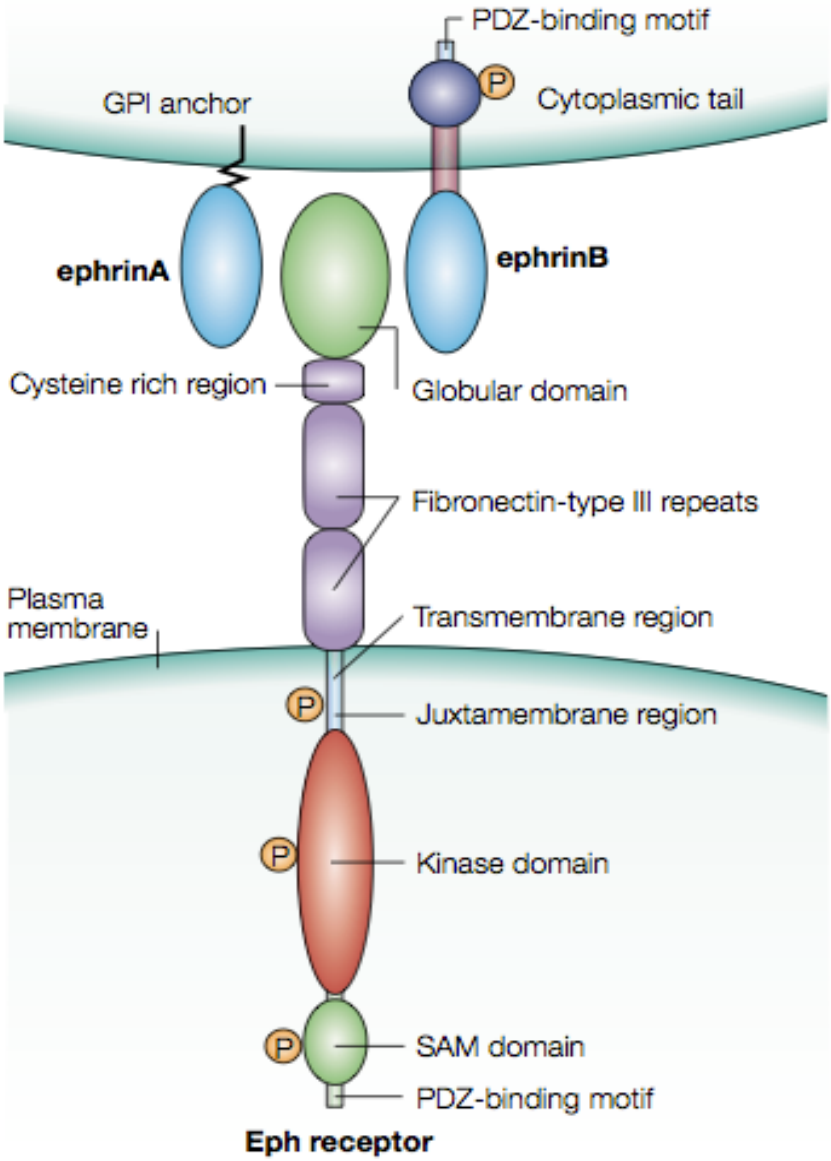

Figure 7 Structure of Eph receptors and their ephrin ligands[70]
PDZ domains are common signalling domains, PDZ being the acronym for the first three proteins found to contain the domain. SAM = sterile alpha motif. GPI = Glycophosphatidylinositol, a glycolipid attached during posttranslational modification to enable membrane anchoring.

Binding of Eph's to ephrin's can also result in 'reverse signalling' through the cytoplasmic domains of the ephrins. Eph binding results in phosphorylation of conserved tyrosine resides in the ephrinB cytoplasmic domain. EphrinBs can also recruit PDZ-domain proteins to a conserved PDZ-binding motif at the tip of their cytoplasmic tail. These PDZ-domain proteins may be adaptor proteins or contain functional domains, and mediate further signalling into the cell that

is independent of the ephrin tyrosine kinase domains.[70] Although ephrinAs lack a cytoplasmic tail, they can still mediate reverse signalling.[72] Cell-cell interaction is terminated (and regulated) by cleavage and trans-endocytosis of the entire receptor complex into either the Eph or ephrin-expressing cell, in the direction of signalling.[72]

Notably, in early vasculogenesis, prior to the onset of flow, arteries and veins are identifiable by reciprocal expression respectively of ephrinB2 and EphB4. EphrinB2 has been reported to be a specific arterial marker and to be absent from veins.[73,71,70] Experiments in which the cytoplasmic tail of ephrinB2 was deleted (and replacement with βgal) demonstrated that reverse signalling is not required for events in early angiogenesis, but neonates were found to die up to 24hrs after birth with defects in cardiac valve development.[71] EphrinB2 is expressed on the downstream surface of developing cardiac valves, and the aortic and pulmonary valves of ephrinB2$^{lacZ/LacZ}$ hearts were grossly thickened.[71] Their mitral (but not tricuspid) valves also appeared hyperplastic, with the increase in size due to increased numbers of mesenchymal cells. It is possible that ephrinB2 reverse signalling regulates the endothelial-mesenchymal transition of endocardial cells that occurs during cardiac valve formation.[71]

A critical requirement for ephrinB2 reverse signalling has been identified in in-vivo lymphatic development by generating two knock-in alleles in its c-terminus.[73] The first, termed ephrinB2$^{\Delta V}$, lacked a functional c-terminal PDZ domain. In the second, ΔY (previously ΔF), the tyrosine residues were replaced with phenylalanine or leucine to block tyrosine phosphorylation (but possibly also interfere with signalling through the PDZ domain).[73] EphrinB2$^{\Delta V\Delta V}$ mice survived the requirement for ephrinB2 in early vasculogenesis, but showed severe lymphatic defects including chylothorax, lymphatic hyperplasia, lack of lymphatic remodelling and a failure to form lymphatic valves. These defects were almost entirely rescued (with normally valved collecting vessels) in ephrinB2$^{\Delta Y\Delta Y}$ mice, indicating that reverse signalling through the ephrinB2 PDZ domain (rather than the tyrosine kinase domains) is critically required for lymphatic development and LV formation.[73] It

has been suggested that ephrinB2 could be required for guiding cell elongation and migration during valve formation.[73] Recently we showed that ephrinB2 is expressed in developing VV, and is required for their development and maintenance.[44] (Appendix 13)

1.7.3 Fox family of transcription factors

The forkhead box (Fox) proteins constitute a large family of transcription factors that share an evolutionarily conserved 100 amino-acid DNA binding domain – the forkhead motif (first identified in the Drosophila gene forkhead*)* with wide ranging roles including development, cell cycle control, metabolism, acquisition of speech and immune function.[74,75] The 'c' subfamily of FOX genes consists of Foxc1 (formerly Mf1) and Foxc2 (formerly Mfh1) which encode proteins with virtually identical DNA-binding domains and generally similar embryonic expression patterns.[74,76]

In man, mutations in FOXC2 cause Lymphoedema Distichiasis in which typically asymmetrical bilateral lower limb lymphoedema of variable age of onset is associated with a double row of eyelashes.[77,78] Mutations in FOXC2 have previously been associated with venous reflux and it has been suggested that the venous valves in these patients are defective.[50] It is interesting to note that these patients are not reported to develop typical venous hypertensive skin changes with ulceration. The mechanism for VV failure in these patients has not been identified.

Mutations in a closely related gene, FOXC1, can cause the Axenfeld-Rieger syndrome, with primarily ocular and craniofacial phenotypes.[79] Although lymphoedema and venous reflux have not been described as part of this syndrome, these phenotypes are often subtle and it is possible that it has been missed (as has recently been described for GJA1 mutations and suggested for GJC2 mutations[58]).

Both Foxc1 and Foxc2 are implicated in cardiovascular development and are expressed in multiple cell types contributing to cardiac outflow tract development, including the secondary heart field, neural crest cells, and

endocardial cells.[76,80, 81] Most compound Foxc1;Foxc2 heterozygotes, as well as all single homozygotes, die pre- or perinatally with a variety of problems including hypoplasia of semilunar valves.[80] Compound Foxc1;Foxc2 null embryos die much earlier and with more severe cardiovascular defects (including hypoplastic semilunar valves) than single Foxc null mutants.[82] Mice that are homozygous for Foxc1 null alleles die pre- or perinatally with phenotypes including the interruption/coarctation of the aortic arch, ventricular septal defects, and aortic and pulmonary valve dysplasia.[83,84] Together these data suggest that Foxc1 and Foxc2 play partially redundant and dose-dependent roles in cardiac development.

In the lymphatic system, Foxc2 is required for maturation of collecting vessels, and deficiency results in abnormal mural cell recruitment around lymphatic valves.[39,40] Foxc2 has been proposed to function downstream of signalling from Vegfr3, consistent with the widespread expression of Vegfr3 and Foxc2 in mesenteric lymphatics. Whilst Vegfr3, Foxc2 and Prox1 expression falls in the lymphangion, expression remains high in the valves.[39,40,85] Signalling through Vegfr2/3 will be discussed further below.

Over 1600 sites where a Foxc2 binding site is very close to a NFATc1 binding site have been identified[39], suggesting that nearby genes are targets of combined activation by Foxc2 and NFATc1. Notable targets include: Gja1 (encoding Cx43), foxp1, SEMA3A, NRP1, EfnB2 (encoding ephrinB2), HEY2, TEK (encoding Tie2), NR2F2 (encoding Coup-TFII). In the lymphatic system, constitutive deletion of Foxc2 (or inhibition of NFAT signalling with ciclosporin) produces a failure to remodel the initial lymphatic plexus into collecting vessels, and an associated failure to form intra-luminal valves.[39,40] SMCs are normally absent around LV's, whereas in Foxc2 null mice, there is abnormal recruitment of SMC's to these sites.[40] This has been hypothesised to be the result of loss of NRP1/semaphorin signalling between lymphatic endothelial cells and pericytes.[86] The role of Foxc2 in the maintenance of the lymphatic system has not previously been studied because of the failure of constitutive knockouts to survive and the lack of tools for conditional Foxc2 deletion.[40]

1.7.4 Notch signalling

In Foxc1 and Foxc2 null murine embryos compound, endothelial cells appear to fail to adopt an arterial identity, and Foxc1/2 are thought to act upstream of Notch in arterial specification.[87,76,88] In vitro, over-expression of Foxc2 produces upregulation of the arterial markers Notch1 and delta-like ligand 4 (Dll4).[76] In pulmonary microvascular endothelial cells Foxc1 and Foxc2 directly activate the Hey2 promotor via upstream forkhead binding elements. In addition, Foxc2 binds the mediator of Notch signalling, Su(H), and so directly contributes to activation of the Hey2 promoter by Notch.[87] Mutations in NOTCH1 have been found to segregate with a spectrum of aortic valve developmental disorders (and subsequent valve calcification).[89] Recently, after completion of the work in this thesis, signalling through Notch1 was found to be required for normal events in early LV formation.[90]

1.7.5 Calcineurin-NFAT signalling

Nuclear Factor of Activated T cells (NFAT) was originally identified in the response of T cells following T-cell receptor binding to antigen-MHC complex. (Figure 8) The NFAT family comprises 5 members with generally non-redundant functions.[91] NFAT1-4 are found in vertebrates. NFAT2, which is a focus of this thesis, is alternatively named NFATc1.[92]

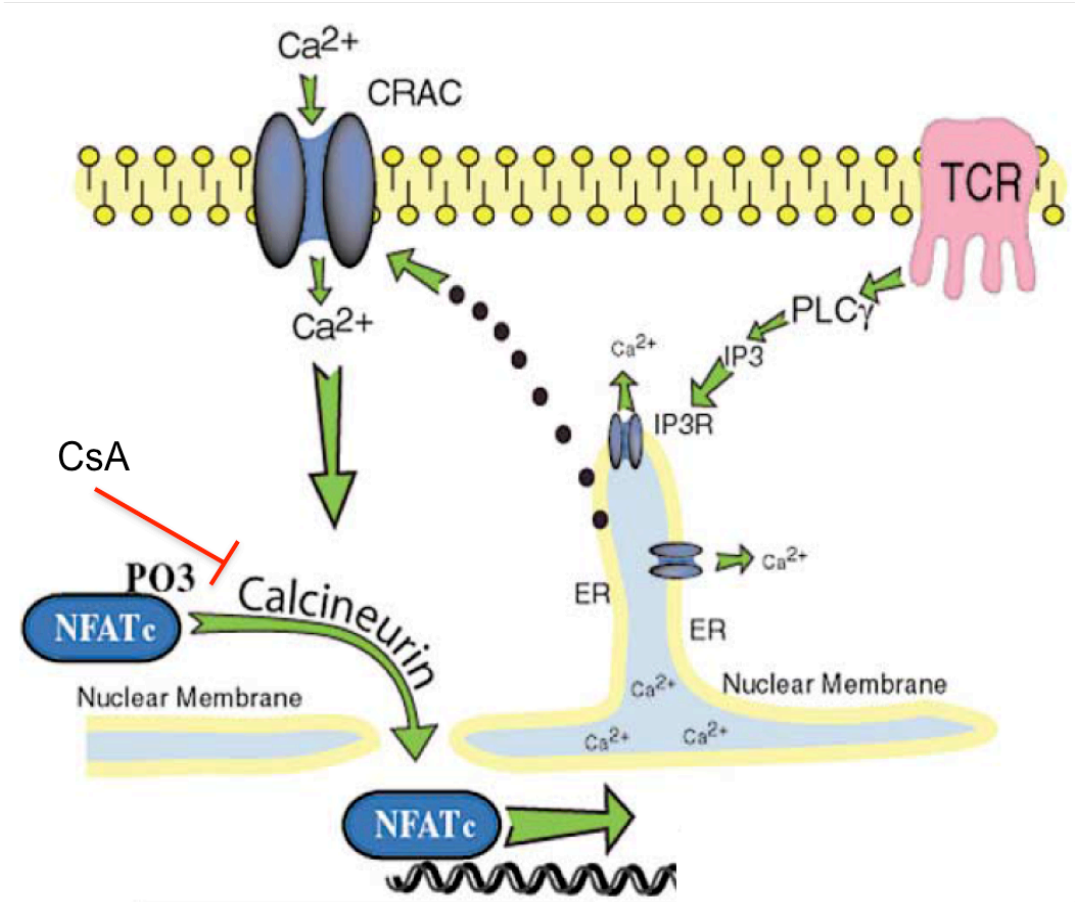

Figure 8 Regulation of NFAT signalling by calcineurin and calcium[92]
In the resting state NFATc is phosphorylated (PO_3) and resides in the cytoplasm. A rise in intra-cellular Ca^{2+} leads to activation of calcineurin, which dephosphorylates NFAT's, revealing a nuclear localization sequence. In the nucleus NFATs act as signal integrators with other proteins. In T lymphocytes (from where most information on NFAT signalling derives), stimulation of a cell surface receptor (TCR) results in activation of phospholipase C (PLC), release of Inositol-triphosphate (IP_3) and release of intracellular Ca^{2+} from intra-cellular stores via the IP_3 receptor. Influx of extra-cellular Ca^{2+} via Calcium Release Activated Ca^{2+} (CRAC) channels is required for full NFAT activation. In cardiac valve formation, it has been suggested that IP_3 may pass between endocardial cells via gap junctions, leading to NFAT activation in neighbouring cells.[92-94] ER= endoplasmic reticulum. CsA= Ciclosporin A, a drug that inhibits calcineurin phosphatase activity.

In the resting state NFATs reside in the cytoplasm but upon an increase in intracellular Ca^{2+} (released from intracellular stores) calcineurin is activated (via calmodulin) and dephosphorylates serine residues on a conserved 300-amino-acid NFAT regulatory domain, resulting in the exposure of a nuclear localization sequence. Once dephosphorylated, NFAT proteins translocate to the nucleus and form complexes with other factors to bind transcriptional targets. NFATs are weak transactivators, and binding with other proteins is typically required for their full downstream effects. The interaction of Foxc2 and NFATc1 in the nucleus to form regulatory complexes on DNA targets has been discussed previously.[39] NFATc1 and NFATc4 bind their own promoters, establishing a positive feedback loop. NFATs are rapidly dephosphorylated by a GSK3 dependent mechanism and exported from the nucleus, allowing discrimination between brief and prolonged Ca^{2+} stimuli. The activity of calcineurin is inhibited by the drug ciclosporin A (CsA), derived from the fungus Tolypocladium inflatum. CsA crosses the placenta and has been shown to block all detectable calcineurin phosphatase activity in embryos. In the cytoplasm it forms a complex with cyclophilin, and the drug–protein composite surface then binds to the interface of the calcineurin A/B complex, which blocks its phosphatase activity by preventing access of the substrate.[95,96] When Ca2+ entry is prevented or calcineurin activity is inhibited the half-life of nuclear NFAT is ~15mins. Additional modulation of this pathway is provided, for example, by DSCR1 inhibition of calcineurin, and DYRK1a-mediated acceleration of phosphorylation. These mechanisms may have important roles in clinical disease, having been suggested to be responsible for the phenotype of Down's syndrome.[97]

NFAT signalling has important roles in cardiac valve morphogenesis. In man, a mutation in NFATc1 has been identified in a patient affected by tricuspid atresia.[98] In murine models it has been demonstrated that in response to local myocardial cues, endocardial cells in the cardiac outflow tract (OFT) and atrioventricular canal (AVC) undergo an endocardial-to-mesenchymal transformation (EMT) to form endocardial cushion cells.[99] NFATc1 is expressed in endocardium and constitutive homozygous deficiency of NFATc1 is fatal at mid gestation due to a failure to form cardiac valves.[100,101]

Conditional deletion of the calcineurin regulatory subunit CnB1 in endocardial cells (mediated by Tie2Cre) results in an almost identical phenotype to constitutive NFATc1 deletion. Aortic, pulmonary, mitral and tricuspid valves all failed to remodel and elongate, with associated lethality at E13.5-E14.5.[96, 102] EMT occurred normally, indicating a specificity for endocardial NFATc1 signalling in valve remodeling. Experiments with CsA indicated a critical time window between E11-E12 in which calcineurin-NFAT signalling is required for valve development.[96]

NFATc1 is required for lymphangiogenesis and maturation of lymphatic collecting vessels, including valve formation.[39, 42, 103] Deletion of CnB1 in endothelial cells inhibited early events in lymphatic valve formation, leading to a broad area of high Prox1 signal, instead of a narrow ring of rotated nuclei.[42] CnB1 was also required for the maintenance of formed lymphatic valves – conditional deletion resulted in a reduction in the length of the leaflet matrix core.[42]

1.7.6 Connexins

Gap junctions form conduits between adjacent cells, and are found joining virtually all cells in solid tissues, mediating the passive diffusion of metabolites, ions and signalling molecules.[104, 105,106] (Figure 9) In vertebrates gap junctions are composed of connexins, integral membrane proteins composed of 4 transmembrane domains with 2 extracellular loops, and a cytoplasmic loop. Both the N- and C- termini are cytoplasmic, with the C-terminal tail of variable length involved in the regulation of channel gating and other functions.[107] Six connexins aggregate to form a hexameric connexon, which may either form a hemi-channel linking the cytoplasm and extra-cellular space, or dock with a connexon from a neighbouring cell to form a gap junction channel. Individual gap junction channels coalesce to form ‘plaques’. 22 connexin genes have been identified in man, with their protein products being named according to approximate molecular weight.[108]

Some connexins have been shown to oligomerise into hexamers with the same (homomeric) or another (heteromeric) connexin, and additionally a gap junction channel may be formed from connexons formed of more than one type (heterotypic junctions). This allows for an increase in the potential combinations of connexins that can contribute to a channel, and variability in the regulation of communication through the channel. Importantly, it is possible for mutated connexins to exert dominant-negative effects, for example in the case of a heterozygous carrier of a mutated protein.[108] At the cell membrane connexins associate with a range of proteins – the 'connexome', and it is possibly through these associated proteins that they exert their non-gap junction-mediated effects, such as on cytoskeletal rearrangements, cell migration and proliferation.[108]

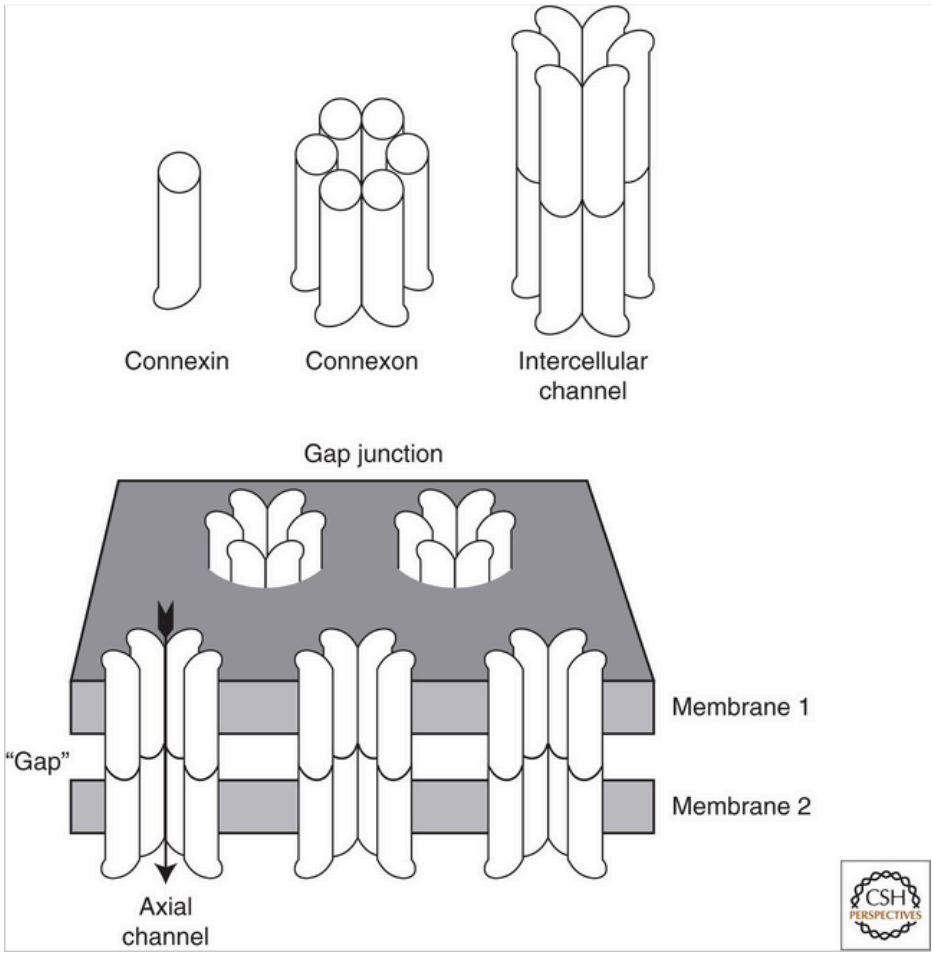

Figure 9 Gap junction channels are composed of connexins[105]
Each connexin protein has four membrane spanning regions, with cytoplasmic N- and C-termini. Six connexins are assembled to form a transmembrane connexon, which may form a hemi-channel or dock with a connexon on a neighbouring cell to form a gap junctional channel, characterized by a narrow core axial channel joining the cytoplasm of the cells.

Connexins have variable permeability to ions and small signalling molecules, (such as cAMP) and variable voltage-gating properties, allowing for a variety of signalling functions even before mixed channels are considered. The identification of the precise signalling molecules responsible for specific defects has remained challenging.[105]

1.7.7 Connexins 43, 47 and 37

The GJC2-eGFP knock-in mouse is not reported to show any lymphatic or venous phenotype, and expression of eGFP was not noted in either system.[61] However, expression of Cx47, Cx43 and Cx37 was recently reported in lymphatic structures using immunohistology.[42, 109] Whilst Cx37 and Cx43 immunostaining was reported in the lymphatic endothelium, Cx47 immunostaining was more restricted and appeared to localise to a subset of valve cells in some mesenteric lymphatic valves, but was more clearly identified in thoracic duct valves.[110] Whilst mesenteric lymphatic valves are composed of 2 layers of endothelial cells, thoracic duct valves are reported to include interstitial cells within their matrix core in a structure more consistent with that which will be described in murine VV in this thesis.[109]

The lack of lymphatic phenotype in the Cx47-eGFP knock-in mouse has been suggested to be as a result of complete loss of the protein, rather than the presence of a mutated form that could exert dominant-negative effects on other connexins.[4, 61] Accordingly, carriers of early nonsense mutations leading to a grossly shorted polypeptide do not show a lymphoedema phenotype.[4]

Mutations in Cx37 have not been associated with human venous or lymphatic disease, but it is required for lymphatic valve development.[109, 111] Recently, it was demonstrated that adult Cx37 knockout mice do not have VV, but the authors were unable to comment on whether Cx37 is required for valve development or subsequent maintenance, or identify the cellular phenotype caused by loss of Cx37.[111] These authors analysed valves after development was complete, and did not examine the localisation of Cx37 during valve

development, or elucidate the cellular processes that go awry with loss of Cx37.

Cx37 also has important roles in the arterial system. In man, a common polymorphism is associated with cardiovascular mortality risk. Cx37 appears to be important in revascularisation as the $Cx37^{-/-}$ mouse recovers limb perfusion more rapidly following induction of hind limb ischaemia.[112-114]

Connexins have important additional functions unrelated to channel activity. For example, knockdown of Cx43 in cortical neurons produces defects in migration that are rescued by channel-dead mutants, suggesting adhesivity between connexins or an effect on migration machinery independent of channel activity.[105] Cx43 is thought to regulate cell polarity and directional migration in vivo and in-vitro, and loss of Cx43 function is associated with abnormal actin stress fiber organization and a loss of polarized cell morphology.[115,116]

Whilst the regulation of connexins has not been examined in the venous system, the intricate pathways linking nuclear transcription factors, lymph flow, and connexins 37 and 43 have been examined in the lymphatic system. Increased Cx37 immunostaining was identified in two regions on opposite sides of lymphatic vessels in their valve-forming region. In the $Cx37^{-/-}$ mouse, $Prox1^{hi}/Foxc2^{hi}$ cells coalesce, but fail to organise into the ring-like constrictions (corresponding to stages 1-2 of VV development) seen in wild-type littermates.[42] Cx37 may be regulated by Foxc2 in lymphatics as this connexin was absent in the jugular lymph sac of $Foxc2^{-/-}$ mice, and its mRNA reduced in LECs from Foxc2-/- mice.[42,109]

In vitro, oscillatory flow produced upregulation of Foxc2, nuclear localisation of Nfatc1 and downregulation of Cx43, mimicking the appearance of valve-forming cells in vivo. Interestingly, upregulation of Prox1 occurred more in response to laminar flow, whilst that of Foxc2 in response to oscillatory flow. In-vitro knockdown of Prox1 and Foxc2 prevent the response of Cx37 and NFatc1 to flow. In addition, Cx37 was required for the NFATc1 response to

fluid flow but remarkably loss of Cx37 did not simply result in uniform failure of nuclear accumulation of NFATc1, but rather in activation in isolated cells. This implies that in-vivo Cx37 (and GJIC) can contribute to the *organisation* of the region of valve forming cells (VFC's). The identity of the molecule that may pass through gap junctions is unknown; two possible candidates for this role are Ca^{2+} and IP_3 (Figure 8).[92, 106]

Taken together, these in-vitro and in-vivo findings by Sabine *et al* point to an accumulation of mechanisms by which a valve-forming region of vein can gradually acquire its phenotype, and VFC's can subsequently organise to form the ring of endothelial cells with upregulated transcription factors that identifies early LV formation. It is expected that those processes demonstrated in lymphatic endothelial cells in-vitro also occur in vivo, and that similar processes may regulate venous valve development.

The larger size of venous valves and the consistent site of development of the proximal femoral valve in mice provides the opportunity to further examine these processes in-vivo, and to develop a model of altered flow in-vivo. The role of Cx47 in VV (or LV) development has not been described, nor has the contribution of Cx43 to early developmental events been shown. Furthermore, whilst Kanady et al recently showed failure of lymphatic-valve formation and lymphatic drainage in $Cx37^{-/-}$;$Cx43^{+/-}$ mice[109], it is not known whether Cx43 deletion alone produces a lymphatic phenotype. Homozygous constitutive loss of Cx43 is lethal within a few hrs after birth due to cardiac right ventricular outflow tract malformation, precluding detailed analysis of lymphatic or venous valve development.[117]

1.7.8 VEGFR2 / VEGFR3 signalling

The vascular endothelial growth factors (VEGF's) are secreted dimeric glycoproteins that include VEGFs A-D and placental growth factor (PLGF).[118] The VEGF receptors (VEGFR's) are members of the receptor tyrosine kinase superfamily, and belong to the same subclass as receptors for the PDGF's and FGF's (Figure 10).[118] VEGF-VEGFR signalling is critically required for

early events in the development of the blood vascular system, and genetic constitutive deletion of VEGFR2 or VEGFR3 results in embryonic lethality.[118]

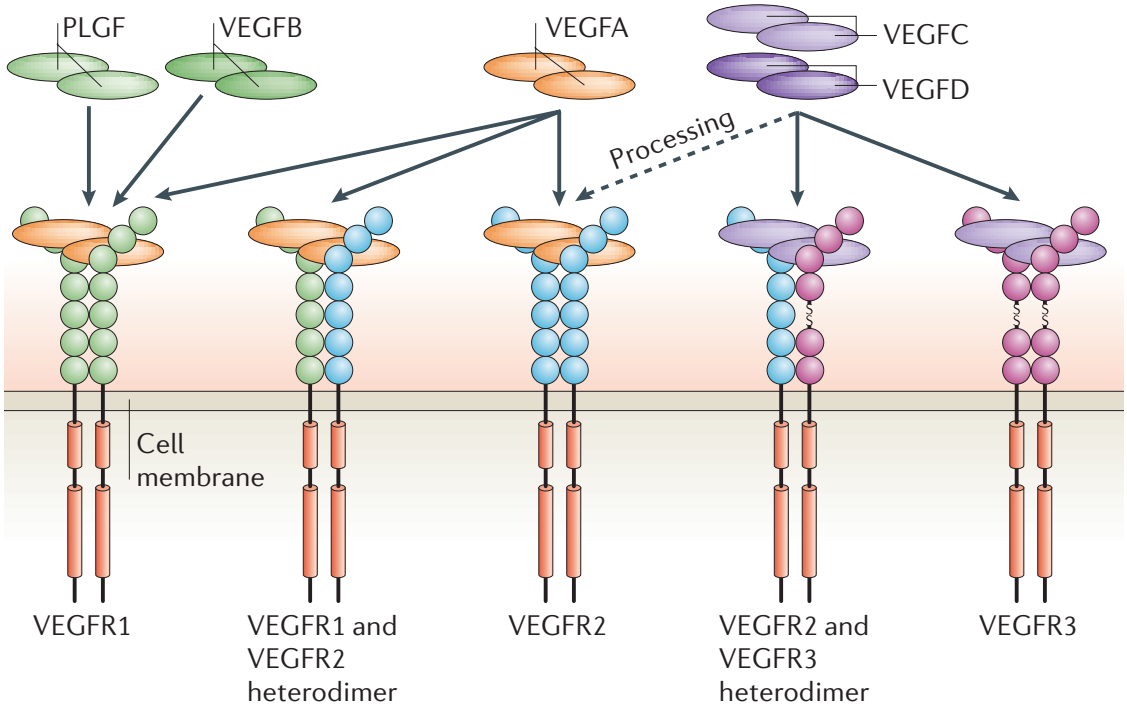

Figure 10 VEGFR ligand binding[118]
VEGFR's consist of 7 extracellular IgG-like domains (6 for VEGFR3, represented by spheres), a single transmembrane domain, and a split intracellular tyrosine kinase domain (represented by red cylinders and affected by mutations causing Milroy's disease). Proteolytic processing is required for VEGFC/D to bind VEGFR2, and these factors bind VEGFR2 with less affinity that VEGFR3. Several protein (not shown) act as co-receptors to VEGFRs, including heparan sulphate proteoglycans and neuropilins (NRP1/NRP2). Binding of ligand guides and stabilises receptor dimerization and is accompanied by activation of the receptor-kinase activity, leading to receptor autophosphorylation. Phosphorylated receptors subsequently recruit interacting proteins and induce activation of signalling pathways. Receptor complexes are subsequently internalized and downgraded. VEGFR3 interacts with (and is regulated by the presence of) EphrinB2 via intermediate proteins. The cell surface glycoproteins neuropilin1 (NRP1) and NRP2 act as non-kinase coreceptors; NRP1 enhances binding of VEGF to VEGFR1/2, and NRP2 enhances binding of VEGFC to VEGFR3. VEGFR's may also form mechanosensory complexes with of platelet-endothelial-cell adhesion molecule-1 (PECAM1), vascular endothelial (VE)–cadherin and integrins. PLGF = placental growth factor. [118,119,120,]

VEGFR3 transduces signals following binding by VEGFC or VEGFD (Figure 10).[121] VEGFR3 inactivation causes significant defects in arterial–venous remodelling of the primary vascular plexus, resulting in lethality by E10.5.[122] At later stages, expression of VEGFR3 was thought to be restricted to the lymphatic endothelial system, but more recently it has been shown to play critical roles in postnatal blood angiogenesis.[123,124] However, in-vivo

postnatal transgenic over-expression of soluble VEGFR3 results in regression of lymphatic vessels, but not major blood vessels, with an associated onset of lymphoedema.[125] Homozygous gene-targeting of VEGFC leads to embryonic lethality at E16.5 as a result of a complete failure in lymphatic vessel formation, whereas VEGFC heterozygous mice survive with lymphatic vessel hypoplasia and lymphedema, but do not appear to exhibit blood vascular defects as found in adults.[15] Notably, homozygous loss of VEGF-C and VEGF-D does not phenocopy loss of VEGFR3 (i.e. embryos survive longer), indicating that other critical signalling processes occur through VEGFR3.[126] These may involve other (unknown) ligands or ligand independent signalling, described as *active* and *passive* pathways.[123] Inhibition of these pathways produces different phenotypes in retinal angiogenesis. Whilst inhibition of ligand-dependent signalling with anti-VEGFR3 antibodies suppressed angiogenesis (with reduced sprouting), conditional endothelial cell-specific VEGFR3 deletion resulted in excessive angiogenesis (increased sprouting).[123, 127] These contrasting results emphasise that inhibition of ligand binding or inhibition of intrinsic tyrosine kinase activity block only some (active pathway) VEGFR3 activities, whilst conditional VEGFR3 deletion will block all.[123]

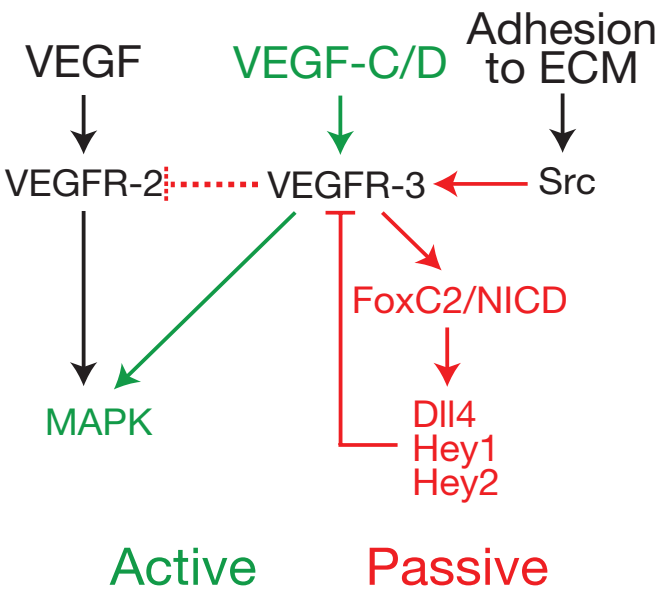

Figure 11 Proposed model of active and passive signalling through VEGFR3[123]

VEGFR3 can be phosphorylated by the tyrosine kinase Src following cell-matrix adhesion, even in the absence of VEGFR3 intrinsic kinase activity. Only the active signalling pathway is targetable by inhibitor molecules, including the small molecule inhibitor MAZ51. Dll4, Hey1 and Hey2 are canonical Notch targets also known to be upregulated by the transcription factor Foxc2. It has become clear that in lymphatics Foxc2 is upregulated downstream of VEGFR3; Foxc2 mRNA was not detected in the endocardium of homozygous VEGFR3lacZ embryos.[40] Subsequently, in retinal angiogenesis, Foxc2 was found to be upregulated by signalling through VEGFR3.[123] ECM=extra cellular matrix, NICD = Notch intracellular domain. PLGF = placental growth factor.

It remains unclear precisely how known human mutations in VEGFR3 result in lymphoedema. Most mutations are missense, although a few deletions and a single splicing variant have been reported.[128] These mutations result in tyrosine kinase–negative receptor proteins with extended cellular half-lives, with the mutant protein residing for longer periods of time at the cell membrane.[128,129] Mutant protein may exert dominant-negative effects.[130] The Chy mouse exhibits constitutive heterozygous loss of VEGFR3 protein tyrosine kinase function, and displays cutaneous lymphoedema.[130] The same mutation carried in the Chy strain was recently reported in a patient with Milroy's lymphoedema, confirming its utility in modelling this disease.[128,130]

1.7.9 A role for flow in valve development

Since the first descriptions of lymphatic and venous valve development in the late 1920's it has been suggested that intraluminal flow has an important role stimulating their development.[22,41] Abnormal blood flow and shear stress adversely affect heart valve formation in the chick and zebrafish,[131-133] and in the mouse flow directs formation of a left-sided aortic arch, indicating the importance of blood-flow in directing morphogenesis.[134] In the lymphatic system, flow has been suggested to have a role in valve formation.[42] To the best of my knowledge a critical requirement for normal flow has not been demonstrated for lymphatic or venous valves in vivo.

Several mechanisms by which flow might modulate valve formation have been proposed. Intravital microscopy has demonstrated oscillatory fluid flow in lymphatics prior to the onset of valve development, and a similar pattern of oscillatory flow might be expected prior to valve development in veins.[42] In vitro, oscillatory blood flow upregulates Foxc2 and Cx37, and acts in concert with Prox1 to regulate LEC morphology.[42] In bEnd3 murine capillary endothelial cells there is an earlier and greater increase in the expression of Cx43 in response to oscillatory flow compared with unidirectional shear stress.[135]

Shear stress induces phosphorylation of the receptor tyrosine kinase Tie2 in endothelial cells and the effect is proportional to flow velocity, leading us to speculate that shear stress induced phosphorylation of Tie2 may be one mechanism in VV development.[136] Blood flow might activate VEGFRs in a ligand-independent manner, by the formation of mechanosensory complexes consisting of PECAM1, (VE)–cadherin, VEGFRs and integrins.[118]

1.8 Background summary

A recent review[85] suggests the following interaction between the previously described pathways (Figure 12), suggesting activation of VEGFR2/3 (possibly interacting with EphrinB2[119]) leading to PLC-IP_3-Ca^{2+}-calmodulin-calcineurin activation of NFATc1, which binds to and signals with Foxc2 in concert with Prox1 to stimulate valve development by upregulating integrinα9 and Fibronectin-EIIIA, and downregulating PDGF-B and Collagen IV.[85] (Data for Figure 12 in this review[85] quotes a personal communication from Prof. T. Petrova, and Appendix 13 [44] to this work.) Both Foxc2 and Prox1 upregulate Cx37, and Foxc2 may downregulate Cx43.[42, 111]. It is possible that signals (possibly IP_3 or Ca^{2+}) pass between endothelial cells via gap junctions to activate calcineurin or otherwise regulate valve development.[92, 106, 109, 111]

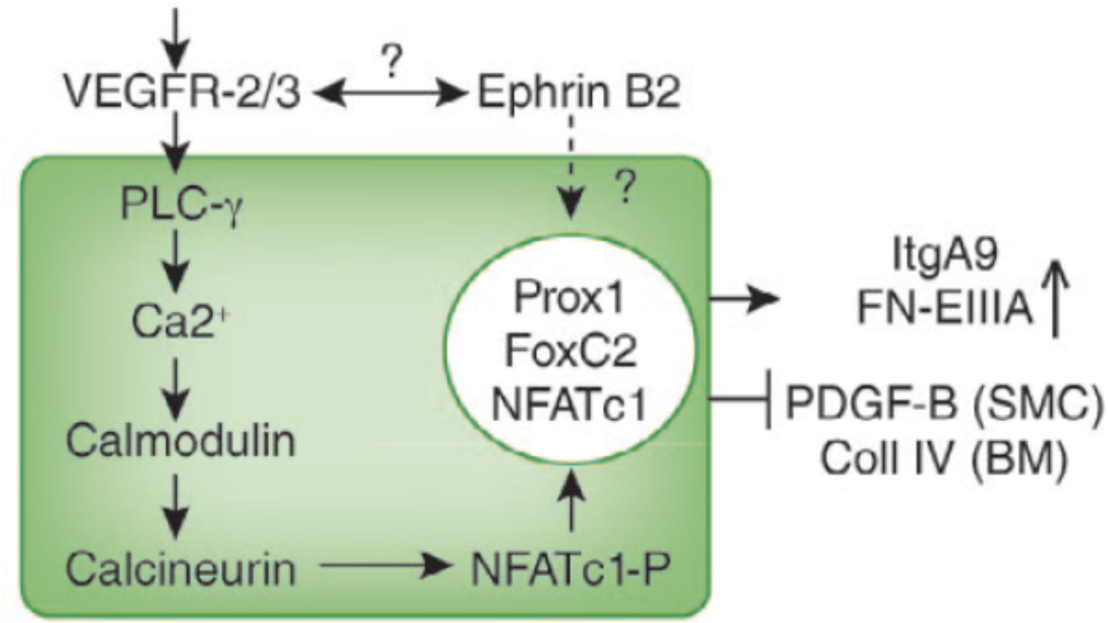

Figure 12 Proposed signalling events in LV formation [85]
A schematic of a valve-forming lymphatic EC is shown (green). The white circle represents the nucleus. It has been proposed[85] that signalling via VEGFR2/3 (arrow above VEGFR2/3), possibly interacting with ephrinB2, acts upstream of Calcineurin-NFAT signalling. Prox1, Foxc2 and NFATc1 are nuclear transcription factors that have roles in LV formation.[85]

Several of these proteins have been described as being specifically expressed in arterial or lymphatic (and not venous) EC's, and Prox1 is widely thought to act as the master regulator of lymphatic EC fate in their differentiation away from venous EC's.[35, 37, 103, 137, 138] However, given the phenotype of venous reflux shown in patients with mutations in FOXC2[49, 50] and VEGFR3[51-53], and some known similarities in the phenotypes of VV endothelial cells[40], this thesis will explore the hypothesis that these factors (and others) regulate VV development in addition to lymphatic/cardiac valve development.

1.9 Rationale for this study

Venous valve failure, associated with venous reflux and hypertension, is commonly found in human venous disease and leads to significant morbidity. A better understanding of the processes involved in the development and maintenance of VV may lead to new therapies that replace absent or dysfunctional valves, and could help alleviate the chronic complications associated with hypertension. This thesis will explore the factors affecting venous valve formation and maintenance in murine models and in man.

Current knowledge of venous valve development relies on histological studies performed in human embryos several decades ago and no methods exist for the study of valve development in rodent models. The use of murine models combined with study of human venous valves could explain the mechanisms of venous valve failure in known single-gene disorders and identify further candidate genes for human venous disease. The ability to understand the processes that regulate venous valve development and maintenance could lead to new treatments to prevent venous valve failure and allow a novel regenerative medicine approach to treat failed valves.

1.10 Hypotheses

1) Venous valve development and maintenance are regulated by processes similar to those identified for cardiac and lymphatic valves.

2) Several human primary lymphoedema syndromes, some previously associated with venous reflux, also involve structural abnormalities in venous valves.

1.11 Aims

1) Develop and characterise venous valve development in the mouse and to use this model (in conjunction with genetic loss of function models involving genes associated with cardiac and lymphatic valve development or disease), to interrogate the mechanisms that regulate valve development in health and disease.

2. Investigate the effects of flow on the development of venous valves in a murine model.

3) Develop methods to locate and measure human venous valves in vivo in order to investigate the effects of known genetic mutations in genes that give rise to primary lymphoedema (VEGFR3, Foxc2, GJC2, and GJA1), on the number and structure of venous valves in these patients.

2 GENERAL METHODS

2.1 In vivo conditional genetic deletion

A constitutive loss of function ("knockout") approach has several limitations including: the potential for increased morbidity and mortality that may limit the utility of the line, difficulty in determining which cell type in a tissue contributes to an observed phenotype, and an inability to study the role of a gene in adult mice after normal development. For example, $Foxc2^{-/-}$ mice on a bl/6 background do not survive beyond the requirement for Foxc2 in cardiac development around E15 and before initiation of venous valve development. $Itga9^{-/-}$ mice die between P6 and P12. Conditional deletion overcomes these limitations by allowing for deletion of an allele in a particular cell type (expressing a particular promoter) and/or at a particular time point after an experimental stimulus.

Several experiments in this study rely on the Prox1CreERT2 line developed by Drs Taija Makinen and Eleni Bazigou using bacterial artificial chromosomes[44] (Appendix 13). In this line Cre recombinase is fused to a mutated ligand-binding domain of the oestrogen receptor (CreERT2) and is expressed under control of the Prox1 promotor.[139,140] Under normal conditions the fusion protein resides inactive in the cytoplasm, bound to heat shock protein 90 (HSP90), which inhibits nuclear translocation. 4OH-Tamoxifen (4OHT, administered i.p. or in feed) displaces HSP90 and results in translocation of CreERT2 to the nucleus and subsequent Cre-mediated deletion of a section of LoxP-flanked DNA - the 'floxed' allele (Figure 13).[141] Use of various floxed alleles allows for spatially and temporally controlled genetic loss of function experiments of each allele during valve development. Deletion of an allele after valve development is complete produces a loss of function experiment to study the role of a particular allele in maintenance of the formed valve. [140]

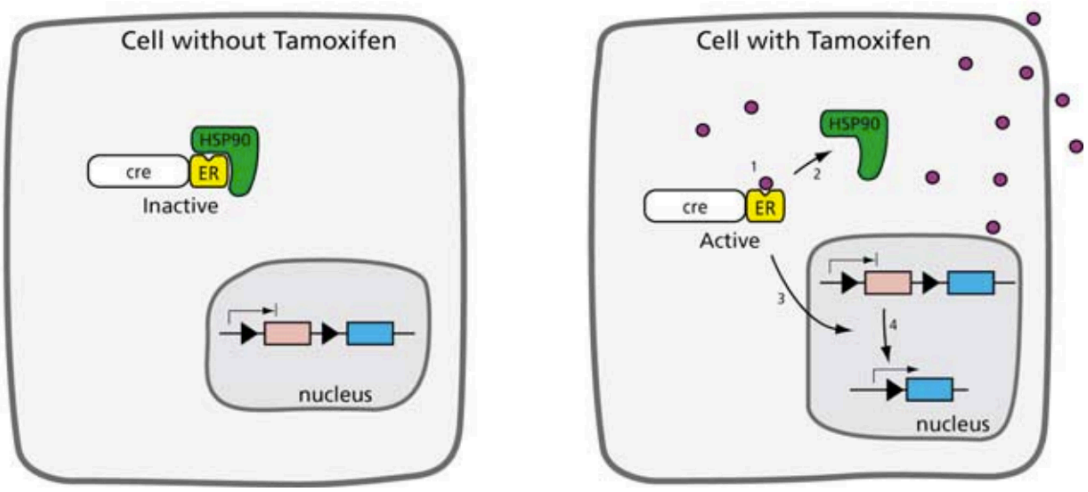

Figure 13 Mechanism of CreERT2 in response to 4OH-Tamoxifen[140]
In the absence of 4OH-Tamoxifen (represented by violet circles) CreERT2 resides in the cytoplasm, bound to HSP90. 4OHT binds the estrogen receptor (1) displacing HSP90 (2), resulting in translocation of the fusion protein to the nucleus (3) and Cre recombinase activity (4). Cre excises DNA between LoxP sites (represented by black triangles). CreERT2 is not activated by endogenous oestrogens.

Various crosses were used to produce the animals described, which resulted in a mixture of CreERT2+ or CreERT2-, heterozygous or homozygous floxed or wildtype alleles. No homozygous CreERT2+ animals were analysed. Littermates were grouped as appropriate into ‘effective genotypes’ of wildtype, heterozygous deletion and homozygous deletion and are referred to as such in the text and figures.

2.2 Animal genotyping

2.2.1 DNA extraction

DNA extraction for animal genotyping was carried out using tail or ear snips and the HotSHOT extraction method. [142]

1. Tissue samples were placed in 100µl PCR tube strips containing 75µl of lysis reagent (pH12.6).
2. Samples were incubated in a thermocycler (Biorad MJ Mini) at 94^{o}C for 30mins, with 1min of vortexing after 15 and 30mins.
3. 75µl of neutraliser reagent (pH5.0) was added to each sample, and the labelled tube strips stored at -20^{o}C.

2.2.2 PCR

Genotyping was carried out by end-product PCR using the HotstarTaq PCR kit (Qiagen) according to the manufacturer's instructions. Primer sequences and PCR conditions are given in Appendix 4.

2.3 Immunofluorescence of venous valves

1. Pups were culled by decapitation, and dissected to allow injection of the infra-renal aorta with heparinised phosphate buffered saline, pH7.4 (PBS)
2. When required, wholemount photographs where taken with a Leica MZ 16F microscope fitted with a Leica DFC 420C camera.
3. Tissues around the femoral vein were removed to allow rapid penetration of fixative, and facilitate subsequent dissection steps.
4. Samples were placed in freshly thawed 4%w/v paraformaldehyde (PFA) for 2hrs on ice.
5. Samples were rinsed in PBS before the vascular bundle from above the bifurcation to the distal femoral vessels was dissected out and stored in blocking solution at 4^{o}C.

6. Samples were incubated with primary antibodies in PBS 24-hrs to 5days on a shaker at 60 rpm at 4^{o}C.
7. Samples were washed for 2hrs at room temperature (RT) on a shaker in copious 0.3% v/v Triton-x100 in PBS (PBST), with changes at 0, 60 and 120mins.
8. Samples were incubated with secondary antibodies (and conjugated primaries) for 2hrs at RT on shaker.
9. Samples were washed for 3hrs at RT on a shaker in PBST, with changes at 0, 60, 120 and 180mins.
10. Samples were further dissected and mounted in Mowiol (Appendix 1) or Prolong Gold (Life Technologies) with a spacer (colour modelling clay, Scolaquip UK) between slide & cover slip.
11. Samples were examined by widefield (Leitz DMRB) or confocal microscopy (Leica SP5). For confocal microscopy, optical sections were obtained at 1024x1024 resolution, 200Hz, 2 frame averages, z-step of 1.5-2µm, pinhole 1Airy Unit. To minimise cross talk, fluorophores were excited sequentially and narrow emission filters were used around the predicted peak for each fluorophore. Offset was set at ~-2.4%, and photomultiplier tube gain adjusted to generate signal within the full range of the detector over the z-depth of the imaged part of the specimen (the vein and few microns either side), whilst avoiding >few% saturated pixels within the VV.
12. Confocal z-stacks were typically 3D median filtered using a kernel size of 3 to reduce background noise. In NIH ImageJ, the stack was cropped, and a 2D maximum z projection was created. Stacks were retained and used to assist in identification of lymphatic vessels and other tissues passing near the vein, and analysis of 3D structure during staging of VV development.

2.4 Immunofluorescence of murine mesenteric lymphatics

1. The small bowel was excised and pinned flat on custom made silastic-lined (Dow Corning) 6-well plates for fixation in freshly thawed 4% PFA at room temperature for 2hrs.
2. Mesenteries were washed and dissected free of the bowel and mesenteric lymph nodes prior to permeabilising in PBST for 2hrs, then blocking in 3% FCS at +4^{o}c in 1.5ml Eppendorf polypropylene tubes overnight.
3. Mesenteries were incubated with primary antibodies in eppendorfs at +4^{o}c for 1-5 days, prior to washing in PBST for 2hrs and incubation with secondary antibodies for 2hrs.
4. Mesenteries were washed for 2hrs and mounted (without spacers) in Prolong Gold, and allowed to cure for 24hrs at room temperature.
5. Imaging was performed with a Leitz DMRB widefield microscope and/or Leica SP5 confocal microscope.

2.5 Drug preparation and administration

2.5.1 4-Hydroxy Tamoxifen (4OHT)

To stimulate nuclear translocation and activity of the CreERT2 construct, dam's received 2mg 4OHT i.p, whilst pups received 50μg i.p. 4OHT, administered in sunflower oil (Sigma) at the times indicated in individual experiments (typically at E15/E15.5 for analysis at P0, or P0/P1 for analysis at P6).

2.5.2 Progesterone

Following 4OHT injection dams are unable to successfully litter to produce viable offspring. Progesterone (Sigma P3972, 37.5μg/g of body weight) was therefore administered (10mg/ml sunflower oil, Sigma S5007, i.p) to prevent

labour and allow explantation of embryos at a time point equivalent to P0 (‘E19’).

2.6 Obtaining human venous valves for comparison with murine valves (structure and protein expression)

The aim of this study was to collect clinically normal venous valves and surrounding vein for use in subsequent experiments. The ethics committee approval number for this study was 10/H0701/68.

1. Patients referred for coronary artery bypass grafting (CABG) were identified by the routine cardiac surgical care team at St Thomas’ Hospital (STH).
2. Patients were consented for participation in the study on admission to hospital. Consent was obtained in accordance with the GMC guideline “Good practice in research and consent to research”. Participants were allocated a unique study code.
3. During routine CABG surgery, any ‘spare’ or unused vein was placed in in a solution of normal saline (as prepared by the scrub nurse).
4. Samples were placed in appropriate containers labelled with the participants unique study code and transferred to the Academic Department of Surgery (ADS) at STH.
5. All samples were allocated an anonymous ‘ADS’ number on entering the laboratory. This was used for labelling of all samples, and subsequent subsamples (eg blocks, slides). All storage, use, processes applied to, and disposal of Relevant Material was recorded in the laboratory Human Tissue Act database. When no longer useful, samples were destroyed in accordance with the Human Tissue Act.

2.7 Preparation of human venous valves for scanning electron microscopy

Veins were collected directly from theatre and opened under a dissecting microscope with blunt-tipped scissors in a distal to proximal direction to avoid causing damage to the valves. Frequently no valves were present in short samples. Any sections of vein containing a valve were pinned onto a cork board and placed upside-down in 2.5%v/v glutaraldehyde fixative and subsequently processed as described in section 3.5 except that samples were visualised in a Hitachi S-3500N scanning electron microscope.

2.8 Preparation of human venous valves for transmission electron microscopy

1. Vein was collected directly from theatre and opened with large blunt-tipped scissors under a dissecting microscope in a distal to proximal (antegrade) direction to avoid causing damage to the valves.
2. A section of vein containing a valve was pinned onto a cork-board and placed upside-down in 2.5%v/v glutaraldehyde fix overnight at +4 ^{o}C.
3. Valves were post-fixed in 1%w/v osmium tetroxide in 0.13M Millonig's phosphate buffer with 0.3M glucose pH7.3 at 4^{o}c for 1.5hrs.
4. Valves were dehydrated for 10mins in 10% ethanol, 30mins in 70% ethanol, and 3x20mins in 100% ethanol at room temperature.
5. Valves were placed in propylene oxide for 2x10min at RT.
6. Under a dissecting microscope a single valve leaflet was dissected from the vein using a razor blade on dental wax.
7. The leaflets was pre-infiltrated in 50:50 100% ethanol:resin (TAAB embedding resin, medium)
8. The leaflet was then infiltrated in 100% resin overnight at 4^{o}C
9. The leaflet was embedded in resin at the correct orientation for cutting sections and polymerised at 70^{o}C for 24hrs. Until the resin hardened,

the orientation of the specimen was checked every 10mins (as convection currents disturbed it)

10. Semi-thin (0.5μm) and ultra-thin (70-90nm) sections were cut using a Reichart OMU4 Ultracut microtome.
11. Semi-thin sections were stained with toluidine blue and examined under a microscope to determine orientation within the specimen.
12. Ultra-thin sections were examined and recorded using a Hitachi H7600 transmission electron microscope fitted with an AMT digital camera system.

Steps 4-8 and 10-11 were carried out by Dr Gema Vizcay-Barrena at the centre for ultrastructural imaging (CUI)

2.9 Preparation of human venous valves for paraffin embedding and sectioning

1. Veins were opened longitudinally using blunt-ended scissors under a dissecting microscope. Alternatively, the vein was probed in a retrograde manner to identify the sites of valves. Maintaining a closed vein was preferable in order to obtain transverse sections of valves that were attached at either end to the vein wall. This prevented them from floating off during processing and avoided 'edge effects'.
2. Samples were fixed in 10% formal saline (4% formaldehyde in 0.9% NaCl) for 24-48hrs.
3. Samples were dehydrated through sequential alcohol washes to xylene and infiltrated with paraffin wax overnight in a TissueTek VIP 5E-F2 automated tissue processor (Sakura Finetek, Netherlands).
4. Samples were embedded in a suitably sized mould and place on a cold plate for at least 1hr before removing the wax block from the mould. For long samples a custom-made deep silastic (Dow Corning) mould was used.
5. 5μm sections were cut for histological analysis.

2.10 Preparation of human venous valves for frozen sectioning

1. Veins were opened longitudinally using blunt-ended scissors under a dissecting microscope. Alternatively, the vein was probed in a retrograde manner to identify the sites of valves and maintained closed.
2. Pieces of vein were placed on a labelled cork disc and snap-frozen in OCT (TissueTek) in isopentane precooled in liquid nitrogen.
3. Samples were wrapped in foil and stored at -80^{o}C until sectioned. Sections were cut at 7-10μm in a cryostat microtome (Bright Instrument Co) set at -26^{o}C.

2.11 General strategies for optimising and detecting antibody binding for immunohistology

Many antibodies used in this project had not previously been optimised for their utility in locating their respective antigens by immunohistochemistry or tissue immunofluorescence and a strategy was developed to expedite the choice of different methods of staining.

Formalin fixed paraffin embedded (FFPE) sections were used initially because they give better preservation of tissue architecture than frozen sections (FS). Initial testing in FFPE sections was with and without heat induced epitope retrieval (HIER), and with retrieval in pH6 and pH9 buffer. Primary antibody concentrations in the range 1-10μg/ml were tested and final concentrations are given in Appendix 3. Initial testing was typically with amplification, for example, using an HRP-polymer-conjugated secondary antibody (Menarini). The proprietary HRP-polymer-conjugate was used with primary antibodies raised in either rabbit or mouse. Alternatively, a biotinylated secondary antibody was used in conjunction either an Extravidin-peroxidase or Extravidin-alkaline phosphatase complex. Microwave heat retrieval was also assessed, as was the use of a tyramide-based amplification system (Perkin Elmer). In general, if

the above strategy failed to localise staining, then staining was attempted in frozen sections, without fixation and using fixation with either 4% PFA at room temperature or acetone at -20^{o}C.

2.12 Immunohistochemistry on paraffin sections

The following is a typical method used during optimising staining. Controls were incubated with IgG to match the species, isotype and concentration of the test antibody.

1. Slides were heated for 30mins in a dry oven at approximately 60^{o}c to melt the paraffin wax. Slides were then washed twice in xylene at room temperature (10mins per wash).
2. Sections were hydrated through graded ethanol 100%, 75% and 50% for 1min each. Care was taken to avoid carry-over of solutions from one bath to the next. Samples were rinsed briefly in running tap water.
3. Heat induced epitope retrieval was performed in an Access Retrieval Unit (Menarini) using Access Antigen Revelation solution (pH 6.0) and Access Super solution (pH 9.0, Menarini) at 124^{o}C for 30secs then allowed to cool to 90^{o}C. Ice was then added to cool the slides to a comfortable handling temp and avoid rapid evaporation and drying-out of sections.
4. Sections were washed in PBS (2x1min) on the 'belly dancer' (Sovall Life Sci) (always at speed setting 5½).
5. Endogenous tissue peroxidase was quenched by incubating the slides in 1% H_2O_2 in industrial methylated spirit (IMS, 3ml of 30% hydrogen peroxide solution in 97ml IMS) for 30mins.
6. Slides were washed in PBS for 2min on the belly dancer.
7. Slides were wiped dry (making sure that the section remained moist) and the tissue section ringed with a hydrophobic pen (DAKO). Specific binding of the primary antibody was facilitated by blocking with neat DAKO super block at RT in a humidity chamber for 7min 30sec. All subsequent incubations were carried out in a humidity chamber.

8. Blocking agent was gently tipped off and sections were incubated at RT for 1hr with primary antibody (in PBS) in humidity chamber.
9. Sections were washed in PBS (5x2min) on the belly dancer.
10. If a primary antibody raised in mouse was used, then sections were incubated for 7.5min with Menarini Universal Probe (rabbit anti-Ms antibody) at RT. Unbound antibody was then washed off in PBS (5x2min) on the belly dancer.
11. Sections were incubated for 15min at RT with Menarini HRP-polymer (proprietary anti-rabbit antibody).
12. Slides were washed in PBS (5x2min) on the belly dancer.
13. HRP activity was localised by incubating with Vector SG substrate (as per the manufacturer's instructions, Vector Labs) for 2-10min whilst monitoring signal development under the microscope.
14. The reaction was stopped by washing in PBS (2x2min) on the belly dancer.
15. Sections were counterstained using Nuclear Fast Red for 11mins.
16. Sections were rinsed for 1min in tap water, dehydrated through graded alcohols (50%, 75%, 100%, 100% and further 100% alcohol) for 1min each and cleared by 2x2min immersions in xylene (BDH, UK).
17. Slides were carefully mounted using DPX (BDH, UK) under cleaned glass coverslips and allowed to dry at room temperature overnight.

2.13 Immunohistochemistry on paraffin-embedded sections using tyramide-based amplification

This method was carried out using the Perkin Elmer Tyramide Amplification kit. Buffer compositions are given in Appendix 1.

1. Slides were warmed for 30mins in dry oven to melt paraffin wax
2. Slides were immersed in xylene (2x10min) at RT.
3. Sections were hydrated though graded ethanol's 100, 75 and 50% (2mins each) and briefly rinsed in running tap water. Heat induced epitope retrieval was carried out using Access antigen revelation solution (pH6.0) and Access super solution (pH9.0) by heating the

slides at 124^{o}C for 30sec and then cooling to 90^{o}C in a digital pressure cooker (Menarini)

4. Slides were washed in TNT buffer for 2x2mins on belly dancer (always set at 5½).
5. Endogenous tissue peroxidase as quenched by incubating the slides in 1% hydrogen peroxide (H_2O_2) in industrial methylated spirit (IMS) for 30mins (3ml of 30% H_2O_2 solution in 97ml IMS).
6. Slides were washed in TNT buffer for 5mins x2 on the belly dancer.
7. Sections were incubated in TNB blocking buffer for 30mins at RT.
8. Remaining block was gently removed and the slide dried around the wax rings. Sections were placed in the humidity chamber and incubation with primary antibody was performed overnight at 4^{o}C. All antibodies were diluted in 1x TNB blocking buffer.
9. Unbound primary antibody was washed off for 5mins x3 in TNT wash buffer on the belly dancer.
10. Sections were then incubated with secondary antibody (biotinylated polyclonal goat anti rabbit IgG) for one hour at RT.
11. Unbound secondary antibody was wash off in TNT wash buffer for 3x5mins on the belly dancer
12. Slides were incubated for 30mins at RT with Streptavidin-HRP conjugate diluted 1:100 in TNB blocking buffer.
13. Slides were washed in TNT wash buffer (3x5mins).
14. TSA biotin signal amplification step:
15. Dilute biotinyl tyramide amplification reagent 1:50 using 1x amplification diluents provided with the kit and incubate for 10mins at RT.
16. Slides were washed three times with TNT wash buffer (3x5mins) on the belly dancer.
17. Slides were incubated with Streptavidin-HRP conjugate diluted 1:100 in TNB blocking buffer for 30mins at RT.
18. Slides were washed with TNT wash buffer (5mins x 4) on belly dancer.
19. Peroxidase activity was localised using the Vector SG substrate kit (Vector Laboratories) and ~200µl of chromagen substrate was applied to each slide. Chromagen substrate was prepared just before use. To 5ml of Dulbecco's PBS pH7.4 (DPBS) was added 3drops (~150µl) of

chromagen, and then 3drops of hydrogen peroxide solution, with mixing after each addition.

20. Slides were washed in TNT wash buffer (3x5mins) on the belly dancer.
21. Tissue sections were counterstained with Nuclear Fast Red (Vector Laboratories) for 10mins at RT
22. Slides were rinsed in running tap water for 30sec.
23. Sections were dehydrated through graded alcohols (50%, 75%, 2x100%) for 1min each and cleared by 2x2min immersions in xylene.

2.14 Immunohistochemistry on frozen sections

The following is a typical method used for optimisation of antibody staining in frozen sections. For uncharacterised antibodies, optimisation was performed by testing at a range of primary concentrations between 1-10μg/ml. All incubations were carried out in a humidity chamber.

1. Slides, stored at -80^{o}C, were allowed to warm to room temperature for 30mins.
2. Sections were fixed in acetone pre-cooled to -20^{o}C for 10mins in a fume hood, then rinsed in PBS for 1min.
3. Slides were wiped dry (making sure that the section remained moist) and the section of tissue ringed with a hydrophobic pen,.
4. Blocking of non-specific binding sites was carried out by treating sections with 3% w/v bovine serum albumin (BSA) in PBS for 3hrs.
5. Block was gently tipped off and sections incubated with primary antibody (diluted in 3% BSA) overnight at +4^{o}C.
6. Sections were washed in PBS (5x2min) on belly dancer (setting 5.5).
7. Slides were incubated for 1hr at RT with a 1/200 dilution of stock Extravidin-alkaline phosphatase complex (Sigma)
8. Slides were washed in PBS (5x2mins)
9. Alkaline phosphatase activity was located using the Vector BCIP/NBT substrate kit (Vector Laboratories), prepared according to the manufacturer's instructions.

10. Staining was stopped by washing for PBS (5x2min)
11. Sections were counterstained with Nuclear Fast Red for 11mins.
12. Slides were washed in PBS for 2min.
13. Sections were dehydrated through graded alcohols (50%, 75%, 100%, 2x100%) for 1min each and cleared by 2x2min immersions in xylene.

2.15 Imaging of stained frozen and paraffin embedded sections of human valves

Sections were photographed using a Micropublisher 3.3RTV camera mounted on a Leitz DMRB microscope with PL Fluotar x5, x10, x20 and x40 lenses (Leica). Micrographs of a 1mm graticule were obtained with each lens to enable the addition of scale bars.

2.16 Animal Husbandry

All UK experiments were performed in accordance with UK Home Office regulations. Animals were maintained at SGUL, CRUK's London Research Institute, UNIL and KCL. Transgenic lines were maintained in house on a bl/6 background. Pregnant and adult Balb/c mice were obtained from Charles River UK.

Animals were maintained on a 12hr light cycle and fed food and water *ad libitum*. Matings were formed overnight; the morning of plug identification was termed E0. Dams littered overnight and were identified in the early morning; this day was referred to as post-natal day 0 (P0).

3 NORMAL MURINE VENOUS VALVE STRUCTURE AND DEVELOPMENT

3.1 Introduction

At the onset of my study, research into the development of valves in the vasculature in animal models was limited to those in the heart [71, 92, 96, 143] and lymphatics [40, 42, 43, 109, 138]. There were no animal models available in which a defined location for VV was described.

3.2 Aims

The aims of the work in this chapter were to carry out the following.

1) Identify a consistent site where a venous valve is present and develop methods for the study of valve development at that site using an endothelial reporter, resin casting, and SEM.

2) Compare the structure of murine and human venous valves.

3) Describe stages in venous valve development to enable the quantification of phenotypes in subsequent experiments.

3.3 Study design and methods

Resin casts of the lower limb venous system and a Tie2LacZ reporter strain were used to identify a consistent site of valve development. Subsequently 143 proximal femoral venous valves were visualised in 84 Tie2LacZ reporter mice (1-2 valves per mouse) at ages from E18 to adult (Table 1).

Wholemount confocal microscopy of the murine femoral vein (as described in the General Methods chapter) was utilised to examine the expression of Prox1 and Foxc2 was at E17, P0 and P6 (≥6 valves per age).

TEM analysis of developing VV was carried out in 3 valves from 3 balb/c mice at P0.

All experiments were carried out as described below or in the general methods chapter. Solutions and antibodies are given in Appendix 1 and Appendix 3.

3.3.1 Visualisation of VV in Tie2LacZ mice

Mice expressing β-galactosidase (βGal) driven by the Tie2 promoter (Tie2LacZ) were maintained on a mixed background (MF1 and FVB). Tie2 is a thought to be ubiquitously expressed in endothelial cells, and LacZ expression driven by the Tie2 promoter allows localisation of endothelium, including the endothelium lining valves.[144] Valves were assigned a developmental stage by an observer blinded to their age. The composition of all solutions used in these studies is given in Appendix 1.

1. Explanted embryo's or pups/adults were culled and rinsed in PBS at 37^{o}c
2. Samples were fixed at 4^{o}c for 90mins and then rinsed in 3x5mins washes (Washing Solution).
3. Samples were placed in Working Staining Solution in the dark at 37^{o}c, and inspected at intervals for an appropriate level of stain. Staining time varied with sample age from a few hours to 1-2days, and was monitored under the microscope.
4. Samples were rinsed in 3x5mins PBS washes prior to fixation in 4% PFA for 2hrs. Samples were then stored in a solution of 70% glycerol, 30% PBS to clear.
5. For imaging, the samples were rinsed with PBS and photographed using a Nikon Coolpix 995 camera mounted on a dissecting microscope (Leica M3C). Veins were opened with either a scalpel over a tungsten needle, or with microscissors (Fine Science Tools).
6. For combined localisation of βGal and SEM of venous valves, samples were processed to visualise βGal activity and photographed with the vein closed and then opened (with scissors or a knife over an intra-luminal tungsten needle). Samples were then pinned to silastic (Dow Corning) boards and fixed for routine processing for SEM.

3.4 SEM of opened murine veins

All buffers and solutions are provided in Appendix 1

1. Pups or adult mice were culled using CO2 confirmed by cervical dislocation. To reduce hair contamination of samples, the fur was wet with 70%v/v ethanol in H20. The abdomen and lower limbs were prepared under a dissecting microscope (Leica M3C).
2. Samples were attached to slides using elastic bands and fixed in 5%v/v formaldehyde and 0.8%v/v glutaraldehyde for 90mins at 4°C
3. Under a dissecting microscope, the femoral vein was opened longitudinally using a curved scalpel blade over an intraluminal tungsten wire.
4. Samples were further fixed in 2%v/v glutaraldehyde and 1%v/v formaldehyde in sodium cacodylate buffer for 24hrs at RT.
5. Samples were trimmed to a small block, osmified (1%v/v osmium) for 24 hours on a rotator, dehydrated through graded alcohols (30mins at each step), critical point dried via CO2, and sputter coated (Polaron SC7640) with gold.
6. Samples were viewed in a Cambridge Stereoscan 360 scanning electron microscope.

3.5 SEM of resin casts of the murine venous system

1. Pups or adult mice were killed using terminal anaesthesia (isofluorane) or CO_2 confirmed by cervical dislocation.
2. The abdomen was opened under a dissecting microscope.
3. Batson's No. 17 (Polysciences) promoter, catalyst, methyl methacrylate monomer and red pigment were mixed as per the manufacturer's instructions.
4. Resin was injected into the IVC using a 30-gauge needle. The IVC was clamped around the needle to prevent leakage. Samples were allowed to cure for 2-3hrs.
5. Samples were placed in several changes of potassium hydroxide at $37^{O}C$ for several days (to weeks) until all tissues had dissolved.
6. Casts were carefully washed and dried in ethanol and mounted on a 15mm SEM stub using araldite. Casts were sputter coated with gold

(Polaron SC7640) and imaged using a Cambridge Stereoscan 360 scanning electron microscope.

3.5.1 Statistical analysis

Change in developmental stage with increasing murine age was analysed by Kruskall Wallis test, with Man Whitney U tests for individual comparisons. All analyses were carried out in SPSS 21 (IBM corporation).

3.6 Results

A valve was consistently identified in the murine proximal femoral vein, and was visualised by localisation of βGal activity in wholemount samples from Tie2LacZ reporter mice (Figure 14). Opening the vein allowed SEM analysis of overall valve structure (Figure 14), and cellular arrangements (Figure 15). Endothelial cells lining the leaflets had a rounded morphology, whilst those of the free edges were always spindle shaped. The free edges of each leaflet fused prior to a common junction with the vein wall at the commissures (Figure 15). Analysis of human VV showed similar macroscopic structural features to murine valves (Figure 16).

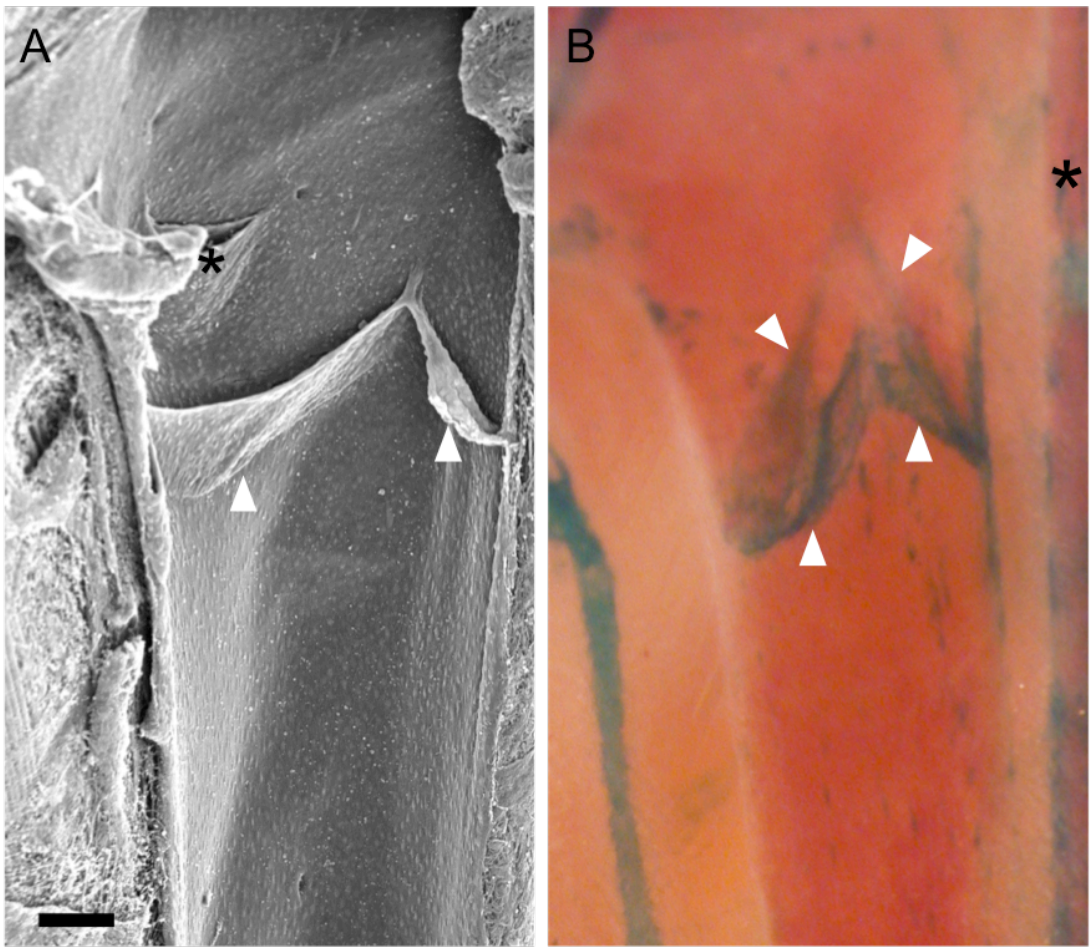

Figure 14 SEM and wholemount images of murine adult left femoral VV
A) SEM of adult venous valve (arrowheads) in the proximal femoral vein. An ostial valve (*) guards the orifice of a tributary vein.

B) Wholemount micrograph in Tie2LacZ reporter strain showing venous valve (arrowheads). The edge of the femoral artery is visible running vertically to the right (*). Both femoral valves are stage 4 (it is not typically possible to stage valves within opened veins). The Tie2 promoter is not active in LECs.[145] Scale bar=100μm. Flow direction is upwards.

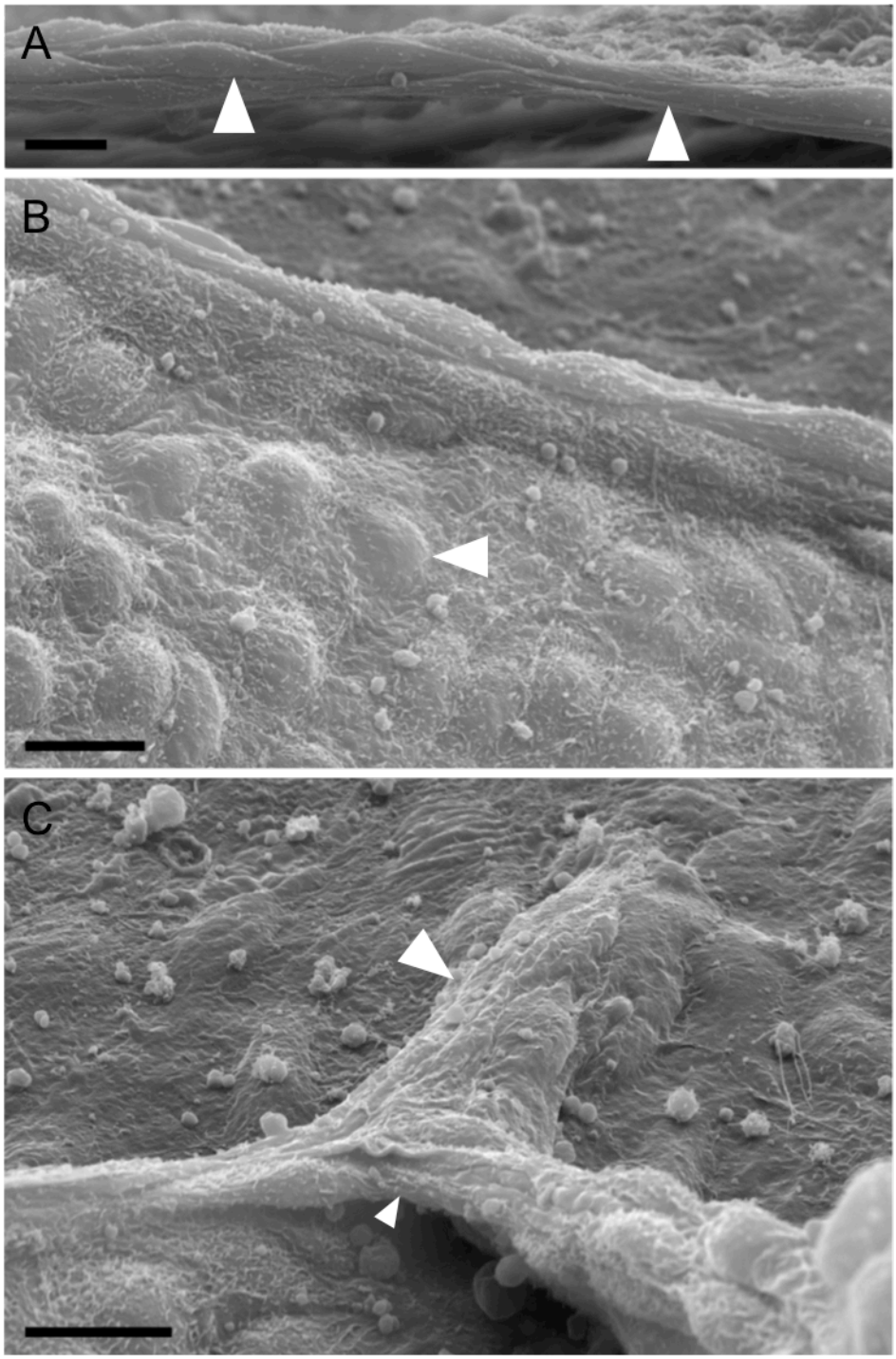

Figure 15 SEM of adult murine venous valve

A) Fusiform free-edge cells (arrowheads).

B) Rounded leaflet cells (arrowhead indicates bulge of nucleus, lumen surface shown) (flow upwards)

C) Commissure (large arrowhead). Note that free edge cells do not insert into the vessel wall but form a complete ring (small arrowhead). Scale bars 10μm. The valve shown is the same as the previous figure.

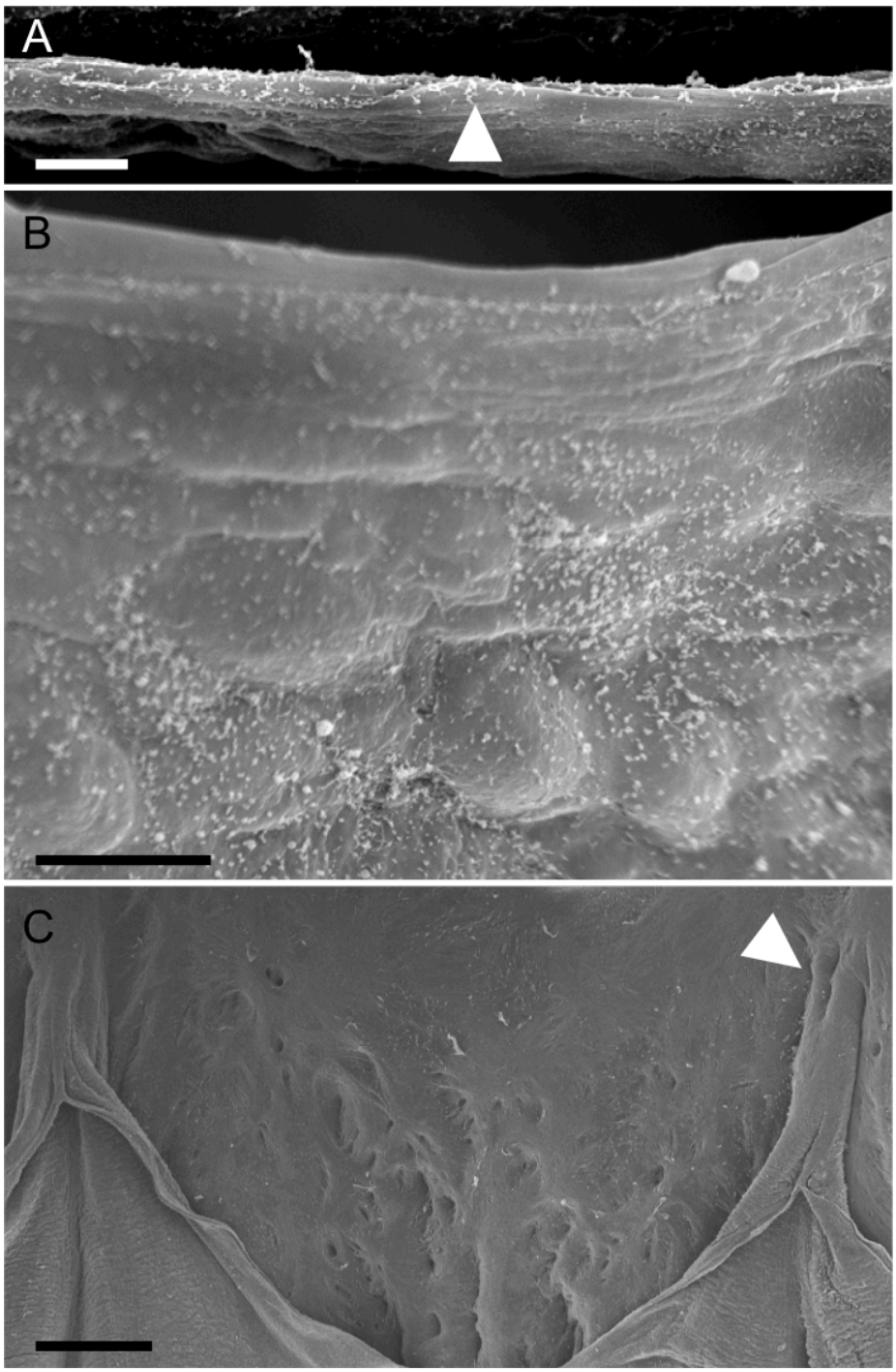

Figure 16 Representative SEM of normal adult human long saphenous vein valve showing similar structure to murine valves

A) Fusiform free edge cells (arrowhead).
B) Rounded cells lining the lumen surface of the leaflet.
C) Commissures are similar to those seen in murine valves, but may branch (arrowhead on right). Multiple small downstream tributaries are seen.
Scale bars: A and B =10μm, C = 500μm. Direction of flow = upwards.

3.6.1 Valve developmental stages using Tie2LacZ and SEM

VV development was assigned stages according to the observed changes in valve structure (Figure 17). Using the Tie2LacZ reporter, at stage 0 no valve structure was seen, whilst at stage 1 an organised ring of rotated cells was present. Ingrowth of a circular shelf of endothelial cells produced stage 2 of development, followed by the development of first one commissure at stage 3 and a second to form stage 4. The presence of a single commissure stage was further identified in a resin cast in an adult mouse (Figure 18). Quantification of VV development in 143 valves at ages from E18 to adult showed a clear stepwise progression in developmental stages with increasing age (Figure 19). The development of valves showed considerable variability (the stages of VV development at selected ages are shown in Figure 20).

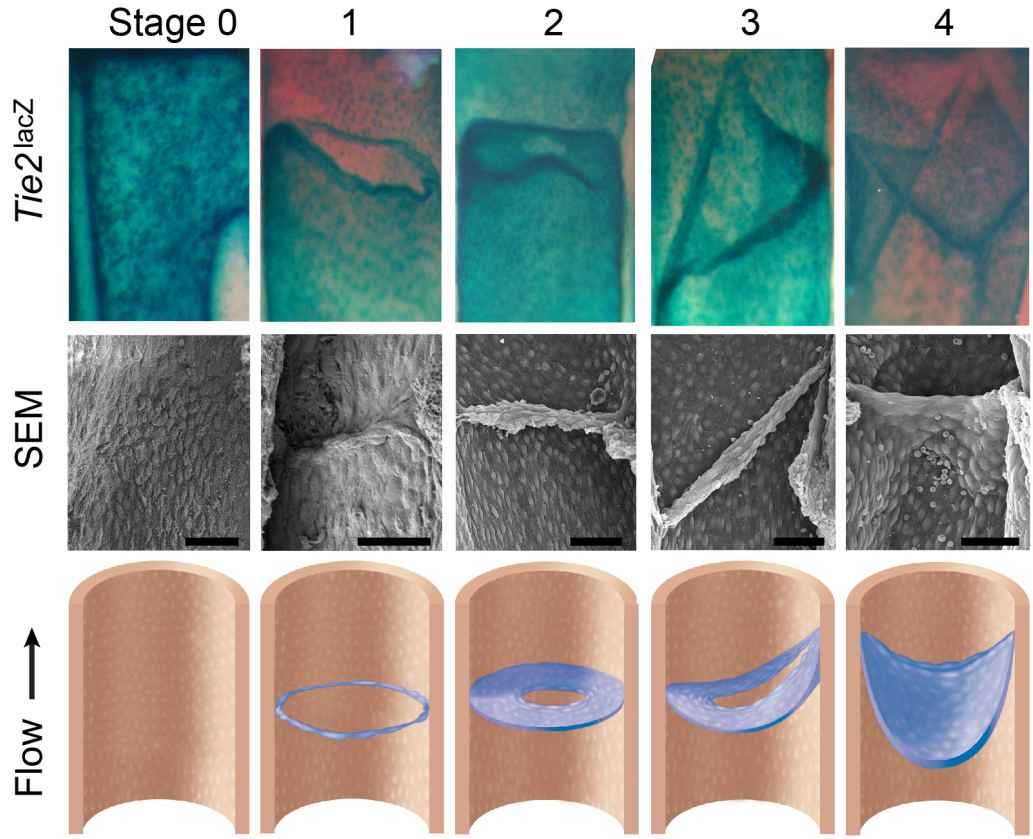

Figure 17 Developmental stages in venous valve formation.
These stages were assigned to VV formation to enable quantification of valve development. See text for definitions used in assigning stages. n=143 Tie2LacZ. Scale 200μm. Direction of flow= upwards (SEM at stage 0 and 1 provided by Dr Eleni Bazigou).

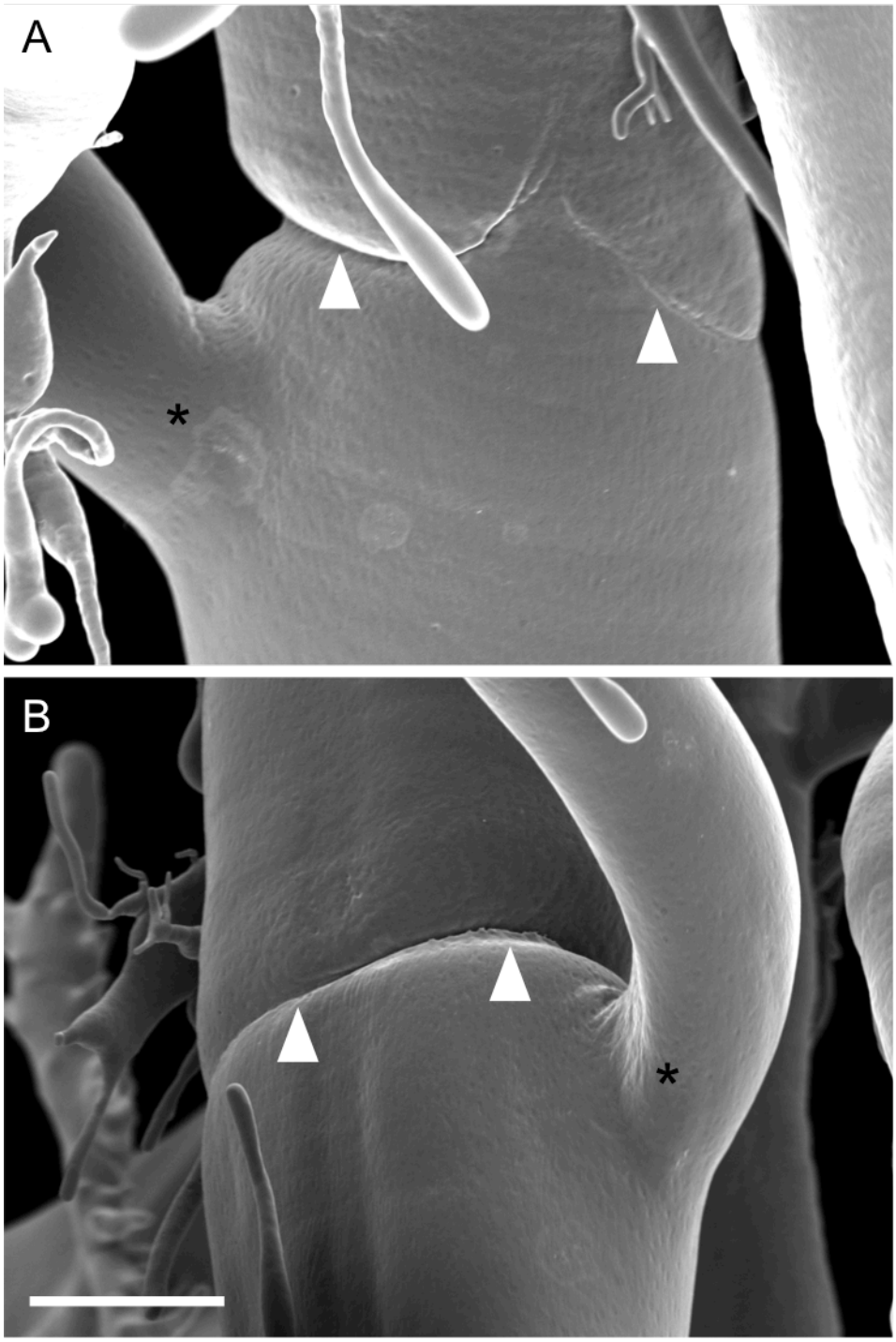

Figure 18 SEM of resin cast of murine Stage 3 valve
A & B show opposing sides of a stage 3 valve that persisted in an adult, visualised by SEM following injection of resin into the venous system. Arrowheads indicate the valve leaflets. A single commissure is shown in A. * indicates a single large tributary. The existence of a single commissure stage has not previously been demonstrated, and was initially identified in valves visualised using the Tie2LacZ reporter. Scale = 250μm

Table 1 Evidence for progression through developmental stages using Tie2LacZ endothelial reporter

Venous valves (N=143) were visualised in 84 Tie2LacZ reporter mice. For this analysis adults were recorded as age 42 days (ie ≥6 weeks). The table provides the number of VV analysed at each age and at each stage

Age	Stage 1	Stage 2	Stage 3	Stage 4	Total
E18	4	1	0	0	5
1	11	15	2	0	28
2	0	2	2	3	7
3	0	2	2	4	8
6	1	11	11	3	26
7	0	0	1	1	2
12	0	0	1	2	3
13	0	0	4	1	5
14	0	0	4	2	6
15	0	4	5	2	11
16	0	0	3	3	6
20	0	0	3	4	7
21	0	1	0	3	4
24	0	0	3	1	4
27	0	0	3	1	4
42	0	0	2	15	17
Total:	16	36	46	45	143

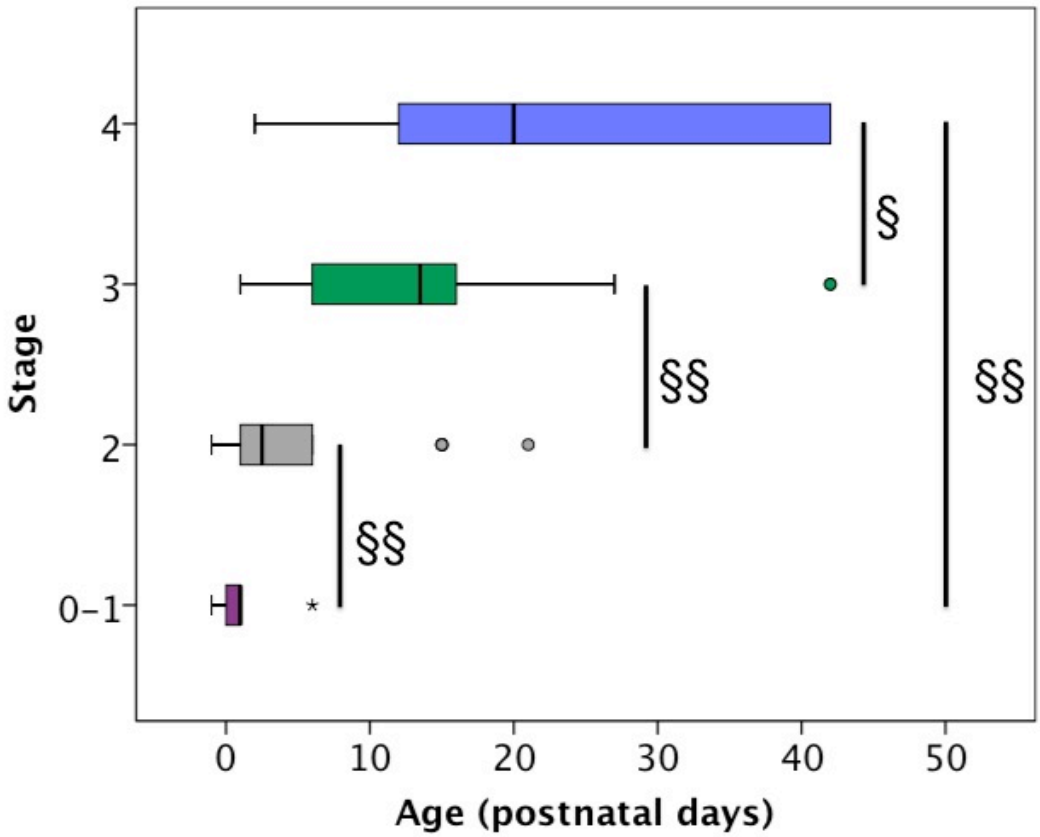

Figure 19 Evidence for valve progression through developmental stages
Analysis of the stage of development in n=143 valves between E18 and adult in n=84 $Tie2^{LacZ}$ reporter mice showed a significant trend in increased age with each stage of development, quantified according to the development of commissures. Box and black line represents inter-quartile range and median. Circles represent outliers and the star an extreme outlier. § P=0.008, §§ P<0.0001. (Mann Whitney U test for individual comparisons, Kruskal Wallis across all four groups) Adults were recorded as age 42 days (i.e. ≥6 weeks). The raw data including the number of VV analysed at each age and stage are provided in Table 1.

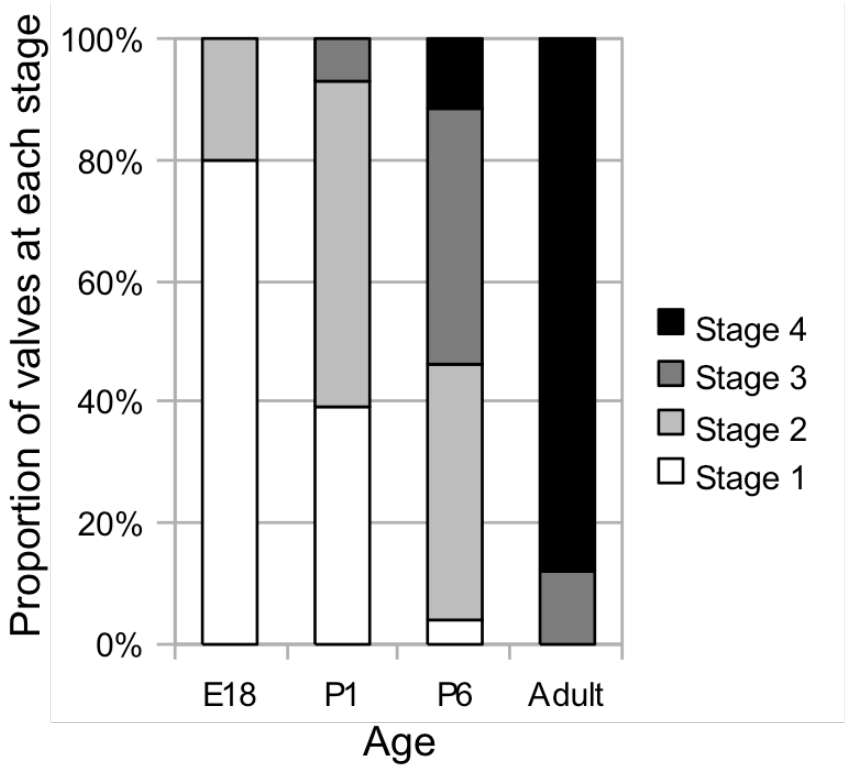

Figure 20 Venous valve developmental stages at selected ages
This graph shows selected ages from staging of Tie2LacZ data, to further illustrate the general trend. The raw data including the number of VV analysed at each age and stage are provided in Table 1.

3.6.2 Immunofluorescence imaging of murine venous valves

Immunolocalisation of Prox1 and Foxc2 at E17 showing widespread heterogeneous signal in femoral vein endothelial cells (Figure 21). Occasional nuclei in the valve region showed higher signal, but no organised valve structures were identified. At P0 rotated and elongated endothelial cells were seen to express higher levels of Prox1 (and other markers including Foxc2) and formed a line of cells in a ring around the vein. This corresponds to the appearances seen at stage 1 of VV development previously described in the Tie2LacZ reporter strain (Figure 17). Elongated nuclei were widely distributed across the vein. The most rotated nuclei were identified in the mid-portion of the vessel. Further imaging at E17, P0 and P2 is given in Figure 68. Detailed analysis of the morphology of $Prox1^{hi}$ valve-forming nuclei (derived from wildtype littermates of Connexin-deleted mice) is given in Appendix 9 (Figure 102, Figure 104, Figure 105).

At P6 stage 3 or stage 4 valves were identified, with well-developed leaflets easily identified by expression of markers such as Foxc2. The free edges of leaflets showed strong signal for Prox1 and Foxc2. Whilst at E17 and P0 SMA-expressing pericytes were seen to uniformly surround the vein in the region of the developing VV, at P6 a reduction of SMA expression was seen in the region of the valve (Figure 21). Quantification of the developmental stages at P0 and P6 is given in subsequent chapters in the analysis of wildtype controls. Additional examples of confocal micrographs at P0 are shown in subsequent chapters in Figure 41, Figure 49, Figure 53 and Figure 56. Further examples at P6 are shown in Figure 25, Figure 33, Figure 42, Figure 51 and Figure 55 (each described in its associated text).

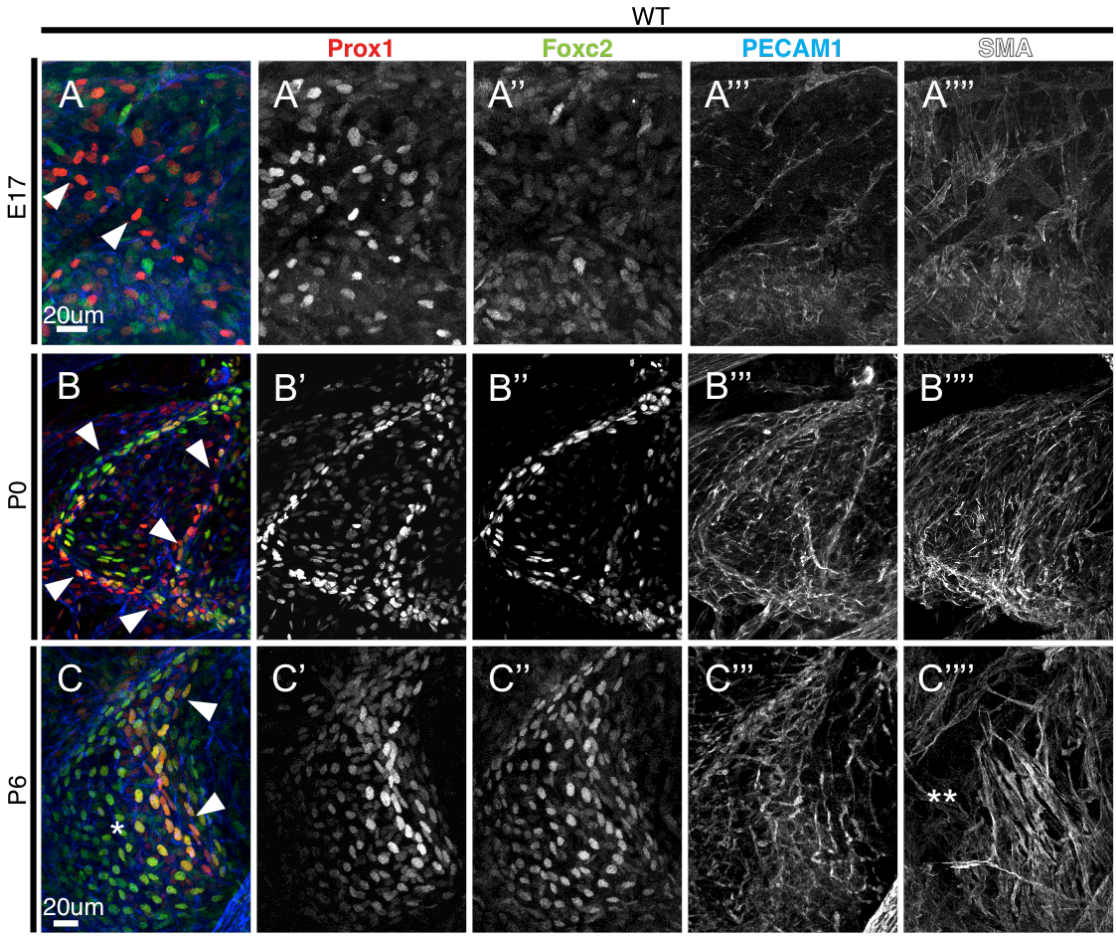

Figure 21 Analysis of developing VV by confocal microscopy
Immunostaining for Prox1, Foxc2 and PECAM1 is overlaid in A-C using the colours indicated above each column. For clarity, localisation of SMA in the same valves (given in A-C'''') is not overlaid. In wildtype mice, immunostaining of Prox1 and Foxc2 was widespread and heterogeneous (arrowheads in A) throughout the valve-forming region of the femoral vein at E17. By P0 rotated and elongated valve-forming Prox1^{hi} and Foxc2hi nuclei are seen (arrowheads in B). Non-VFC Prox1 immunostaining tends to be higher upstream, whilst Foxc2 is higher downstream. At P6 rotated free-edge cells (nuclei identified by arrowheads in C) form the free edges of the leaflets, whilst cells lining the valve leaflets (* in C) have rounded nuclei. Note deficiency in SMA-expressing cells that appears by P6 (** in C''''). Representative confocal micrographs of n≥6 at each age. Flow direction left to right (in landscape format).

3.6.3 TEM imaging of murine VV at P0

In preliminary analysis of femoral veins at P0, developing VV were clearly identified as unique structures protruding into the vein lumen at the previously characterised site of VV formation. Even at this early stage numerous interstitial cells were seen and the microscopic VV structure illustrates the potential complex cellular interactions occurring during development (Figure 22). Taken with SEM and confocal analysis at the same time point, the cells at the edge of this structure (Figure 22) are assumed to be the rotated Prox1^{hi} valve-forming cells that have been described to form a ring at stage 1, and subsequently line the leaflet free edge at all later stages. Endothelial cells lining the primitive leaflet (Figure 22) have a rounded morphology in SEM analysis (Figure 15) and also express Prox1 and other markers (Figure 21 and subsequent chapters). Because of the lack of strongly expressed markers, interstitial cells could not be very clearly identified by confocal microscopy.

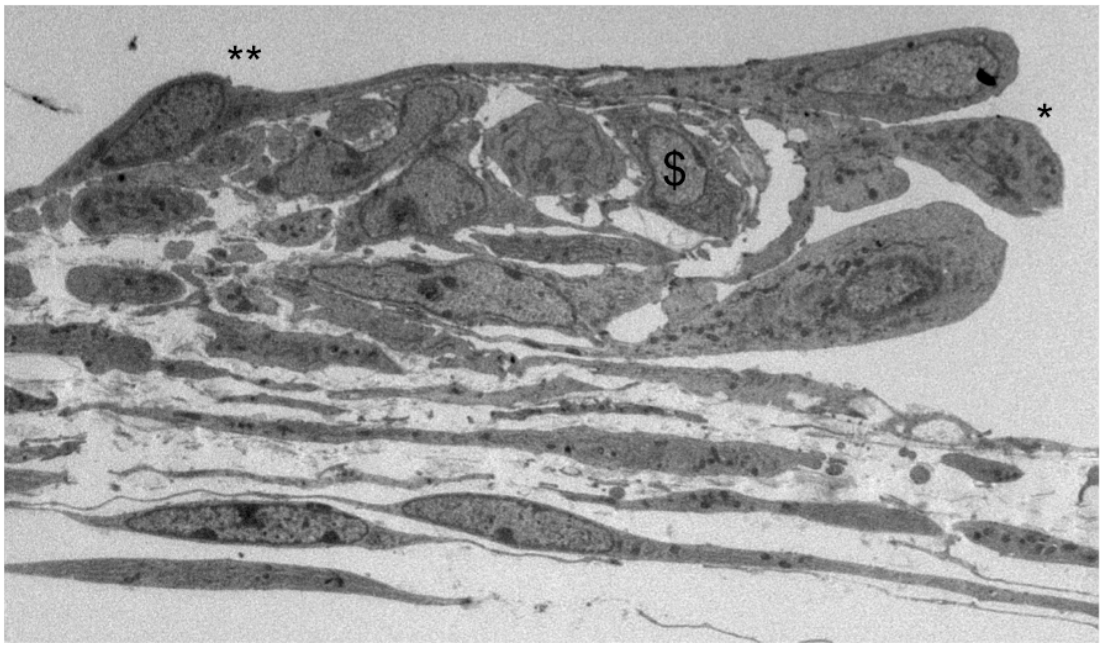

Figure 22 TEM of developing VV at P0
A longitudinal section of the region of the femoral vein containing a developing venous valve leaflet is shown. At P0 numerous interstitial cells were already present in the early venous valve. ** leaflet endothelial cell, $ interstitial cell nucleus, * free-edge (rotated) cell. The relatively loose attachment of the free-edge cell to the underlying matrix and interstitial cells is reminiscent of that described at similar stages in LV development.[146] Representative of N=3 balb/c valves at P0. Scale bar 10μm. Flow direction left to right.

3.7 Discussion

Whilst venous valves have been described in the pig, mouse, rat and duckling and other animals using various imaging techniques, a consistently positioned valve has not been identified in a small animal model.[11, 26,31,33,33] Here I describe the localisation of a venous valve in a consistent location in the proximal femoral vein. Initial experiments with a Tie2LacZ reporter line revealed venous valves distributed throughout the lower limb veins of the mouse. The largest valve, and the only one consistently found at the same position, was in the proximal femoral vein. The finding of the consistent position of this valve has facilitated subsequent studies of early valve development, by enabling targeted analysis even at the earliest time points. The limit of 2 analysed valves per mouse raises the number of animals required in any experiment. Subsequent to this work being carried out, others have used immunohistochemical and resin casting techniques to confirm the presence of valves throughout the lower limb veins in Bl/6 mice aged 10wks and 2yrs.[147] Valves were identified most frequently, albeit in only 68% of mice, in the region of the 'sapheno-femoral junction'. This relatively low frequency likely relates to the sensitivity of the methods used to identify valves, as I identified a valve at this site in near 100% limbs.

Initial analysis of VV in the Tie2LacZ reporter line showed wide variability in valve structures, and frequently different structures on either side of the same mouse, obscuring any developmental series. To the best of my knowledge a unicommissure stage (stage 3) has not previously been described. Subsequent analysis of a large number of valves across a wide age range, according to the acquisition of commissures, showed a clear progression with age. In was not methodologically possible to image valve structure in vivo and these data necessarily derive from single time points, but the developmental sequence proposed is supported by the progressive development at increasing age.

Significant variability was found in analysing valves in the Tie2LacZ line, which could relate to difficulty in assigning stages to valves visualised only with the

reporter line, or to true increased variability, for example as a result of their background (mixed FVB/MF1).

Confocal microscopy of whole (unopened) veins following immunostaining with various markers for both the vessel and valve endothelial cells (Prox1, Foxc2, PECAM1 and SMA), facilitated localisation of valve forming cells at earlier stages than identified using the Tie2LacZ reporter. This also revealed that cellular rotation events occurred at an earlier stage than previously identified[44, 148] and are well developed by P0. It has only very recently been possible to visualise the valve-forming region at the earliest stages (E15-E18) and this remains a methodological obstacle to detailed analysis of events at this early stage.

Prior to P0, Prox1 and Foxc2 expression was widespread and heterogeneous, which is surprising given their previous characterisation as lymphatic and arterial/lymphatic markers, respectively, and the finding that Prox1 is a master regulator for the differentiation of LECs from veins[44, 149] In lymphatic valves, Prox1 and Foxc2 are more highly expressed on one side of the vessel, prior to 'circularisation' and extension of this cellular phenotype around the vessel to form a complete ring, or 'domain'.[42,148] These stages were not identified in the developing normal venous valve, where the ring of rotated cells seen at P0 appeared to arise from heterogeneous $Prox1^{hi}$ and $Foxc2^{hi}$ cells scattered throughout the valve forming region. It is possible that a highly transient stage of development was not identified, or that development proceeds via different early stages in the venous and lymphatic systems. Future work should aim to examine the polarity of VFCs (indicating any directional migration to form the early valve ring) by immunolocalisation of polarised organelles.[145]

A technique for TEM analysis of developing VV at P0 has only very recently been developed, and preliminary TEM data at P0 showed very early leaflet formation, consistent with rotated cells at the free-edge. Free-edge cells were seen to be loosely attached to underlying cells, with a similar appearance to that recently described at a similar stage in LV development,[146] suggesting that a similar process involving planar cell polarity proteins may have a role in

VV development. This supports the idea that leaflet development occurs at the site of these rotated cells, which appear to be already forming the free edges of the leaflet. Immunostaining of the initiation of VV matrix deposition was hindered by the lack of a commercially available laminin-α5 antibody with which to clearly label the developing leaflet matrix.

Whilst human VV interstitial cells are identifiable by immunostaining with antibodies raised against smooth muscle alpha actin (SMA), similar SMA immunostaining was not identified in mice VV leaflets. Analysis by TEM, however, confirmed the presence of interstitial cells within murine VV leaflets as early as P0. This is consistent with the description of interstitial cells in other animals, although their appearance during development has not previously been described.[11] The identity and roles of these cells remain unknown but their presence at such an early stage suggests the possibility of a functional role. For example, these cells may produce the matrix that forms the core of the leaflet. No strongly-expressed markers for these cells have been identified. In future work, identification of a specific marker could allow conditional deletion in these cells and analysis of their potential role in VV development and/or maintenance.

The conformational changes accompanying development of the valve commissures have yet to be clearly described. It has been cautiously assumed that the valve commissures develop at the sites of apparent commissures seen in the ring of rotated cells at P0, but direct evidence for this is lacking. In particular, it is notable that whilst the potential positions of two commissures might be indicated by the positions of cells at stage 0, at stage 2 there may be little indication of where subsequent commissures will develop. Similarly at stage 3 there is little indication of where the second commissure will develop. This process requires the appearance of relatively proximal cells to form the second commissure, and also a ‘split’ in the rounded shelf of the stage 3 valve Mechanisms regulating these processes remain to be explored.

Similar to lymphatic valves, a reduction in SMA-positive pericytes was seen around the mature venous valve at P6. In the lymphatic system, this ‘gap’

forms part of the phenotype of the collecting vessels, and abnormal recruitment of pericytes to this region is a key part of the phenotype of Foxc2$^{-/-}$ mice, which model the human disease lymphoedema distichiasis.[40] Contrary to events in the lymphatic system, in the veins this gap appears later in development, and was not seen at earlier stages.

It is not clear what stimulates the cell-rotation events at P0. Remarkably, cells exposed to gradients of wall shear stress in vitro rotate perpendicular to the direction of flow.[150] This raises the possibility that blood flow could be a stimulus to these events. Intra-vital microscopy of murine lymphatics has shown that fluid flow is 'oscillatory', or 'reversing' prior to the onset of valve formation.[42] A similar requirement for oscillatory blood flow has been suggested in developing zebrafish cardiac valves.[131,133] Altered flow through the chick heart has similarly been demonstrated to produce outflow tract malformations.[132] Fluid flow through the venous valve-forming region prior to valve development has yet to be directly observed or modelled. It remains unclear what effect a tributary downstream of the site of endothelial cell rotation may have. The effect of flow on leaflet development is studied and discussed in a chapter 10.

In these experiments the Tie2^{LacZ} reporter line was used to identify the vessel endothelium, but it appears likely that signalling through Tie2 plays a role in valve formation, as Tie2 reporter activity appeared to differ on either side of the forming valve region in a similar way to Prox1 expression. Foxc2 has been shown to upregulate Ang2, a ligand for Tie2, and the Ang-2 knockout mouse fails to develop lymphatic valves.[39,151]

3.7.1 Limitations of the study

- The vein that forms the external iliac has been called the femoral or saphenous vein; in this work the term femoral vein has been preferred throughout.
- It has been assumed that Prox1hi cells identified at E17/18 are the rotated and elongated Prox1hi cells identified at P0, and that these cells subsequently form the free-edges of the leaflets. The latter is reasonable given the particular morphology of these cells, which distinguishes them from the surrounding endothelium, and the TEM findings at P0.
- At earlier stages it becomes increasingly challenging to differentiate presumptive valve-forming cells from surrounding endothelium.
- The limit of 2 valves per mouse raises the number of animals needed in any experiment. This, together with the requirement for 3 periods of tissue dissection in order to process samples for wholemount imaging, increases the risk of loss of data through damage and limits the amount of data that can be obtained from a single animal, which makes sample variability more difficult to assess than in analysis of LV development.
- The use of other modalities, such as micro-computed tomography (CT) and high frequency ultrasound was explored (data not shown) without success in imaging murine VV, although the femoral vein was readily identifiable in adult mice. Further antibody-labelling techniques with tracers could enable this to become a viable modality in future.

4 THE ROLE OF INTEGRINA9 IN VV DEVELOPMENT

4.1 Introduction

Integrinα9 is expressed in LV, and is required for normal LV development.[43] Loss of integrinα9 results in a failure to remodel fibronectin-EIIIA and to develop the LV matrix core.[43] We recently localised integrinα9 on murine venous valves and showed that conditional deletion of Itga9 after birth resulted in a failure to develop normal valve leaflets, whilst deletion in adult mice resulted in a failure to maintain VV.[44] These samples were analysed by luminal SEM (as described in the General Methods chapter). Because this requires the vein to be opened, it was not possible to comment on the intact valve structure, or quantitatively assess defects in VV formation following Itga9 deletion.[44]

4.2 Aims

1. To replicate our finding of expression of integrinα9 on VVs using an improved imaging technique.
2. To replicate the finding that integrinα9 is required for leaflet development using an improved method of analysis, and quantify the resulting phenotype.
3. To localise integinα9 in adult human VV leaflets by immunohistochemistry.

4.3 Design and Methods

4.3.1.1 Localisation of integrinα9 in VV

Immunolocalisation and confocal microscopy of wholemount unopened veins was carried out as described in Chapter 3.

4.3.1.2 Itga9^{lx};Prox1CreERT2 mice

A conditional loss of function approach was used to investigate the role of integrinα9, using a previously described transgenic line incorporating loxP sites around exon 8 of the Itga9 gene.[152] Itga9lx;Prox1CreERT2 mice were maintained in a colony at CRUK on a bl/6 background.[152,43,44]

4.3.1.3 mTmG reporter mice

The spatial and temporal activity of the Prox1CreERT2 line in femoral vein endothelial (valve-forming) cells was assessed using a previously described transgenic double-fluorescent Cre reporter line, termed mTmG.[153] In this line alleles for the fluorescent proteins tdTomato and eGFP are placed under the control of a strong promoter at the ubiquitously expressed Rosa26 locus, and are separated by a stop sequence such that under normal conditions only tdTomato is expressed. The tdTomato allele and stop sequence are flanked by loxP sites, such that after Cre mediated excision of LoxP flanked segments, the tdTomato allele and stop site are excised and GFP expression results. Ongoing GFP production therefore permanently identifies those cells (and their progeny) in which the Prox1 promoter was active at the time of injection of 4OHT. Both GFP and tdTomato are tagged with membrane localisation sequences, which allows analysis of cellular morphology.[153] Itga9lx;Prox1CreERT2 mice were crossed with the Rosa26mTmG reporter line to provide localisation of Cre recombinase activity and endothelial cells.[153]

4.3.2 Conditional deletion of Itga9

Crosses were made to obtain double transgenic offspring either homozygous of heterozygous for a floxed Itga9 allele, and carrying either 1 or no copies of Prox1CreERT2. Prox1CreERT2^{-} offspring were analysed as effective wildtype. To enable improved visualisation of the vasculature and confirm Prox1CreERT2 in the femoral vein, some crosses were performed on a Rosa26mTmG background. For analysis at P6, pups were injected at P0. 22 effective wildtype mice, 8 mice with heterozygous deletion, and 7 mice with homozygous deletion were analysed (up to 2 valves each). Numbers of VV visualised in each group are provided in the results table.

4.3.3 Genotyping and immunofluorescence

Genotyping and immunofluorescence imaging of murine VVs were carried out as described in the General Methods chapter. Solutions are given in Appendix 1, antibody concentrations/dilutions in Appendix 3 and primers in Appendix 4.

4.3.4 Localisation of integrinα9 in adult human VV

Sections of long saphenous vein were obtained from patients undergoing coronary artery bypass grafting (Section 2.6) and integrinα9 was immunolocalised using tyramide-based signal amplification as described in the General Methods chapter with antibody concentrations given in Appendix 3).

4.3.5 Statistical analysis

For comparison of stage of valve development Fisher's exact test was used, comparing wildtype with either heterozygous or homozygous knockouts for each stage. Data from multiple litters were necessarily pooled. All analyses were carried out in SPSS 21 (IBM corporation).

4.4 Results

4.4.1 Expression of integrinα9 in murine & human VV

Confocal microscopy of immunolabelled murine venous valves confirmed expression of integrinα9 in murine VV leaflets (Figure 23). Subsequent tyramide-amplified immunohistochemistry localised integrinα9 to normal adult human venous valves. Integrinα9 was localised in a membranous pattern and expression was widespread in the valve. Integrinα9 was localised to the fluid-facing as well as matrix-facing membranes of EC's, and in interstitial cells (Figure 24).

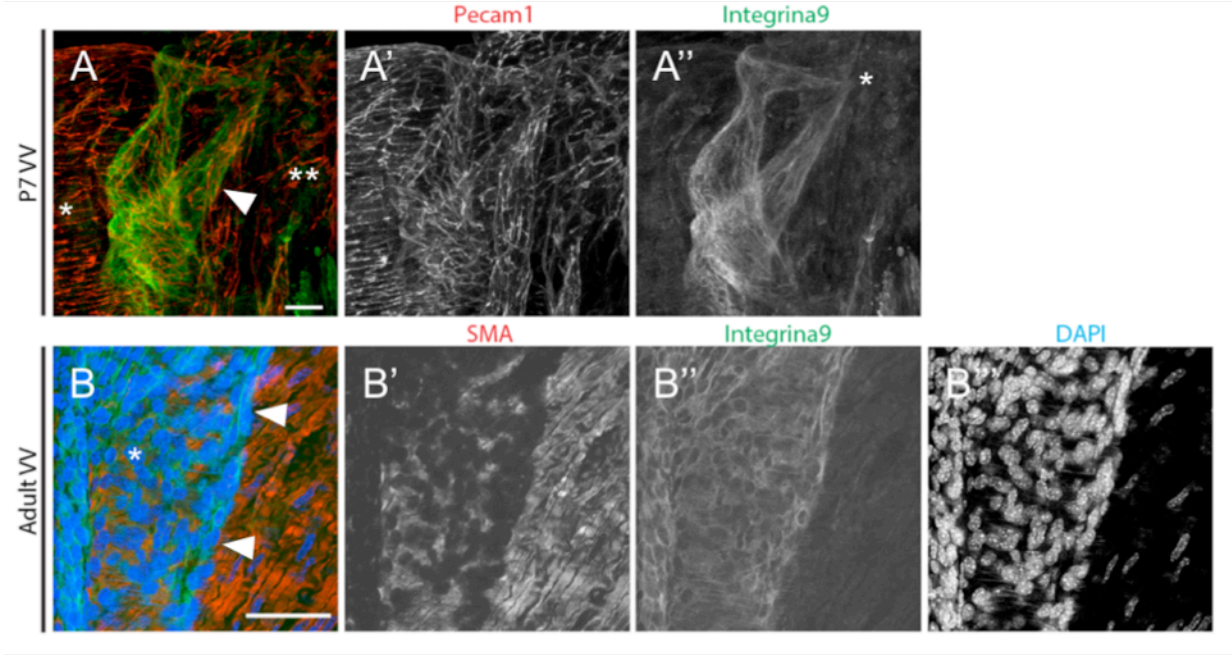

Figure 23 Immunolocalisation of integrinα9 on murine venous valves

A-A'') Immunolocalisation of Pecam1 and Integrinα9 at P6-7 (n>6). Upstream cells (* in A) have an elongated morphology, as outlined by membranous Pecam1. Cells downstream of the valve (** in A) are rounded and more disorganised. A commissure is marked with a * in A''

B-B'') Immunolocalisation of SMA and integrinα9 in a small region of the edge of an adult valve in an opened femoral vein, with nuclei identified by DAPI. The valve leaflet (* in B) does not express SMA, which is localised to pericytes (B'). Free edge cells/nuclei are identified by arrowheads in B. (n=1). Scale bars 50μm. 2D projections of confocal z-stacks. Flow direction from left to right.

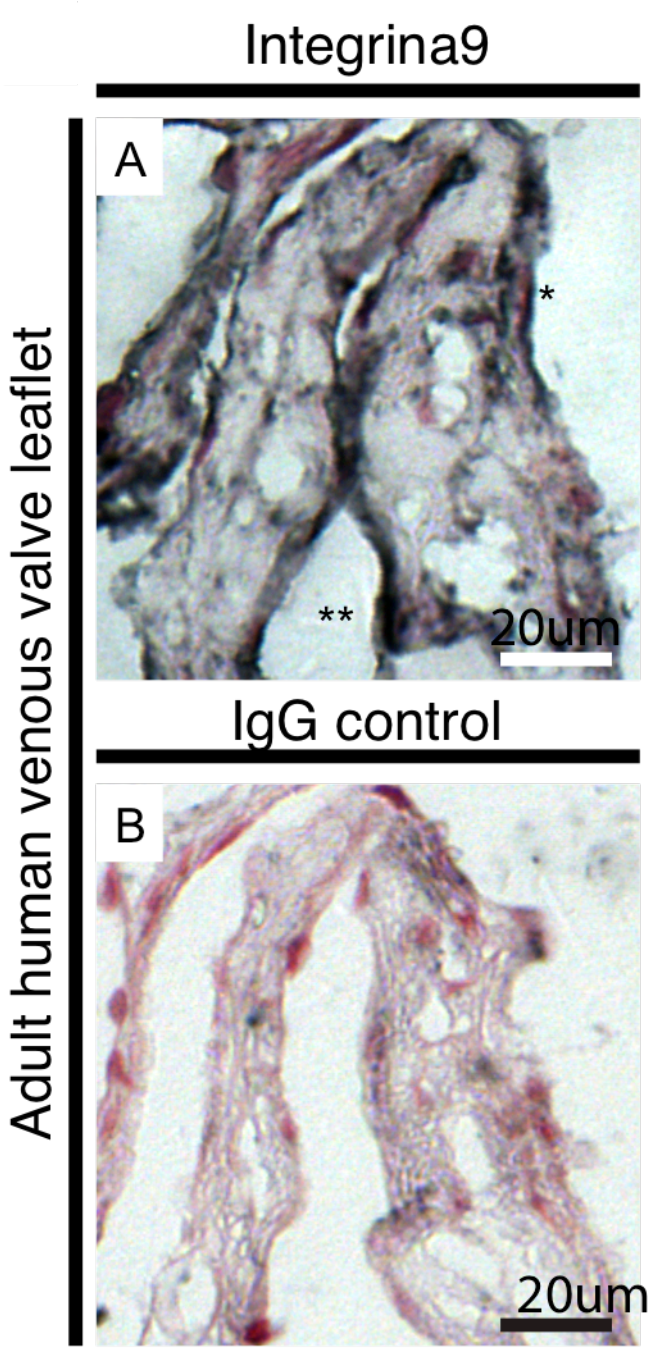

Figure 24 Localisation of integrinα9 in adult human venous valve
A) Immunolocalisation of integinα9 in transverse sections of adult human long saphenous vein VV. Positive signal (* and **) is shown in black, counterstained with nuclear fast red. * identifies the leaflet lumen surface, ** marks the sinus surface.

B) Non-immune IgG negative control.

The opposing leaflet is shown to the top left of A and B.

4.4.2 Conditional loss of function of integrinα9 from P0

Whilst control valves developed normally, conditional homozygous deletion of Itga9 from P0 resulted in a severe phenotype with failure to develop valve leaflets, with a significant increase in the proportion of valves at Stage 1 (P<0.0005) and reductions in those reaching stages 3 (P<0.0005) and 4 (P=0.026). No valves were seen at stages 2-4 (Figure 25). Prox1^{hi} rotated endothelial cells remained identifiable at P6 (Figure 26B). Heterozygous deletion did not produce a statistically significant phenotype. Widespread expression of GFP at P6 in Rosa26mTmG;Prox1CreERT2+ mice (Figure 26B) confirmed previously demonstrated utility of Prox1CreERT2 in producing Cre recombinase activity in these cells at this time point.

A

	Effective wildtype	Heterozygous deletion		Homozygous deletion	
	n	n	P	n	P
Stage 0	0	0	-	1	ns
Stage 1	0	2	0.057	12	**<0.0005**
Stage 2	5	3	ns	0	ns
Stage 3	23	7	ns	0	**<0.0005**
Stage 4	12	1	ns	0	**0.026**
Total	40	13		13	

B

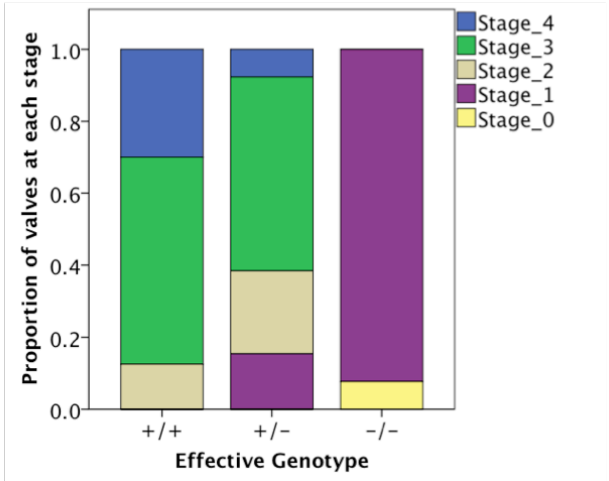

Figure 25 Valve development at P6 following conditional deletion of integrinα9 from P0

A) The table provides the total number of VV analysed for each genotype and the number of VV identified at each stage. P= Fisher's exact test. ns=P>0.05 (Fisher's exact test); n=number of VV analysed.

B) The proportion of valves at each stage is shown for each genotype. Deletion of

integrinα9 from P0 produced a severe phenotype with almost complete failure to develop valve leaflets at P6. Heterozygous deletion did not produce a significant phenotype. +/+ = wildtype (N=22 mice), +/- = heterozygous deletion (N=8), -/- = homozygous deletion (N=7).

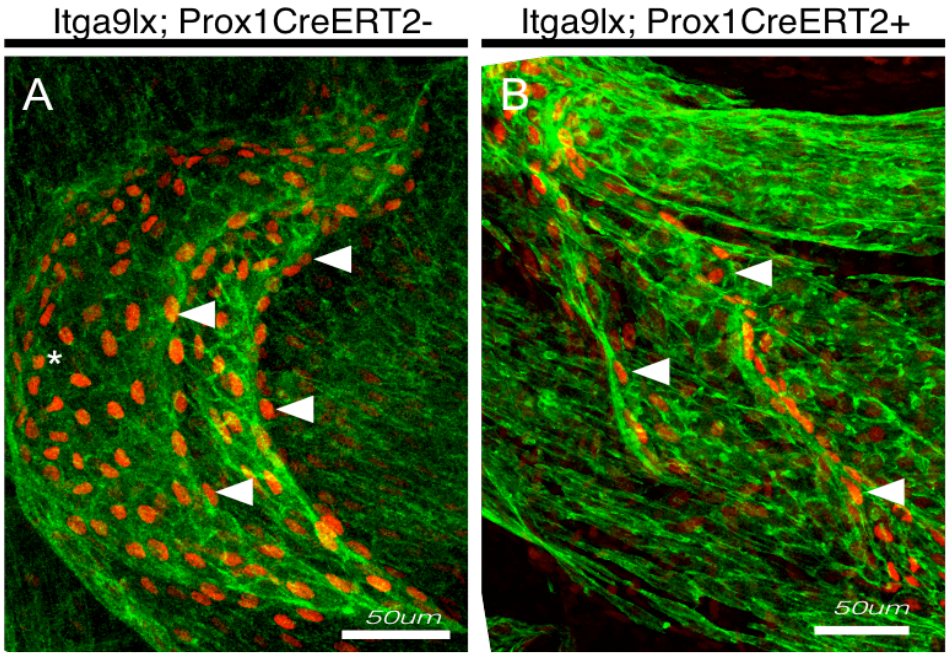

Figure 26 Valve morphology at P6 following conditional deletion of integrinα9 from P0

In control littermates valves developed normally (A) whilst homozygous conditional Itga9 deletion (B) produced a failure of leaflet formation. Free edge cells (arrowheads) are marked in A and B, but leaflets (*) are seen only in A. The ring of rotated Prox1^{hi} endothelial cells was relatively intact (arrowheads in B). Blood flow is from left to right. For clarity membrane-targeted tdTomato (in A) and eGFP (in B) are both displayed as green. Scale 50μm

4.5 Discussion

Expression of integrinα9 and its role in venous valve development was investigated using immunofluorescence/confocal imaging techniques and a conditional loss of function approach. These revealed a critical requirement for integrinα9 in the development of the valve leaflets. Integrinα9 did not appear to be required for the maintenance of the Prox1^{hi} free-edge cell phenotype, as these cells tended to remain identifiable (albeit not as a complete ring) at P6. It is likely that integrinα9 is required for the interaction between valve leaflet EC's and the matrix core of the VV, as has been suggested in LV.[43] The finding that integrinα9 is critical to the development of both VV and LV provides clear evidence that venous and lymphatic valves may be regulated by similar mechanisms.

Expression on human VV, combined with the requirement for integrinα9 in murine VV maintenance, suggests a potential role for this protein in human disease. One known ligand for integrinα9, tenascinC, has been implicated in the pathology of varicose veins and it is possible that disrupted signalling through integrinα9 could form part of the disease process in man.[154]

4.5.1 Limitations of the study

A potential role for integrinα9 prior to P0 has not been examined. At the time this study was carried out the techniques for preparation of immunostained venous valves at E16-P0 (and loss of function from E15) used elsewhere in this thesis had not been developed. It would be interesting to examine the expression pattern of integrinα9 and its ligands during these very early stages in development. It is possible that integrinα9 could have a role during these earlier stages of valve development, but the persistence of free edge cells at P6 after deletion from P0 suggests that integrinα9 does not have a role in earlier patterning events for these cells.

5 THE ROLE OF EPHRINB2 IN VV DEVELOPMENT

5.1 Introduction

EphrinB2 reverse signalling is required for normal cardiac and lymphatic valve development.[71, 138] In addition, we recently described a requirement for ephrinB2 signalling in VV development and subsequent maintenance, a surprising finding given previous reports that ephrinB2 expression is restricted to arteries and lymphatics (Appendix 13).[44, 138] Previously, ephrinB2 promoter activity, indicating likely expression, was examined using the EfnB2GFP reporter line, using confocal microscopy of opened murine veins, and expression was described in scattered endothelial cells between P0 and P2.[34]

5.2 Aims

1. Explore the activity of the EfnB2 promoter at P0.
2. Quantify the phenotype resulting from conditional loss of ephrinB2.

5.3 Design and Methods

5.3.1 EfnB2GFP

EphrinB2 promoter activity was visualised at P0 using a previously described GFP reporter line in which the start codon of EfnB2 was replaced with H2BGFP cDNA (generating a null allele and nucleus-targeted GFP).[155] Six valves in 3 EfnB2GFP mice were visualised at P0. The EfnB2GFP colony was maintained in house on a bl/6 background.

5.3.2 EfnB2^{lx} mice

To investigate the role of ephrinB2 prior to P6, a conditional loss of function approach was selected, using a previously described transgenic line incorporating LoxP sites inserted around exon 2 of EfnB2 by homologous recombination.[156] The Efnb2^{lx} colony was maintained in house, on a bl/6 background.[44] Crosses were made to obtain double transgenic offspring either

homozygous of heterozygous for a floxed EfnB2 allele, and either heterozygous or wildtype for Prox1CreERT2. Prox1CreERT2^{-} offspring were analysed as effective wildtype. To enable improved visualisation of the vasculature and confirm Prox1CreERT2 in the femoral vein, some crosses were performed on a Rosa26mTmG background as described in the previous chapter.[153] For analysis at P6, pups were injected at P0. 3 effective wildtype, 3 mice with heterozygous deletion and 2 mice with homozygous deletion were analysed. 2 valves were visualised in each animal.

5.3.3 Genotyping and immunofluorescence

Immunofluorescence confocal microscopy of murine VVs and genotyping were carried out as described in the general methods and Chapter 3. Solutions are given in Appendix 1, antibodies in Appendix 3 and primers in Appendix 4.

5.3.4 Statistical analysis

All analyses were carried out in SPSS 21 (IBM corporation). For comparison of stage of valve development Fisher's exact test was used, comparing wildtype with either heterozygous or homozygous knockouts for each stage. Data from multiple litters were pooled.

5.4 Results

5.4.1 EfnB2GFP reporter localisation at P0

Using an improved method of immunostaining, with the vein remaining unopened, ephrinB2 reporter activity was detected earlier than we previously reported (Figure 27). At P0 reporter activity was clearly identified in some Prox1^{hi} valve forming cells (Figure 27), and downstream of the developing valve. Reporter signal was much lower in veins than in neighbouring arteries.

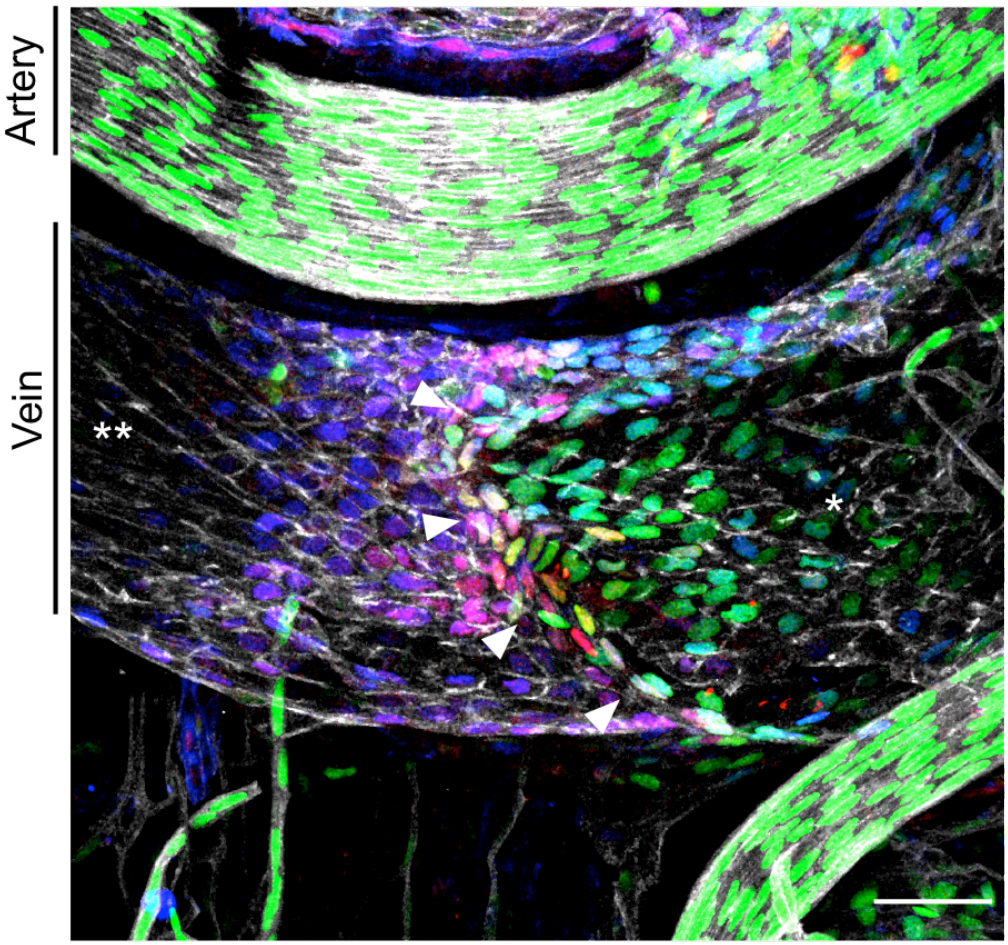

Figure 27 EfnB2GFP reporter activity and immunolocalisation at P0
EfnB2 promoter activity at P0 was examined using the EfnB2GFP reporter (green) with immunolocalisation of Prox1 (red) NFATc1 (blue) and Pecam1 (white). GFP is targeted to the nucleus. These mice express one copy of wildtype ephrinB2; no clear phenotype was seen following heterozygous conditional deletion of EfnB2 at P6, indicating that heterozygous deletion at P0 is not expected to produce a phenotype. GFP signal was clearly localized to rotated valve-forming cells (arrowheads) and in the downstream region (*), but signal was very weak/absent in upstream cells (**). Analysis of ephrinB2 expression is hampered by a lack of specific antibodies for use in wholemount imaging. Further examples are given in Appendix 5. Split channels for this figure are given in Figure 28. Representative confocal micrographs of n=6 valves (3 mice) at P0. Flow left to right. Scale 50μm

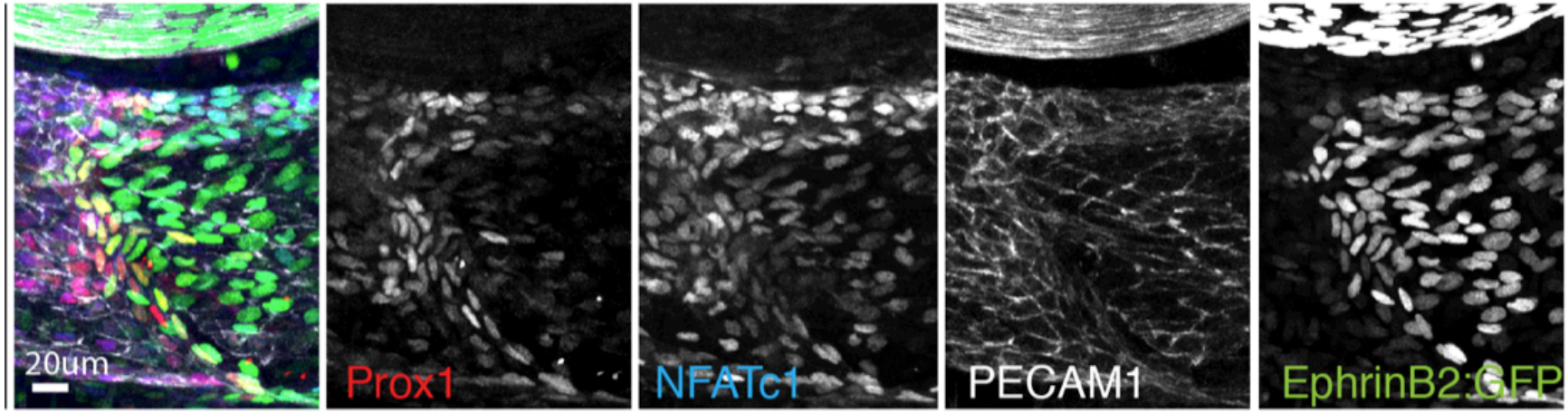

Figure 28 EfnB2GFP reporter activity: separated signals
This panel of micrographs is a reproduction of Figure 27 with the individual channels separated to highlight the overlapping expression domains of Prox1, NFATc1 and ephrinB2. Scale 20μm

5.4.2 Conditional deletion of EfnB2 from P0

Whilst control valves developed normally, homozygous EfnB2 deletion from P0 resulted in a severe phenotype with near complete loss of valve leaflets at P6 (Figure 29). No valves reached stages 1-4. Some rotated Prox1^{hi} cells remained at P6 (Figure 30). Heterozygous deletion did not produce a statistically significant phenotype.

A

	Effective wildtype	Heterozygous deletion		Homozygous deletion	
	n	n	P	n	P
Stage 0	0	0	-	4	**0.005**
Stage 1	0	0	-	0	-
Stage 2	0	1	1	0	-
Stage 3	6	4	.455	0	**0.005**
Stage 4	0	1	1	0	-
Total analysed	6	6		4	

B

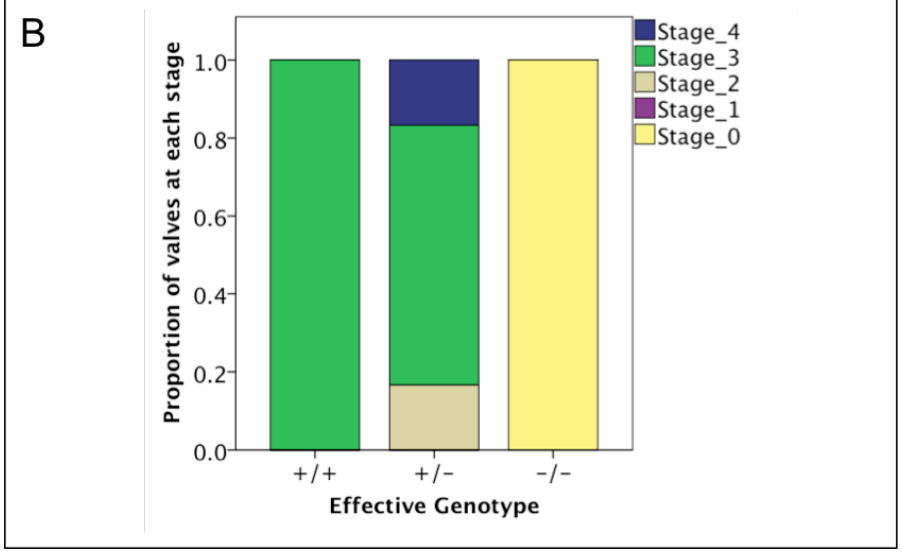

Figure 29 Valve development at P6 following conditional deletion of ephrinB2 from P0

A) The table provides the total number of VV analysed for each genotype and the number of VV identified at each stage. Homozygous deletion of ephrinB2 resulted in a severe phenotype, with no leaflet development in these mice. ns=P>0.05 (Fisher's exact test) ; n=number of valves.

B) The proportion of valves at each stage is shown for each genotype. Deletion of EfnB2 from P0 produced a severe phenotype with complete failure to develop valve leaflets at P6. Heterozygous deletion did not produce a significant phenotype. +/+ = wildtype (N=3 mice), +/- = heterozygous deletion (N=3 mice), -/- = homozygous deletion (N=2 mice).

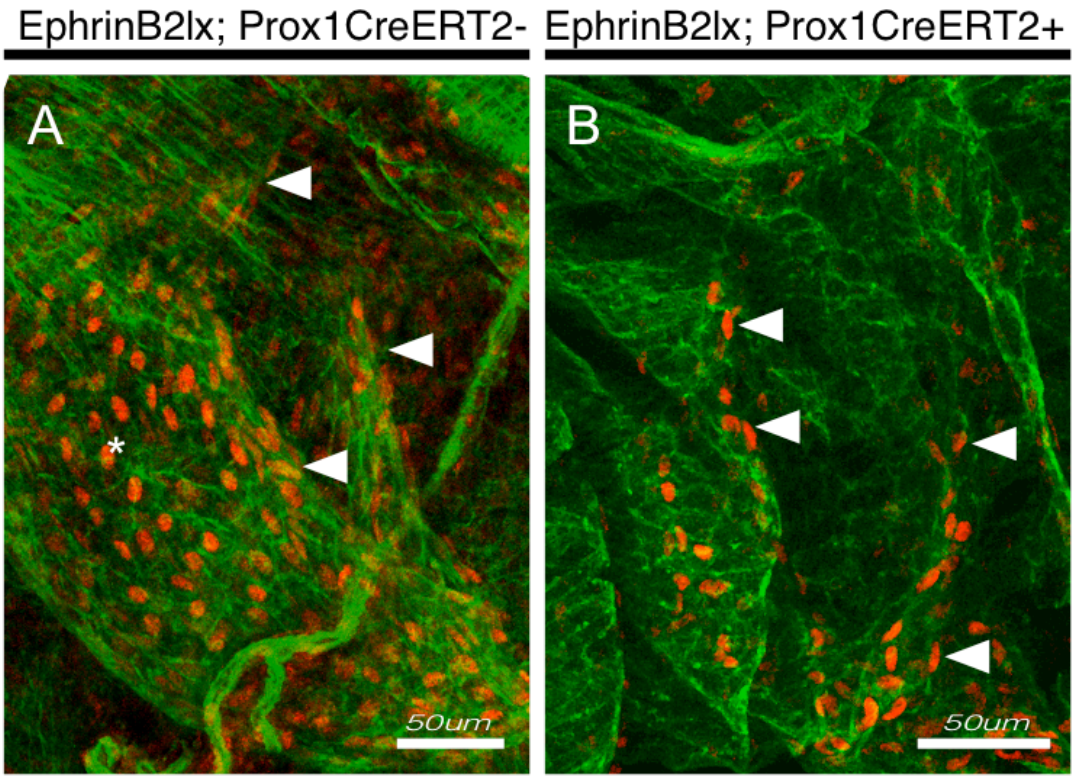

Figure 30 Valve morphology at P6 after conditional deletion of EfnB2 from P0

(A) Valves in wildtype littermates appeared to develop normally.

(B) Homozygous conditional deletion of ephrinB2 resulted in complete loss of leaflets with a few remaining Prox1^{hi} valve cells.

Red = Prox1 immunostain, Green = membrane-targeted tdTomato or eGFP respectively for CreERT2- and CreERT2+ valves. (mTmG reporter line).

Representative of n= 6 wildtype littermates and 4 homozygous knockout VV.
Arrowheads = examples of Prox1^{hi} cells. Scale 50μm

5.5 Discussion

This work aimed to determine the pattern of ephrinB2 reporter activity at P0, and quantify using an improved visualisation method the phenotype seen with conditional deletion of ephrinB2. Homozygous conditional EfnB2 deletion from P0 and analysis at P6 resulted in a severe phenotype with almost complete regression of valve development, albeit with some remaining Prox1^{hi} EC's. This is consistent with work carried out on the open vein that showed a requirement for ephrinB2 in VV development at P6, and subsequent maintenance of the formed valves.[44] Contrary to data (obtained by opening the vein), with the whole mount method revealed that some rotated Prox1^{hi} cells remained at P6, indicating that ephrinB2 is not required for maintenance of the free-edge cell phenotype.[44] This is consistent with the finding that EfnB2GFP reporter activity was not identified in free edge cells at P6, and raises the possibility that these free-edge cells express an ephrinB2 receptor (such as EphB4) at this time point.[44] EphB4 has a widespread expression in murine cutaneous veins at P1,[73] but expression in the large central veins has not been reported.[73] EfnB2lx;Prox1CreERT2^{-} are expected to produce normal amounts of ephrinB2, but valves did not quite reach the expected normal range of developmental stages at P6, since in most groups analysed at P6 approximately half have reached stage 4, and half stage 3. This may be because of the low number of samples available for analysis, but it is also possible that the floxed Efnb2 allele is hypofunctional. The latter concern is probably excluded by the lack of a significantly worse valve phenotype following heterozygous deletion, and it is therefore more likely that an unusual random variation affected this sample.

Confocal microscopy on whole mount veins, revealed EfnB2GFP reporter activity at earlier ages and developmental stages than identified by the open vein technique.[44] Previously, studies using opened vessels showed scattered EfnB2GFP reporter activity at P2 amongst apparently disorganised Prox1^{hi} cells, whilst at P0 almost no GFP expression was seen[44], which is inconsistent with the valve developmental stages presented in the previous chapters, or the localisation of EfnB2GFP in the whole mount studies with the vein remaining intact. My whole mount analysis showing elongated and rotated valve-forming

cells at P0 is consistent with immunostainings for VFC's presented in earlier chapters. These findings illustrate the benefit of confocal imaging with the vein intact (both in allowing more complete imaging of the valve, and also facilitating location of the valve site).

The EfnB2GFP reporter allows visualisation of promoter activity; these results should be interpreted with some degree of caution given the inability to confirm protein expression, and the haploinsufficiency of the reporter. Importantly, the expression of Prox1 and NFATc1 appeared relatively normal in the reporter line. Organisation of VFC's did not appear entirely normal in all reporter valves analysed. It was not possible to quantify this EfnB2 constitutive heterozygous knockout phenotype in the low number of samples available for analysis; although the striking pattern of EfnB2GFP activity at P0 strongly suggests ephrinB2-based cell sorting could be involved in patterning the early VFC's. In endothelial cells the cognate receptor for ephrinB2 is EphB4[70] and so it is therefore likely that EphB4 is expressed in the VV forming region and has a role in early VV formation.

Whilst $EfnB2^{GFP}$ reporter activity has been identified in some $Prox1^{hi}$ cells at P0, is absent from $Prox1^{hi}$ free-edge cells at P6, suggesting that it is differentially regulated at the two time points.[44] It is possible that signalling through ephrinB2 is involved in the selection of free-edge cells at P0, and in maintenance of their phenotype. In experiments involving ectopic expression of full length and truncated Eph's and ephrins in excised zenopus caps, bidirectional signalling was required for cell-cell repulsion and the maintenance of a tissue boundary; repulsion of each cell type was required to prevent invasion into the territory of the other.[157] It remains to be seen whether uni- or bi-directional signalling is required to establish the ephrinB2 expression pattern observed at P0 in VV development. In the same xenopus ex-vivo experimental system, unidirectional signalling was sufficient for suppression of gap junction communication between tissue compartments.[157] It is therefore possible that one role of ephrinB2 expression seen in early VV development is to prevent gap junction inter-cellular communication between the upstream region and valve forming cells. The roles of gap junction proteins in VV

development is discussed further in Chapter 8. Further work could examine gap-junctional communication between compartments.

It remains to be determined whether an Eph-ephrin interaction is required for normal organisation up to P0 and it is unclear how the marked boundary in ephrinB2 reporter activity at P0 arises. Limited availability of the ephrinB2^{GFP} line, prevented examination of the activity of the ephrinB2 promoter at earlier stages. Further work at these stages could elucidate the pattern by which this clear boundary in ephrinB2 expression arises. It is possible that ephrinB2 is upregulated in endothelial cells in a heterogeneous pattern, and that subsequent ephrin-dependent cell sorting and migration results in the organised ring of valve-forming endothelial cells identified at P0 (and clearly associated ephrinB2 expression boundary now identified at P1). Reporter activity was also identified downstream of the valve-forming cells, consistent with the previous report of expression in this region at P6.[43] One possibility is that ephrinB2 is upregulated in this region by Foxc2 and NFATc1, both of which are expressed in valve forming cells, and in the region downstream of the rotated cells at P0.[39]

A phenotype in Prox1^{hi} valve-forming cells at P0, which exhibit ephrinB2 reporter activity (and assumed Eph expression on upstream cells), would suggest that reverse signalling is likely to occur into these cells. This would be consistent with the known requirement for reverse signalling in cardiac and lymphatic valve formation.[73] It is reasonable to speculate that reverse signalling (and likely through the PDZ motif) is required for VV development. This could be investigated further using ephrinB2$^{\Delta V/\Delta V}$ mice. In this discussion it has been assumed that these ephrinB signalling events are confined to the endothelium. It is possible that signalling with pericytes and/or interstitial cells is involved.[158]

EphrinB protein interactions have been implicated in other critical signalling pathways at the cell membrane, involving numerous membrane proteins including the VEGF receptors, integrins, and connexins. Notably, ephrinB2 and its PDZ domain are required in-vivo for normal sprouting angiogenesis,

and in this context ephrins are required for endocytosis and full signalling through both VEGFR2 and VEGFR3.[72] In the absence of ephrinB2, VEGFR2/3 were not endocytosed even in the presence of VEGFA, resulting in reduced downstream signalling into the cell.[72,119] It is possible that ephrinB2 functions to regulate VEGFR2 and/or VEGFR3 in venous valve development in a similar manner.[119]

EphrinB's have not been directly implicated in human venous reflux, but insufficiency of the receptor, EphB4, has recently been implicated in human capillary malformation-arteriovenous malformation (CA-AVM) in a pathway with ephrinB2 and RASA1 (in a zebrafish model).[159] It is striking to note the finding of ephrinB2 reporter activity in veins as well as arteries (the present study and[44] as it has been suggested that defective ephrinB2-EphB4 signalling may account for the recurrence of CA-AVM in adults following treatment. It has been suggested that rapamycin (used to inhibit mTOR) in this pathway, may avoid recurrence of CA-AVM in man. Previous data suggest a requirement for ephrinB2 in VV maintenance, suggesting that one side effect of this therapy could be VV failure.[44, 159,160] It is likely that Eph-ephrin signalling plays different roles in the vasculature at different time points during development and in adult life. Signalling through these proteins is required for normal arteriovenous separation in vasculogenesis, but expression of ephrinB2 in veins at the site of VV formation would suggest a different role in more mature vessels. This is not consistent with an ongoing requirement for Eph-ephrin signalling to avoid CM-AVM. A likely explanation is differential regulation in new sprouting vessels in adults. Alternatively an effect of the different levels of ephrinB2 promoter activity (expression) seen in murine arteries and veins, and regulation at a different step in the pathway may be involved. EphrinB2 has previously been thought to be a specific and critical marker for arterial or lymphatic endothelial cells, and the finding of its expression in venous endothelial cells and valves is surprising.[73] Reported activity was found at much lower levels in the femoral vein than femoral artery and it was therefore difficult to visualise both together as a result of saturation of the arterial signal.

The expression and critical requirements for ephrinB2 in cardiac valve and lymphatic valve development[71, 138], together with the finding that ephrinB2 is required for venous valve development, reinforces the concept that similar pathways are required for cardiac, lymphatic and venous valve development.

5.5.1 Limitations of the study

- All tested commercially available ephrinB2 antibodies are not specific for ephrinB2, as demonstrated by continued binding in ephrinB2 knockout mice (Dr Taija Makinen, personal communication 2013). It has therefore not been possible to confirm whether ephrinB2 promoter activity results in protein expression in the valve-forming cells and downstream regions. The finding of a clear phenotype at P6 following ephrinB2 deletion is strongly suggestive of ephrinB2 expression at this time.
- It was not possible to quantify the phenotype in the EfnB2GFP (heterozygous for wildtype EfnB2) reporter at P0, because of the mild phenotype seen and low number of samples available for study.
- Similarly, limited availability of the floxed EfnB2 line did not allow investigation of its role prior to P0 by conditional deletion.

6 ROLE OF FOXC2 IN VV DEVELOPMENT

6.1 Introduction

The nuclear transcription factor Foxc2 has been strongly implicated in cardiac and lymphatic valve development.[39, 40, 47, 80, 82, 161]. In lymphatics, loss of Foxc2 is associated with a failure of maturation of the collecting vessels, and absence of the gap in SMA-expressing pericytes that is found around normal LV.[40] Constitutive deletion of Foxc2 in mice is fatal from E13.5 up to shortly after birth due to cardiac abnormalities.[80, 161, 162]. A recently described Foxc2^{lx} line[163] now allows conditional Foxc2 deletion, enabling investigation of the role of Foxc2 in VV development (and in lymphatic vessel maintenance). In man, mutations in FOXC2 cause lymphoedema distichiasis and in addition to their abnormal lymphatics, these patients have been shown to suffer reflux in their veins, implying an additional venous phenotype.[47, 50] Foxc2 has been suggested to act upstream of Notch1 pathway signalling.[88] Mutations in Notch1 are associated with abnormal cardiac valve in man.[89] Recently, and after completion of this work, a role for Notch1 was described in LV development.[90] The expression of Foxc2 in developing VV is described in Chapter 3.

6.2 Aims

1) Validate the use of the Prox1CreERT2 line in deleting floxed alleles prior to P0.

2) Confirm the presence of a phenotype resulting from use of a newly described Foxc2^{lx} line, by identifying a requirement for Foxc2 in LV maintenance.

3) Investigate whether there is a requirement for Foxc2 in early or late VV development.

4) Investigate whether there is a requirement for Notch1 signalling during early or late valve formation.

6.3 Design and Methods

6.3.1 Mice

A conditional loss of function approach was used to investigate the role of Foxc2 in VV development and circumvent the lethality of constitutive deletion. This was done using a recently described transgenic line incorporating a floxed Foxc2 allele.[163] This line was imported for this work from the laboratory of Professor Tsutomo Kume, (Northwestern University, USA) rederivatised and crossed with the Prox1CreERT2 line to allow conditional deletion of Foxc2 in Prox1-expressing cells as previously described.[44] The mTmG line is described in Chapter 4.

6.3.1.1 Validation of Prox1CreERT2 recombinase activity

Rosa26mTmG;Prox1CreERT2 dams were injected at E15 and VV in embryos analysed at late E18. 3 VV in 3 mice were analysed by confocal microscopy as described in Chapter 3.

6.3.1.2 Conditional deletion of Foxc2

Crosses were made to obtain double transgenic offspring either homozygous of heterozygous for a floxed Foxc2 allele, and either heterozygous or wildtype for Prox1CreERT2. Prox1CreERT2- offspring were analysed as effective wildtype. For analysis at P0, dams received i.p. 4OHT at E15, whilst for analysis at P6, pups were injected at P0+P1.

At P0, 12 effective wildtype mice, 7 mice with heterozygous deletion and 8 mice with homozygous deletion were analysed. At P6, 12 effective wildtype mice, 6 mice with heterozygous deletion and 7 mice with homozygous deletion were analysed. Numbers of VV visualised in each group are provided in the results tables.

P6 mesenteric lymphatics (following administration of 4OHT at P0) were immunostained as described in the general methods. Mesenteries were examined using a fluorescence microscope (Leitz DMRB) and the number of mesenteric lymphatic valves per ray counted and recorded in Excel (Microsoft,

Redmond). For quantitative analysis of the requirement of Foxc2 for lymphatic valve maintenance, the number of LV in radial lymphatics was quantified in wildtypes (n=9 mesenteries, 56 vessels), in littermates with heterozygous deletion (n=4 mesenteries, 26 vessels) and homozygous deletion (n=3 mesenteries, 24 vessels). Data were exported into SPSS (IBM) for analysis.

6.3.1.3 Conditional deletion of Notch1

In vitro, Foxc2 upregulates Notch1 and the downstream Notch pathway components Hes and Hey.[123, 164] It was therefore decided to analyse a potential role for Notch signalling in venous valve formation using mice with conditional deletion of Notch1 from E15 and P0. AT P0, 8 effective wildtype and 7 homozygous conditional deletion mice were analysed. At P6, 4 effective wildtype and 4 homozygous conditional deletion mice were analysed. Numbers of VV visualised in each group are provided in the results tables.

6.3.2 Genotyping and immunofluorescence

Immunofluorescence imaging of murine VV and mesenteric LV, and genotyping were carried out as described in the general methods chapter and Chapter 3. Solutions are given in Appendix 1, antibody concentrations in Appendix 3 and primers in Appendix 4.

6.3.3 Statistics

Fisher's exact test was used to compare the stage of VV development, in wildtype mice with either heterozygous or homozygous knockouts for each stage. Data from multiple litters were pooled.

For analysis of the number of mesenteric LV per vessel, P values represent Bonferroni post hoc after ANOVA for heterozygous/homozygous deletion Vs wildtype.

All analyses were carried out in SPSS 21 (IBM corporation).

6.4 Results

Widespread expression of Prox1 in the murine femoral vein was confirmed at late E18. Analysis of VV in mTmG;Prox1CreERT2 mice showed widespread GFP expression, confirming cre-mediated deletion in endothelial cells following 4OHT injection at E15-16 (Figure 31).

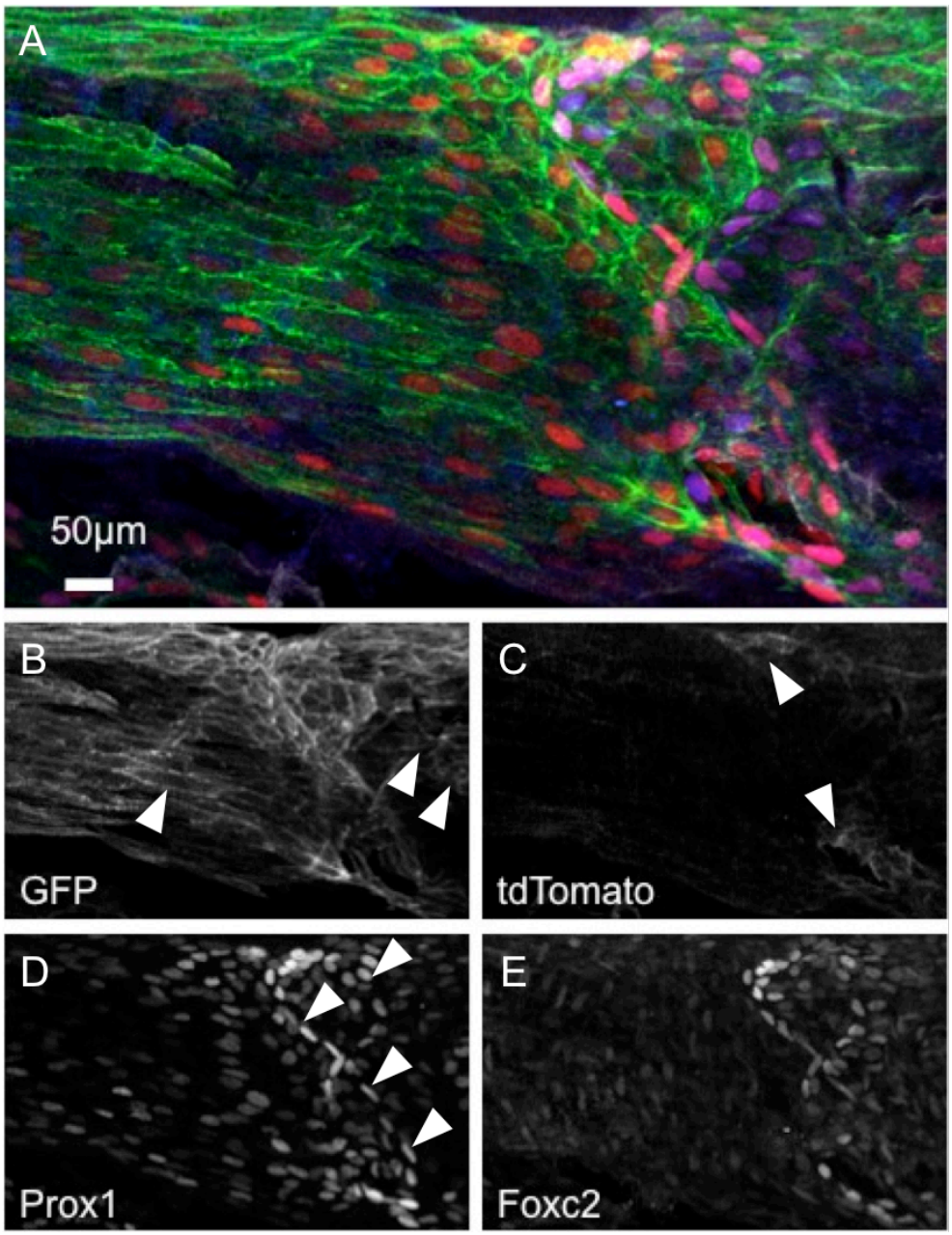

Figure 31 Prox1CreERT2 produces recombination in developing VV
A) R26mTmG;Prox1CreERT2, 4OHT at E15-16, analysed very late E18. GFP (green), Prox1 (red), tdTomato (white), Foxc2 (blue). Separated channels are shown in B-E. GFP expression, indicating cre-mediated recombination, is seen in almost all cells in the femoral vein, and almost all valve forming cells (arrowheads in D). Note elongated upstream cells (single arrowhead in B) and rounded downstream cells (double arrowhead in B). Some cells immediately downstream of the valve (arrowheads in C) express tdTomato and not GFP, indicating lack of recombination. Flow from left to right. Representative of n=3 VV. 2D maximum projection of confocal z-stack.

6.4.1 Conditional deletion of Foxc2 from E15

Conditional deletion of Foxc2 from E15 did not produce a significant phenotype in the development of VV (Figure 32)

A

	Effective wildtype	Heterozygous deletion		Homozygous deletion	
	n	n	P	n	P
Stage 0	0	2	ns	2	ns
Stage 1	17	10	ns	11	ns
Total analysed	17	12		13	

B

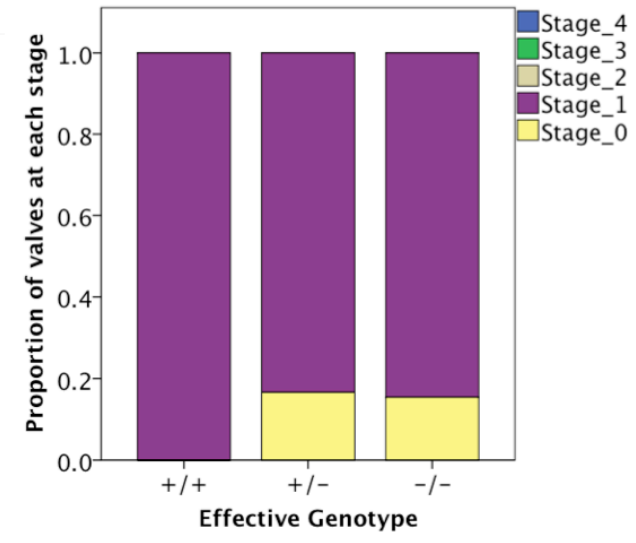

Figure 32 Valve development at P0 following conditional deletion of Foxc2 from E15

A) The table provides the total number of VV analysed for each genotype and the number of VV identified at each stage. Analysis of VV at P0 following conditional deletion of Foxc2 from E15 did not show any significant phenotype in valve developmental stage. ns=P>0.05 (Fisher's exact test); n=number of VV analysed.

B) The proportion of valves at each stage is shown for each genotype. +/+ = wildtype (n=12 mice), +/- = heterozygous deletion (n=7), -/- = homozygous deletion (n=8).

6.4.2 Conditional deletion of Foxc2 from P0

Homozygous conditional deletion of Foxc2 from P0 resulted in inhibition of valve development with a significant (P=0.017) increase in the proportion of VV remaining at stage 0 at P6. No VV reached stage 4 (Figure 33).

A

	Effective wildtype	Heterozygous deletion		Homozygous deletion	
	n	n	P	n	P
Stage 0	0	0	ns	4	**0.017**
Stage 1	0	0	ns	1	ns
Stage 2	1	0	ns	2	ns
Stage 3	15	7	ns	5	ns
Stage 4	7	2	ns	0	0.07
Total analysed	23	9		12	

B

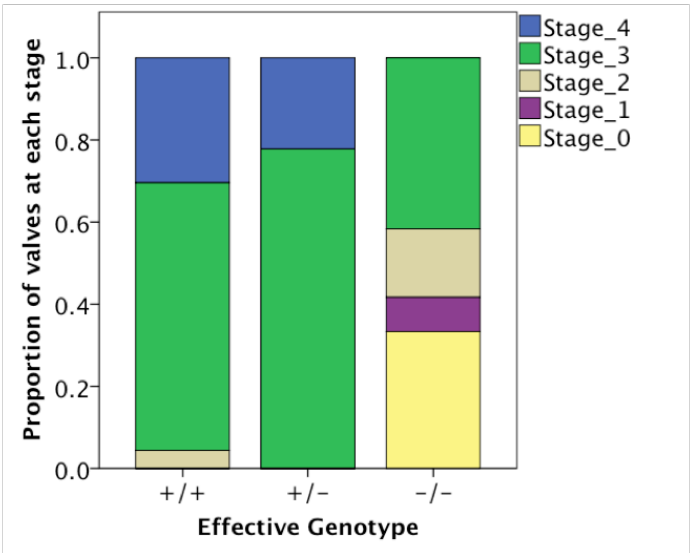

Figure 33 Valve development at P6 following conditional loss of Foxc2 from P0

A) The table provides the total number of VV analysed for each genotype and the number of VV identified at each stage. Analysis of VV at P0 following conditional deletion of Foxc2 from P0 showed an increase in the proportion of valves at stage 0. ns=P>0.05 (Fisher's exact test); n=number of VV analysed.

B) The proportion of valves at each stage is shown for each genotype. +/+ = wildtype (n=12 mice), +/- = heterozygous deletion (n=6), -/- = homozygous deletion (n=7).

6.4.3 Effect of conditional Foxc2 deletion on mesenteric LV maintenance

Conditional deletion from P0 produced significant lymphatic phenotypes at P6 (Figure 34, Figure 35), and some mice developed chylothorax, chylous ascites, and reflux of lymph (chyle) into the femoral lymphatics, confirming the efficacy of Cre mediated excision of Foxc2 on lymphatic phenotype in these animals. Homozygous conditional deletion was noted to result in lethality from around P6-8.

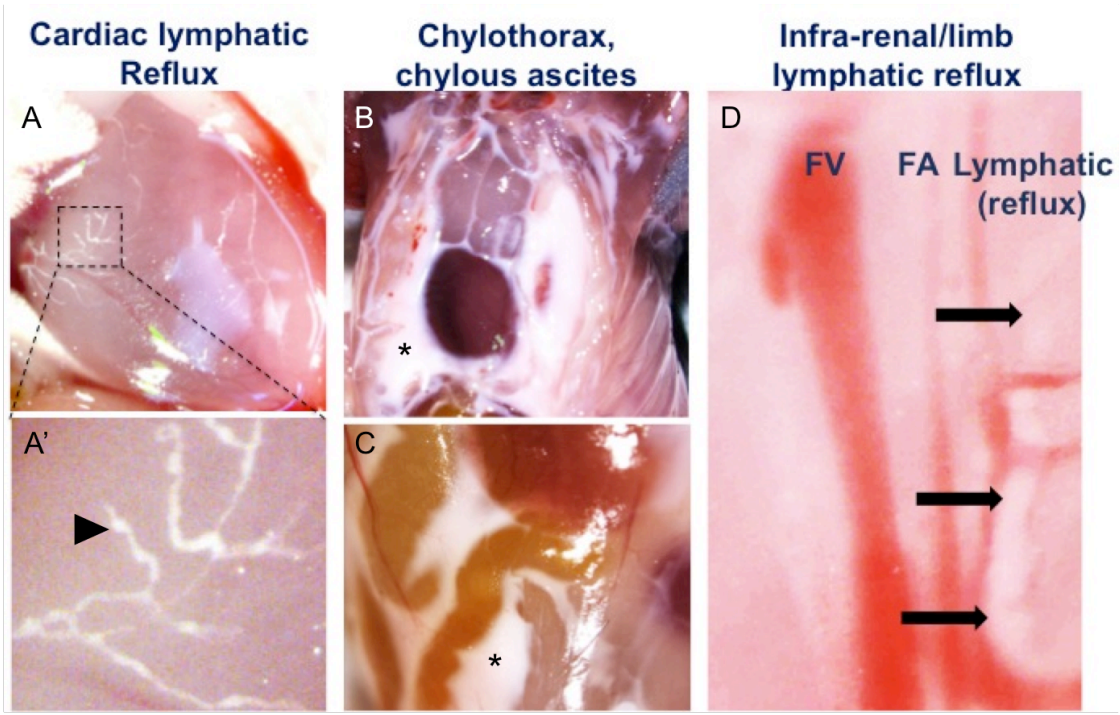

Figure 34 Conditional deletion of Foxc2 and lymphatic phenotype at P6
Sporadic lymphatic phenotypes included reflux of chyle into cardiac lymphatics (A and A', arrowhead in A'), chylothorax (B, *), chylous ascites (C, *), and reflux of chyle into femoral lymphatics (D, arrows). Photographs taken immediately post-mortem using Leica dissecting microscope. FV = femoral vein, FA = femoral artery.

Conditional homozygous deletion of Foxc2 from P0 resulted in a significant reduction in the number of lymphatic valves per vessel, compared with wildtype littermates (respectively 1.00 Vs 4.55, P<0.0005, Figure 35). The reduction in LV numbers seen with heterozygous conditional deletion did not reach statistical significance (P=0.052).

A

Genotype	n mesenteries (n vessels)	Mean LV per radial vessel	P
Effective wildtype	9 (56)	4.55	-
Heterozygous deletion	4 (26)	3.62	0.052
Homozygous deletion	3 (24)	1.00	<0.0005

B

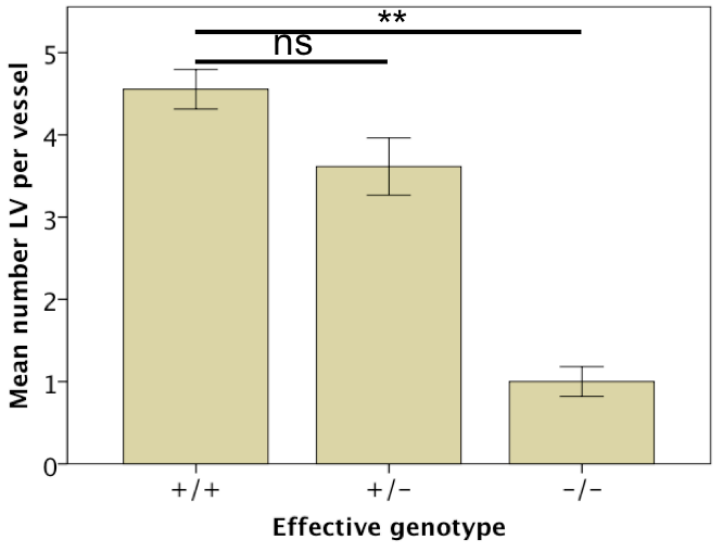

Figure 35 Foxc2 is required for LV maintenance after P0

A) The table provides the total number of mesenteries (mice) and lymphatic vessels analysed for each genotype and the mean number of LV identified at each stage. Conditional homozygous deletion of Foxc2 from P0 resulted in loss of LV by P6. P=Bonferroni post hoc, Vs WT, after ANOVA (ANOVA P<0.0005). Error bars represent 1SEM. +/+ = wildtype, +/- = heterozygous deletion, -/- = homozygous deletion. ns= P>0.05, ** = <0.0005 (+/+ Vs -/-)

6.4.4 Conditional deletion of Notch1 at E15

Analysis at P0 following conditional deletion of Notch1 from E15 showed a phenotype of reduced organisation of the Prox1^{hi} valve-forming cells, with failure to reach stage 1 of VV development (P<0.0005, Figure 36, Figure 37).

A

	Effective wildtype	Homozygous deletion	
	n	n	P
Stage 0	0	13	<0.0005
Stage 1	14	1	<0.0005
Total analysed	14	14	

B

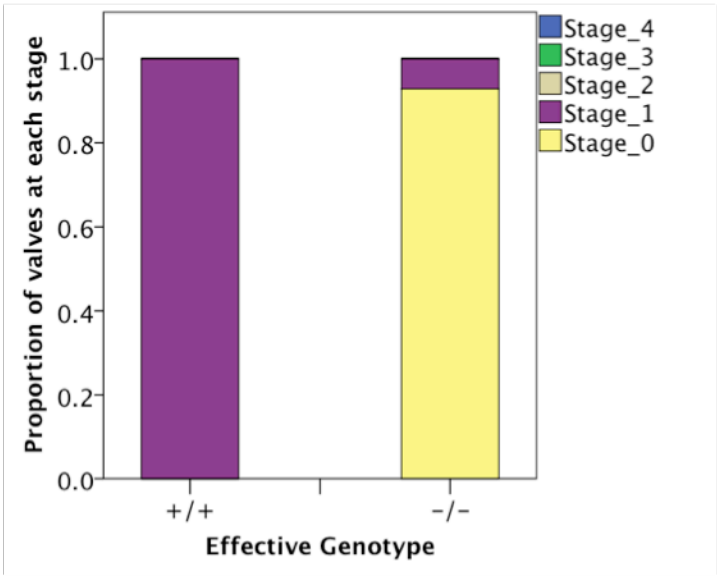

Figure 36 Valve development at P0 following conditional deletion of Notch1 from E15.5

A) The table provides the total number of VV analysed for each genotype and the number of VV identified at each stage. Conditional deletion of Notch1 from E15.5 resulted in failure of normal organisation of the Prox1^{hi} valve forming cells at P0, whilst VV developed normally in wildtype littermates. P= Fisher's exact test.

B) The proportion of valves at each stage is shown for each genotype. +/+ = wildtype (n=8 mice), -/- = homozygous deletion (n=7 mice).

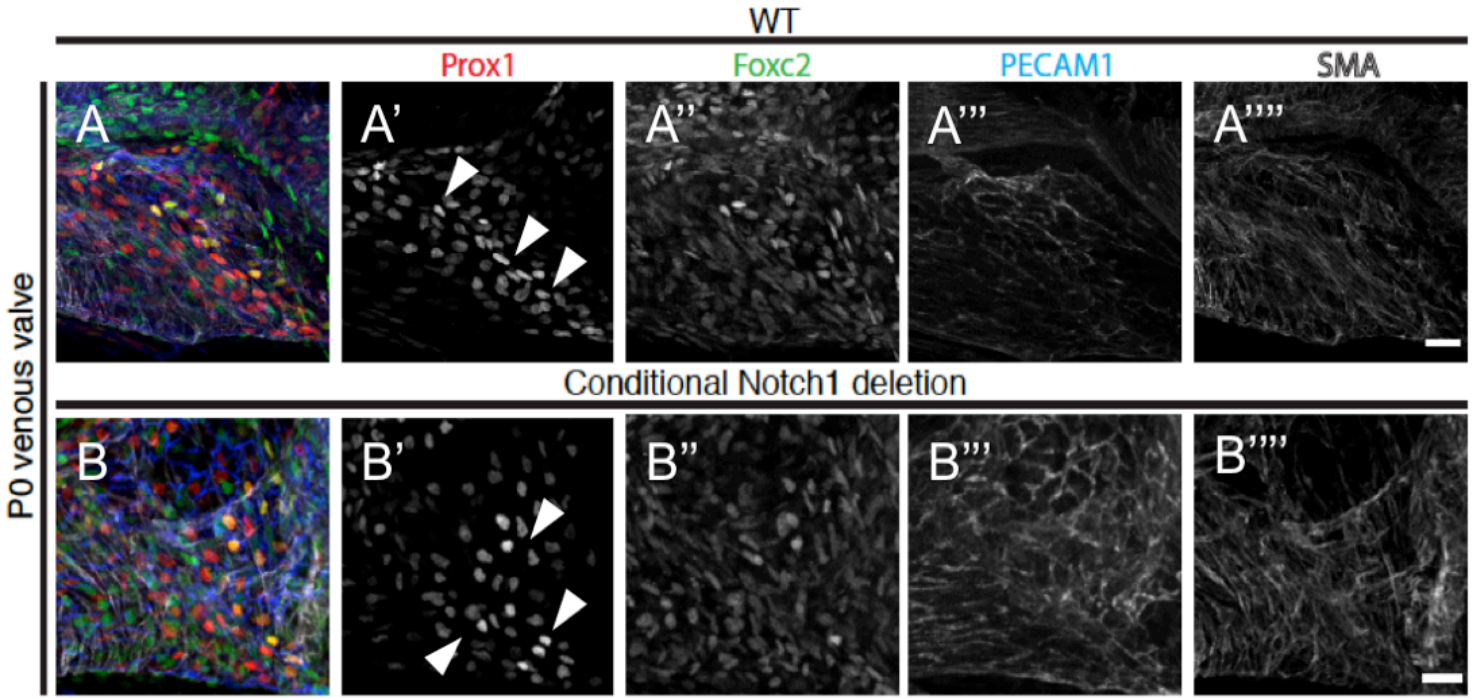

Figure 37 Valve morphology at P0 following conditional deletion of Notch1 from E15

A-A'''') shows a VV at P0 in a wildtype littermate, whilst B-B'''' shows a VV region following conditional Notch1 deletion from E15. Wildtype controls showed rotated and elongated Prox1hi nuclei (arrowheads in A'). B) Conditional homozygous Notch1 deletion resulted in a broader region of Prox1^{hi} cells, that did not elongate and rotate (arrowheads in B'). Immunostaining is as indicated, for Prox1 (red, A', B') Foxc2 (green, A'', B'') PECAM1 (blue, A''', B''') and SMA (white, A'''', B''''). Scale bars 20μm

6.4.5 Conditional deletion of Notch1 from P0

Notch1 was not required for later events in VV formation, and VV developed normally to P6 following 4OHT injection at P0 (Figure 38).

A

	Effective wildtype	Homozygous deletion	
	n	n	P
Stage 3	2	3	ns
Stage 4	6	5	ns
Total analysed	8	8	

B

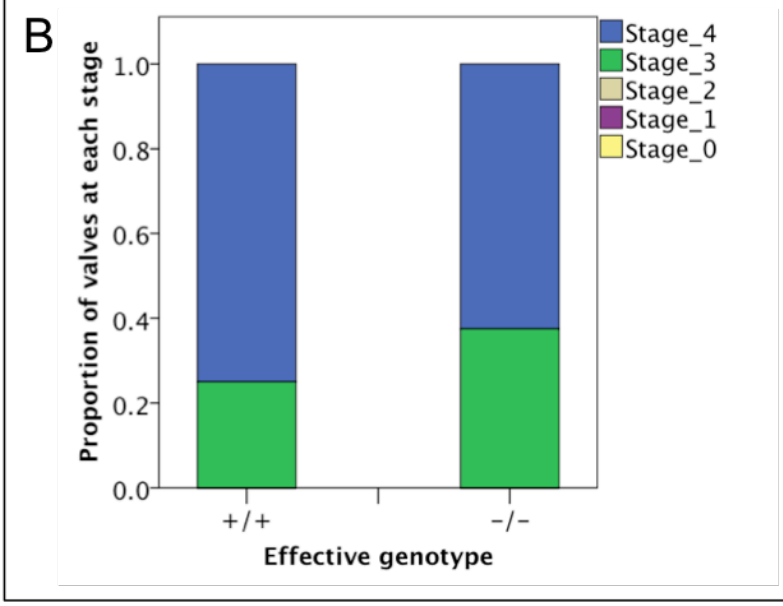

Figure 38 Valve development at P6 following conditional deletion of Notch1 from P0

A) The table provides the total number of VV analysed for each genotype and the number of VV identified at each stage. Analysis at P6 after conditional Notch1 deletion from P0 did not show any discernable phenotype. P= Fisher's exact test.

B) The proportion of valves at each stage is shown for each genotype. +/+ = wildtype (n=4 mice), -/- = homozygous deletion (n=4 mice).

6.5 Discussion and conclusions

Analysis at late E18 of Prox1CreERT2;Rosa26mTmG valves following injection of 4OHT at E15-16 revealed widespread GFP expression in the femoral vein. This experiment confirms that the activity of the transgenic Prox1 promoter is widespread in the femoral vein ECs around E15-16, and supports my earlier data using antibody immunolocalisation of Prox1 that suggested widespread protein expression at E17. This is surprising given the previous characterisation of Prox1 as a master regulator of lymphatic cell fate.[149] Some endothelial cells did not express GFP; this may be because of a true absence of promoter activity, or a degree of mosaicism in the activity of CreERT2. Expression of GFP was found in almost all Prox1^{hi} valve-forming cells, confirming the utility of the Prox1CreERT2 line in subsequent conditional loss of function experiments in these cells. This finding is reinforced by the strong phenotype following conditional deletion of Notch1, which will be discussed further below. It was noted that some tributaries expressed tdTomato rather than GFP, despite staining positively for Prox1 at E18 (not shown). This suggests that Prox1 expression may become increasingly widespread after E15-16, at least in these vessels. The complete absence of GFP expression in Cre- valves (not shown) confirms the failure of endogenous oestrogens to activate ERT2 in these mice and the consequent absence of Cre-mediated excision in control groups in this thesis.

Given the clear venous phenotypes seen in patients who are heterozygous for mutations in FOXC2[50], it was expected that conditional deletion of Foxc2 in VFC's would produce a clear early defect in VV development.[50] Surprisingly no significant effect was seen with deletion prior to P0, and only relatively mild phenotypes with analysis after deletion prior to P6. It was not possible to analyse VV at later stages because this deletion was lethal (likely as a result of the identified lymphatic defects) around P8. The observed lack of strong phenotype at P0 following earlier Foxc2 deletion is unlikely to be as a result of a failure of deletion, because the Prox1CreERT2 line has demonstrated activity in a Cre reporter (mTmG) line, has produced strong phenotypes with other floxed alleles, and produced strong lymphatic phenotypes in the same animals. One plausible explanation for my findings is redundancy in signalling

between Foxc2 and NFATc1, which is expressed in VFC's in a similar pattern to Foxc2, or expression of Foxc1. Although Foxc1 and Foxc2 are often co-expressed in the blood vascular system and demonstrate some redundancy[80] loss of even one copy of Foxc2 is sufficient to produce lymphoedema in mice, and both lymphoedema and venous reflux in man.[40, 50] Whilst Foxc2 is known to be expressed in venous and lymphatic valves, expression of Foxc1 has not previously been described in the lymphatic or venous systems in either mouse or man, and this transcription factor has not been implicated in their development.[40] Investigation of the possibility of Foxc1 expression in venous but not lymphatic valves was hampered by a lack of anti-murine Foxc1 antibodies for use in wholemount immunofluorescence. A tested antibody (not shown) produced very weak nuclear localisation. Other investigators have similarly failed to find a suitable antibody (Petrova.T, personal communication 2013). Western blot analysis of lysed isolated human VV leaflets (but not non-valve vein wall) did, however, show a strong band near the expected molecular weight with a monoclonal Foxc1 antibody (Figure 95). If we accept the generally observed similarity between the expression profile of human and murine VV, this finding suggests that Foxc1 is expressed in murine venous valves, leading to the speculation that Foxc1 may be able to compensate for loss of Foxc2. This hypothesis could be examined in vivo by combined conditional deletion of Foxc1 and Foxc2; unfortunately a floxed Foxc1 allele was not available for study during this work. Redundancy between Foxc1/Foxc2 and NFATc1 also remains unexplored and could be addressed by using ciclosporin to inhibit calcineurin-NFAT signalling, and floxed Foxc1/2 alleles.

Notch1 deletion from P0 produced no phenotype at P6, in contrast to the finding that deletion from E15 produced a clear phenotype at P0. It is possible to speculate that Notch1 plays a role in the selection and/or maintenance of the VFC phenotype at very early stages in VV development, and this will be a focus of future work. Because of the need to explant embryos following administration of 4OHT, it was not possible to study the later effects of early Notch1 deletion. In man, mutations in Notch1 have been associated with

bicuspid aortic valve, and mutations in Notch3 with varicose veins, suggesting clinically important roles for Notch signalling in man.[89,165]

6.5.1 Limitations of the study

- The immunolocalisation pattern of Notch1 was not described at early stages, because antibodies for wholemount imaging are not yet well characterised. Similarly the localisation of Notch1 ligands remains to be explored.
- Given the possible redundancies between Foxc2, Foxc1 and NFATc1 it is not possible to conclude that Foxc2 does not play a role in VV development prior to P0 without analysis of concurrent deletion or inhibition of Foxc1/NFATc1. Immunolocalisation of Foxc1 in murine and human venous valves was attempted to support my western blot analysis of valve lysate, but this was not successful.
- The quantification of valve developmental stages that has been applied consistently throughout this work is not well suited to describing the cellular events prior to P0; it is possible that new methods of quantification will be required to describe events at these time points.

7 CALCINEURIN-NFAT SIGNALLING IN VV

7.1 Introduction

Calcineurin-NFAT signalling has been clearly implicated in the development or cardiac and lymphatic valves.[39,42,93,96,100,101] I therefore hypothesised that it may also be expressed in VV, and required for their normal development. Calcineurin is a heterodimer consisting of a catalytic α subunit and regulatory β subunit. The β subunit exists as two isoforms, CnB1 and CnB2. CnB1 is expressed in the vasculature and is encoded by PPP3R1.[166] Calcineurin is a protein phosphatase, and in response to a rise in intracellular $Ca2^{+}$, dephosphorylates NFATs to reveal their nuclear localisation sequence, leading to nuclear translocation and transcriptional activity (Figure 8).[92] Calcineurin activity is rapidly and effectively inhibited by the drug ciclosporin A.[39, 96, 103] A more refined approach has been enabled by a murine strain with floxed PPP3R1 alleles, allowing conditional deletion of CnB1.[166] In lymphatics conditional PPP3R1/CnB1 deletion has been associated with shorter LV leaflets[42], and I therefore decided to analyse VV leaflet length in addition to VV developmental stage in this conditional knock out.

7.2 Aims

1) Investigate whether there is a requirement for calcineurin-NFAT signalling in venous valve development after P0, using the calcineurin inhibitor ciclosporin.

3) Investigate whether there is a requirement for Calcineurin signalling during early or late valve formation, utilising conditional deletion of PPP3R1, encoding CnB1.

3) Quantify the effect of conditional deletion of PPP3R1 from P0 on leaflet length.

4) Localise NAFTc1 in human VV by immunohistochemistry

7.3 Design and Methods

7.3.1 PPP3R1^{lx} mice

Crosses were performed to obtain Prox1CreERT2^{+} and Prox1CreERT2^{-} littermates, all PPP3R1^{lxlx} [42, 166], with 4OHT administered to the dam at E15.5

(for analysis at P0) or pups at P0 (for analysis at P6). Mice were maintained at University of Lausanne on a bl/6 background.[42] AT P0, 5 effective wildtype and 5 conditional homozygous deletion mice were analysed. At P6, 16 effective wildtype and 8 homozygous conditional deletion valves were analysed. The numbers of VV visualised at each stage are provided in the results table.

7.3.2 Ciclosporin inhibition of calcineurin-NFAT signalling

Ciclosporin (Calbiochem 239835) was reconstituted to 100mg/ml in Dimethysulfoxide and stored at 4^{o}c and diluted 1:10 in sunflower seed oil (Sigma S5007) prior to injection (50μg/g.wt of pup, bid). Balb/c (wildtype) littermates in 2 litters were randomly allocated to a ciclosporin or control group. The ciclosporin (n=7 pups) or vehicle (n=7 pups) was administered bid from P1-P5 with a further dose administered immediately prior to termination of the experiment at P6. All mice were culled and analysed at P6 by immunofluorescence and confocal microscopy. Six valves were successfully analysed following control treatment, and 8 following ciclosporin treatment.

7.3.3 Measurement of VV leaflet length

Leaflet length was measured in a 2D maximum projection of each confocal z-stack. In NIH ImageJ, a standard template was referenced to allow 8 measurements of leaflet length to be obtained at standardised positions (Appendix 7). Analysis was performed in 11 effective wildtype valves and 14 littermates following homozygous conditional deletion.

7.3.4 Immunohistochemistry for NFATc1

Vein was obtained from patients undergoing CABG, and 5um sections cut from paraffin-blocks of embedded valved segments, followed by immunohistochemistry for localisation NFATc1, all as described in the General Methods chapter.

7.3.5 Genotyping and immunofluorescence

Immunofluorescence imaging of murine VV and genotyping were carried out as described in the General Methods and Chapter 3. All solutions are given in

Appendix 1, antibody concentrations/dilutions in Appendix 3 and primers in Appendix 4.

7.3.6 Statistics

For comparison of stage of VV development following administration of ciclosporin or conditional deletion of PPP3R1 Fisher's exact test was used, comparing wildtype with either heterozygous or homozygous knockouts for each stage. Data from multiple litters were pooled.
For analysis of the change in VV leaflet length with PPP3R1 deletion, an independent samples t test was used.

All analyses were carried out in SPSS 21 (IBM corporation).

7.4 Results

7.4.1 Normal expression pattern of NFATc1

At E18 NFATc1 was heterogeneously expressed in endothelial cells of the femoral vein in the region of the developing valve. At P0, NFATc1 was expressed by Prox1^{hi} VFC's, but signal was more widespread than that from Prox1. At P6 NFATc1 was heterogeneously expressed in free-edge cells, and also in the valve leaflet endothelium (Figure 39). Another example of NFATc1 localisation at P0 is given in Figure 27.

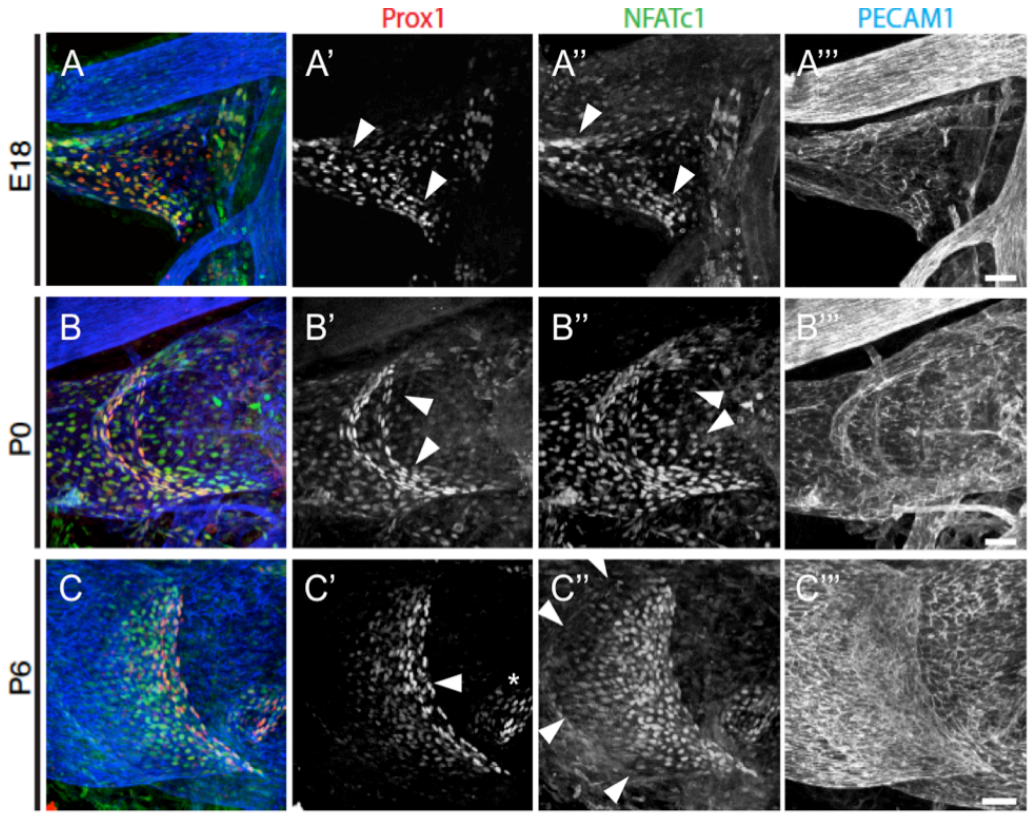

Figure 39 Expression of NFATc1 in wildtype venous valves

Immunolocalisation of NFATc1 (green), Prox1 (red) and PECAM1 (blue) are shown at: A-A''') E18, B-B''') P0, C-C''') P6. At E18 NFATc1 and Prox1 were heterogeneously expressed by endothelial cells (arrowheads in A' and A''). At P0 Prox1^{hi} VFC's were organized into a ring of rotated and elongated cells (arrowheads in B') whilst NFATc1 retained a more widespread expression pattern (arrowheads in B''). At P6 Prox1 signal was strongest in free edge cells (arrowhead in C'), but NFATc1 was expressed throughout the valve leaflets (outlined by arrowheads in C''). A valve guards the orifice of a downstream tributary in C (* in C'). Representative confocal micrographs from n≥6 per group. Bars 50μm.

7.4.2 Effect of inhibiting NFAT signalling with ciclosporin

Three ciclosporin-treated pups did not survive to P6 (leaving 4 for analysis), compared with complete survival of the solvent treated pups. Ciclosporin treated pups failed to gain weight normally compared with littermate controls, ($P=0.015$, ANOVA, Figure 96). Vein samples in this experiment were surrounded by an unusual amount of fat, which interferes with the laser, and prevents complete staging of valves. Because a strong phenotype was clear, (Figure 40B) valves were classified as having a normal appearance or thin valve leaflets. Inhibition of calcineurin-NFAT signalling by administration of ciclosporin resulted in a failure of valve leaflet development (n=6 VV, Figure 40A, compared with valves in pups receiving vehicle control (n=8 VV), which developed normally ($P<0.05$, Fisher's exact test).

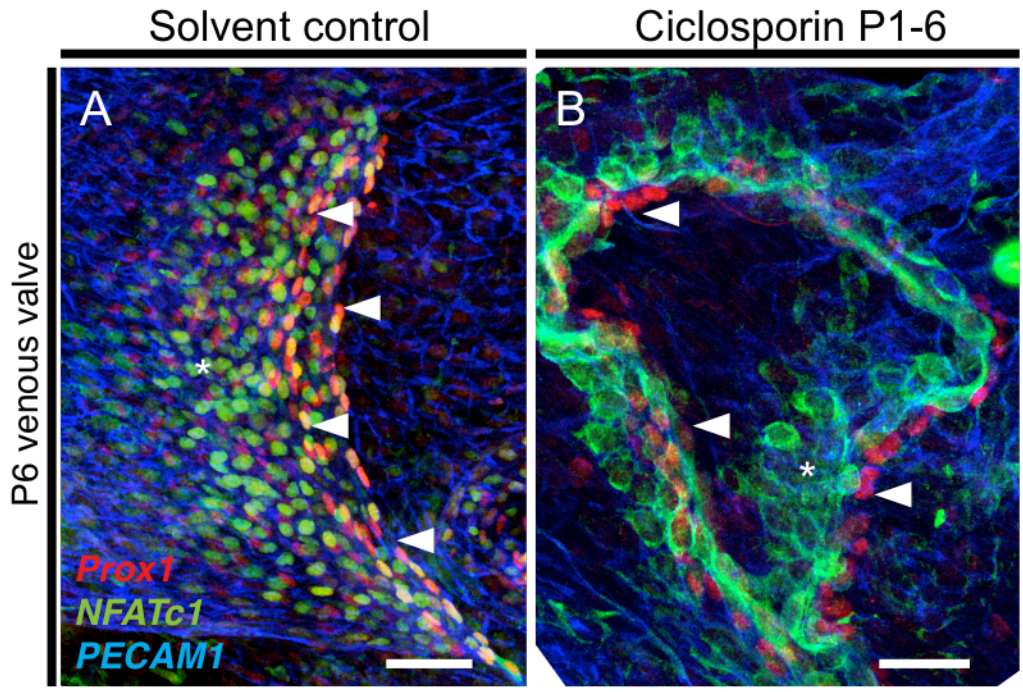

Figure 40 Morphology of valves at P6 after inhibition of NFAT signalling at P0-6
A) The table provides the total number of VV analysed for each treatment and the number of VV identified at each stage. P= Fisher's exact test. B-C) Valves in pups receiving solvent control developed normally (B) whilst ciclosporin treated valves (C) had thin leaflets. In B+C, arrowheads indicate free edge cells, * indicates leaflets. Note predominantly cytoplasmic staining pattern of NFATc1 signal (green) following treatment with ciclosporin (C) compared to nuclear pattern in control valves (B) consistent with loss of calcineurin phosphatase activity on NFATc1. The nuclear localization in control valves indicates active NFATc1 signalling at this stage. Scale bars 50μm

7.4.3 Inhibition of NFAT signalling at P0 following conditional deletion of PPP3R1 (CnB1) from E15

Conditional homozygous deletion of PPP3R1 (encoding CnB1) from E15 did not produce a significant valve phenotype at P0 (Figure 41).

A

	Effective wildtype n	Homozygous deletion n	P
Stage 0	0	2	ns
Stage 1	7	7	ns
Total analysed	7	9	

B

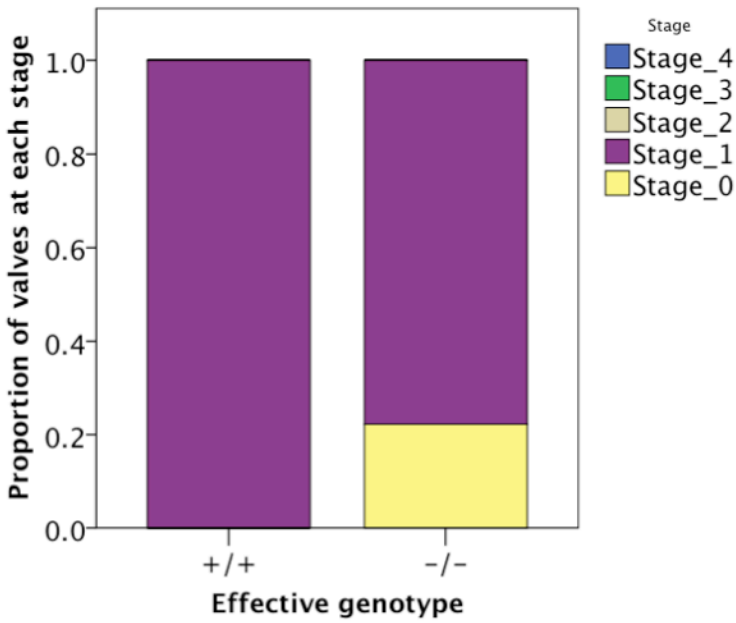

Figure 41 Valve development at P0 following conditional deletion of PPP3R1 (CnB1) from E15

A) The table provides the total number of VV analysed for each genotype and the number of VV identified at each stage. Homozygous deletion of PPP3R1 (encoding CnB1) from E15 had little effect on valve phenotype and the majority of VV developed to stage 1 at P0. P= Fisher's exact test. ns= >0.05.n=number VV analysed.

B) The proportion of VV at each stage is shown for each genotype. +/+ = wildtype (n=5 mice), -/- = homozygous deletion (n=5 mice).

7.4.4 Valve development at P6 after inhibition of NFAT signalling by conditional deletion of PPP3R1 (Calcineurin B1) from P0

Whilst control valves developed normally to stages 3-4, conditional homozygous loss of CnB1 from P0 inhibited the development of VV leaflets, with a failure to progress beyond stage 1 of VV development (Figure 42). The initial ring of rotated endothelial cells remained entirely intact (Figure 43).

A

	Effective wildtype n	Homozygous deletion n	P
Stage 0	0	1	ns
Stage 1	0	9	**<0.0005**
Stage 2	0	1	Ns
Stage 3	20	4	**0.030**
Stage 4	12	1	**0.036**
Total number	32	16	

B

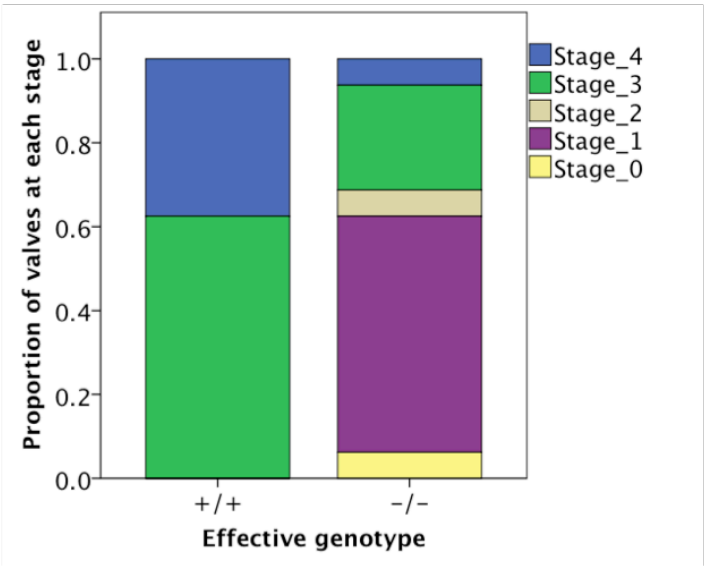

Figure 42 Valve development at P6 following conditional deletion of PPP3R1 (CnB1) from P0

A) The table provides the total number of VV analysed for each genotype and the number of VV identified at each stage. Homozygous conditional deletion of CnB1 from P0 resulted in failure to develop valve leaflets, compared to wildtype littermates that developed normally. P= Fisher's exact test. ns= >0.05

B) The proportion of valves at each stage are shown for each genotype. +/+ = wildtype (n=16 mice), -/- = homozygous deletion (n=8).

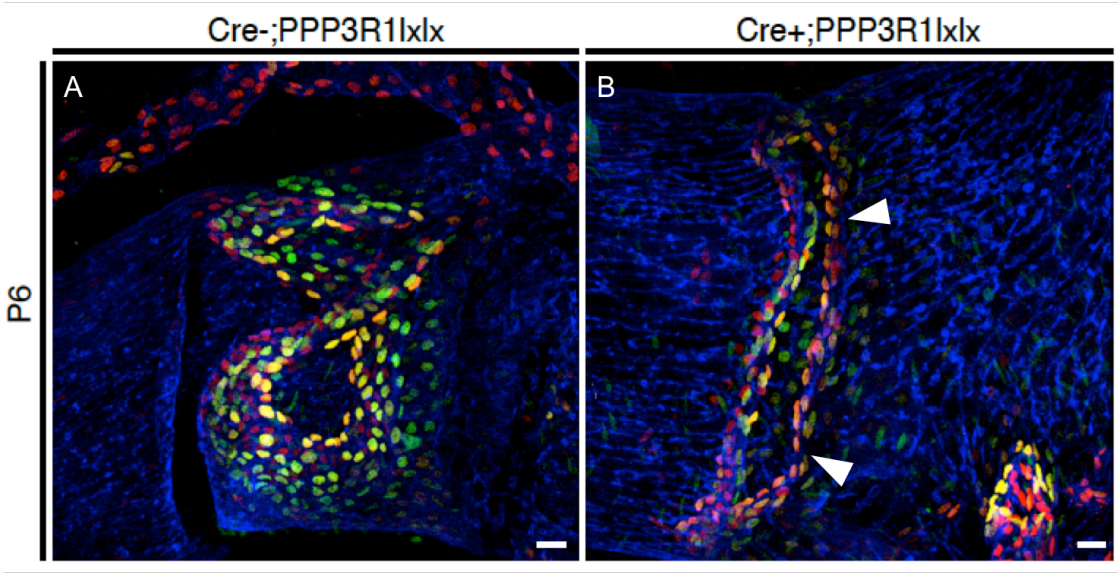

Figure 43 Morphology of valves at P6 following conditional deletion of PPP3R1 (CnB1) from P0

A) Prox1CreERT2^{-} (effective wildtype) valves developed normally. B) Conditional deletion of PPP3R1 (encoding Calcineurin B1) resulted in a failure of leaflet development at P6 (arrowheads in B). Scale bars 20μm. Green = Foxc2, Red = Prox1, Blue = PECAM1.

7.4.5 Effect of PPP3R1 deletion on venous valve leaflet length at P6

Conditional homozygous deletion of PPP3R1 from P0 resulted in significantly shorter leaflets at P6 (P=0.021), compared with wildtype littermate controls. (Figure 44)

A

Genotype	Number of leaflets analysed	Mean normalised leaflet length (arbitrary units)	P
Effective wildtype	11	1.00	-
Homozygous deletion	14	0.59	0.021

B

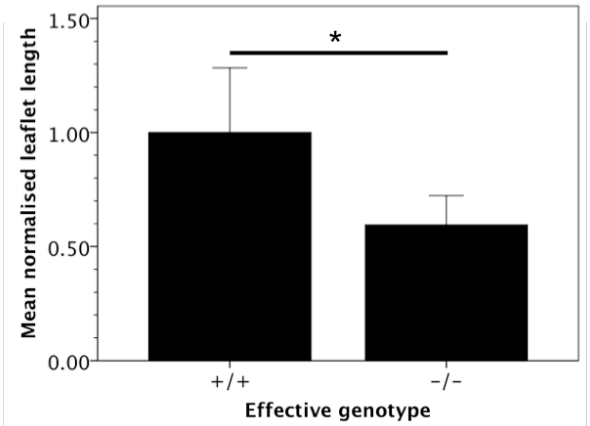

Figure 44 Conditional deletion of PPP3R1 (CnB1) from P0 analysed at P6.
A) The table provides the total number of VV analysed and the mean normalized leaflet length for each genotype. Homozygous conditional deletion of CnB1 from P0 resulted in significantly shorter valve leaflets, compared to wildtype littermates that developed normally. P= independent sample t test.

B) The mean normalized leaflet length for each genotype is shown. Error bars represent 2SEM. +/+ = wildtype (n=6 mice), -/- = homozygous conditional deletion (n=7 mice). * P=0.021

7.4.6 Localisation of NFATc1 in human VV

NFATc1 was localised to nuclei of endothelial cells lining the lumen surface of the VV leaflets, suggesting active calcineurin-NFATc1 signalling in these cells.

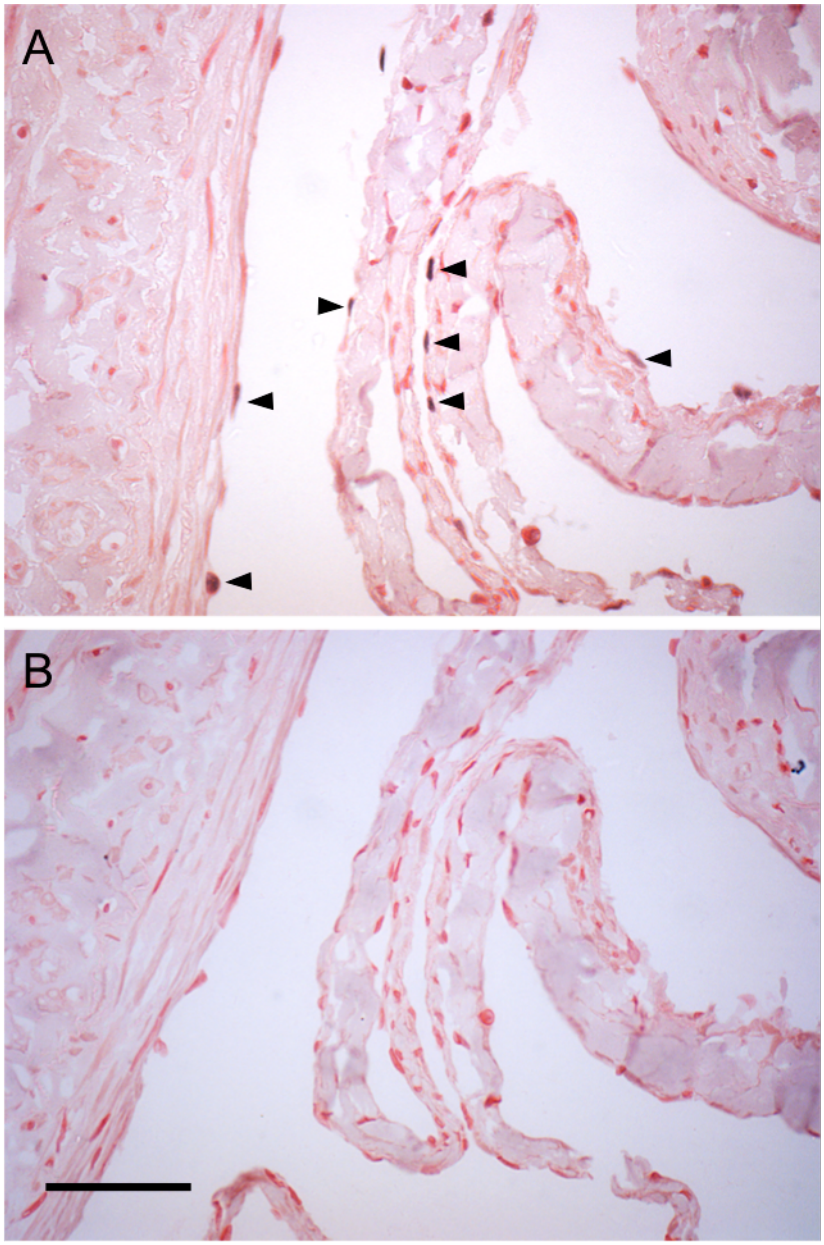

Figure 45 Immunohistochemical localisation of NFATc1 in human VV
A) NFATc1 was localised to nuclei of endothelial cells lining the luminal surface of two opposing VV leaflets in FFPE transverse sections of human VV. (arrowheads).

B) No signal was detected with concurrent use of non-immune IgG on a section on the same slide.

Scale bar 50μm

7.5 Discussion

Endothelial deletion of the regulatory subunit of calcineurin, CnB1 (encoded by PPP3R1) from P0 restricted subcellular localisation of NFATc1 to the nucleus and effectively blocked VV development beyond stage 1, with approximately 40% shorter valve leaflets at P6. This suggests a cell-autonomous function for calcineurin-NFAT signalling in VV development. A similar defect was found with inhibition of calcineurin phosphatase activity by administration of CsA, although this caused other, systemic effects including failure to gain weight.

NFATc1 is thought to be critically required for valve elongation in cardiac and lymphatic valves[42, 96] and our results appear to confirm the underlying hypothesis that some similar mechanisms regulate cardiac, venous and lymphatic valve development. The mechanism by which leaflet elongation fails is unknown. It is possible that endothelial cells fail to proliferate, since NFATc1 has been shown to promote proliferation of human pulmonary valve endothelial cells in vitro.[167]

NFATc1 and Foxc2 show similar patterns of immunolocalisation in the developing valve (and downstream region) and it is likely that these proteins interact in VV development, as has previously been demonstrated in lymphatic collecting vessel maturation.[39, 40]. Conditional deletion of either CnB1 or Foxc2 in endothelial cells from E15 did not result in a significant valve phenotype at P0. It was not possible within the time and geographical constraints of this work to analyse the phenotype of double transgenics, or following Foxc2 deletion with CsA. NFATc1 binds to GATA5, and it is notable that loss of GATA5 function produces an abnormally bicuspid aortic valve, demonstrating a role for GATA-binding proteins in valve formation. Whilst GATA5 has not been identified in VV, the related protein GATA2 has been immunolocalised to human VV and could also interact with NFATc1 in valve development. NAFTc1 associates with GATA2 in skeletal muscle.[168] Whilst mutations in GATA2 can lead to lymphoedema, it is not known whether these patients are affected by VV failure. [169,98,165] This will be the focus of future work.

In the pro-valve endocardium an enhancer within the first intron of NFATc1 functions as an autonomous cell-specific enhancer leading to high expression of NFATc1 in valve endocardium.[170] It is an intriguing possibility that the same enhancer directs expression in venous and lymphatic valve development.

Endothelial-mesenchymal transition has never been suggested to occur in LV or VV development, although the origin of VV interstitial cells remains unknown. Analysis of venous valves in Prox1CreERT2;Rosa26mTmG mice at P6 following administration of 4OHT at P1+P2 did not reveal GFP-expressing interstitial cells (Appendix 11), indicating that Prox1-expressing EC's at P1 had not become interstitial cells by P6. This preliminary result does not exclude EMT at earlier stages (prior to P1). Whilst murine LV do not have interstitial cells (except in the thoracic duct), pericytes are consistently identified near the valve agger. [146]

7.5.1 Limitations

Activity of other NFAT's has not been examined in the context of venous valves. NFATs other than NFATc1, if present in VV endothelium, would similarly be inhibited by CsA or CnB1 deletion. It is an intriguing possibility that NFATc3 or NFATc4 in pericytes may play a role in VV and LV development, analogous to their role in myocardium. The VV phenotype (prevention of valve elongation) observed in the limited number of valves imaged after postnatal CsA administration was similar to that seen with endothelial CnB1 loss of function in Prox1CreERT2;PPP3R1^{lxlx} mice and is consistent with the findings of Chang et al [96] regarding the endocardial requirement for CnB1 in cardiac valve elongation. Experiments were carried out to examine the hypothesis that earlier administration of CsA prevents valve development, but were complicated by early littering (data not shown). It remains possible that other NFATs are expressed and may play a role in VV (and LV development).

Calcineurin activity is calcium dependent, but the upstream stimulus to calcineurin-NFAT signalling in VV development has not been studied. Ca^{2+} has been suggested as a candidate carrier for valve-regulatory signals

passing between endothelial cells via gap junctions, and will be discussed further in Chapter 8.[106]

The requirement for calcineurin-NFAT signalling in maintenance of the formed VV has not been examined. The nuclear localisation of NFATc1 in adult human VV demonstrates on-going active signalling via this pathway, and a requirement for VV maintenance could lead to a detrimental VV phenotype in patients treated with ciclosporin (or other calcineurin inhibitors such as the clinically-used drug FK506).

8 ROLE OF CONNEXINS 37, 43, 47 IN VV DEVELOPMENT

8.1 Introduction

Connexins are transmembrane proteins that have important roles including the formation of gap junctions between adjacent cells.[105] In man, mutations in GJA4 (encoding Cx43) and GJC2 (encoding Cx47) have recently been shown to cause lymphoedema.[4, 57] In mice, Cx37 and Cx43 have been found to be required for normal lymphatic valve development.[42, 109] Uniquely for primary lymphoedema, the lymphoedema caused by GJC2 mutations in man has been attributed to a functional rather than structural lymphatic defect, possibly related to abnormal lymphatic pumping.[4] Whilst Cx47 expression has been identified in adult VV and LV, no lymphatic or venous phenotype with loss of Cx47 in mice has been described.[61, 111]

Recently, and after this work on Cx37 was completed, it was found that adult Cx37 homozygous knockout mice have absent VV; the mechanisms underlying this finding have not been described.[111]

8.2 Aims

1) Characterise the expression pattern of Cx37, Cx43, and Cx47 at P0.

2) Analyse the VV developmental phenotypes produced by genetic loss of function of Cx37, Cx43 and Cx47.

3) Develop and apply novel techniques for analysis of the cellular phenotypes seen in these experiments.

8.3 Design and Methods

8.3.1 Mice

Transgenic mice were maintained at the University of Lausanne on a Bl/6 background. For immunolocalisation of connexins 37 and 43, balb/c mice from Charles River UK were used and ≥3 VV analysed per connexin.

8.3.1.1 Constitutive deletion of GJA1 (Cx37)

In this line the majority of the single coding exon of GJA1 has been deleted. [171] $Cx37^{-/-}$ females are infertile and therefore $Cx37^{+/-}$ females were interbred with $Cx37^{-/-}$ or $Cx37^{+/-}$ males. At P0, 3 wildtype, 11 heterozygous knockout and 14 homozygous knockout littermates were analysed. At P6 2 wildtype, 18 heterozygous knockout and 16 homozygous knockout littermates were analysed. Numbers of VV visualised at each age and stage for each genotype are provided in the results.

8.3.1.2 Conditional deletion of GJA4 (Cx43)

Prox1CreERT2+ and Prox1CreERT2– littermates, all $GJA1^{lxlx}$ were analysed, with 4OHT administered to the dam at E15.5 (for analysis at P0) or pups at P0 (for analysis at P6). At P0, 6 effective wildtype and 6 homozygous conditional deleted littermate mice were analysed. At P6 2 wildtype and 4 homozygous conditional deleted littermates were analysed. Numbers of VV visualised at each age and stage for each genotype are provided in the results.

8.3.1.3 Constitutive deletion of Cx47 in Cx47GFP reporter

In this line the coding region of GJC2 is replaced by eGFP.[61] eGFP in these mice is not specifically targeted to the nucleus, and has been identified in the nucleus and cytoplasm.[61] At P0 4 wildtype, 5 heterozygous knockout and 8 homozygous knockout littermate mice were analysed. At P2 2 wildtype, 2 heterozygous knockout and 6 homozygous knockout mice were analysed. Numbers of VV visualised at each age and stage for each genotype are provided in the results. GFP signal was amplified with a biotinylated anti-GFP antibody and streptavidin-conjugated Dylight-488 secondary antibody.

8.3.2 Correlation between nuclear and cellular morphology measurements in mTmG reporter

The correlation between valve-forming cell nuclear and cellular morphology in wildtype mice at late E18 was assessed using membrane targeted GFP in the mTmG Cre reporter line, crossed with Prox1CreERT2, in 2 VV (Figure 31).[44,153]

1. Rosa26mTmG;Prox1CreERT2 mice were injected at E15-16 to produce recombination and therefore membrane-targeted eGFP expression in the valve-forming cells at late E18. Valves were immunostained for Prox1 and Foxc2 and confocal z-stacks were obtained as described in the General Methods Chapter and Chapter 3.

2. Measurements were made of the nuclear and cellular maximum length and width of $Prox1^{hi}$ cells in NIH ImageJ software, using single optical sections within Z stacks. For cell measurements, the centre of the line of membrane-tagged GFP fluorescence was taken as the boundary of the cell. Only cells where the nuclear and cell boundaries could be clearly identified were measured. Cells throughout the valve were included.

3. Data were exported into Excel and SPSS 21 (IBM) for analysis.

8.3.3 Quantification of effect of connexin deletion on nuclear elongation and rotation at P0

A total of 3382 nuclei were measured. The numbers of nuclei contributing to the analysis in each group are provided in the results section in Table 2 and Table 3. For Cx37, 6 wildtype, 4 heterozygous knockout and 8 homozygous knockout littermate VV were analysed. For Cx43, 6 wildtype and 11 homozygous conditional deleted littermate VV were analysed. For Cx47, 5 wildtype, 6 heterozygous knockout and 6 homozygous knockout littermate VV were analysed.

1. Confocal z-stacks of VV were created as described in Chapter 3.

2. The Prox1 channel was isolated and a XY maximum projection produced and reflected/rotated so that the centreline of the vessel was horizontal in the image with blood flow from left to right.

3. Following the method of Tatin *et al*,[146] length and width were measured in NIH ImageJ software for all nuclei with Prox1^{hi} immunosignal above the background of adjacent vessel endothelium in the valve-forming region. The composite (four channel) z-stack was used to identify the boundaries of the vein and avoid measurement of non-venous nuclei.

4. The centre and angle of the length measurement line were extracted and used for nuclear position and rotation, respectively.

5. Data were exported to Microsoft Excel. The length:width ratio was calculated for each nucleus.

6. To appropriately convert nuclear rotation (0-360^{o}) into deviation away from the midline (0-90^{o}), the angle derived from each length measurement was converted to radians, and the following function applied:

Converted angle = asin(sqrt(sin^2) of original angle

The results of this equation are shown in Appendix 9.

7. The position of each nucleus was calculated relative to the most superior and inferior nucleus in the valve, generating a 'centile value' for the position of the measured nucleus across the vessel from superior to inferior. For grouped analyses each nucleus was automatically assigned to 1 of three groups (tertiles) according to its geometric position in the valve (y axis). The superior, middle, and inferior regions were respectively numbered tertiles 1-3 as shown in Figure 46.

8. Data for the length:width ratio and position of each nucleus were exported to SPSS 21 for analysis.

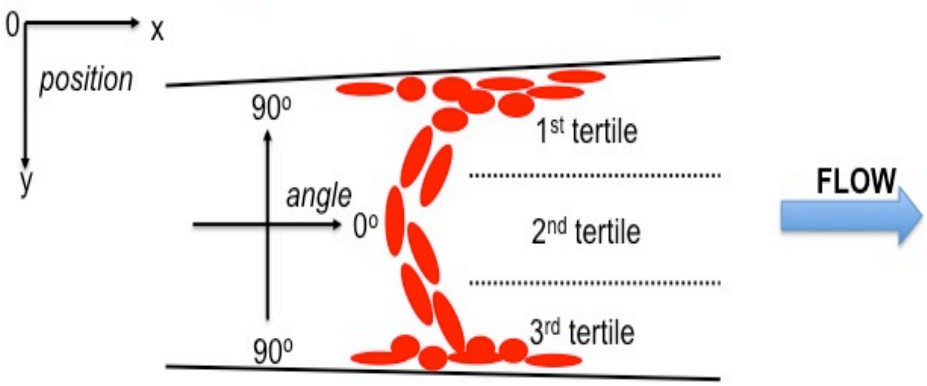

Figure 46 Quantification of nuclear phenotypes in venous valves
Nuclei were split into three groups according to position within the vein, according to the y coordinate of the center of the nuclear length measurement. Rotation was measured relative to the midline of the vessel.

8.3.4 Genotyping and immunofluorescence

Immunofluorescence imaging of murine VV and genotyping were carried out as described in the General Methods and Chapter 3. Confocal z-stacks of Cx37 and Cx43 immunolocalisation were not filtered. All solutions are given in Appendix 1, antibodies in Appendix 3 and primers in Appendix 4.

8.3.5 Localisation of Cx43 and Cx47 in human long saphenous vein VV

Segments of vein from patients undergoing coronary artery bypass grafting (with clinically normal long saphenous veins) were obtained and immunolocalisation for Cx43 and Cx47 was performed on acetone-fixed frozen sections using HRP-polymer amplification (Menarini diagnostics) and Vector SG substrate (Vector) as described in the General Methods chapter.

8.3.6 8.3.6 Statistical analysis

For comparison of stage of VV development Fisher's exact test was used, comparing wildtype with either heterozygous or homozygous knockouts for each stage. Data from multiple litters were pooled.

To assess for correlation between nuclear and cellular morphology (elongation, rotation) scatter plots were produced, and the Pearson's r and O value calculated.

For the analysis of the proportions of nuclei in each region of the vein that were elongated (length:width ratio ≥2) a chi square test was used, comparing heterozygous or homozygous deletion with wildtype littermates. Similarly, a Chi square test was used for the proportion of elongated nuclei in each region that were rotated ≥40degrees.

For analysis of the proportion of analysed nuclei that were located in each region of the vessel, an independent samples t-test was used for homozygous or heterozygous deletion compared with wildtype littermates.
All analyses were carried out in SPSS 21 (IBM corporation).

8.4 Results

8.4.1 Connexin expression at P0

At P0 Cx37 immunosignal was primarily detected around valve-forming cells, particularly in the upper and lower regions of the vein. Cx43 was not detected around Foxc2-expressing valve-forming cells, but rather in the upstream region in the upper half of the vein (Figure 47). Cx47 promoter activity was detected in a Cx47GFP reporter strain (which is heterozygous or homozygous knockout for Cx47) using anti-GFP antibodies. As expected, in labelled cells signal was detected not in a membranous pattern but distributed throughout the cell (Figure 48). GFP+ve cells were identifiable in the femoral vein distal to the valve region and in the region of the developing valve (Figure 48, Figure 57)

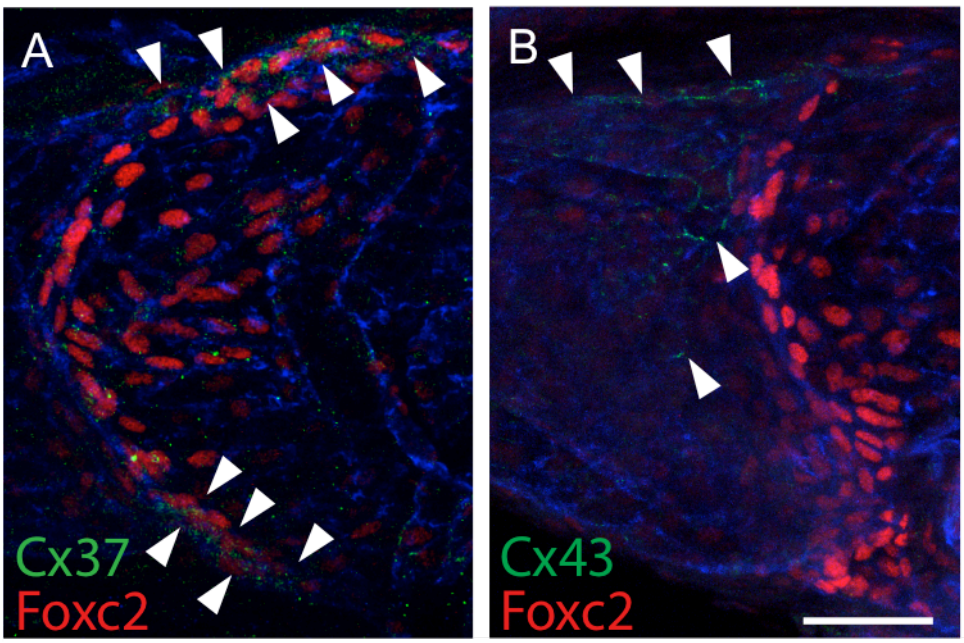

Figure 47 Expression of Cx37,43 in the valve-region at P0
A) At P0, Cx37 was most strongly localized around the Prox1+ VFC's (between the arrowheads in A)

B) Cx43 was localized to the upstream region of the vein in an endothelial pattern (area outlined by arrowheads in B). Blue = Pecam1. Representative images from n≥3 per group. Scale 50μm.

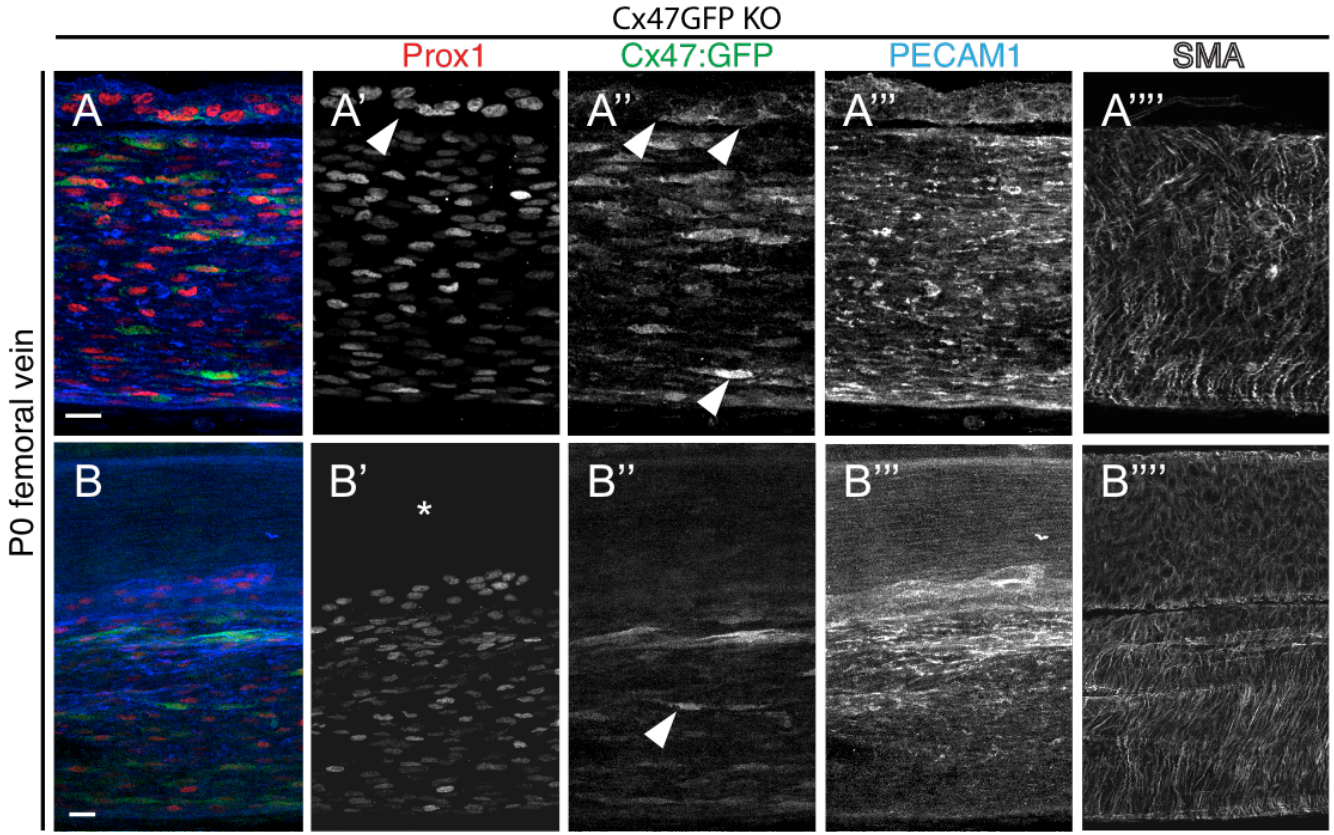

Figure 48 Cx47GFP signal in distal femoral vein at P0
A and B) Two examples of Cx47GFP reporter (Cx47 knockout) signal in the distal femoral vein (not the valve region) at P0, with immunolocalisation of Prox1, PECAM1, SMA. GFP^{+} cells are readily identifiable in the FV (large arrowheads in A'' and B''), and in lymphatics (small arrowheads in A''). Prox1 expression in the lymphatic is marked by an arrowhead in A'. * in B' marks the position of an artery, seen to be GFP^{-} in B''. Scale bars 20μm. Flow direction left to right. For clarity SMA signal is omitted from A and B.

8.4.2 Effect of constitutive deletion of Cx37 (GJA4) analysed at P0

Whilst wildtype and heterozygous constitutive Cx37 knockout valves developed normally to stage 1, homozygous deletion almost entirely prevented progression to stage 1 of development (Figure 49). Prox1^{hi} cells were still identified across the vein at P0, but appeared disorganised with a failure to show a normally elongated and rotated morphology (Figure 50).

A

	Wildtype	Heterozygous knockout		Homozygous knockout	
	n	n	P	n	P
Stage 0	0	0	ns	22	**<0.0005**
Stage 1	6	16	ns	2	**<0.0005**
Total analysed	6	16		24	

B

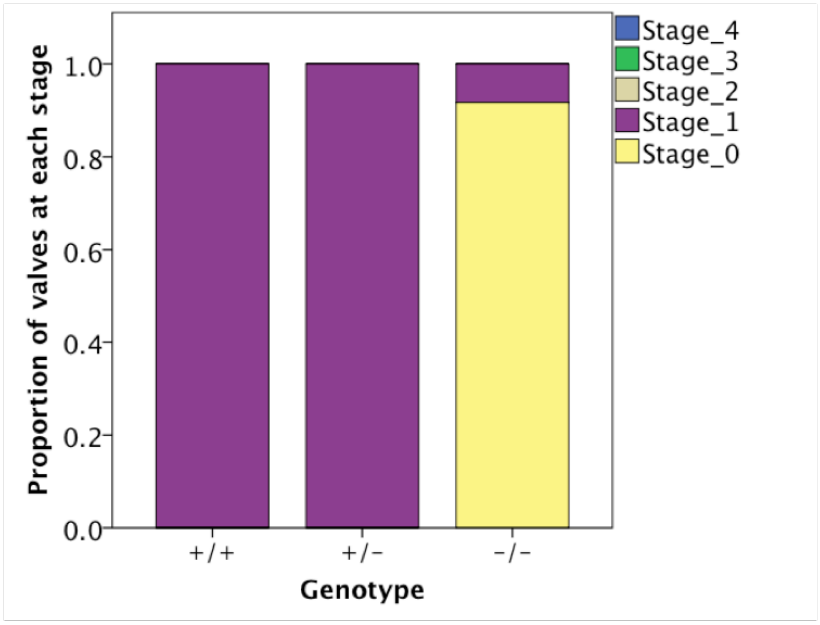

Figure 49 Valve development at P0 following constitutive deletion of Cx37
A) The table provides the total number of VV analysed for each genotype and the number of VV identified at each stage. Homozygous knockout of Cx37 resulted in a failure of normal organisation to reach stage 1 of VV development, compared to heterozygous knockout and wildtype littermates that developed normally. Fisher's exact test. ns= >0.05

B) The proportion of valves at each stage is shown for each genotype. +/+ = wildtype (n=3 mice), +/- = heterozygous knockout (n=11) -/- = homozygous knockout (n=14).

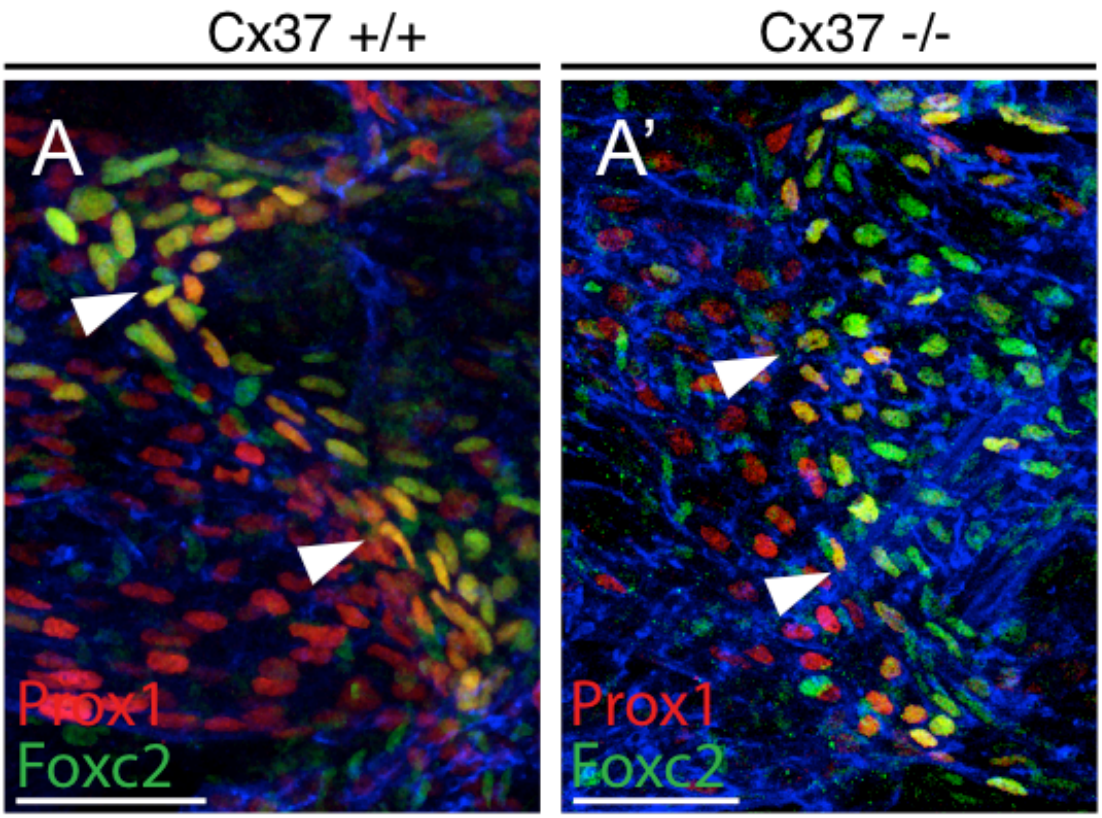

Figure 50 Morphological changes in valve development at P0 following constitutive deletion of Cx37

Analysis at P0 following constitutive homozygous deletion of Cx37 showed a failure of organisation with reduced elongated and rotation of valve-forming cells (arrowheads in A'), compared with wildtype littermates in which normally elongated and rotated VFC's are seen (arrowheads in A). Arrowheads indicate line of Prox1^{hi} VFC's (not individual specific nuclei). Scale bar 50μm. Green = Foxc2, red = Prox1, blue=Pecam1 immunolocalisation. Flow left to right.

8.4.3 Effect of constitutive deletion of Cx37 (GJA4) analysed at P6

At P6, whilst wildtype controls and heterozygous constitutive deletion did not affect valve development, homozygous deletion of Cx37 resulted in complete absence of Prox1^{hi} valve cells (Figure 51). Accordingly, no gap was seen in SMA positive pericytes (Figure 52).

A

	Wildtype	Heterozygous knockout		Homozygous knockout	
	n	n	P	n	P
Stage 0	0	0	ns	29	**0.011**
Stage 2	0	3	ns	0	ns
Stage 3	1	23	ns	2	ns
Stage 4	1	10	ns	0	ns
Total analysed	2	36		31	

B

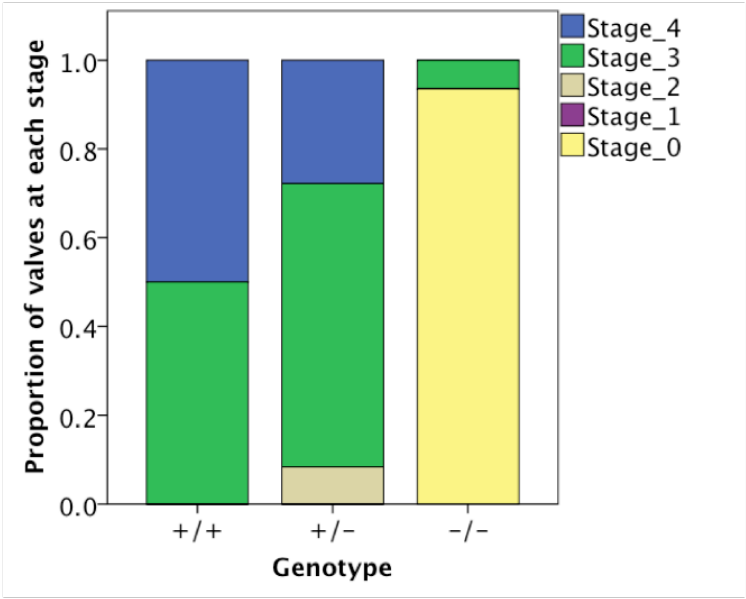

Figure 51 Valve development at P6 following constitutive deletion of Cx37
A) The table provides the total number of VV analysed for each genotype and the number of VV identified at each stage. Homozygous knockout of Cx37 resulted complete absence of identifiable Prox1^{+} or Foxc2^{+} valve cells at P6, compared to heterozygous knockout and wildtype littermates that developed normally. Fisher's exact test. ns= >0.05

B) The proportion of valves at each stage is shown for each genotype. +/+ = wildtype (n= 2 mice), +/- = heterozygous knockout (n=18 mice), -/- = homozygous knockout (n=16 mice).

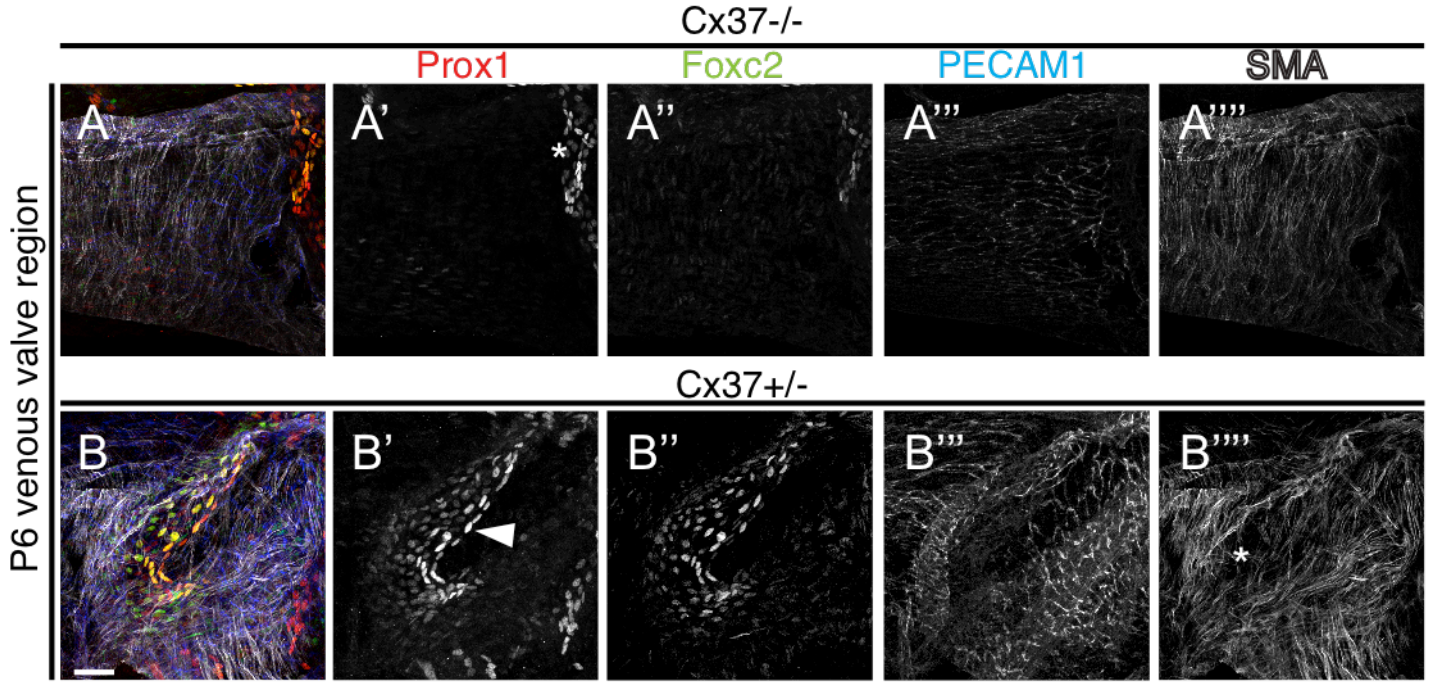

Figure 52 Valve morphology at P6 in mice with constitutive deletion of Cx37
A-A'''') Shows the region where a VV is normally found in a homozygous Cx37 knockout pup.

B-B'''') Shows the same region in a heterozygous knockout littermate, which has developed a normal-appearing stage 4 valve.

Homozygous constitutive deletion resulted in complete loss of Prox1^{hi} valve cells by P6, whilst heterozygous Cx37 deletion resulted in normal valve development (arrowhead in B') Homozygous deletion was associated with loss (in A'''') of the normal reduction (* in B'''') in SMA-expressing pericytes around the VV. A Prox1^{+}, Foxc2^{+} lymphatic is marked with * in A'. Scale bar 50μm. Blood flow is from left to right.

8.4.4 Effect on valve development at P0 of conditional deletion of Cx43 (GJA1) from E15.

Conditional deletion of GJA1 (encoding Cx43) from E15 resulted in a loss of normal valve organisation at P0, albeit the phenotype was not as strong at that seen with deletion of Cx37 or Cx47 (Figure 53, Figure 54). Relative to other connexin deletions, there was increased variability in the Cx43 homozygous deletion VV phenotype when analysed at P0, with some valves appearing relatively normal (Figure 53).

A

	Effective wildtype	Homozygous deletion	
	n	n	P
Stage 0	0	9	**0.005**
Stage 1	7	4	**0.005**
Total analysed	7	13	

B

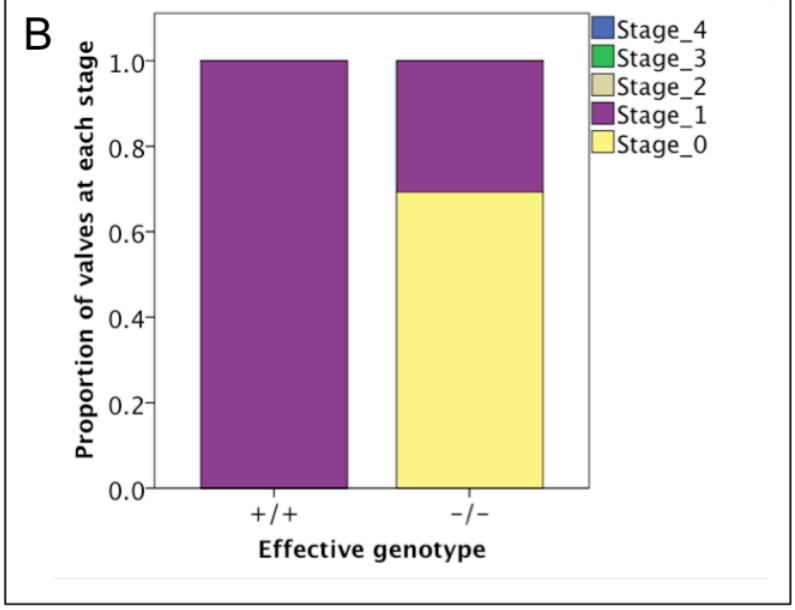

Figure 53 Valve development at P0 after conditional deletion of Cx43 from E15

A) The table provides the total number of VV analysed for each genotype and the number of VV identified at each stage. Homozygous conditional deletion of GJA1 (Cx43) resulted in significantly fewer valves reaching stage 1 compared to wildtype littermates that developed normally. Fisher's exact test.

B) The proportion of valves at each stage are shown for each genotype. +/+ = wildtype (n=6 mice), -/- = homozygous conditional deletion (n=6 mice).

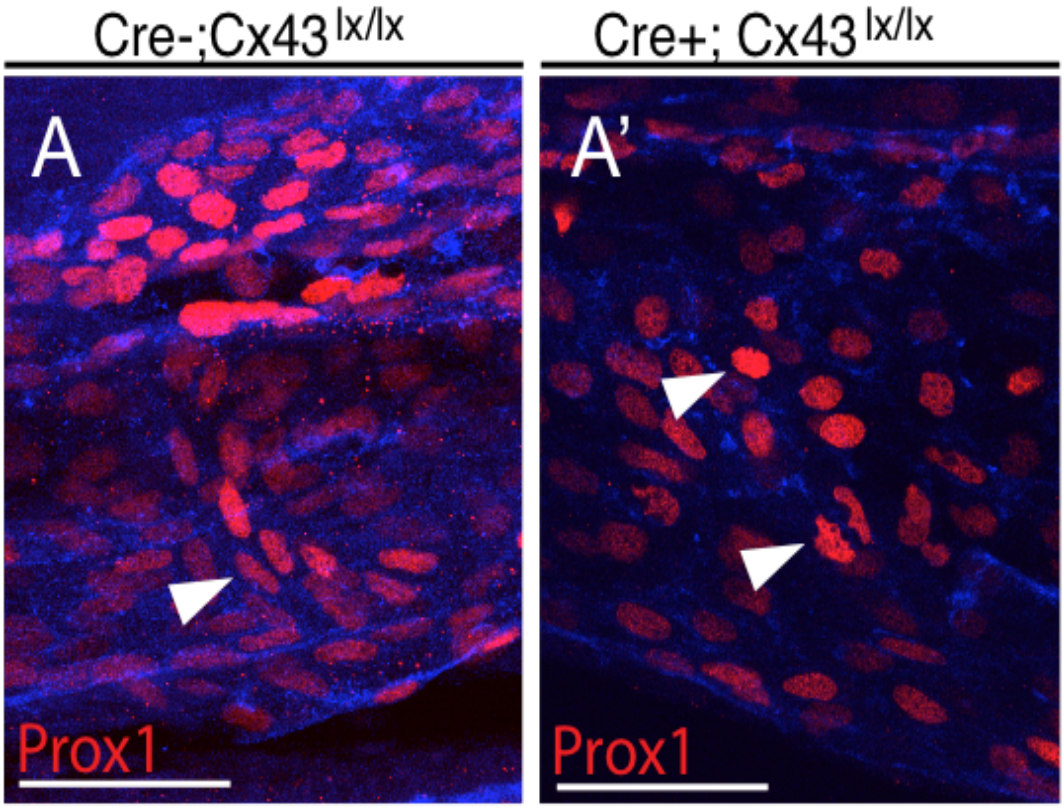

Figure 54 Conditional deletion of Cx43 analysed at P0

A) Wildtype littermates developed relatively normally and showed a line of rotated Prox1^{hi} valve-forming cells (line marked by arrowhead in A)

A') Conditional homozygous deletion of Cx43 resulted in a phenotype in which Prox1^{hi} valve-forming cell nuclei were identifiable but did not appear normally organized, and appeared less elongated and rotated (two examples identified by arrowheads in A').

Red = Prox1, blue=Pecam1. Blood flow left to right. Scale bar 50μm

8.4.5 Effect of conditional deletion of Cx43 (GJA1) from P0 on valve development at P6

No significant phenotype was detected at P6 following conditional deletion of Cx43 at P0 (Figure 55), indicating that the critical requirement for Cx43 activity is limited to around P0.

A

	Effective wildtype	Homozygous deletion	
	n	n	P
Stage 2	0	1	ns
Stage 3	3	5	ns
Stage 4	1	2	ns
Total analysed	4	8	

B

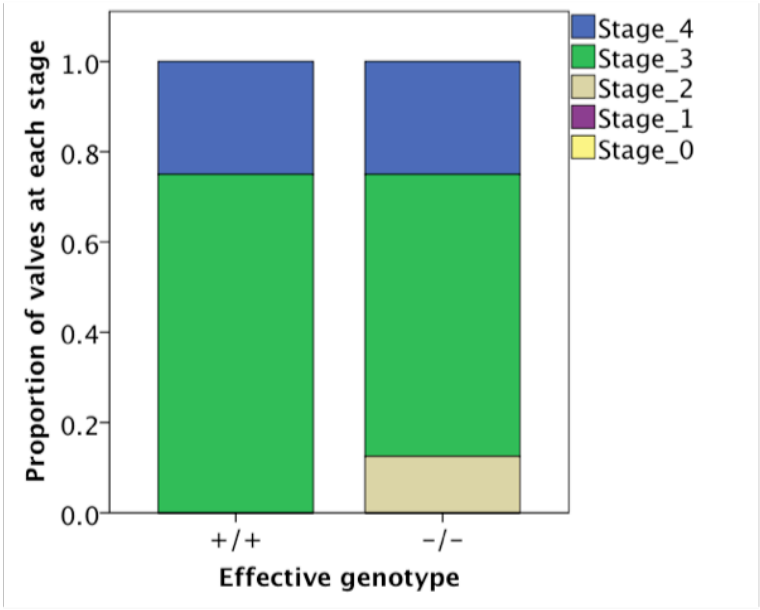

Figure 55 Valve development at P6 following conditional deletion of Cx43 from P0

A) The table provides the total number of VV analysed for each genotype and the number of VV identified at each stage. Conditional deletion of Cx43 from P0, analysed at P6, did not reveal any significant phenotype. Fisher's exact test. ns=P>0.05

B) The proportion of valves at each stage is shown for each genotype. +/+ = wildtype (n=2 mice), -/- = homozygous conditional deletion (n=4 mice).

8.4.6 Constitutive deletion of GJC2 (Cx47) analysed at P0

Whilst valves in wildtype littermates and those with heterozygous deletion of Cx47 from E15 developed normally, homozygous constitutive deletion resulted in a failure of organisation of Prox1^{hi} valve-forming cells (Figure 56, Figure 57). The lack of any amplified GFP signal in wildtype littermates confirmed the specificity of the anti-GFP antibody and imaging of Cx47:GFP signal (Figure 57).

A

	Wildtype	Heterozygous knockout		Homozygous knockout	
	n	n	P	n	P
Stage 0	0	0	ns	11	**0.001**
Stage 1	8	10	ns	3	**0.001**
Total analysed	8	10		14	

B

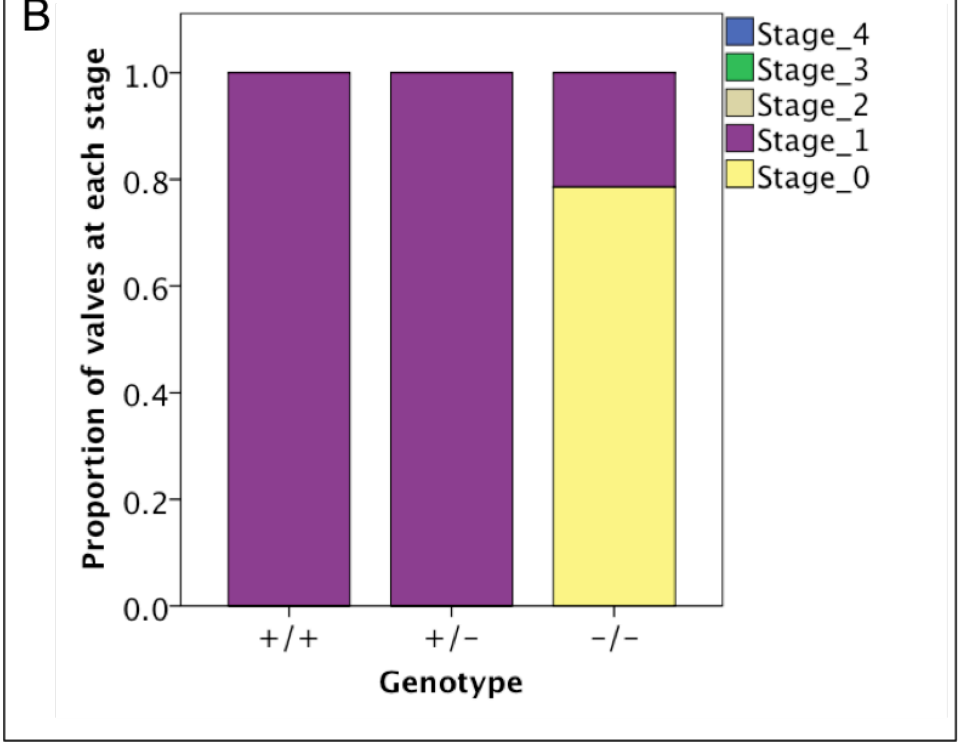

Figure 56 Constitutive deletion of Cx47 in Cx47GFP reporter at P0.
A) The table provides the total number of VV analysed for each genotype and the number of VV identified at each stage. Constitutive homozygous knockout of Cx47 resulted in failure of organisation to stage 1 of development. Prox1^{hi} cells remained identifiable. Heterozygous deletion of Cx47 did not produce a phenotype. Fisher's exact test.

B) The proportion of valves at each stage is shown for each genotype. +/+ = wildtype (n=4 mice), +/- = heterozygous knockout (n=5), -/- = homozygous knockout (n=8).

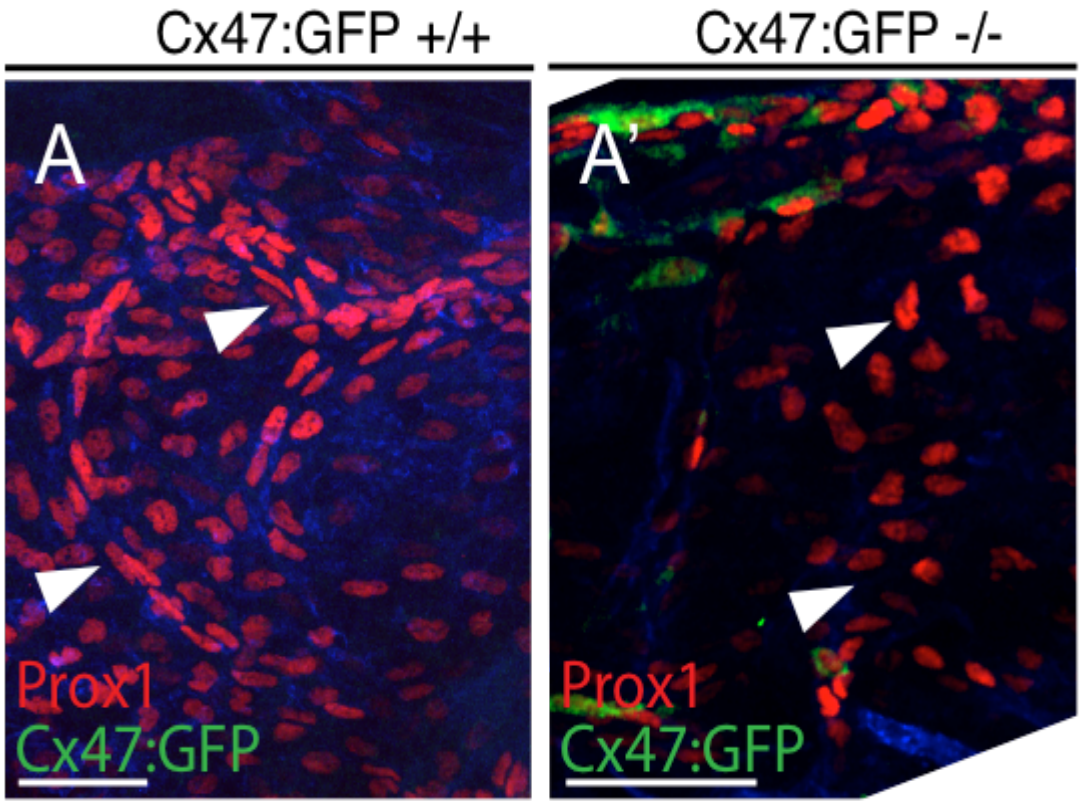

Figure 57 Constitutive Cx47 deletion analysed at P0

A) In wildtype littermates a line of rotated and elongated Prox1^{hi} valve-forming cell nuclei was clearly identified (indicated by arrowheads in A)

A') Homozygous knockout of Cx47 (in the Cx47GFP reporter) resulted in a clear phenotype in which Prox1^{hi} valve-forming cell nuclei remained identifiable in a band across the vein (position indicated by arrowheads in A'), but appeared less elongated and rotated, and overall less organized.

Scale bar 50μm. Green = amplified GFP in Cx47:GFP reporter. Note absence of GFP signal in WT littermate (A). Blue=Pecam1. Flow left to right.

8.4.7 Constitutive deletion of GJC2 (Cx47) analysed at P2

Analysis of homozygous Cx47 deleted valves at P2 showed a similar phenotype to Cx37 deletion at P6, with a complete absence of Prox1^{hi} valve cells (Figure 58, Figure 59). This indicates a critical requirement for Cx47 in the maintenance of the abnormal valve structure forming at P0, and a clear structural phenotype caused by loss of GJC2. In additional, GFP^{+} cells were greatly reduced and almost undetectable in the vein at P2 (but were detectable in other structures, Figure 59). No significant phenotype was seen in the limited number of VV analysed following heterozygous deletion (Figure 58, Figure 59).

A

	Wildtype	Heterozygous knockout		Homozygous knockout	
	n	n	P	n	P
Stage 0	0	0	ns	12	**0.001**
Stage 1	2	1	ns	0	ns
Stage 2	0	1	ns	0	-
Stage 3	2	2	ns	0	ns
Total analysed	4	4		12	

B

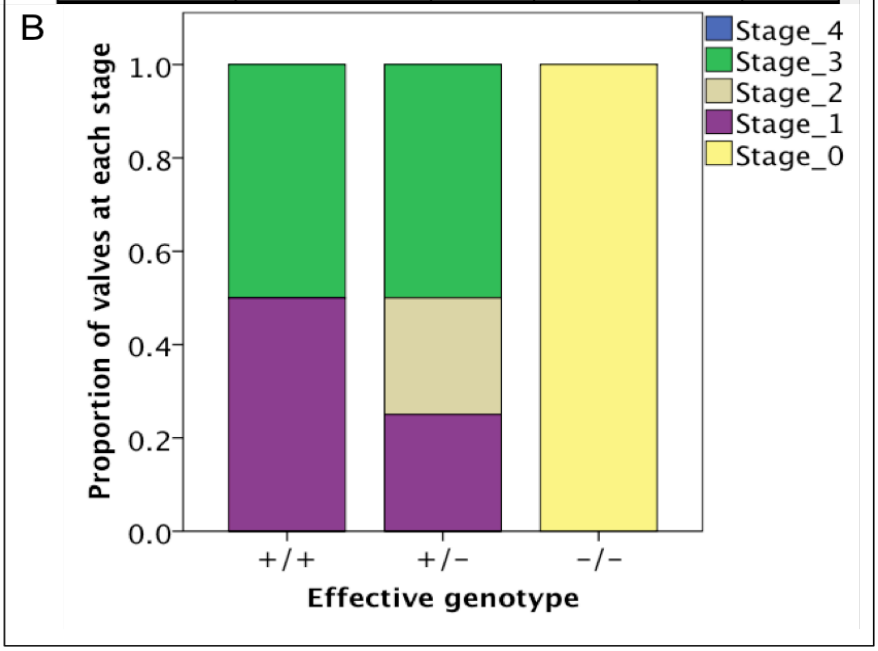

Figure 58 Constitutive deletion of GJC2 analysed at P2

A) The table provides the total number of VV analysed for each genotype and the number of VV identified at each stage. Homozygous knockout of Cx47 resulted in almost complete absence of valve cells by P2. Heterozygous knockout of Cx47 did not produce a phenotype. Wildtype littermates developed relatively normally, although none were observed at stage 4. P= Fisher's exact test. ns=P>0.05

B) The proportion of valves at each stage is shown for each genotype. +/+ = wildtype (N=2 mice), +/- = heterozygous knockout (N=2), -/- = homozygous knockout (N=6).

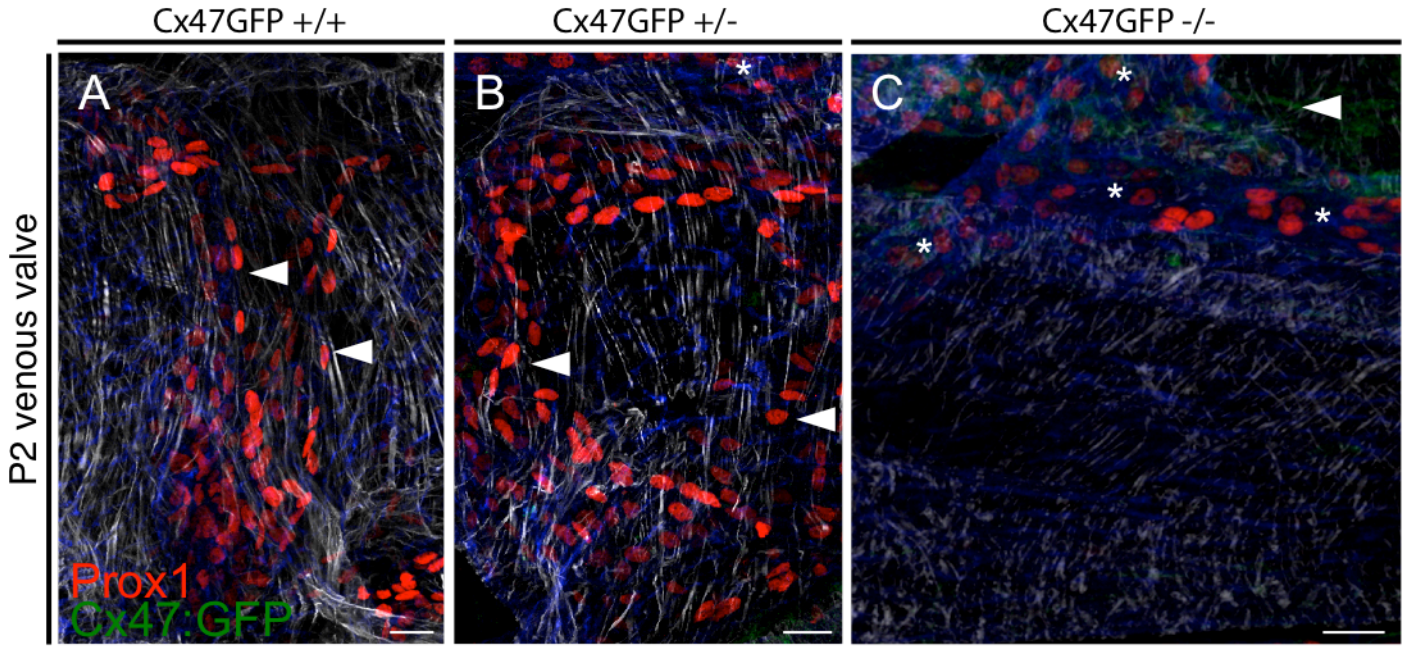

Figure 59 Constitutive Cx47 deletion analysed at P2

VV developed normally in wildtype littermates and heterozygous knockouts (arrowheads in A and B). Prox1hi VFC's were absent from homozygous knockouts at P2 (C) but Prox1 remained identifiable in neighbouring lymphatics (* in B and C). GFP signal from Cx47-expressing cells was greatly reduced at P2 compared to P0, but was still detectable around the neighbouring artery (arrowhead in C). Note in A & B Prox1 signal is barely detectable in the vein around the valve. Scale bars 20μm. Flow left to right.

8.4.8 Correlation of nuclear and cellular morphology in valve-forming cells at P0

Analysis of nuclear and cellular morphology in Prox1^{hi} valve-forming cells at late E18 showed a strong significant correlation between measurements of nuclear and cellular rotation (Pearson's r=0.99, P<0.0001, Figure 60), and nuclear and cellular elongation (Pearson's r=0.81, P<0.0001, Figure 61). A 2D maximum projection of a z stack (from which measurements were obtained in individual optical sections) is shown in (Figure 27). The nuclear specificity obtained by immunolocalisation of Prox1 is demonstrated in which Prox1 colocalises with nuclear-targeted GFP. These results indicate that in these cells at this time point, measurement of nuclear morphology based on Prox1 immunostaining could be used as a marker for cellular morphology.

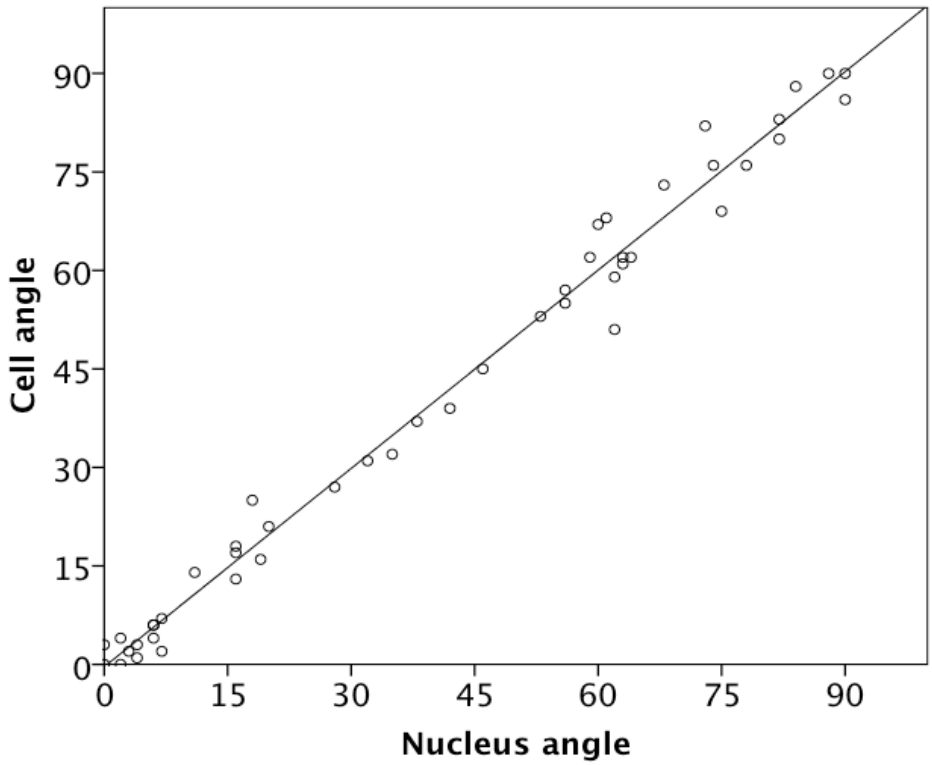

Figure 60 Correlation between cell rotation and nucleus rotation in VFC's

The angle of the long axis of the nucleus and the cell were measured in 47 cells in 2 valves. Pearson's r=0.99, P<0.0001. A line of best fit through the origin is shown. Prox1CreERT2;mTmG mice were given tamoxifen at E15 and analysed at late E18 with immunostaining for Prox1. Only Prox1^{hi} valve-forming cells, where the cell membrane was clearly defined, were measured. Rotation was measured relative to the axis of the image.

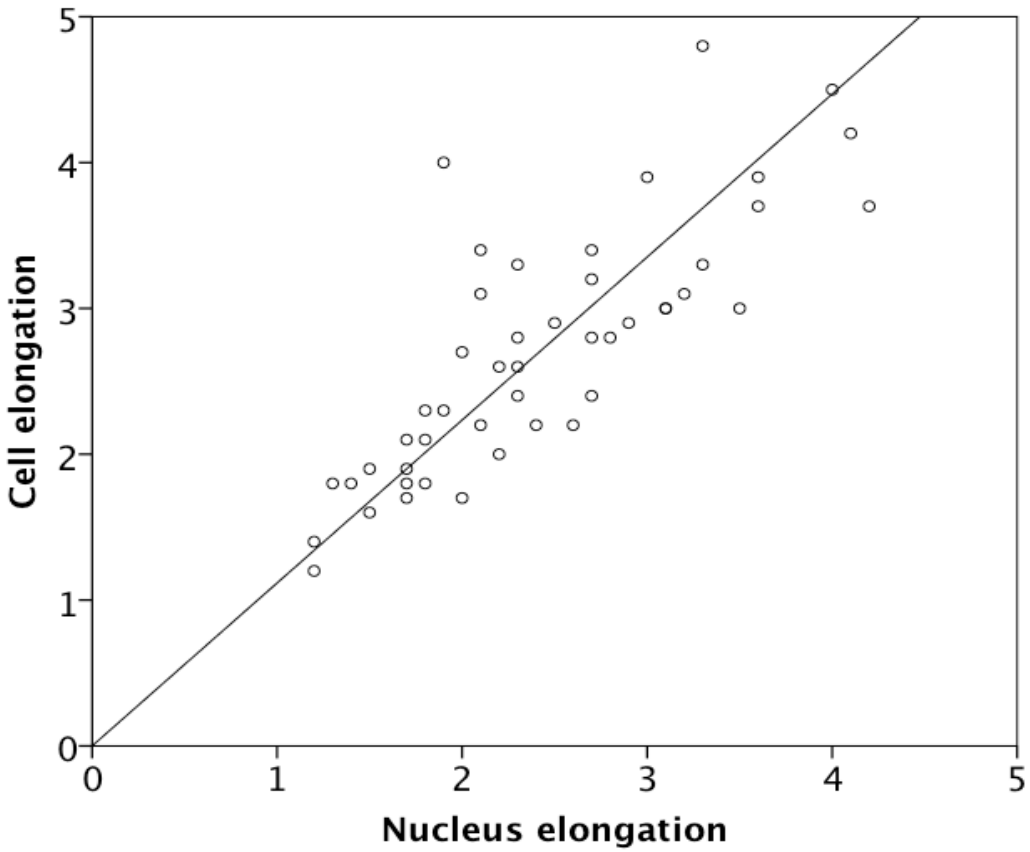

Figure 61 Correlation of cell and nucleus elongation in VFC's

The length of the long axis of the nucleus and of the cell, as marked by membrane-tagged GFP, were measured in 47 cells in single optical sections from confocal z-stacks. Pearson's r= 0.81, P<0.0001. A line of best fit through the origin is shown. Prox1CreERT2;mTmG mice were given tamoxifen at E15 and analysed at late E18 with immunostaining for Prox1, and only Prox1^{hi} valve-forming cells where the membrane was clearly defined were measured. Elongation (of cell or nucleus) = length:width ratio. Although this correlation is weaker that that for rotation, it remains strong and it can be seen that the cutoff of nuclear elongation of 2 used in subsequent analyses will correctly identify elongated cells.

8.4.8.1 Morphology of wildtype Prox1^{hi} nuclei at P0

No correlation was found between elongation and rotation of individual nuclei, and these parameters were analysed separately. (Appendix 9, Figure 102). Analysis of the variation in WT Prox1^{hi} nuclear rotation across the y-axis (from superior to inferior) demonstrated clear variation, with the most rotated nuclei present in the central region of the vessel. (Appendix 9, Figure 103, Figure 104) This is consistent with the qualitative description of VV development given in Figure 21. No substantial variation was seen in WT Prox1^{hi} nuclear elongation across the vessel (Figure 105). Because the variation in nuclear morphology across the vein precluded pooled analysis of all nuclei,

subsequent analyses in this chapter were performed within each tertile (1st – superior third, 2nd – middle third, 3rd – inferior third, Figure 46).

8.4.9 Cellular morphology phenotypes following GJA1, GJA4, GJC2 deletion

The elongation of Prox1^{hi} valve-forming cells was analysed in wildtype littermates and following constitutive deletion of Cx37 or Cx47, or conditional deletion of Cx43 (Table 2, Figure 62-Figure 64). The upper (1st tertile), middle (2nd tertile) and lower (3rd tertile) of the vein was analysed separately, because these regions displayed different mean nuclear rotation in a pooled analysis of wildtype cells (Figure 46). The proportion of nuclei with length:width ratio ≥2 was significantly reduced in the 2nd and 3rd tertiles following homozygous loss of Cx37. Homozygous deletion of Cx43 produced significant reductions in elongation in all regions, whilst homozygous deletion of Cx47 resulted in reduced elongation only in the 1st tertile.

Nuclear rotation was analysed for nuclei that were elongated with length:width ratio ≥2 (Table 3, Figure 62-Figure 64). The proportions of nuclei rotated ≥40^0 was significantly reduced compared with wildtype littermates, in all regions of the vein following constitutive homozygous Cx37 deletion. Conditional homozygous deletion of Cx43 or constitutive homozygous deletion of Cx47 resulted in reductions in nuclear rotation in the upper and middle regions of the vein.

Table 2 Prox1^{hi} nuclear elongation phenotypes with connexin deletion.
P values represent Chi square analysis of heterozygous or homozygous deletion versus WT for the proportion of nuclei of each genotype elongated ≥2. Tertiles refer to the y-axis position across the vein

Protein	Tertile	Genotype	n cells	Median elongation	n elongated ≥2	Proportion elongated ≥2	p Vs WT
Cx37	1st	WT	209	2.2	127	61%	-
		Het	161	2.3	100	62%	ns
		KO	142	2.1	79	56%	ns
	2nd	WT	161	2.2	105	65%	-
		Het	98	2.3	73	74%	ns
		KO	67	1.6	18	27%	**<0.0005**
	3rd	WT	189	2.4	132	70%	-
		Het	31	2.4	20	65%	ns
		KO	138	2.0	73	53%	**0.002**
Cx43	1st	WT	157	2.3	114	73%	-
		KO	189	2.2	118	62%	**0.045**
	2nd	WT	133	2.3	93	70%	-
		KO	186	2.1	107	58%	**0.024**
	3rd	WT	185	2.4	127	69%	-
		KO	165	2.0	89	54%	**0.005**
Cx47	1st	WT	171	2.5	137	80%	-
		Het	268	2.5	199	74%	ns
		KO	114	2.3	76	67%	**0.01**
	2nd	WT	80	2.2	52	65%	-
		Het	95	2.2	57	60%	ns
		KO	90	2.0	50	56%	ns
	3rd	WT	103	2.2	66	64%	-
		Het	141	2.6	104	74%	ns
		KO	109	2.0	58	53%	ns
		(Total:	**3382**		**2174)**		

Table 3 Prox1^{hi} elongated nuclear rotation phenotypes with connexin deletion.

Rotation was only analysed in nuclei elongated ≥2. P values represent Chi square analysis of heterozygous or homozygous deletion versus WT for the proportion of nuclei rotated ≥40 degrees relative to the long axis of the vessel.

Protein	Tertile	Genotype	Cells analysed	Median angle	n rotation ≥40	Proportion rotated ≥40	p Vs WT
Cx37	1st	WT	127	26	32	25%	-
		Het	100	18	28	28%	ns
		KO	79	15	7	9%	**0.004**
	2nd	WT	105	37	51	49%	-
		Het	73	31	29	40%	ns
		KO	18	21	3	17%	**0.01**
	3rd	WT	132	27	48	36%	-
		Het	20	14	7	35%	ns
		KO	73	22	11	15%	**0.001**
Cx43	1st	WT	114	28	34	30%	-
		KO	118	24	12	10%	**<0.0005**
	2nd	WT	93	24	43	46%	-
		KO	107	18	18	17%	**<0.0005**
	3rd	WT	127	28	29	23%	-
		KO	89	16	22	25%	ns
Cx47	1st	WT	137	16	26	19%	-
		Het	199	11	9	5%	**<0.0005**
		KO	76	8	4	5%	**0.006**
	2nd	WT	52	50	33	63%	-
		Het	57	36	27	47%	ns
		KO	50	16	16	32%	**0.001**
	3rd	WT	66	21	14	21%	-
		Het	104	24	20	19%	ns
		KO	58	28	19	33%	ns
		(Total	**2174)**				

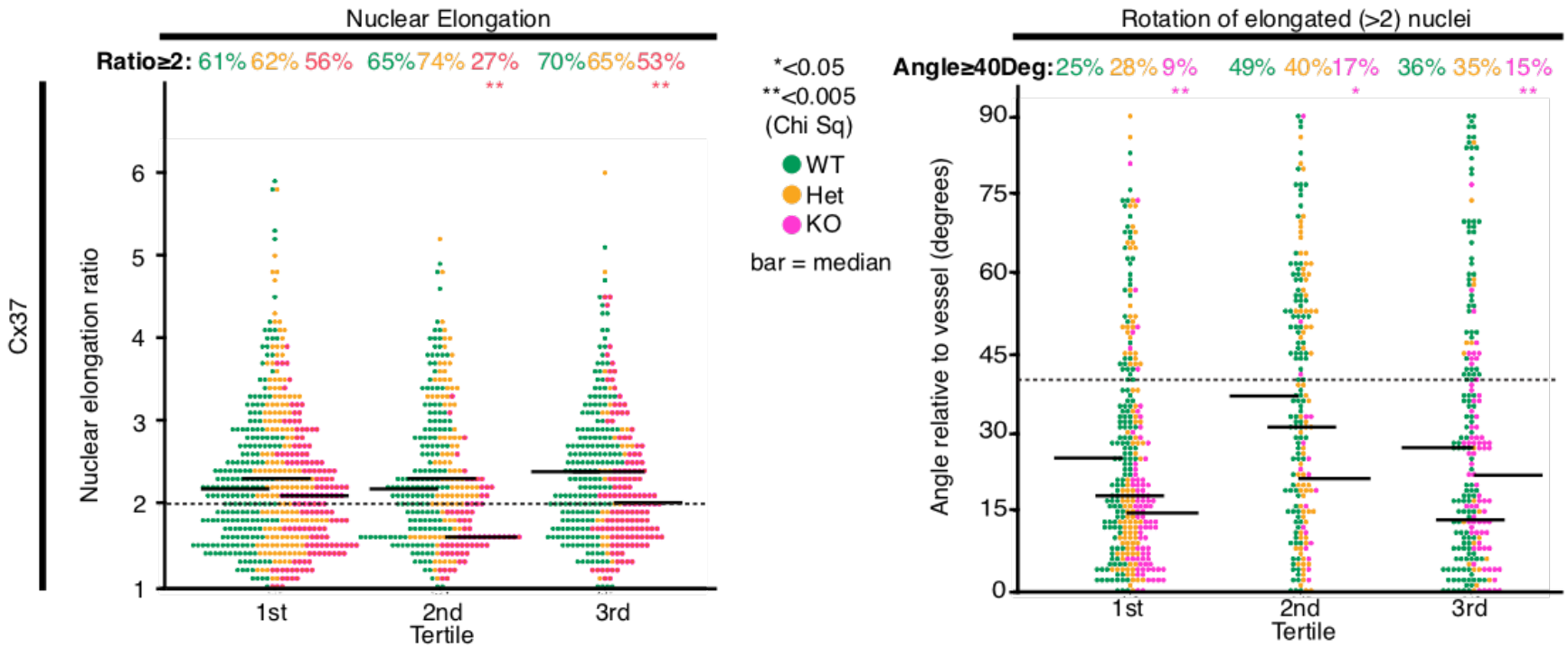

Figure 62 Analysis of nuclear morphology following Cx37 deletion

Each dot represents a single Prox1^{hi} nucleus. The proportion of nuclei elongated ≥2 (dotted line) was analysed for each region and is shown above each group. Rotation was examined in elongated nuclei, and the proportion rotated ≥40^{0} (dotted line) is shown above each group. Tertiles refer to the y axis position across the vein (see Figure 46).

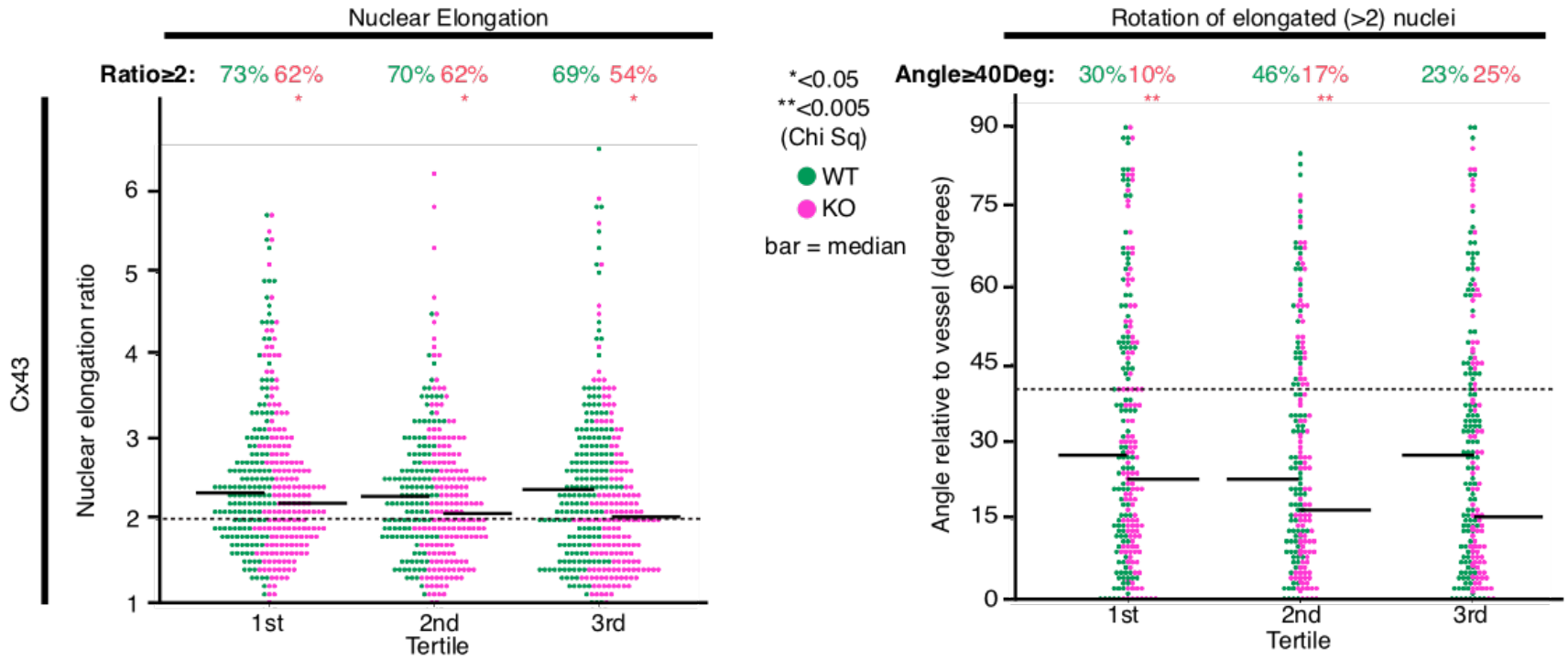

Figure 63 Analysis of nuclear morphology following Cx43 deletion

Each dot represents a single Prox1^{hi} nucleus. The proportion of nuclei elongated ≥2 (dotted line) was analysed for each region and is shown above each group. Rotation was examined in elongated nuclei, and the proportion rotated ≥40^{0} (dotted line) is shown above each group. Tertiles refer to the y axis position across the vein (see Figure 46).

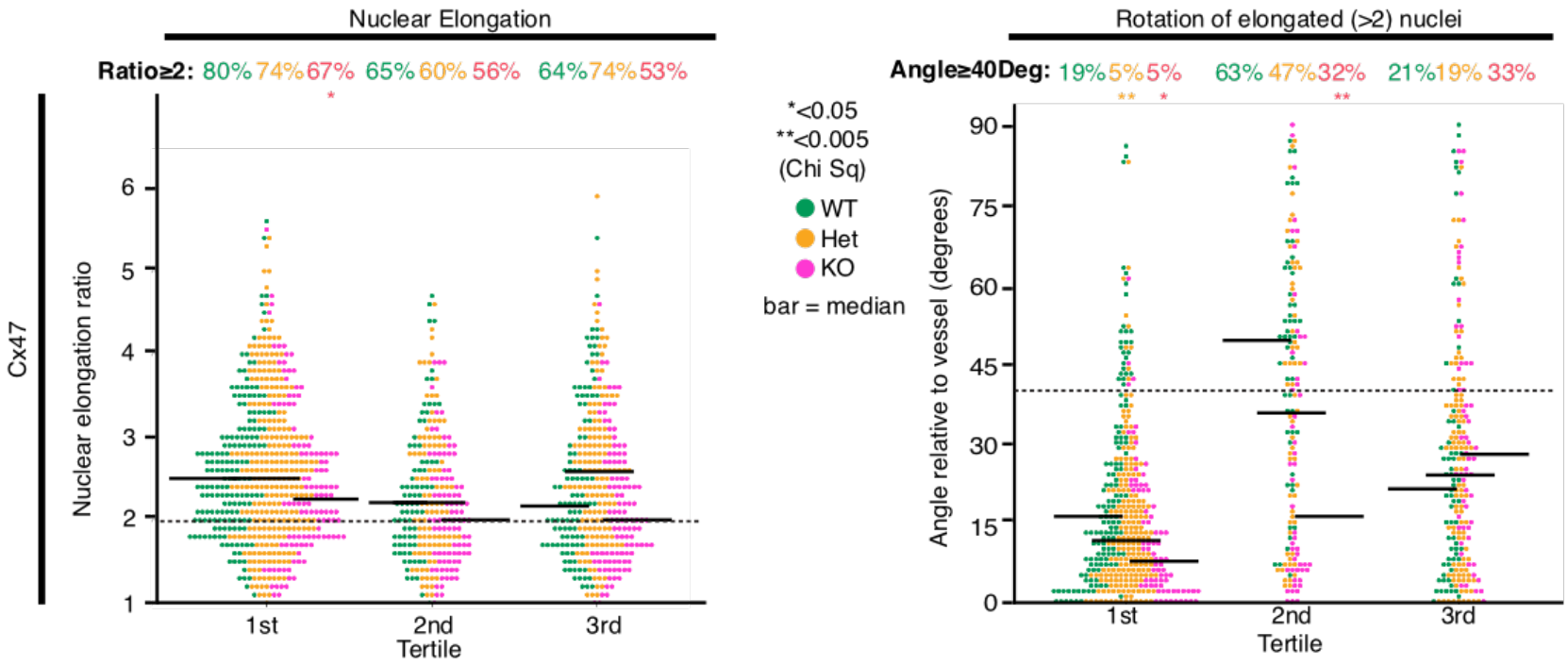

Figure 64 Analysis of nuclear morphology following Cx47 deletion

Each dot represents a single Prox1^{hi} nucleus. The proportion of nuclei elongated ≥2 (dotted line) was analysed for each region and is shown above each group. Rotation was examined in elongated nuclei, and the proportion rotated ≥40^{0} (dotted line) is shown above each group. Tertiles refer to the y axis position across the vein (see Figure 46).

8.4.10 Proportions of measured VFC's in each region of the vein at P0

It has been suggested that VFC's migrate around the lymphatics vessel to form the ring in early lymphatic valve formation (equivalent to VV stage 1).[42] Analysis, in each VV, of the proportion of VFC's in each region of the vein (by tertile) showed no difference in the proportions of cells in each region for conditional homozygous deletion of Cx43 or constitutive heterozygous knockout of Cx47. Homozygous knockout of Cx37 resulted in a lower proportion of Prox1^{hi} cells identified in the central region of the vein. The mean proportion in wildtype valves was 0.280 Vs 0.195 in homozygous knockout valves, P =0.003 (independent samples t test).

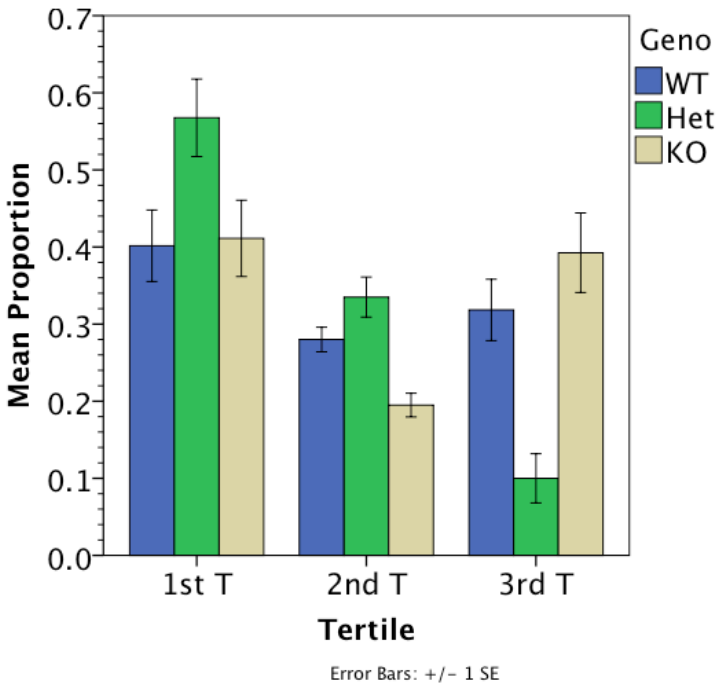

Figure 65 Proportion of measured VFC's in each region of vein at P0 following Cx37 knockout

Knockout of Cx37 resulted in significantly lower proportion of Prox1^{hi} cells identified in the 2nd tertile (central region). Mean proportion (wildtype) 0.280 Vs (KO) 0.195, P=0.003 (independent samples t test). Corresponding increases in the proportion in tertiles 1 and 3 did not reach statistical significance. Heterozygous deletion resulted in a significantly higher proportion of cells in tertile 1 and corresponding reduced proportion in tertile 3 (P=0.046 and P=0.004, respectively), compared with wildtype.

8.4.11 Expression of connexins 43 and 47 in human adult normal venous valves

Connexins 43 and 47 were immunolocalised in human long saphenous vein valve leaflets. Signal from Cx43 was preferentially detected on the sinus surface of the leaflet (Figure 66), whilst Cx47 signal was detected throughout the leaflet (Figure 67). Both proteins were localised in a membranous-type expression pattern.

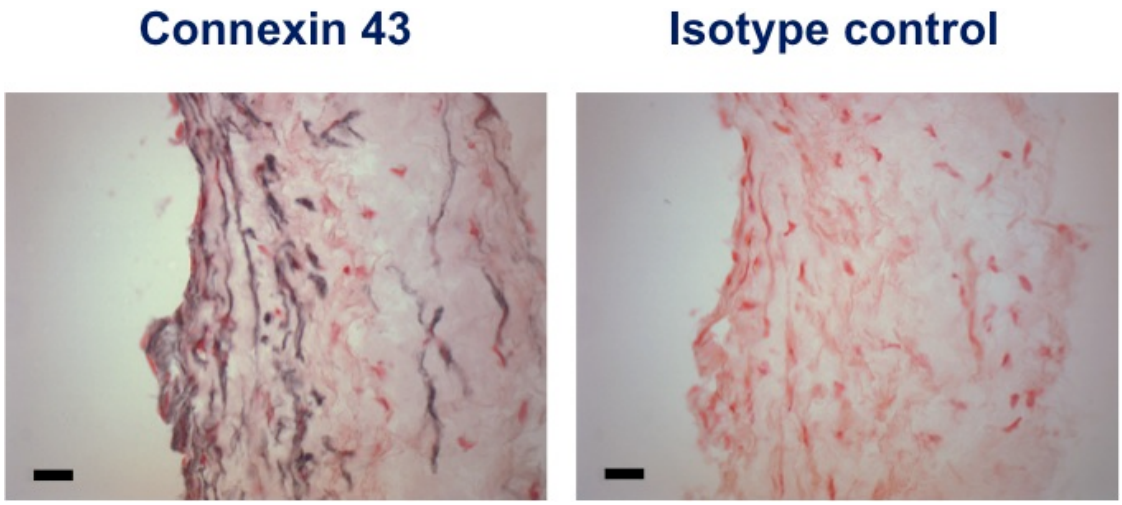

Figure 66 Localisation of Cx43 in human long saphenous vein valve leaflets by immunohistochemistry.
Cx43 was localised to the sinus side of the valve leaflets, including interstitial cells. Nuclear fast red counterstain. Scale 20μm.

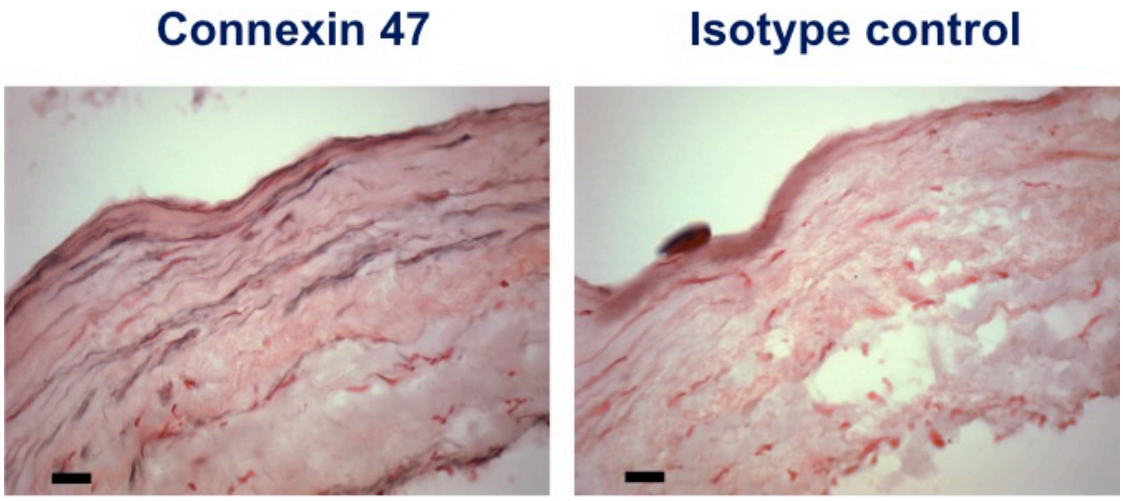

Figure 67 Localisation of Cx47 in human long saphenous vein valve leaflet by immunohistochemistry.
Nuclear fast red counterstain. Scale 20μm. Cx47 immunostaining was identified throughout the leaflet.

8.5 Discussion

After these result were obtained, and consistent with these findings, it was reported that adult Cx37$^{-/-}$ mice lack venous valves.[111] The cellular cause of this abnormality has not previously been described, and to the best of my knowledge no VV phenotype associated with loss of Cx43 or Cx47 has been described.

A genetic loss of function approach to connexins 37, 43, 47 produced a grossly similar phenotype for all three proteins. At P0 the Prox1^{hi} VFC's were generally identified in the correct region of the vein, and were distributed across the width of the vein, but they displayed abnormal morphology, as measured by immunostaining of their nuclei. Importantly, almost all VFC's were unidentifiable at P6 or P2 following loss, respectively, of Cx37 or 47, whilst conditional deletion of Cx43 in Prox1-expressing cells after P0 showed no phenotype. Taken together with the observation that Prox1^{hi} VFC's were present at P0, these results strongly suggest that the failure of normal events around P0 are responsible for failure to develop normal VV in these mice. The increasingly severe phenotype from P0 to P2/6, together with the previously reported adult Cx37$^{-/-}$ phenotype, excludes developmental delay. It remains unclear whether failure of on-going valve formation is caused by loss of connexin function, or secondary to the abnormal organisation of Prox1^{hi} cells seen at P0, which presumably affects other signalling processes.

Connexins 37, 43 and 47 had very different expression patterns around the developing VV at P0. Whilst Cx37 immunosignals were strongest around the Prox1^{hi} VFC's, signal for Cx43 was localised to upstream endothelium and not VFC's. This is consistent with previous work showing that Foxc2 upregulates Cx37, and suggesting that Foxc2 may downregulate Cx43, as Foxc2 is highly expressed (albeit heterogeneously) in VFC's.[42, 111] It remains unclear why immunosignals for Cx43 were consistently increased in he upper half of the vessel. Additionally, despite this expression pattern, conditional loss of Cx43 produced a significant reduction in VFC elongation in the lower third of the vessel.

In man, mutations in GJC2, encoding Cx47, have been demonstrated to cause lymphoedema, but it has been suggested that this phenotype results from a functional, rather than structural lymphatic defect.[4] Given the observed similarities between venous and lymphatic valves it is therefore surprising to find a clear structural VV defect resulting from loss of Cx47. It is possible that a structural defect in GJC2-mutated lymphatics remains to be discovered. Similarly, mutations in GJA1, encoding Cx43, were very recently described as causing human lymphoedema.[57] Both Cx43 and Cx47 were immunolocalised to normal human venous valve leaflets, and the structure of VV in patients carrying mutations in GJC2 and a single participant carrying a GJA1 mutation will be examined in a subsequent chapter.

It is possible that the conditional deletion approach may not phenocopy known human syndromes, since these (human) mutations could result in dominant negative effects whilst genetic deletion reproduces protein loss. Further more, combination of different proteins in heteromeric connexons or heterotypic gap junctions could extend the effects of a mutated protein to signalling events predominantly produced by other connexins.[105] Induced loss of one connexin results in downregulation of other connexin, which could present a particular problem with a constitutive rather than conditional knockout approach.[172,141]

It is notable that with loss of all three connexins, VFC's were distributed across the width of the vein. If the disoriented appearance of VFC's is accepted as indicating disordered directional cell migration, this is inconsistent with a model in which differentiation of VFC's occur in a clump on one side of the vessel followed by migration around the vessel to form the ring at Stage 1. Instead, these findings would be more consistent with an alternative process - VFC differentiation in situ. VFC migration has not been directly observed (in VV or LV) and could be an interesting focus for future work.

It remains to be confirmed whether the connexin's expressed around the VFC's at P0 form functional gap junctions. TEM analysis at P0 did not identify clear gap junctions, but this is likely to be because of difficulty in identification

of these structures in ex-vivo samples (Figure 22). For Cx43, the phenotype observed following endothelial-specific gene deletion confirms the endothelial localisation of the protein. Given the known roles for Cx37 and Cx43 in endothelial cells, it seems likely that these connexins (and likely Cx47) form functional gap junctions during VV development.[105] It was not possible in this work to determine the messenger that may be communicated between VFC's. Ca^{2+} has been suggested as a candidate for this role, and could subsequently act upstream of calcineurin-NFAT.[94] Cx45 has been shown to play a critical role in cardiac outflow tract development, and acts upstream of NFATc1 signalling.[92, 93] Expression of Cx45 has not been described in LV or VV, but it is an intriguing possibility that Cx45 could also play a role in peripheral valve development. In future work it would be informative to attempt to demonstrate GJIC compartments via the injection of dye into VFC's.

Cx43 regulates cell polarity and directional migration via a channel independent effect on the cytoskeleton.[116] In this work Cx43 was immunolocalised to the upstream endothelial cells rather than VFC's, whilst the observed phenotype was in the VFC's themselves. This suggests that signalling between upstream cells and VFC's was perturbed by loss of Cx43, rather than a direct effect of loss of Cx43 in VFC's themselves.

8.5.1 Limitations:

- Cellular phenotypes resulting from connexin loss of function were analysed by measuring length and width of $Prox1^{hi}$ nuclei. This was performed in blinded fashion, but selection of nuclei could be susceptible to bias. Use of automated software to threshold Prox1 nuclei was attempted but was unsuccessful (data not shown). Signal intensity varies with depth in a z-stack, and this is not appreciable in a 2D maximum projection. In a 2D projection of 3D data, nuclei may appear to overlap, and be measured as a single object by automated software, particularly given the variation in nuclear intensity between and within nuclei. Analysis of z stacks was also attempted using 3D

volume rendering software, but nuclear volumes were distorted by section thickness and the limited z-resolution of the objective. Analysis of a 3D stack would require time-consuming thin section scanning and deconvolution, and even within z-stacks, automated thresholding remained susceptible to errors. Nuclear sphericity has previously been analysed as indicative of disordered migration.[145]

- In future work, loss of cell polarity could be further investigated by co-staining polarised cellular organelles.

9 ROLE OF VEGFR2/3 IN VV FORMATION

9.1 Introduction

Signalling through the tyrosine kinase VEGFR3 is critically required for early blood vascular and lymphatic development.[122, 125] In man, mutations in VEGFR3 and its ligand, VEGFC, cause Milroy's disease (lymphoedema).[53] These patients have an increased incidence of venous reflux, suggesting a developmental venous defect.[50, 53] Our previous work has identified VEGFR3 promoter activity in developing VV using a VEGFR3LacZ reporter line,[44] but expression has never been confirmed by immunolocalisation and the timing of onset of VEGFR3 expression has not been described. It is not known whether signalling through VEGFR3 is required for VV development.

9.2 Aims

1. To investigate the expression pattern of VEGFR3 is expressed on VVs
2. To investigate whether there is a role for VEGFR3 signalling in VV development.

9.3 Design and Methods

Inhibition of the various forms of signalling through VEGFR3 can be achieved with different and complementary methods. For inhibition of valve induction, blocking antibodies would require administration to the dam, and the antibody is not widely available. Both the Chy mouse (which exhibits constitutive heterozygous loss of VEGFR3 protein tyrosine kinase function) and a mouse line with a floxed VEGFR3 allele were not available.[123, 130] For these reasons, and because patients affected by Milroy's disease carry mutations inactivating the tyrosine kinase domain, I elected to examine the effect of VEGFR tyrosine kinase inhibitors in vivo. A recently described small molecule tyrosine kinase inhibitor, Maz51, has selectivity for VEGFR3 over other VEGFR's, and has previously been characterised for use in in-vivo murine models.[124, 173] In-vivo, Maz51 significantly prevents tyrosine phosphorylation of VEGFR3 but has little effect on VEGFR2, and its effect has ben verified when administered at 10mg/kg OD.[124, 173]. In vitro, Maz-51 inhibited ligand-independent auto-phosphorylation and also (ligand-dependent) phosphorylation in response to VEGF-C.[173] Axitinib is a well-characterised small molecule tyrosine kinase inhibitor, with selectivity for VEGFR1, VEGFR2 and VEGFR3.[174, 175]

9.3.1 Axitinib

Axitinib was administered at 12.5µg/g.mouse weight in acidified water.

Axitinib was prepared as follows:

1. 600µl PEG400 (Sigma) and 1ml sterile water (Baxter, UK) and 100µl 1M HCl were added to 5mg axitinib (LC laboratories) in a 2ml polypropylene tube (Eppendorf) and sonnicated (Sonnicator 230HT, Crest Laboratories) for 10mins at RT.
2. The resulting solution was made up to 2ml with 70% v/v PEG400 in water, adjusted to pH2 with HCl.

9.3.1.1 Effect of axitinib administration from E16, analysed at P0

Pregnant dams were administered axitinib 12.5µg/g.mouse wt or solvent control (70% v/v PEG400 in water, adjusted to pH2) i.p. b.d. from late E16 and analysed at P0. Six animals were analysed after treatment with axitinib and 4

after solvent control. Eight control and 9 axitinib-treated valves were visualised.

9.3.1.2 Effect of axitinib administration from P0, analysed at P2

Pups in two litters were randomly assigned to receive Axitinib or solvent control s/c b.d from P0 to P2, and were culled for analysis at P2. 3 pups received Axitinib and 3 solvent control.

9.3.2 Maz51

Maz51 (Calbiochem 676492) was administered at 10µg/g OD in DMSO from a stock solution of 10µg/µl diluted to 1µg/µl. Dose volume was therefore 1µl x animal weight in grams (i.p to dams, s/c to pups). Controls received solvent alone.

9.3.2.1 Effect of Maz51 administration from E16, analysed at P0

Pregnant dams were administered Maz51 or solvent control i.p o.d. from late E16. All dams received a single dose of 37.5µg/g Progesterone (Sigma P3972) in sunflower oil (Sigma S5007) to prevent early labour. Embryos were explanted at 'E19' and analysed as P0. Four animals were analysed after receiving Maz51 and 5 after receiving solvent control.

9.3.2.2 Effect of Maz51 administration from P0, analysed at P6

Pups in two litters were randomly assigned to receive Maz51 or solvent control from P0 to P5, and were culled for analysis at P6. Twelve pups were analysed after receiving Maz51 and 5 after receiving solvent control. Eight control and 19 Maz51-treated valves were visualised.

9.3.3 Genotyping and immunofluorescence

Immunofluorescence imaging of murine VV and genotyping were performed as described in Chapter 3. Solutions are given in Appendix 1 and antibodies in Appendix 3.

9.3.4 Statistical analysis

For comparison of stage of VV development Fisher's exact test was used, comparing wildtype with either Axitinib or Maz51-treated VV compared to each solvent control for each stage. All analyses were carried out in SPSS 21 (IBM corporation).

9.4 Results

9.4.1 Normal expression of VEGFR2/3

At E17 VEGFR3 immunosignal was readily detected in lymphatics (Figure 68) but not in the femoral vein in the region of the developing valve. At P0 and P2 VEGFR3 signal was detected, particularly around Prox1^{hi} VFC's.

VEGFR2 is known to be widely expressed in the blood vasculature; expression was confirmed in the valve-forming region of the vein at E18 (Figure 69).

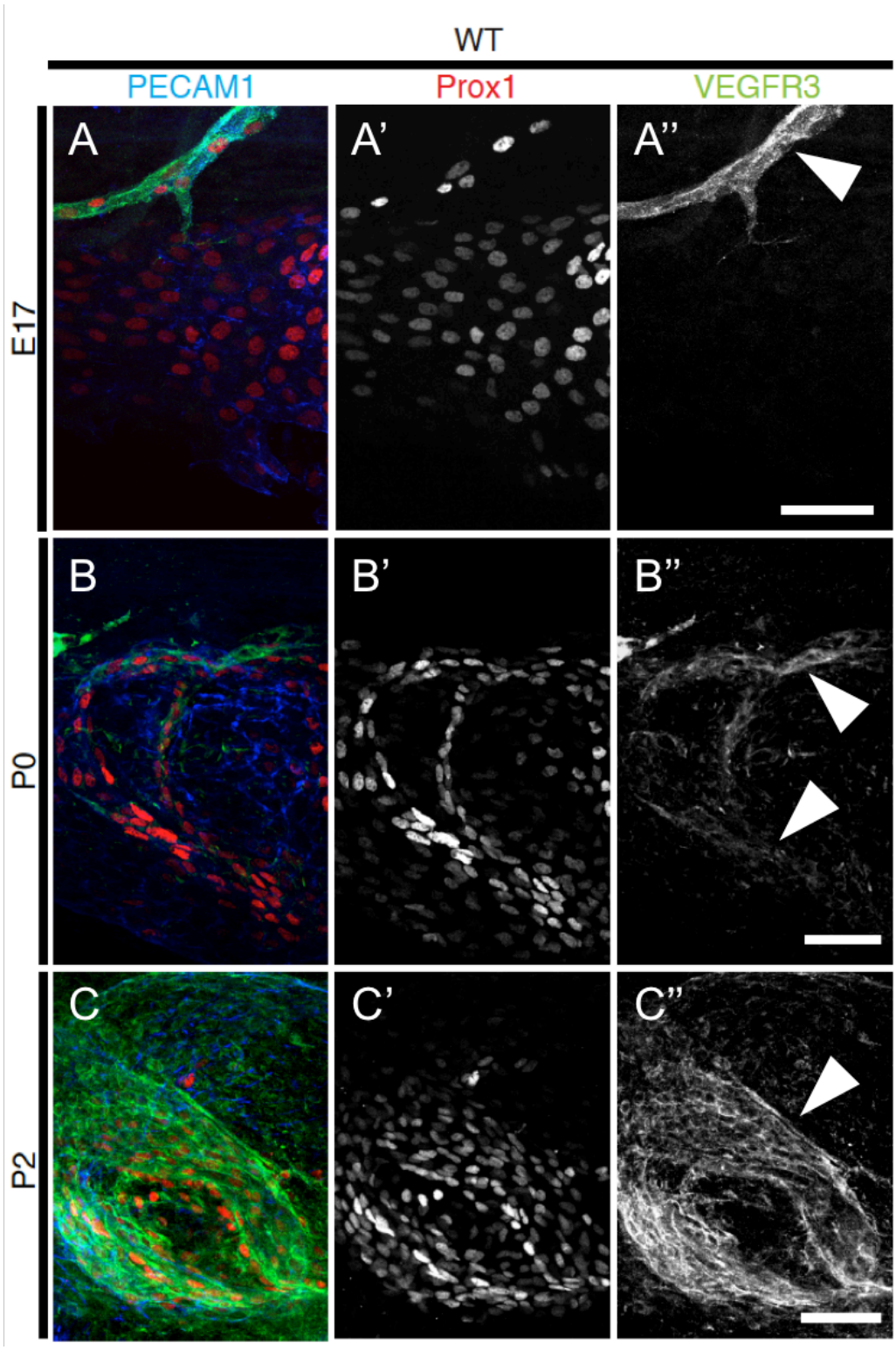

Figure 68 Timing of *VEGFR3* expression in the valve-forming region
Immunolocalisation of Prox1, VEGFR3 and Pecam1 is shown at E17 (A-A''), P0 (B-B'') and P2 (C-C''). VEGFR3 was not detected at E17 (but was readily detectable in lymphatics, arrowhead in A''). VEGFR3 was detected at P0, primarily around Prox1^{hi} valve-forming cells (arrowheads in B''). Valve leaflets expressed VEGFR3 at P2 (arrowhead in C''). Scale bars 50μm.

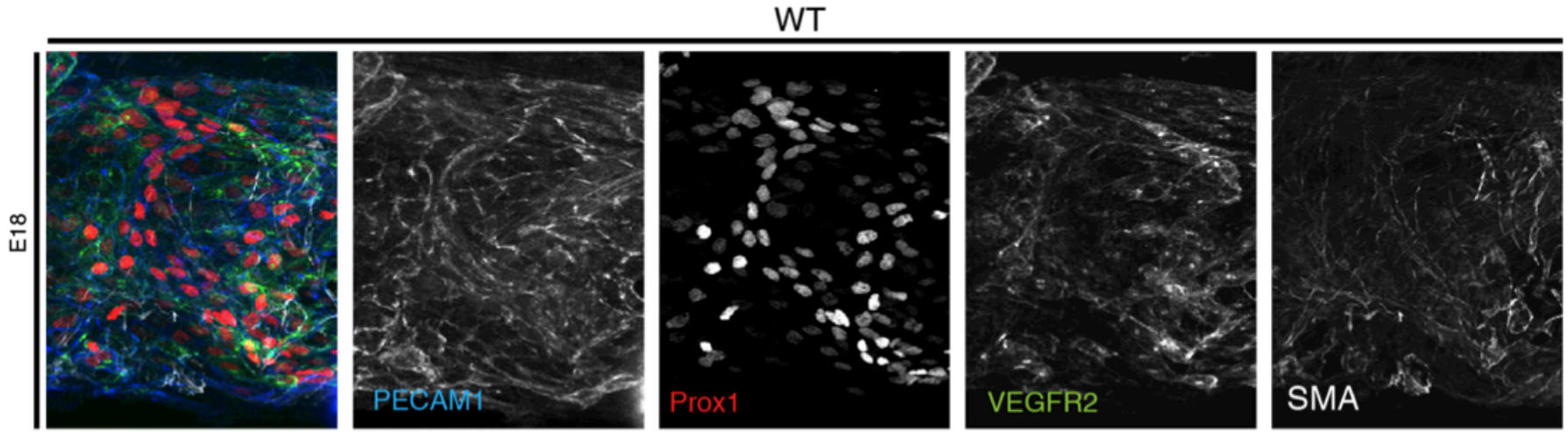

Figure 69 Immunolocalisation of *VEGFR2* at E18
VEGFR2 was expected to be expressed by blood endothelial cells at all time points. Expression in the region of the developing valve was confirmed at E18 (representative confocal micrograph of n=2 VV)

9.4.2 Effect of treatment with axitinib or Maz51 analysed at P0

Treatment with the pan-VEGFR tyrosine kinase inhibitor axitinib, but not the more VEGFR3-specific Maz51, resulted in complete failure of induction of valve formation (Figure 70). Although expression of VEGFR3 was not detected at E17, inhibition with Maz51 was started from late E16 in case low levels of receptor expression had not been detected.

A

Effect of MAZ51 from E16, analysed at P0			
	Control	Maz51	
	n	n	p
Stage 0	0	1	ns
Stage 1	8	7	
Total	8	8	

B

Effect of axitinib from E16, analysed at P0			
	Control	Axitinib	
	n	n	p
Stage 0	0	9	<0.0005
Stage 1	8	0	
Total	8	9	

C

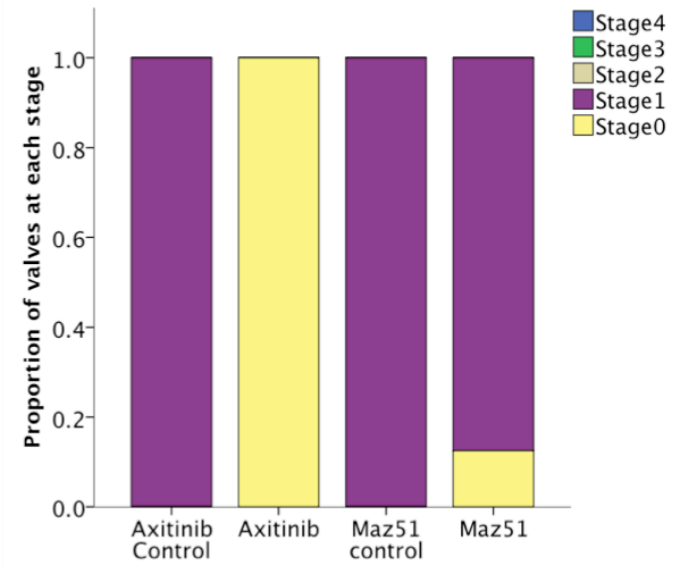

Figure 70 Analysis at P0 of pups treated with Axitinib or Maz51.
A-B) The tables provides the total number of VV analysed for each treatment and the number of VV identified at each stage. Whilst treatment with axitinib prevent VV development whilst treatment with MAZ51 had no effect. P= Fisher's exact test.

C) The proportion of valves at each stage are shown for each treatment group. Because inhibitors were given i.p. to pregnant dams, the control and inhibitor groups necessarily derive from different litters treated immunostained and imaged at the same time. Axitinib & Maz51 experiments were carried out separately.

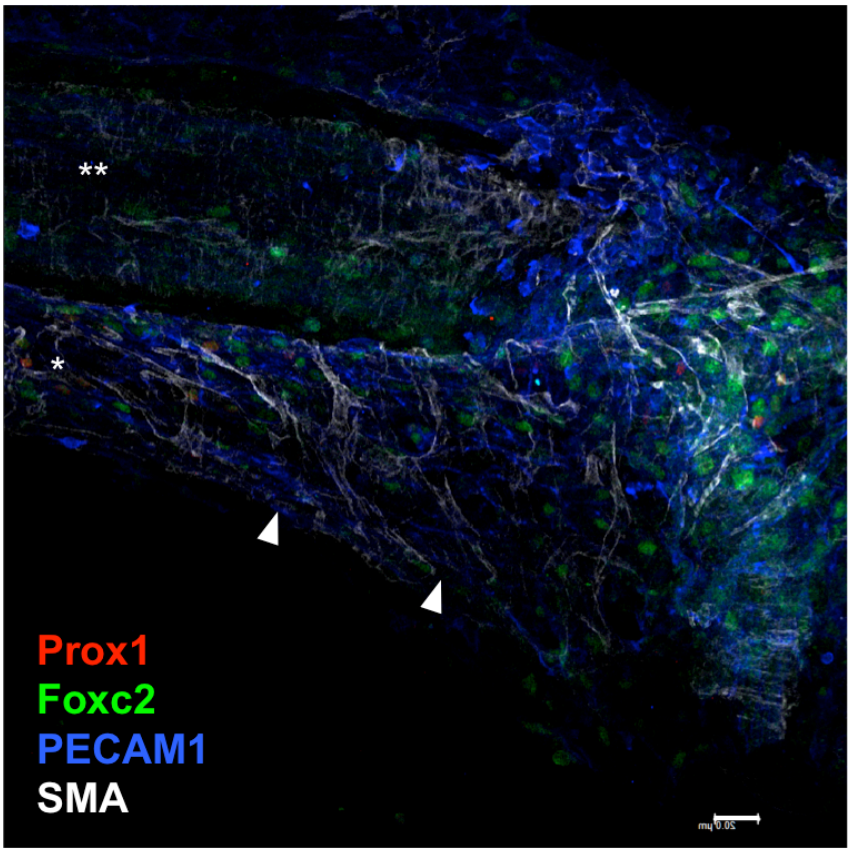

Figure 71 Representative image of an axitinib-treated femoral vein at P0. Note the abnormal lack of Prox1 signal in femoral vein, but presence of Foxc2 immunostaining in femoral veins. The femoral vein is identified by * and femoral artery by **. The normal site of the developing VV is approximately marked by arrowheads. Prox1 signal was identified in lymphatics elsewhere in the sample and in control valves. 2D maximum projection of confocal z-stack. (Prox1: Red, Foxc2: Green, SMA: White, PECAM1 Blue) Scale 20μm. Blood flow from left to right.

9.4.3 Effect on VV of treatment with Axitinib from P0

Axitinib treatment resulted in significant mortality and analysis could not be carried out beyond P2. No deaths were seen in littermates treated with solvent alone. Survival curves and analysis of pup weight are provided in Figure 99 and Figure 100, respectively. At P2, no significant VV phenotype was seen following treatment with axitinib (Figure 72).

A

Effect of Axitinib from P0, analysed at P2			
	Solvent control	Axitinib	
	n	n	p
Stage 2	2	3	ns
Stage 3	4	3	
Total	6	6	

B

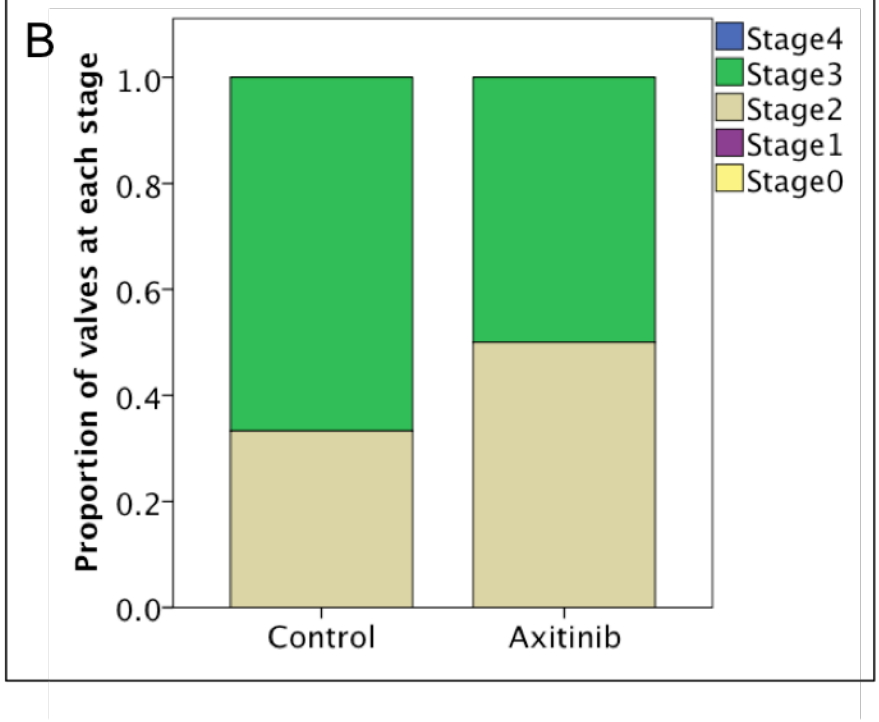

Figure 72 Venous valve phenotype after treatment with axitinib to P2
A) The table provides the total number of VV analysed and the number of VV identified at each stage. Treatment with axitinib did not produce a significant phenotype when the experiment was terminated early at P2. Data includes two pups that died just prior to analysis. P= Fisher's exact test.

B) The proportion of valves at each stage are shown for each treatment group.

9.4.4 Effect of treatment with MAZ51 from P0

All animals survived to P6 and appeared healthy and VV development progressed normally (Figure 73). Analysis of mesenteric lymphatics at P0 revealed almost complete absence of Prox1 immunosignal positive lymphatics (and absence of lymphatic valves) in 6/6 samples analysed, compared to a normal appearance of lymphatics in 5 pups receiving solvent control (P<0.0005).

A

Effect of Maz51 from P0, analysed at P6			
	Solvent control	Maz51	
	n	n	p
Stage 1	0	1	ns
Stage 3	5	10	ns
Stage 4	3	8	ns
Total	8	19	

B

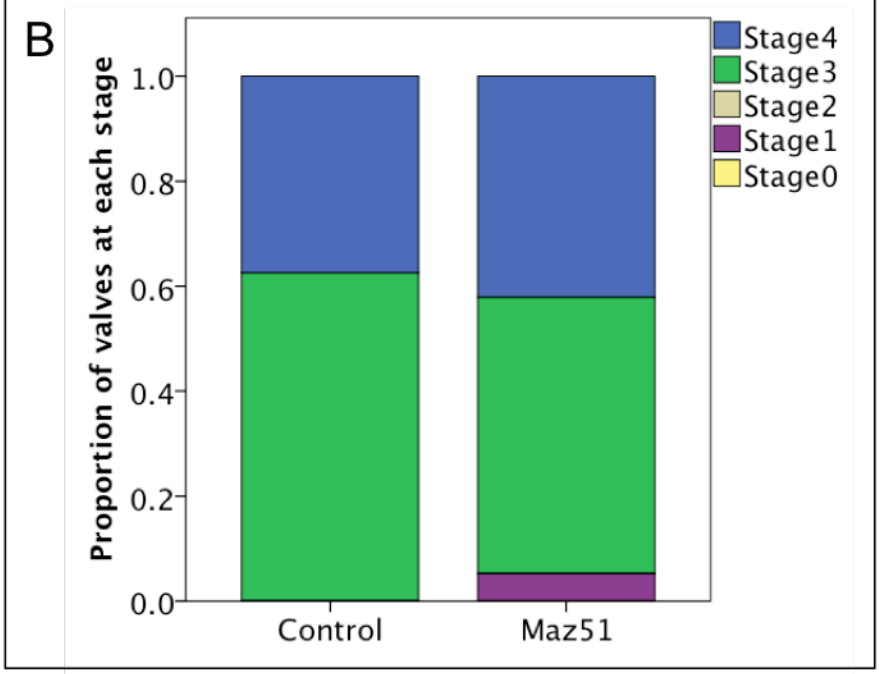

Figure 73 Effect of treatment with Maz51 from P0 to P6
A) The table provides the total number of VV analysed and the number of VV identified at each stage. Treatment with Maz51 from P0 to P6 had no discernable effect on valve development at P6. P= Fisher's exact test. ns=P>0.05. n=number VV analysed.

B) The proportion of valves at each stage is shown for each treatment group.

9.5 Discussion

Whilst immunolocalisation of VEGFR2 showed the expected widespread distribution, signals for VEGFR3 were more localised to the developing valve. This is consistent with the general absence of VEGFR3 from the venous system,[125] and our finding of VEGFR3 promoter activity in developing but not adult venous valves.[44]

Combined inhibition of the tyrosine kinase activity of both VEGFR2 and VEGFR3, but not VEGFR3 alone, resulted in complete failure of valve induction at P0. The activity of MAZ51 was confirmed at P6 by analysis of mesenteric lymphatics, which showed gross abnormalities in all treated mice. Unfortunately postnatal treatment with axitinib resulted in lethality, and no clear phenotype was observed at P2. Some pups were noted to be cyanosed, suggesting lethality could have resulted from a failure of pulmonary angiogenesis. Postnatal inhibition of VEGFR3 with MAZ51 had no discernable effect.

Prox1 expression was undetectable in the femoral vein at P0 following Axitinib treatment, and Prox1 has previously been reported to be required for VV formation; it is possible that loss of Prox1 could be responsible for the VV defect observed.[176] Taken together these results suggest that signalling through VEGFR2, or at least VEGFR2 tyrosine kinase activity, (but not VEGFR3 tyrosine kinase activity) may be required for expression of Prox1 in these veins at this time point. Foxc2 immunosignal in the femoral vein remained easily detectable despite axitinib treatment, which is surprising given the suggested role of signalling through VEGFR2/3 in upregulation of Foxc2 and Notch targets, and suggests that other mechanisms could maintain Foxc2 in veins despite inhibited VEGFR2/3 signalling (Figure 11).[40, 123]

Tyrosine kinase inhibitors distribute widely and can be expected to have systemic effects, as shown by the post-natal non-viability of axitinib treatment. It is difficult to exclude effects caused by a general failure of development. For

axitinib the whole vessel appeared abnormal and it is entirely possible that the defect observed is due to a general failure of EC growth.

In further work, it may be possible to inhibit ligand binding to VEGFR3 in-vivo with a specific rat monoclonal IgG2A antibody, which is expected to cross the placenta.[177] Blocking antibodies are also available against VEGF-c and VEGFR2. These approaches still do not result in cell type-specific loss of function and it would also be important to analyse conditional deletion of VEGFR3 and VEGFR2 in endothelial cells using floxed alleles, in order to block passive signalling.[123]

10 THE ROLE OF FLOW ON VV DEVELOPMENT IN VIVO

10.1 Introduction

Fluid flow has been implicated in the normal development of cardiac and lymphatic valves, but has not previously been found to be required for VV development.[42, 131, 133, 178] A requirement for normal flow has been suggested for LV development in vitro, but not in an in-vivo model.[42]

Understanding the role of flow in valve development requires surgical intervention at an early post-natal age. To the best of my knowledge there are no published data available demonstrating safe anaesthesia or surgery in mice below P6. Methods have been described for performing minor procedures in P6 mice and P1 rats.[179, 180] Gotoh *et al* have experience in operating successfully in mice at P4 (Gotoh.H, personal communication, 2010). Major problems particularly affecting pup anaesthesia include a large surface area:volume ratio predicating to hypothermia, practical difficulties in animal handling and restraint, skin closure and post-operative rejection by the mother - cannibalism rates in the range of 75% have been reported.[179, 180]

10.2 Aims

1. Develop techniques for anaesthesia of P0 murine pups
2. Develop a model of altered flow during venous valve development in vivo, to test the hypothesis that normal flow is required for valve development.

10.3 Methods

10.3.1 Development of anaesthetic technique in P0 pups

Induction was carried out in a custom made small chamber made from a pipette-tip box (approximately 12x8x6cm) fitted with a 1ml pipette tip to allow connection to the gas supply tubing from the anaesthetic machine. The induction chamber was pre-warmed on a heated pad to avoid hypothermia. Immediately after induction warmed EMLA cream was placed over the operative site. Pups were administered warmed weight-adjusted buprenorphine in 5% dextrose saline to provide intra-operative and post-operative pain relief and fluid replacement. Maintenance of anaesthesia was performed via gas inhalation of isofluorane anaesthesia delivered by a Univentor 4000 anaesthetic unit. Intra-operative monitoring was carried out by manual counting of respiratory rate. Although invasive monitoring has become possible in rodent pups, it is doubtful that this is feasible at P0; the equipment is expensive and the setup time would add to the duration of anaesthetic.

10.3.2 Development of the surgical model

Surgery was performed on a heated pad to avoid hypothermia. Minimal chlorhexidine skin preparation was used as this removes heat in evaporation. The pup was placed on a warmed cotton pad on a heating pad and covered with a sterile sheet. Instruments were obtained from Fine Science Tools. A 2-3mm incision was made using blunt-tipped scissors, which were subsequently used for all dissection. Occasionally superglue or compression under a fat pad was used for haemostasis, but effective haemostasis was generally achieved by avoidance of vessel injury.

The vein distal to the site of the developing valve was identified and dissected free of the femoral nerve. The vein could not be dissected free of the artery as there is no tissue plane between them at this age. Attempts to alter flow were as follows.

10.3.2.1 Occlusive vascular clip

Placement of a venous clip aimed to reduce or alter blood flow through the vein without causing venous or arterial damage. This was technically demanding and depended on the optimal mechanical properties and shape of the clip, which was sequentially optimised. Titanium wire was selected as it does not induce a biological reaction, could be sterilised, and is malleable. Initially 250μm Titanium (Ti) wire was used and cut into short lengths with a scalpel under a microscope. This was done with the wire attached to autoclave tape so that the short segments of wire remained in place. The centre of each short length of wire was then depressed into the thickness of the tape with a blunt portion of scalpel blade to create a "V" shape. Wires were then placed in a 50ml falcon tube (without the lid) and sterilised in an autoclave.

The 250μm Ti wire was found to be too large in diameter, and so 50μm Ti wire was tested. Unfortunately Ti wire proved too malleable at 50μm to be able to compress the vein – on compression the V shape of the wire tended to bend around the vascular bundle.

Following a review of wires available Tungsten (W) wire at 50μm was used. This harder metal was far more difficult to cut to length, and to bend, but this was subsequently performed prior to surgery. Intra-operatively W wire tended to bend at the existing "V" to produce two straight portions of wire that compress the vein more successfully. The shape of the wire clip was then modified to produce a narrower portion at the base of the "V". As the compression force is applied at the top of the "V", and the vein is positioned at the base, this new shape gave better compression of the vein, and avoided compression of the femoral artery.

10.3.2.2 Ligation of the vein

In order to determine whether a single point of flow interruption could sufficiently alter flow through the valve, the vein and artery were ligated between the site of the valve and the first distal tributary at P0 and VV analysed at P6.

10.3.2.3 Ligation and bisection

The femoral vein and artery were double ligated (10/0 vicryl on a round bodied needle) and the vein divided between the ligatures, at a point between the valve and first distal tributary. 20 control valves and 16 flow-altered valves were successfully analysed.

10.3.2.4 Wound closure

Skin closure was initially attempted with tissue glue on the recommendation of the local veterinary surgeon but the mothers repeatedly removed the glue causing wound dehiscence. Use of skin clips has previously been recommended, but none could be located of suitable size for P0 pups.[179] Subsequently the skin was closed with running 10/0 monofilament vicryl on a curved needle, knotted at either end, using a micro-needle holder. No complications arose from wound closure with this technique.

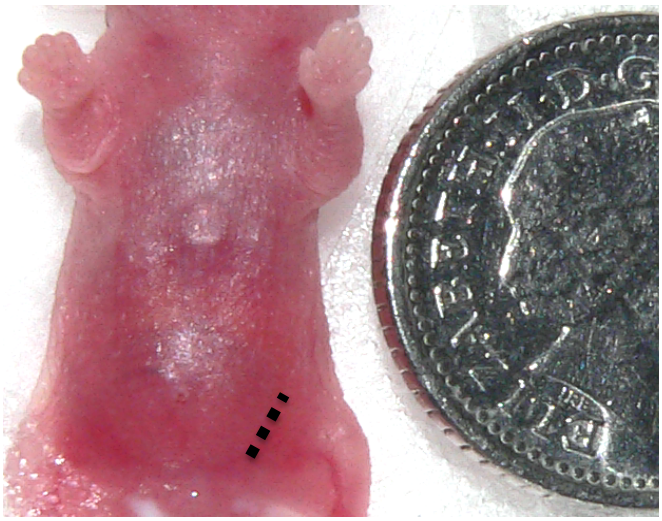

Figure 74 Incision site
Dotted line marks the incision for ligation upstream of proximal femoral venous valve in a P0 pup. Coin=5p, for scale.

10.3.3 Post-operative Care

Pups were returned to a heated recovery nest made from their mothers nesting material and supplied with oxygen until they are clinically judged to have returned to a level of responsiveness appropriate for their age. This

included movement, attempts at self-righting, and some squeaking. Pup surface temperature was assessed using an infra-red thermometer to avoid over or under heating during the recovery stage. The majority of pups had developed some degree of intra-operative hypothermia. The cage was placed in a hot box overnight following surgery. Pups were periodically monitored during the recovery phase, bearing in mind that each additional disturbance may increase the chances of rejection by the mother, and also that disturbing the nest appeared to reduce the density of nesting material and allow pups to become more easily dispersed.

10.3.4 Immunofluorescence imaging

Immunofluorescence imaging of murine VV was performed as described in the General Methods chapter. Solutions are given in Appendix 1 and antibodies in Appendix 3.

10.3.5 Statistical analysis

For comparison of stage of VV development Fisher's exact test was used, comparing wildtype with either heterozygous or homozygous knockouts for each stage. For analysis of the effect of flow on vein diameter, VV area, or diameter:area ratio, independent samples t tests were used. Data from multiple litters were pooled. All analyses were carried out in SPSS 21 (IBM corporation).

10.4 Results

10.4.1 Optimisation of the surgical model

Use of a clip was found to be ineffective at altering flow by P6 and valves developed entirely normally. Ligation of the vein at a single point had no effect on valve development; revascularisation was seen to bridge the point of ligation and flow through the normal route appeared restored by P6. Ligation of the vein at two points with division of the vein was successful; revascularisation was seen to occur from the point of ligation, with blood flow diverted via an alternative route (arrow in Figure 75A). Double ligation and dissection of the vein was carried out on 21 pups, and VV successfully visualised after processing in 20 control veins and 16 operated veins.

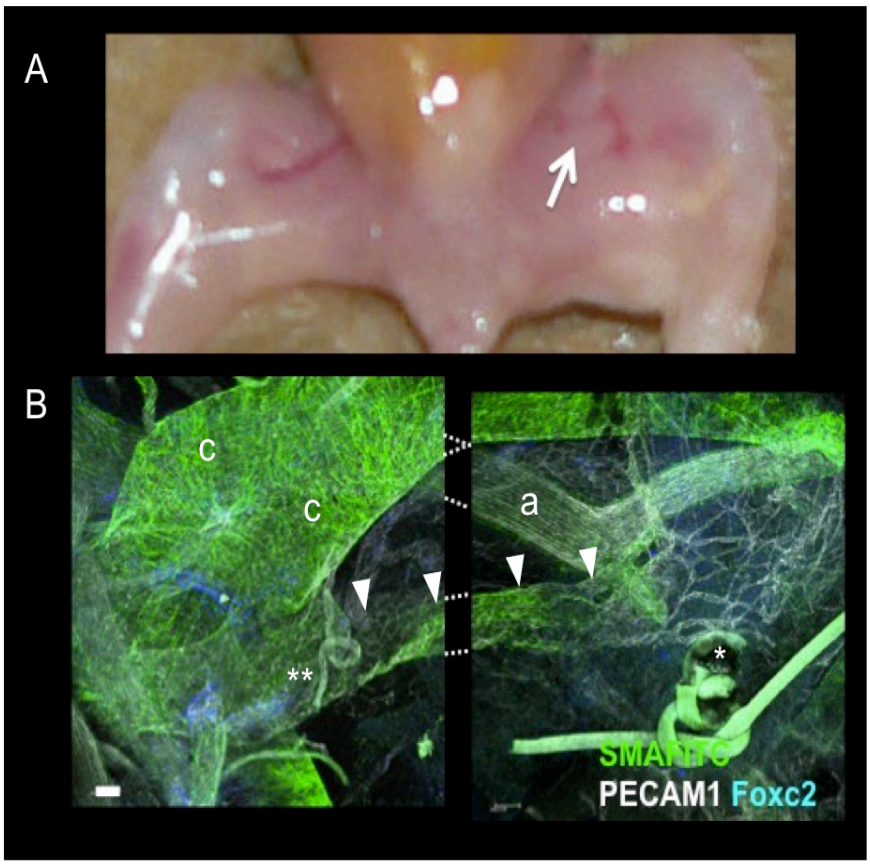

Figure 75 Imaging at P6 following flow alteration by vein ligation and vein bisection at P0.

A) A micrograph of a P6 pup following left sided surgery at P0. The normal route of femoral vein been diverted (arrow indicates the normal route; the diverted bloodflow is seen above this).

B) Confocal images of the operated region identified by the arrow in A are shown. The femoral vein is marked by arrowheads and * = the site of the occlusion at the proximal knot. The vein has been divided distal to this point. Flow is diverted through collaterals (c) that re-enter the femoral vein just downstream of the valve, which is abnormally small (**). In B flow is from right to left. Scale bar 50μm.

10.4.2 The effect of altered flow on valve development

Anaesthetic techniques were successful in allowing surgery at P0 and induction of a flow-altering lesion by double ligation and division of the femoral vein upstream of the developing valve. Operated pups gained weight normally, and no correlation was detected between subsequent pup weight at P6 and valve area (Figure 110, Figure 111, Appendix 12).

Flow alteration was associated with qualitatively smaller valves compared with control (unoperated) valves on the other side of the same mouse (Figure 77). Valve area was reduced by over 4-fold following altered flow (Figure 76). Because the change in vein diameter at the site of the valve approached statistical significance (Figure 76), valve area:diameter ratio was calculated, and confirmed a significantly smaller valve at P6 in association with alteration of blood flow from P0 (Figure 79). Flow alteration was also associated with a failure of valves to develop normally, with a significant increase in the number of valves at stage 2 of development (Figure 80).

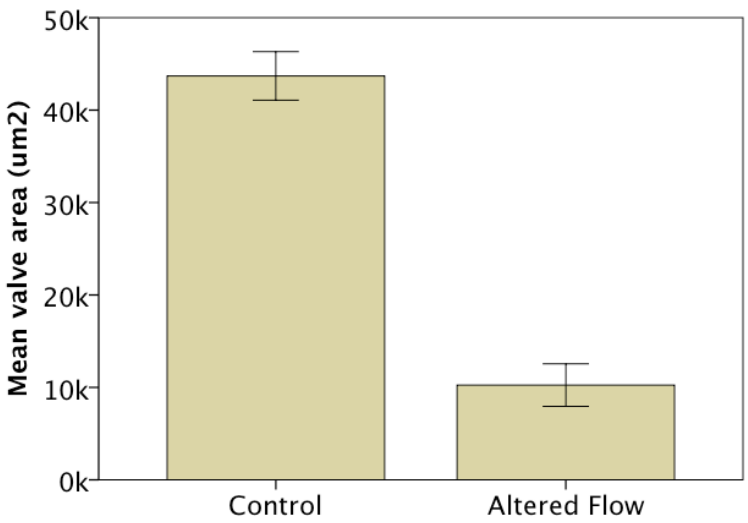

Figure 76 Valve area is reduced following flow alteration
Error bars represent sem. P<0.0001 (independent samples t test). Area of Foxc2 immunostained valve leaflet was measured in a 2D maximum projection of a 3D confocal z-stack.

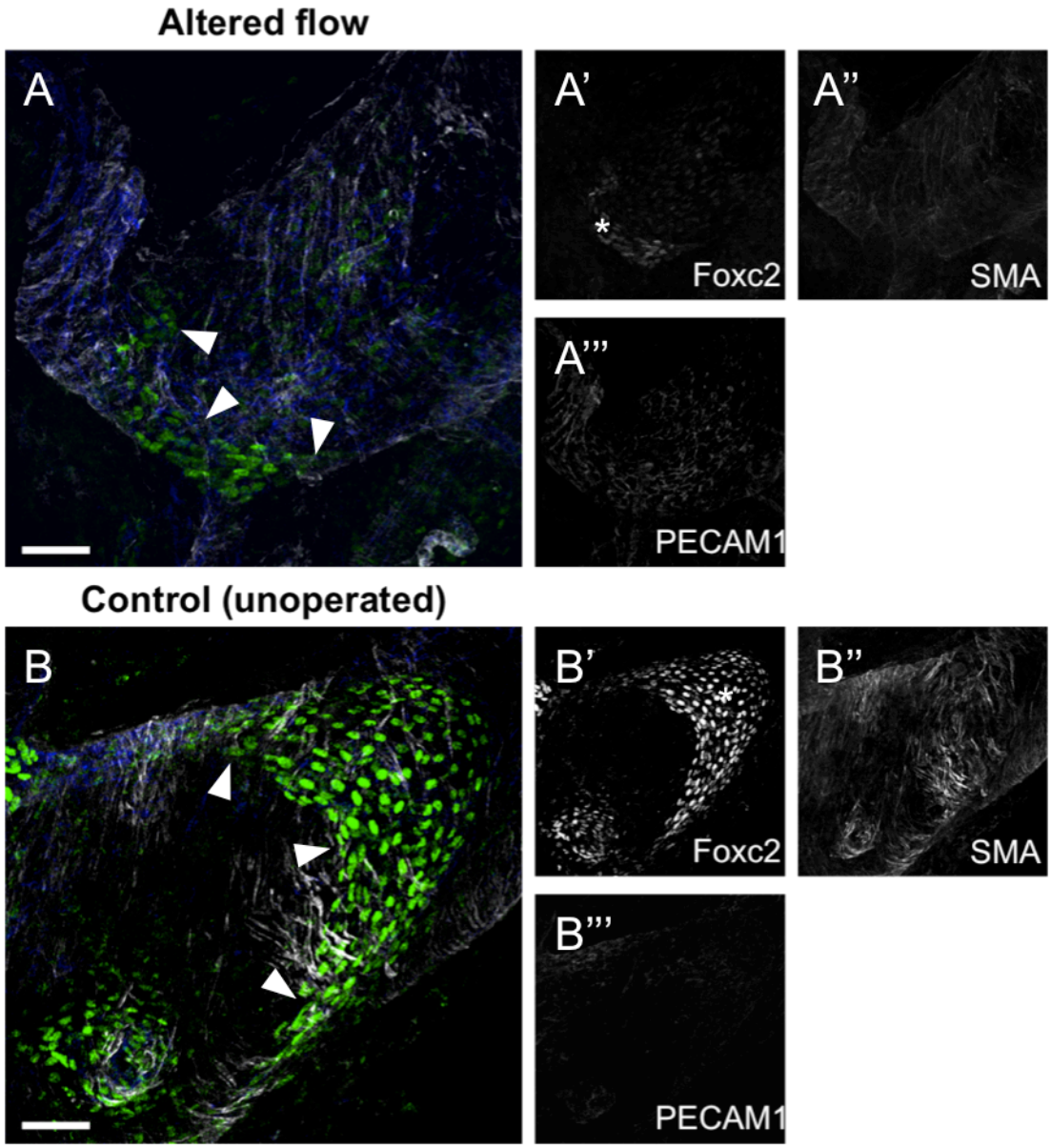

Figure 77 Smaller valves following flow alteration.
A) A venous valve (arrowheads in A, * in A') at P6 following induction of a flow altering lesion at P0.

B-B''') The corresponding control valve (arrowheads in B, * in B') for A.

The valve developing in conditions of reduced flow (A-A''') is smaller. It was not possible to quantify a reduction in Foxc2 immunosignal (A').

2D maximum projections of confocal z-stack. Scale 50μm. Upper panel flow L>R, lower panel flow R>L.

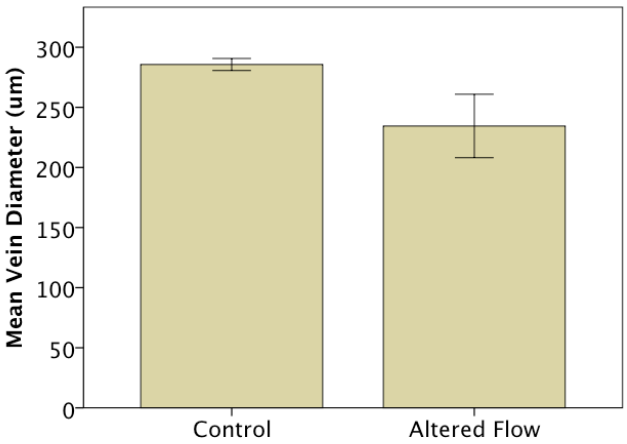

Figure 78 No significant change in vein diameter at the valve site
Diameter was measured perpendicular to the vessel axis, at the center of the valve in 2D projection of confocal z-stack. P=0.096 (independent samples t test with equal variance not assumed as Levene's test P<0.001). Error bars represent 1SEM. (Note that with equal variance assumed P<0.05)

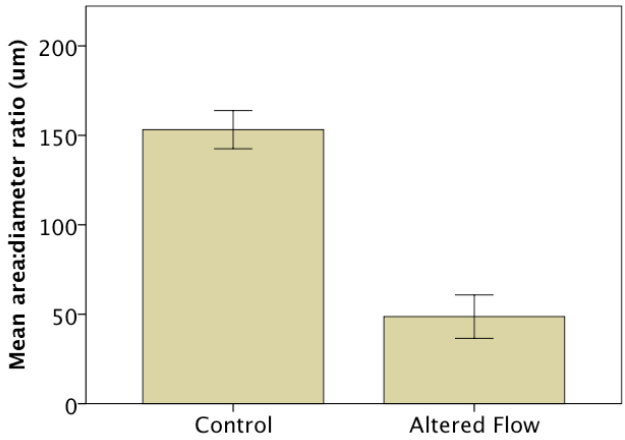

Figure 79 Flow alteration reduces valve area:vein diameter ratio of valve
Induction of flow alteration at P0 caused a significant reduction in area:vein diameter ratio at P6 (P<0.0001, independent samples t test). Error bars represent 1SEM.

A

Effect of operative intervention from P0, analysed at P6			
	Control valves	Flow altered valves	
	n	n	p
Stage 0	0	2	ns
Stage 1	0	1	ns
Stage 2	0	6	**0.004**
Stage 3	7	1	ns
Stage 4	13	6	ns
Total analysed	20	16	

B

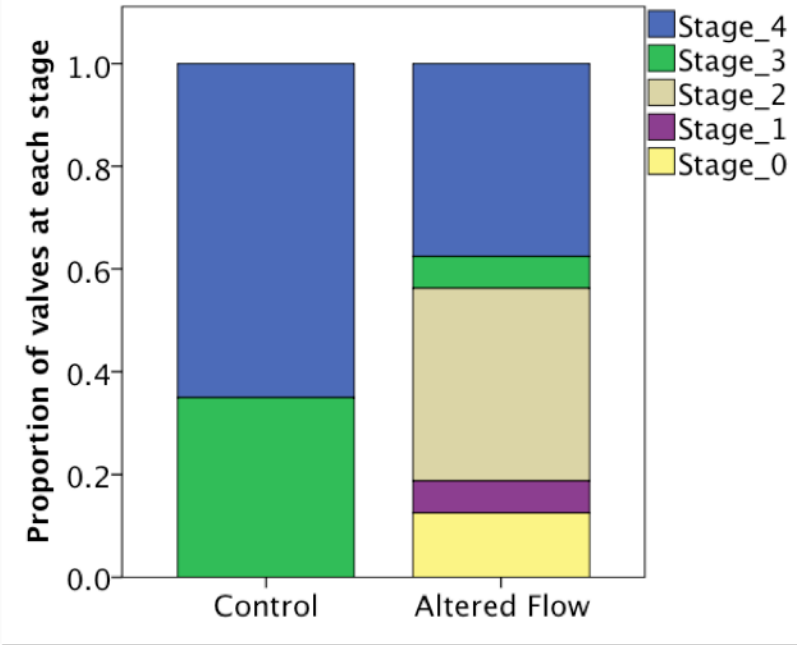

Figure 80 Flow alteration delays developmental progression

A) The table provides the total number of VV analysed and the number of VV identified at each stage. N=21 operated pups. Flow alteration at P0 resulted in defective development at P6, compared to the contralateral control valve, which developed normally. P= Fisher's exact test. ns=P>0.05. n=number of VV analysed.

B) The proportion of valves at each stage is shown for each treatment group.

10.5 Discussion

The anaesthetic techniques described were successful in avoiding any rejection by the mother, despite approximately 1hour of separation. This is likely to be because pups were not returned to the mother until they were normothermic and appeared to be behaving normally. It was observed that mothers did not care for pups that did not respond to them. No olfactory conditioning (other than using the mother's bedding for the anaesthetic recovery nest) was required. Perioperative mortality was noted to increase with duration of anaesthesia above approximately 12mins.

The surgical model was optimised to produce a flow-altering lesion that was resistant to the rapid neovascularisation observed. Double ligation and division of the femoral vein resulted in diversion of flow via an alternative route, with flow typically regaining the truncal vein via tributaries at the site of the developing valve, or just downstream. Flow was therefore maintained at the valve site. No thromboses were seen in any veins.

Alteration in the blood flow experienced by the developing valve from P0 resulted in reduced valve development at P6 when compared with the unoperated contralateral control valve in the same pup. Valves exposed to altered flow had a significantly smaller 2D area, despite correction for the size of the vein. These data suggest that valve endothelial cells are sensitised to their local flow, and suggest for the first time that normal flow is required for full VV development in-vivo. This finding is consistent with previous data in cardiac and lymphatic valve formation.

10.5.1 Limitations

- I was unable to examine the effect of flow on valve position relative to branch points or in early cell rearrangements, as anaesthesia and surgery are currently not practicable in embryos. In future work it may be possible to characterise a VV that develops at a consistent site postnatally, enabling intervention to alter flow during earlier stages of VV development.

- As the control contralateral limb was not operated on, I cannot entirely exclude the possibility of effect from application of the suture or division of the downstream vein. The increase in mortality with increased anaesthetic time precluded a sham operation on the contralateral limb. It is highly unlikely that the procedure affected valve development other than by a direct effect on the vein, given that repeated experiments with dissection, application of titanium or tungsten clips, and ligation of the vein and artery (without double ligation and venous division) all failed to affect valve development.

- It was not possible with the existing experimental setup to record the effect of the procedure on blood flow, or the anatomy of revascularisation of the veins. It is possible that selecting mice in which flow was successfully diverted away from the femoral vein would increase the severity of the valve developmental phenotype.

- The size of the valves at P6 precluded the acquisition of material for analysis of changes in protein expression in response to altered flow. In future work it would be interesting to attempt to replicate in-vitro findings of effects of flow on critical regulators of valve development such as Foxc2 and Cx37. [42] It is entirely possible that the observed phenotype is due to a general effect of reduced flow on venous endothelial cells, rather than a specific effect on the valve endothelial cells.

- The hypothesis that that normal flow is required for the maintenance of venous valves was not examined in this work. Preliminary experiments to alter flow in adult mice failed due to rapid revascularisation around the suture used to occlude flow (data not shown). Flow patterns around valves at junctions are likely to be complex, and be modified by the shape of the valve orifice as well as an interacting stream from the tributary. It has been suggested that paired venous valves are specifically non-aligned to produce (or in response to) helical flow patterns.[181] Further work will revisit the role of flow in the maintenance of valve structure and function, which may play roles in human diseases. For example the progression of venous reflux in varicose veins could be exacerbated by a response of the valves to abnormal flow patterns.

The reduced flow experienced by endothelium surrounded by thrombosis could conceivably contribute to valve failure in Post Thrombotic Syndrome.

11 IN-VIVO IMAGING ANALYSIS OF HUMAN VENOUS VALVES

11.1 Introduction

Venous valve structure has not been systematically assessed in vivo in man. Duplex ultrasonography is a common imaging modality used for assessing venous disease in man as it is non-invasive, does not involve ionising radiation, and no contrast agents are required for the production of high resolution images. Dynamic imaging allows assessment of venous reflux and any obstruction to flow that may be caused, for example, by thrombus. Facilities for ultrasound scanning are widely available, and are relatively cost-effective compared with other imaging modalities.[182]

The use of ultrasound for measurement of popliteal venous valve leaflet thickness shows that leaflet thickness increases slightly with age.[182] Measurement of leaflet thickness was not validated in other veins, and only one valve was measured per individual. Ultrasound has also been employed to assess the suitability of venous valves for repair, using a visual assessment of flow pattern and measurements of vein diameters in deep and superficial veins of the lower limb.[183]

11.2 Aims

1. Develop an ultrasound-based method for in-vivo quantification of the presence of venous valves and structural abnormalities in the valves
2. Analyse venous valve phenotypes in patients with known genetic defects.

11.3 Methods

11.3.1 Study participants

The National Research Ethics Service provided ethical approval for the study. Controls without clinical venous disease were recruited locally. Patients with known genetic mutations were recruited from the Lymphoedema Clinic at St George's Hospital, London.

11.3.2 Ultrasound examination of valves

All valve ultrasound examinations were performed by full-time vascular ultrasonographers in the Ultrasonic Angiology department at Guy's & St Thomas' NHS Foundation Trust.

Veins were scanned using a Phillips IU22 clinical ultrasound machine. An L17-5MHz transducer was used for most veins. An L9-3MHz transducer was used for particularly deep veins.

The following veins were scanned:

Upper limb

- Brachial vein from ACF to axillary vein (medial brachial vein if paired).
- Basilic vein from ante-cubital fossa (ACF) to axillary vein

Lower limb

- Popliteal vein from adductor hiatus to trifurcation
- Short saphenous vein from SPJ if within 10cm of knee skin crease to 20cm BK.

The basilic, brachial, popliteal and short saphenous veins were examined. Each vein was scanned along its entire length, switching between longitudinal and transverse views to detect valves. The positions of identified valves were recorded in a standardised reporting sheet, using the distance from agreed surface landmarks. An image of each valve was saved. B-mode cine loops were recorded of each valve in B-mode and with colour Doppler. Valve maximum leaflet measurements were taken offline using Phillips Xcelera Cath Lab software. Due to time constraints in imaging, limited consent for imaging

lower limb veins or prior vein ablation, not all veins were imaged in all participants.

11.3.3 Statistical analysis

Age matching was confirmed using an independent samples t test, and sex matching using a Fisher's exact test.

Reproducibility in counting the number of valves in a vein was assessed using a scatter plot and an Intraclass Correlation Coefficient, because Pearson's r is not suitable for low integer variables.

Reproducibility in measurements of leaflet length (derived from analysis of the same scan, or repeated scanning) was assessed using a scatter plot and Pearson's r.

For analysis of human VV structural phenotypes (number of valves and valve length), t tests were used for each genotype compared with the control group.

All analyses were carried out in SPSS 21 (IBM corporation).

11.4 Results

11.4.1 Participants recruited

Table 4 Genotypes of recruited participants

GJC2 encodes Cx47 and GJA1 encodes Cx43. Several participants were members of affected families.

	StudyID	Family	Age	Sex	Genotype
Controls	2012-01	-	25	M	
	2012-02	-	30	F	
	2012-03	-	24	F	
	2013-01	-	24	M	
	2013-24	-	37	M	
	2013-25	-	42	F	
FOXC2	2013-12	-	22	F	c.595dupC
	2013-13	-	42	F	298C>T p.Gln100x
	2013-21	1	21	M	c.438G>A p.Trp146x
	2013-22	1	54	M	
	2013-23	-	31	F	c.361C>T p.Arg121Cys
	2013-17	2	47	M	c.223T>G
	2013-18	2	20	M	
	2013-26	-	51	M	c.595dupC
VEGFR3	2013-10	-	48	M	c.A3344G p.Y1115C
	2013-11	-	26	F	c.2554G>A p.G852S
	2013-16	-	36	F	c.2554G>C p.Gly852Arg
GJC2	2013-19	3	20	F	p.P316L
	2013-20	3	71	M	
	2013-27	4	46	M	143C>T p.S48L
	2013-28	4	17	F	
GJA1	2013-29	-		F	c.617A>G p.K206R

11.4.2 Participant age and sex matching

Study participants were statistically matched for age and sex, although some study participants were older than the controls (Table 5, Figure 81).

Table 5 Age and sex matching of participant groups
Age was compared using independent samples t tests. Sex (proportion female) was compared using a fisher's exact test.

Group	Mean age (years)	p	N Females (males)	p
Control	30.33	-	3 (3)	-
FOXC2	36.00	0.357	3 (5)	1
VEGFR3	36.67	0.338	2 (1)	1
GJC2	38.50	0.570	2 (2)	1
GJA1	44.0	-	1 (0)	-

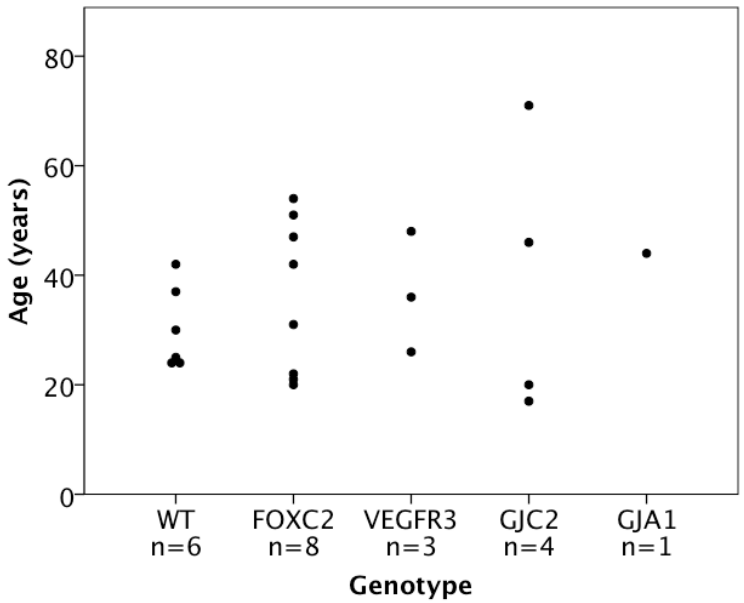

Figure 81 Ages of participants for each genotype studied
The scatter plot identified some participants who were older than the controls, although all groups are statistically matched.

11.4.3 Validation of valve quantification by ultrasound

Analysis of the number of valves identified by two vascular ultrasonographers examining the same veins on different days showed a high and significant correlation, with intra-class correlation of 0.896 and P<0.0005 (Figure 82). Reproducibility in measuring the ultrasound-detected leaflet length was assessed by two methods. Analysis of two ultrasonographers analysing the same images showed a high and significant correlation of r=0.953 and P<0.0005 (Figure 83). The correlation was weaker when based on separate scans obtained on different days, but still showed a reasonable correlation with r = 0.735 and P<0.0005 (Figure 84).

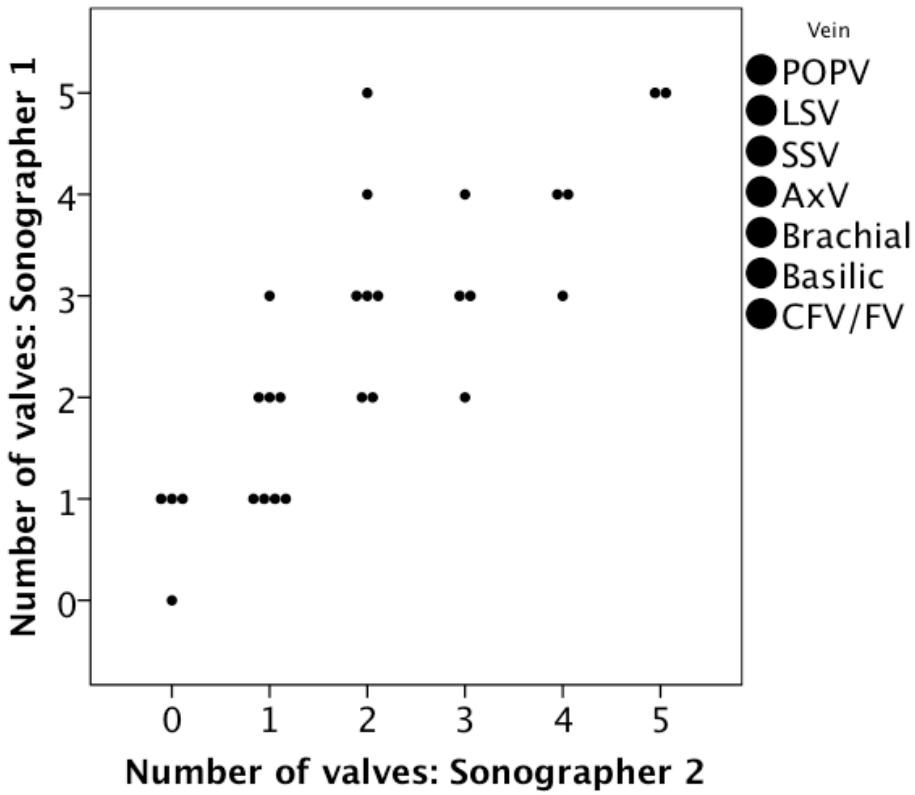

Figure 82 Reproducibility of counting number of valves
This graph shows a strong correlation between repeated measures of the number of valves in a vein by two different ultrasonographers. Intraclass correlation coefficient 0.896, P<0.0005. Identical integer values are shown side by side. A graph of the same data plotted as continuous variables and including a line of best fit is shown in Figure 108.

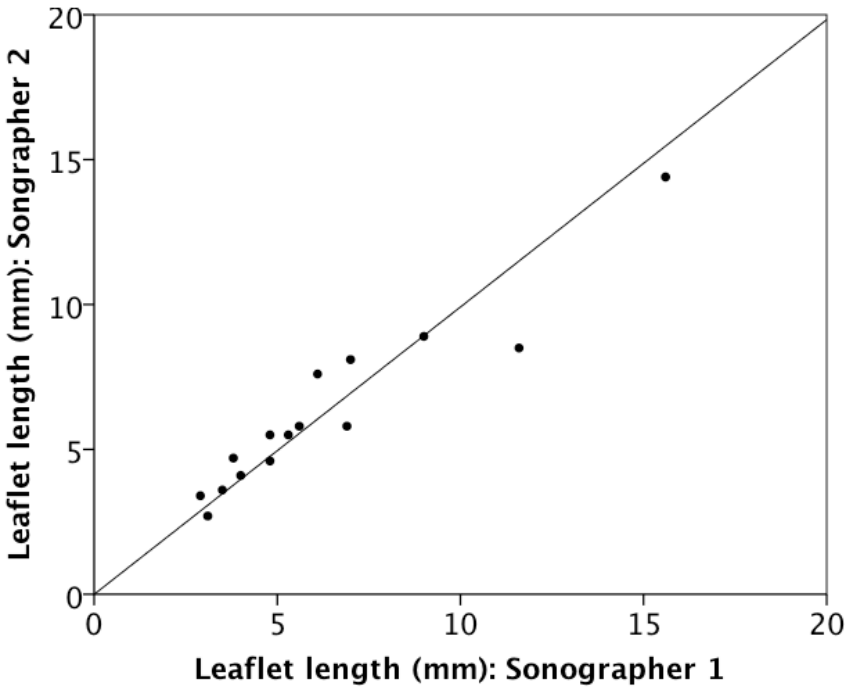

Figure 83 Reproducibility of length measurements from same scan
This graph shows the extremely strong correlation between repeated measurements of valve length derived from two sonographers analyzing the same images. Pearson's r = 0.953 P<0.0005 A line of best fit through the origin is shown.

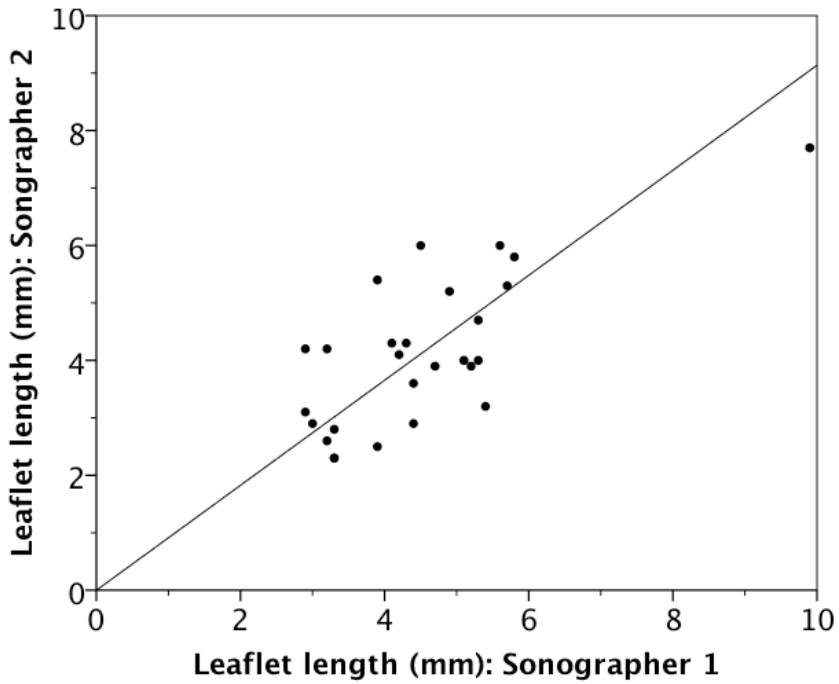

Figure 84 Reproducibility of length measurements from different scans
There was a strong correlation between repeated measurements of valve length derived from two sonographers performing independent scans. Pearson's r= 0.735 p<0.0005. The line of best fit through the origin demonstrates some effect from the outlying data point.

11.4.4 Venous valve phenotypes in patients carrying genetic mutations and controls

The number of valves identified by ultrasound in the popliteal vein, short saphenous vein (SSV), brachial vein and basilic vein in each group are given in Table 6, and shown in Figure 85. The length of each identified valve is also provided, and shown in Figure 86. In the control group typically only one valve was detected in the popliteal vein whilst a mean of 4.13 valves were detected in the SSV. In the upper limbs, 2.10 and 2.40 VV were detected by ultrasound respectively in the brachial and basilic veins.

Mutations in VEGFR3 were associated with reduced number of valves in the SSV. Mutations in FOXC2 were associated with a more substantial phenotype, and were associated with reduced number of valves and shorter valves in all veins. Mutations in GJC2, encoding Cx47, were associated with reduced number of valves in the SSV, brachial and basilica veins and shorter valves in the popliteal, SSV and basilica veins. The sole participant with a mutation in GJA1, encoding Cx43, had a significantly reduced number of valves in the SSV.

Vein	Group	Mean number of valves per vein			Mean leaflet length		
		n (limbs)	mean	p	n (valves)	mean	p
Popliteal	Control	8	1	-	8	7.00	-
	VEGFR3	5	0.80	0.606	4	5.05	0.199
	FOXC2	16	0.25	**0.001**	3	2.33	**0.004**
	GJC2	6	0.50	0.200	3	2.53	**0.004**
	GJA1	2	1.00	1	2	10.80	0.062
SSV	Control	8	4.13	-	22	3.78	-
	VEGFR3	4	1.75	**0.015**	6	2.93	0.212
	FOXC2	16	0.81	**<0.0005**	13	1.62	**<0.0005**
	GJC2	8	2.25	**0.020**	18	2.29	**0.001**
	GJA1	2	1.00	**0.026**	2	2.95	0.471
Brachial	Control	10	2.10	-	20	3.80	-
	VEGFR3	4	1.25	0.850	5	3.32	0.519
	FOXC2	16	0.69	**<0.0005**	10	2.29	**0.012**
	GJC2	8	0.63	**0.003**	5	3.76	0.966
	GJA1	2	0.50	0.059	1	3.10	0.664
Basilic	Control	10	2.40	-	24	4.86	-
	VEGFR3	5	1.60	0.146	7	3.73	0.170
	FOXC2	16	0.38	**<0.0005**	6	1.58	**<0.0005**
	GJC2	8	1.25	**0.027**	10	2.55	**0.002**
	GJA1	2	2.50	0.900	5	3.96	0.327

Table 6 Quantification of human VV phenotypes in controls and patients
P valves derive from independent samples t-tests for each genotype Vs control. GJC2 encodes Cx47 and GJA1 encodes Cx43. SSV = short saphenous vein

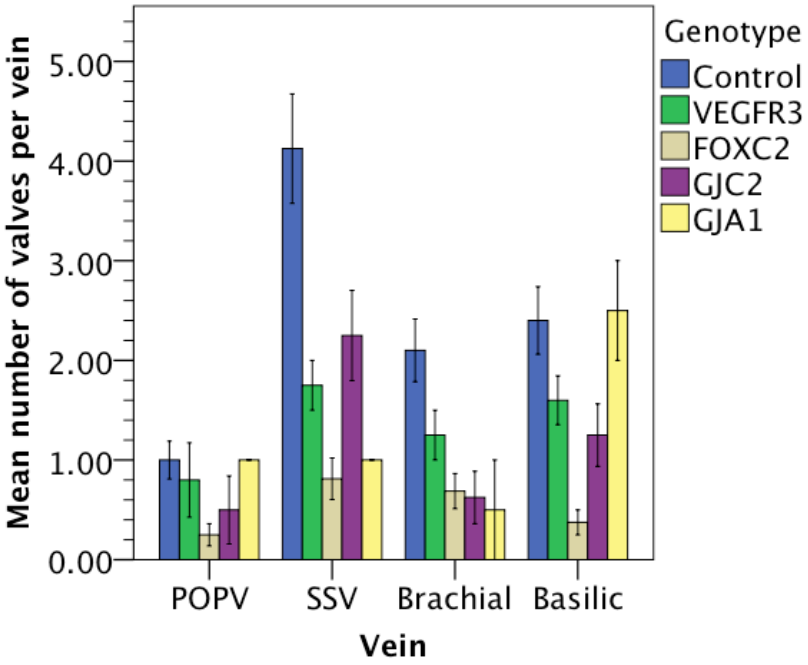

Figure 85 Number of ultrasound detected VV per vein in patients and controls

Error bars represent SEM. Original data and P values for comparisons are provided in Table 6. POPV = popliteal vein, SSV = short saphenous vein

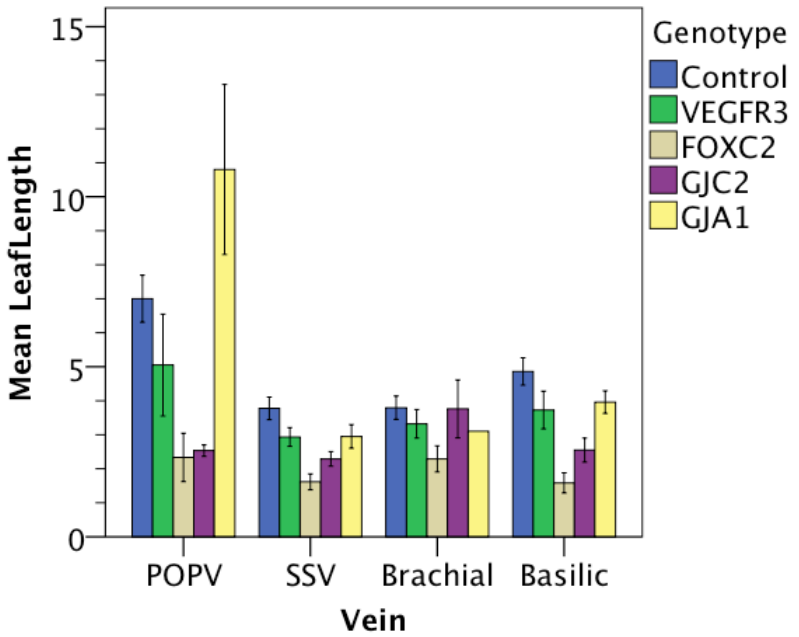

Figure 86 Mean VV length in patients and controls

Error bars represent SEM. Original data and P values for comparisons are provided in Table 6. POPV = popliteal vein, SSV = short saphenous vein

11.4.5 Analysis of normalised results

Because of the variable number of valves and length of leaflets found in each veins in the control group, it was not possible to combine raw data from different veins. The data for each valve/vein were therefore normalised to the corresponding values for that vein in the control group. Summary means were calculated that reflect the global effects on the observed ultrasound parameters in each group. (Figure 87, Figure 88) These data necessarily combine deep and superficial veins. In a subsequent analysis no significant differences were found between deep and superficial veins when analysed sepatately (Figure 89, Figure 90).

Significant reductions in the normalised number of valves were identified in participants carrying mutations in FOXC2, GJC2, VEGFR3 and GJA1 compared with the control group. The phenotype was strongest for FOXC2 mutations, as participants had approximately 80% fewer valves than the control group. Mutations in VEGFR3, FOXC2 and GJC2 but not the mutatiion in GJA1 were associated with significantly shorter normalised valve lengths. The strongest phenotype was again seen in association with FOXC2, where valves were on average 46% shorter. (Table 7, Figure 87, Figure 88)

Table 7 Comparison of the number and length of human venous valves in various genotypes.
Number and length were normalised to controls for each vein.

Group	Mean normalised number of valves per vein			Mean normalised leaflet length		
	n (veins)	mean	p	n (valves)	mean	p
Control	36	1	-	74	1	-
VEGFR3	18	0.634	**0.006**	22	0.786	**0.018**
FOXC2	64	0.233	**<0.0005**	32	0.455	**<0.0005**
GJC2	30	0.464	**<0.0005**	36	0.616	**<0.0005**
GJA1	8	0.631	**0.039**	10	0.954	0.723

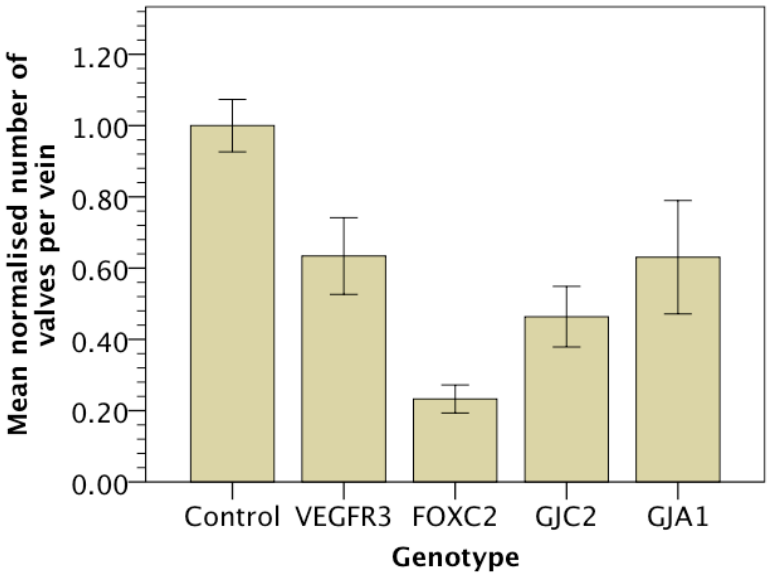

Figure 87 Normalised analysis of number of valves per vein
This graph shows the differences in mean normalized number of valves per vein for each genotype studied. Error bars represent SEM. P values for comparisons are given in Table 7. GJC2 encodes Cx47, GJA1 encodes Cx43.

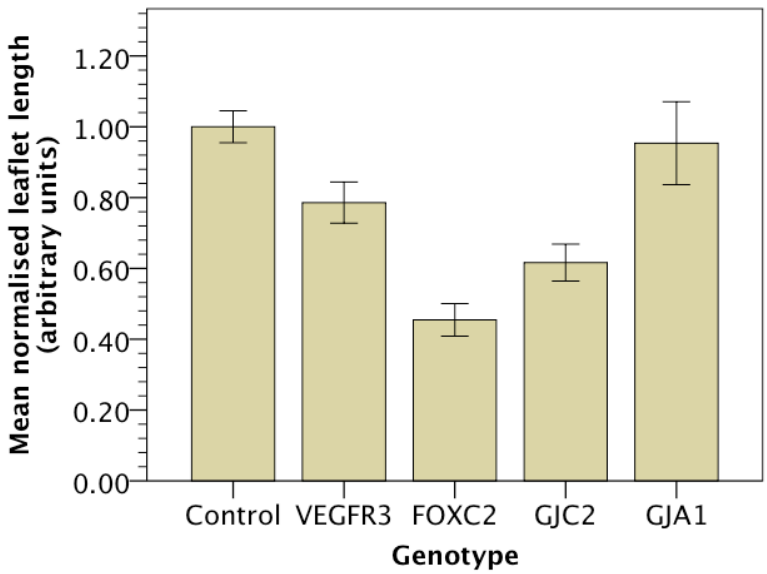

Figure 88 Normalised analysis of valve length
This graph shows the differences in mean normalized valve length for each genotype studied. Error bars represent SEM. P values for comparisons are given in Table 7.

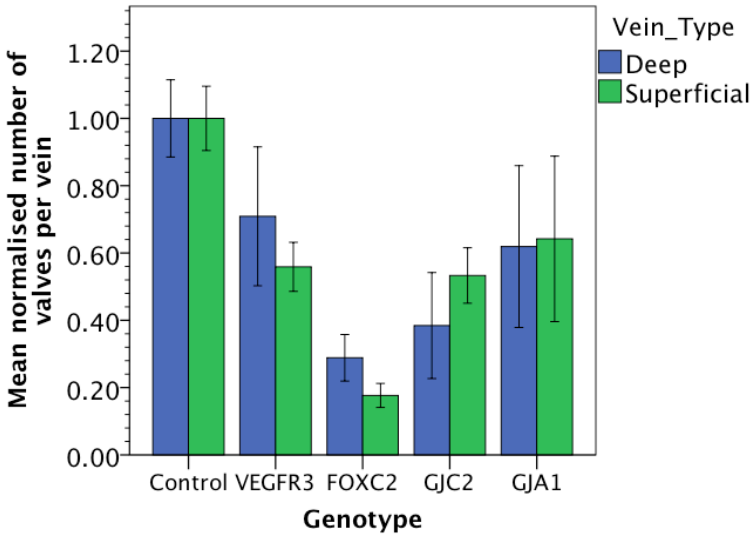

Figure 89 Normalised number of valves according to vein type
This graph shows that there was no difference in normalized number of valves per vein, when comparing deep and superficial veins for each genotype studied. P=ns (t test) for all comparisons. Error bars represent SEM.

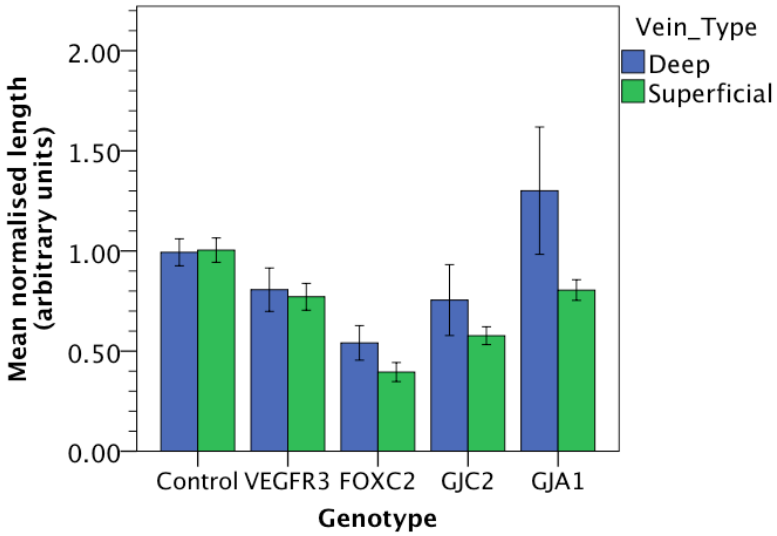

Figure 90 Normalised leaflet length according to vein type
This graph shows that there was no difference in normalized valve length, when comparing deep and superficial veins for each genotype studied. P=ns (t test) for all comparisons (deep vs superficial veins) Error bars represent SEM.

Two members of a family affected by the same mutations in GJC2 (encoding Cx47) demonstrated markedly different severity in their VV phenotype. Participant 2013-19 (age 20) was affected with clinically worse four-limb lymphoedema than her grandfather, 2013-20 (age 71). 2013-19 also showed a substantial VV structural defect with significantly shorter venous valves. No significant difference was seen in the number of valves identified (P=ns). Mean values for normalized leaflet length were 2013-19: 0.46, 2013-20: 0.87. P=0.005 These data suggest that an unknown interaction between the P316L mutation in the intracellular region of Cx47 and the granddaughters background has resulted in a clinically significant failure of VV leaflet structure. This mutation has also been reported in Ref[4] No significant difference was seen between two members of the second GJC2 family analysed.

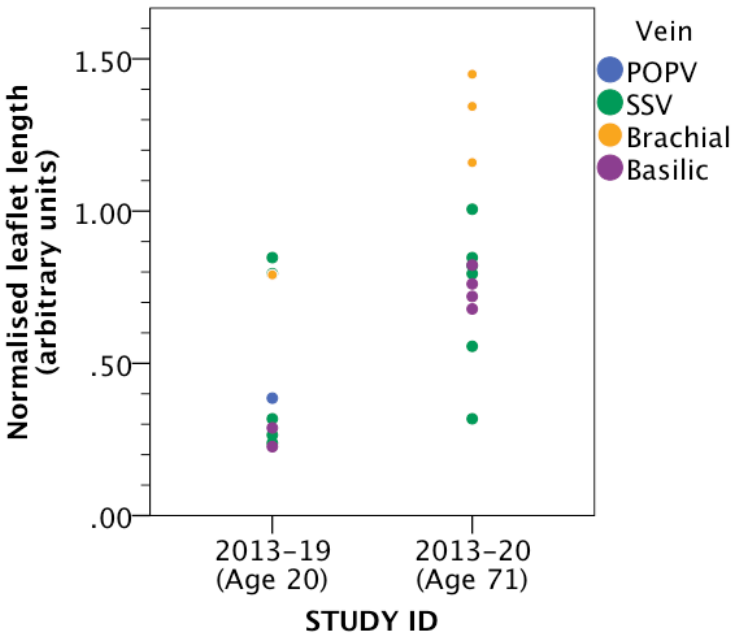

Figure 91 Two members of the same family affected by a GJC2 mutation
Each circle represents a single valve measurement. Participant 2013-19 (Table 4, age 20) was affected with clinically worse four-limb lymphoedema than her grandfather, 2013-20 (age 71). 2013-19 also showed a substantial VV structural defect with significantly shorter venous valves. No significant difference was seen in the number of valves identified (P=ns). Mean values for normalized leaflet length were 2013-19: 0.46, 2013-20: 0.87. P=0.005 POPV = popliteal vein, SSV = short saphenous vein.

11.5 Discussion

11.5.1 Ultrasound analysis of VV

Venous valves were systematically assessed in study participants with known genetic mutations, and age and sex matched healthy volunteers. To the best of my knowledge the systematic assessment of venous valves has not previously been described, and few reports have been made of the use of ultrasound (US) to study these structures. Assessment of the number of valves in each vein, and in the measured length of valve leaflets, showed a degree of reproducibility consistent with utility. Although US measurement of popliteal vein valve leaflet thickness has been described[182], leaflet thickness was not measured in this study as this measure nears the limit of ultrasound resolution and therefore felt to be unreliable.

The correlation between length measurements by different observers was higher when based on the same images (r=0.95) than when based on separate scans (r=0.74). For measurements taken from different scans, error may include difficulty in identifying the same valve for measurement. Measurement error in valve number or leaflet length would be expected to increase the variability seen in the data and reduce the likelihood of statistically significant results. Whilst the use of ultrasound to assess the structure of a single valve (for example in pre-operative planning) has not been specifically validated in this work, these results demonstrate that it is reasonable to use ultrasound to compare valves in groups of patients. The short saphenous vein contained the highest number of valves identified by ultrasound, and therefore tended to produce statistically significant reductions of valves in patients. In future work it may be possible to perform a more focused assessment on this vein. The LSV is the most commonly treated varicose vein, but was not scanned because of its long length and the need to reduce the total amount of scanning time.

11.5.2 VV phenotypes in patients with known genetic defects

Compared to controls, patients with mutations in FOXC2, VEGFR3, GJA1, or GJC1 all showed defects in the normalised number of valves identified. This was most striking for FOXC2, with affected patients possessing only 23% the

normal complement of valves. Patients carrying mutations in VEGFR3, FOXC2, GJC2 but not the single patient with a mutation in GJA1 showed a reduction in the normalised length of valve leaflets. This is consistent with the previous finding that patients carrying mutations in FOXC2 or VEGFR3 show increased rates of venous reflux.[50]

It is particularly notable that patients carrying mutations in GJC2 show clear VV structural defects, since the lymphatic phenotype in these patients has been attributed to a functional rather than structural defect.[4] The present data suggests that either the lymphatic and venous phenotypes arise by quite different mechanisms, or a lymphatic structural phenotype remains to be identified in these patients. Interestingly, two members of the same family, both carrying the same mutation in GJC2, show different severity of their phenotype, suggesting a possible interaction effect with other genes. This was not seen in the second family affected by a GJC2 mutation.

It is unclear why mutations in FOXC2 and VEGFR3 cause lower limb, but not upper limb lymphoedema. Patients with VEGFR3 mutations (causing Milroy's disease) typically have lower limb lymphoedema at birth, prior to assuming an upright stature. This implies that gravitational effects are not the cause. Lymphatic defects have been identified in the upper limb of patients with Milroy's.[48] Significant venous valve defects were not identified in the upper limbs of patients with Milroy's, but this may be as a result of the relatively low number of patients studied.

Patients with lymphoedema were only examined at a single time point. Further work could examine the temporal change in valve structure and function. It is possible that a failure to maintain normally developed valves could contribute to a later onset of lower limb swelling, for example in lymphoedema distichiasis. It would also be interesting to investigate, using these more detailed assessments, whether VV failure progresses distally or proximally within a limb affected by varicosities. It may also be possible to assess the effect of thrombosis on VV, both as a direct effect, and also any effect due to altered blood flow.

11.5.3 Limitations

- The venous valve scanning protocol required approximately 2hrs of ultrasonographer and patient time in order to visualise valves in all four limbs. The protocol was therefore limited in the number of veins that could be assessed. In addition, it was not practicable to assess reflux and vein diameter alongside valve structure. Future work could focus on the short saphenous and an upper limb vein whilst utilising a more detailed assessment. Measurements of the number of valves or of leaflet length were normalised to the corresponding values from the same veins in the control groups. The resulting normalised values showed a substantial variability (not shown). More accurate data could result from normalising to the diameter of the vein at the site of each vein. These data were not available for the present analysis. In addition a more focused scan could prove efficient for clinical use in assessing venous valves, as has previously been suggested.[183]

- It was not possible within the scope of this work to compare the number of valves identified by ultrasound with imaging by another modality, such as contrast venography. This invasive procedure represents the gold standard for in-vivo imaging of veins, but requires ionising radiation and potentially nephrotoxic contrast agents. It is therefore not possible to comment on the accuracy of the described ultrasound technique in detecting venous valves. This does not detract from the utility of ultrasound in comparing groups of patients. The most definitive data on valve location derives from post-mortem studies.[184, 185] In the popliteal vein, 1 valve has been reported to be commonly found just distal to the adductor hiatus, with a second valve just above the trifurcation in some individuals.[184] In the basilic vein, a mean of 9.3 valves was identified.[185] These findings are consistent with the results in this chapter.
- Ultrasonographers were blinded to the genotype of study participants during scanning and offline length measurements. Lymphoedema is frequently mild and difficult to identify, but it is not possible to exclude that some affected individuals were identifiable.

- Participant recruitment was limited by the availability of patients with known rare mutations. In particular, only one patient was available with lymphoedema caused by a mutation in GJA1, since this disease has only very recently been described (in the same family).[57] An abnormally long popliteal valve in a dilated vein in one limb is likely to represent an outlier and skewed the mean measurement for this patient. As discussed, normalising to vein diameter could avoid this problem in future work.

12 GENERAL DISCUSSION & LIMITATIONS

12.1.1 Methodologies

This work has provided several methods for the study of venous valve development in mice, including confocal microscopy, TEM, SEM of the vein endothelium, and SEM of resin casts of the vascular lumen (Chapter 3). Widefield and confocal microscopy of immunofluorescence stained VV with the vein intact enabled a quantification of VV developmental phenotypes in genetic loss of function experiments, or after administration of drug inhibitors. In addition, confocal microscopy allowed imaging in fluorescent reporter lines alongside immunolocalised proteins. Using these techniques it was also possible to visualise valve development at earlier stages than has previously been described, leading to the finding that valve development begins earlier than previously identified. Building on previously described work in lymphatics, methods were developed for the detailed analysis of morphology of VFC's at P0, allowing a detailed examination of phenotypes at this stage (Chapter 8).[146]

12.1.2 Requirements for specific proteins

Critical requirements are described for several proteins in venous valve development (Table 8, Table 9, Figure 92). These include Foxc2, NFATc1, Notch1, Cx37, Cx43, Cx47, integrinα9 and ephrinB2. After the requirement for Cx37 was identified in this work, others have described a requirement for Cx37 for the presence of VV in adult mice.[111] The current data build on these findings by describing the expression pattern of Cx37 at earlier stages, and identifying the developmental stage at which the VV abnormality arises.[111]

It is notable that several proteins previously identified as specific and critical regulators of arterial and lymphatic identity are found to be expressed in the region of the developing venous valve, including ephrinB2, Prox1, Notch1, VEGFR3 and Foxc2.[88, 186] In particular, Prox1, which has been described as a master regulator of lymphatic cell fate, has been found to be widely expressed in the femoral vein in the region of the developing VV at E17, and subsequently to be strongly expressed in VFC's.[44, 73, 149] This finding is confirmed by the activity of the Prox1CreERT2 transgene in venous EC's, and

the finding that Prox1 is required for VV development near the lymphovenous junction.[176] Nevertheless, these data do not dispute earlier findings for example that in arterio-venous specification ephrinB2 is expressed in arteries and EphB4 in veins, or that Prox1 is required for venous EC's to adopt a lymphatic identity and sprout from the veins as iLECs. The finding that at later stages of development proteins characterised as regulators of arterial/lymphatic development are expressed in veins suggests that after vessel specification events are complete, these proteins may perform further roles in vessel maturation (including valve formation).

12.1.3 The role of blood flow

It has previously been demonstrated that fluid flow is oscillatory prior to the onset of LV formation, and lymphatic EC's respond to fluid flows in vitro. I have shown for the first time that normal blood flow is required between P0 and P6 for normal VV developing in-vivo. It was not possible to examine the effects of altered flow on protein expression or localisation, or to examine the requirement for normal flow in events prior to P0. In vitro, Cx37 and Foxc2 (amongst other examples) are upregulated in lymphatic EC's by shear stress[42], and it is likely that a similar pathway operates in VV development in-vivo.

12.1.4 Events leading to stage 1 of VV development

Characterisation of the timing of normal events in VV development enabled experimental manipulation of the process at different time points. It was possible to identify proteins that are only required for the early stages (leading up to stage 1) of VV development, or later stages (leaflet and commissure formation).

The earliest events in venous valve development were the heterogeneous expression of valve-forming cell (VFC) markers, identifiable in the valve-forming region of the vein by E17, although it remains impossible to identify definite VFC's at this stage. In VV by P0, wildtype VFC's had organised into a ring of rotated and elongated cells aligned circumferentially around the vein lumen. Three connexins – Cx37, Cx43, Cx47 – were found to have very

different expression patterns during early valve development. The importance of connexins in LV development, and a requirement of Cx37 for the presence of VV in the adult mouse have been described previously.[42, 94, 109, 111] Loss of Cx37, Cx43 or Cx47 resulted in grossly similar phenotypes of VV disorganisation at P0, with defects in the normal elongation and rotation of endothelial cells. Similarly, loss of Cx47 resulted in complete absence of VFC's by P2, and by P6 for loss of Cx37. This may be due to defective communication between VFC's, either directly through loss of gap junction components, or lack of cell contact secondary to failed organisation events. In valves lacking Cx37 there were proportionally fewer VFC's in the central region of the vein than in wildtype littermates. This finding is susceptible to bias in the identification of Prox1^{hi} VFC's, although no differences were identified for Cx43 or Cx47. Whilst this is consistent with the suggestion that the Cx37 phenotype could also involve defective migration of cells into this region, this idea is not supported by the finding that an overall similar phenotype is seen following loss of Cx43/47 without any change in the proportion of cells in each region.[42] These loss-of function approaches to connexin function showed that valve development appears to progress relatively normally up until P0, by which time these connexins are critically required, and so these data suggest that failure of organisation at this stage is likely to be the mechanism involved in the human Cx43 and Cx47-related VV structural phenotypes identified in this work.

Conditional deletion of Notch1 had no effect after P0, but deletion from E15.5 resulted in a phenotype at P0 of a widened region of Prox1^{hi} VFC's, and an observed lack of rotated and elongated VFC's. After this work was completed, comparable findings were published following Notch1 deletion in lymphatic valve development.[90] Expression of a dominant negative Mastermind-like transgene resulted in a more severe phenotype than deletion of Notch1, suggesting that other Notch proteins may also be signalling in LV formation. In cultured cells, activation of Notch1 or Notch4 induced integrin α9, fibronectin EIIIA and Cx37 expression.[90] It was not possible within the timeframe of this work to identify antibodies suitable for localisation of Notch1 by wholemount confocal microscopy at P0, and the expression pattern of Notch1 in VV at this

stage remains unknown. In LV, it has been noted that conditional deletion of Notch1 resulted in a similar phenotype to Cx37 knockout.[90] In VV, this is again seen, and in addition the phenotype is comparable to that seen following Cx47 knockout or deletion of Cx43.

It remains to be determined whether the phenotypes observed with loss of Cx37, Cx43 or Cx47 result from a loss of gap junctional intercellular communication or non-junctional roles. The different expression patterns of the connexins, particularly Cx43 in the upstream region and Cx37 in VFC's, suggests that domains of GJIC may be established that allow VFC's to act in a coordinated fashion. Given the recent finding that Notch1 intracellular domain activity upregulates Cx37 (and Foxc2), Notch1 could act in VFC's to select VFC's and establish this signalling.[90]

EfnB2 promoter activity was imaged using a fluorescent reporter line, and was identified much earlier than previously described. It remains unclear how the patterns of protein expression seen at P0 are established. Levet et al have demonstrated a requirement for BMP9 (likely acting via ALK1) in lymphatic valve formation, and shown that BMP9 upregulates Foxc2, Cx37 and EphrinB2 in LECs. It is likely that BMP9 is also involved in VV development, and it could act upstream of these factors at early stages to upregulate Foxc2 and EphrinB2 in VFC's and the downstream region.[45]

The expression pattern of ephrinB2 identified in Chapter 0 indicates that Cx43 expression upstream of the VFC's is in an ephrinB2 non-expressed domain, with VFC's and downstream cells expressing ephrinB2. This again suggests that ephrinB2-based cell sorting could be involved in patterning the valve at P0. EphrinB2 and ephrinB1 are structurally closely related, and ephrinB1 physically interacts with Cx43 and regulates GJIC in craniofacial development.[187] In the frontal bone of chimeric embryos, whilst plaque-like Cx43 immunostaining was observed between ephrinB1-null cells, and between wildtype cells, almost no Cx43 plaques were observed between ephrinB1-null and wildtype cells, suggesting that ephrin based cell sorting may assist in the production of GJIC domains of EC's.[187] Given the high degree of homology between ephrinB1 and ephrinB2, it is interesting to speculate that

ephrinB2 could also interact with Cx43. Treatment of ephrinB1 over-expressing cells with soluble EphB receptor resulted in loss of membranous Cx43 expression.[187] In VV development, this hypothesis would be consistent with the presence at P0 of Cx43 just upstream of the line of VFC's (which express ephrinB2).

12.1.5 Leaflet and commissure development after stage 1

Surprisingly neither Foxc2 nor Calcineurin-NFAT signalling were required for the earliest events in valve formation. This work does not exclude the possibility that redundancy between Foxc2 and NFATc1 allows for compensation, or for unidentified expression of other Fox family members such as Foxc1. Both NFATc1 and Foxc2 were required for normal maturation of the valves beyond P0; loss of NFAT-Calcineurin signalling resulted in particularly marked failure of leaflet development. The mechanism underlying this failure is not known; it is possible that NFATc1 induces proliferation of leaflet cells.

The membrane-bound matrix receptor integrinα9 was previously identified, along with ephrinB2, to be critically required for VV development after P0 and also maintenance of the adult VV.[44] These findings were confirmed using an improved method, allowing staging of valve development. Conditional homozygous deletion of ephrinB2 or integrinα9 from P0 resulted in complete loss of valve leaflets, but in both cases rotated Prox1^{hi} endothelial cells could still be identified at P6, although not to the same extent as seen following loss of NFAT-calcineurin signalling, suggesting that entegrina9 and ephrinB2 might be required for maintenance of the free-edge cell phenotype, to some degree, or at least that the mechanisms of valve failure following these deletions differs. EphrinB2 was previously described to be expressed in leaflet endothelial cells but not free-edge cells, compatible with a requirement for reverse signalling into leaflet cells after P0.[44] It was not possible to determine whether reverse or forward signalling is required for VV development, but given the previously identified requirement for ephrinB2 reverse signalling for lymphatic valve development, it is possible that reverse signalling is similarly required for VV development.[73]

Table 8 Summary of murine VV phenotypes shown in this thesis
The table provides a summary of the phenotypes seen with the genetic loss of function approaches and model of altered blood flow employed in this thesis.

	Requirement in early VV development: **Phenotype at P0 after early deletion (≈E15) / inhibition**	**Requirement in later VV development:** **Phenotype at P6 after later deletion (≈P0) / inhibition**
Integrinα9	*unknown*	Failure to develop leaflets. Residual Prox1hi rotated EC's seen at P6
EphrinB2	*unknown* Suggested role in patterning the ring of rotated cells at P0 (Stage 1)	Failure to develop VV leaflets. Some residual Prox1hi rotated EC's seen at P6
Cx37	Disorganisation of Prox1^{hi} cells, possibly reduced proportion of Prox1hi cells in centre of vein (constitutive knockout)	Complete absence of any VV cells at P6 (constitutive knockout). Loss of gap in pericytes
Cx43	Disorganisation of Prox1^{hi} cells (constitutive deletion)	No phenotype at P6 following conditional deletion from P0.
Cx47	Disorganisation of Prox1^{hi} cells (constitutive knockout in reporter)	Complete absence of any VV cells at P2 (constitutive knockout).
Foxc2	No clear phenotype at P0 (conditional deletion)	Inhibited VV development
Nfat-calcineurin	No clear phenotype at P0 (conditional CnB1 deletion)	Marked failure to developed VV leaflets, but ring of Prox1^{hi}/Foxc2^{hi} rotated cells entirely intact
Notch1	Disorganised Prox1^{hi} cells at P0	No phenotype at P6 following conditional deletion from P0.
VEGFR3	No phenotype with drug inhibition of VEGFR3 (but strong phenotype with combined inhibition of VEGFR1,2,3)	No phenotype with drug inhibition of VEGFR3
Altered blood flow	*unknown*	Inhibited valve development and smaller valve

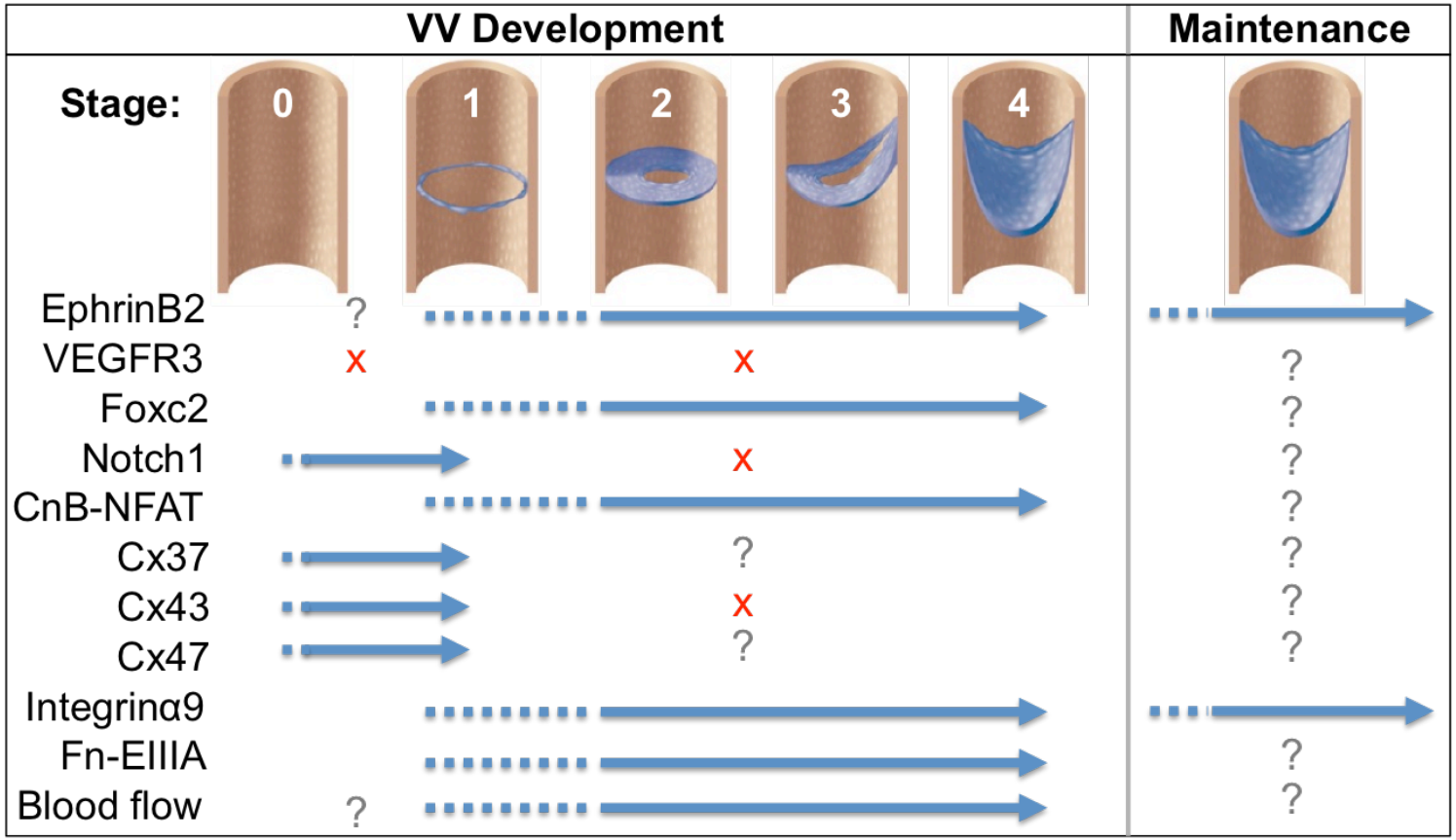

Figure 92 Summary schematic: factors required for murine VV development and maintenance
The schematic summarises the timing of the known requirements for VV development and maintenance, as shown in Table 8 and Table 9. X= shown to be not required. ?= unknown, due, for example, to experiments not performed or lack of a floxed allele to allow conditional deletion. Data sources are given in Table 9.

Table 9 The factors known to be responsible for VV development and maintenance in murine models and in man

The table summarises existing knowledge of the factors responsible for VV development and/or maintenance in mice and in man. * = work in this thesis. *U* = unknown. In man, expression refers to adult VV in patients with clinically normal veins. It is unlikely that Cx43 or Notch1 are required for maintenance of the formed VV, since deletion of either from P0 did not give a phenotype at P6, but their role in maintenance has not been specifically examined in this thesis. Fn-EIIIA = EIIIA splice variant of fibronectin. Ref[44] is given in Appendix 13.

Protein/Factor	Murine VV Development	Murine VV Maintenance	Man
Prox1	Expressed [44] and required [176]	*U*	Expressed [44]
Integrinα9	Required [44] and *	Ref[44]	Expressed *
Fn-EIIIA	Required [44]	Ref[44]	*U*
EphrinB2	Required [44] and *	Ref[44]	*U*
Cx37	Required [111] and *	*U*	*U*
Cx43	Required *	*Unlikely* *	Expressed and VV defect *
Cx47	Required *	*U*	Expressed and VV defect *
Foxc2	Expressed [40] and required *	*U*	Reflux [50] and VV defect *
Nfat-calcineurin	NFATc1 expressed and calcineurin activity required *	*U*	NFATc1 expressed *
Notch1	*	*Unlikely* *	*U*
VEGFR3	Expressed but possibly not required *	*U*	Reflux [53] and VV defect *
(GATA2)	*U*	*U*	Expressed *
Normal blood flow	Required *	*U*	*U*

12.1.6 Cardiac, Venous and lymphatic valve formation

Apart from Cx47, all the proteins identified in this work as critical regulators of VV development have previously been shown to play roles in cardiac and/or lymphatic valve development. It has previously been noted that cardiac and lymphatic valves share some regulatory pathways.[39] For example, loss of Calcineurin-NFAT signalling results in a failure of leaflet elongation in the semilunar, venous and lymphatic valves.[42, 96]. Whilst the interactions between several of the proteins studied in this work remain to be examined, it will be interesting to determine whether these interactions are consistent in cardiac, lymphatic and venous valves. It is likely that work in any one valve type will continue to illuminate potential mechanisms of valve formation in others. The finding of a structural VV defect following Cx47 knockout is notable as the lymphatic phenotypes observed in patients carrying mutations in GJC2 have been attributed to a functional and not structural defect.[4]

12.1.7 Analysis of human VV and phenotypes in patients

SEM, TEM and immunohistological analysis of murine and human venous valves suggest similar cellular structure and protein expression patterns, consistent with previous descriptions of human VV.[11] Several proteins, including integrinα9, NFATc1, Cx43 and Cx47 were localised in adult human venous valves. We have previously described expression of Prox1 in human VV.[44]

The use of ultrasound to quantify structural defects in human VV was validated, allowing the identification of VV structural defects in patients with known genetic defects. Analysis of valves in patients with mutations in FOXC2, VEGFR3, GJC2 (encoding Cx47) and GJA1 (encoding Cx43) showed generally reduced numbers of valves and shorter valve leaflets. Although patients with Milroy's disease carry mutations that inactivate the tyrosine kinase domain of VEGFR3, inhibition of this domain in the murine model had no effect on VV development, either up to P0, or to P6. This unexpected result suggests the possibility that mutations carried by patients exert effects that are not directly mediated by loss of tyrosine kinase activity. It has previously been demonstrated that kinase-dead VEGFR3 proteins reside for a greater period of time at the cell membrane, and it is possible that mutant VEGFR3 interferes

with normal function of other proteins at the membrane, for example VEGFR2 or ephrinB2.[119, 129] It was not possible to explore these possibilities in the current work.

12.1.8 Limitations and future work

This work has several limitations. Unlike some other vascular model systems (for example retinal sprouting angiogenesis), in venous (and lymphatic) valve development sequentially occurring processes are not clearly spatially separated. In combination with the variability seen in the morphology and timing of venous valve development, this complicates interpretation of expression data and genetic loss of function phenotypes.

It is not possible to quantify loss of protein in VV following Cre-mediated excision of LoxP-flanked sequences. This is likely to vary with different genes, due for example to differing rates of protein turnover. Confocal microscopy and (in particular) immunohistochemistry are not quantitative techniques and so it is not possible to identify small changes in protein expression (although large variations may be clearly apparent). There is no technique for isolation of valve cells from tissue, and even if this were possible it is highly unlikely that sufficient protein would be available for quantitative analysis. mRNA could be examined by qPCR (or in situ) but this would not confirm loss of protein.

The analysis of constitutive knockouts (for example of Cx37 or Cx47) may be complicated by distant and unidentified effects of protein loss. Where possible this has been avoided by the use of conditional deletion in Prox1-expressing EC's, allowing analysis of cell-autonomous roles. In addition, the appropriate presence of VFC's at P0 in Cx37 and Cx47 constitutive knockouts suggests that steps up until this time point have proceeded relatively normally.

It is possible for a floxed allele to result in slightly less protein production that a wildtype allele, even in the absence of Cre recombinase. Most of the phenotypes observed in this thesis required homozygous deletion, with relatively normal development occurring following heterozygous deletion. This suggests that any relatively small reduction in protein expression in Cre-

animals carrying floxed alleles is likely to have a negligible effect. Similarly, the lack of a strong phenotype following heterozygous deletion of ephrinB2 or Cx47 suggests that the expression patterns observed in the EfnB2GFP reporter or Cx47:GFP reporter (both heterozygous knockouts) are relatively normal. The lack of a conditional heterozygous ephrinB2 deletion phenotype at P6 does not exclude a phenotype from earlier deletion prior to P0. It has been shown in the vasculature that knockdown of one connexin can reduce levels of others.[105] This possibility was reduced where possible with the use of conditionally targeted alleles.

The methodology for the analysis of nuclear morphology in Chapter 8 builds on previous work in lymphatic valve development.[146] Whilst analysis of wholemount samples is critical to understanding events in-vivo, it is possible that measurements of nuclear morphology could have been affected by areas of distortion or damage to the vessel. This was avoided by co-immunolocalisation of endothelial and smooth muscle markers, avoidance of any distorted tissue, and analysis of a large number of nuclei in many samples. Windowing of displayed immunosignal can result in an apparent change in the dimensions of a structure, but should not affect rotational angle. Any variation should be very small within a sample. It was not possible to use a signal threshold to identify Prox1hi cells, and this selection was performed manually (as previously described in ref [146]). Bias in VFC selection could therefore have affected the analysis, particular for analysis of the number of VFC's in each region of the valve.

Inhibitors were used to study the effects of inhibition of calcineurin activity, and inhibition of VEGFR tyrosine kinase activity. It is not possible the exclude a contribution of off-target effects to the observed phenotypes. Axitinib, in particular, resulted in general toxicity and the observed phenotype may be due to general inhibition of EC growth. It was not possible to analyse the effect of conditional deletion of VEGFR2/3.

Calcineurin-NFAT inhibition was analysed using ciclosporin and conditional CnB1 deletion by Prox1CreERT2. Whilst conditional CnB1 deletion was

confined to EC's by Prox1CreERT2, ciclosporin would additionally inhibit signalling in all other cells. Both approaches would inhibit nuclear translocation of all NFAT's, including NFATc1. NFATc1 was localised to the developing VV, and is critically required for cardiac and lymphatic development. It is not possible to exclude potential roles for other NFATs in VV development.

A major limitation to the progress of this study has been the paucity of data obtained from a single mouse, which possesses only two proximal femoral vein valve sites. This contrasts with common methods for study of lymphatic valves (in the mesentery and ear) where many valves are analysed in a single sample. These techniques lack the advantage of the development of a valve at a consistent position. Additionally, the requirement for sample dissection three times to process wholemount specimens from 'mouse to slide' limits the number of samples that can be processed. The model could be improved by development of techniques to allow wholemount confocal microscopy of other veins, containing more valves for analysis. This would be facilitated by use of endothelial reporter lines.

In further work, it is necessary to perform conditional deletion experiments to examine the roles of Cx37, Cx47, VEGFR2/3, during later VV development, and also in maintenance (Figure 92, Table 9). The role of Foxc2 and Calcineurin-NFAT signalling in maintenance has not been examined, and could be explored with the use of conditionally targeted deletion and/or ciclosporin. No requirement was shown for Foxc2 or Calcineurin-NFAT in early VV development, and it will be important to determine whether redundancy between Foxc1/Foxc2/NFATc1 is present in early VV development.

The identity, source(s) and role(s) of interstitial cells have not been examined in this thesis. The line used for conditional deletion produces recombination only in the VV EC's. It is likely that interstitial cells play important roles in VV development, which may include production or maintenance of the VV matrix core, and also roles in signalling with EC's. It is interesting to speculate that neural crest cells, which play critical roles in cardiac valve development, could

also have a role in VV (and LV) formation. This could be investigated in a fate mapping study with use of a Wnt1Cre line with an appropriate reporter (for example mTmG).

Signalling events between VV EC's and pericytes have not been examined in this thesis, but are likely to be required for formation of the 'gap' in SMA-expressing pericytes seen around the formed VV, in a similar way to the process that occurs in LV development.

The role of blood flow in early VV development or maintenance has not been successfully examined. Analysis of the role of flow in maintenance could have particular relevance to human VV disease, potentially including the VV failure associated with thrombosis and varicosis. Additional work is required to elucidate the mechanotransduction pathways that incorporate signals from blood flow into the genetic program of VV development (and possibly maintenance).

13 REFERENCES

1. Meissner M, Moneta G, Burnand K, Gloviczki P, Lohr J, Lurie F, Mattos M, McLafferty R, Mozes G, Rutherford R. The hemodynamics and diagnosis of venous disease. *Journal of Vascular Surgery*. 2007;46:S4-S24

2. Mozes G, Gloviczki P. New discoveries in anatomy and new terminology of leg veins: Clinical implications. *Vasc Endovascular Surg*. 2004;38:367-374

3. Phillips MN, Jones GT, van Rij AM, Zhang M. Micro-venous valves in the superficial veins of the human lower limb. *Clin Anat*. 2004;17:55-60

4. Ferrell RE, Baty CJ, Kimak MA, Karlsson JM, Lawrence EC, Franke-Snyder M, Meriney SD, Feingold E, Finegold DN. Gjc2 missense mutations cause human lymphedema. *Am J Hum Genet*. 2010;86:943-948

5. Bergan JJ, Schmid-Schonbein GW, Smith PD, Nicolaides AN, Boisseau MR, Eklof B. Chronic venous disease. *N Engl J Med*. 2006;355:488-498

6. Coleridge-Smith.PD. Leg ulcer treatment. *J Vasc Surg*. 2009;49:804-808

7. Eberhardt RT. Chronic venous insufficiency. *Circulation*. 2005;111:2398-2409

8. Raffeto.J KR. Mechanisms of varicose vein formation: Valve dysfunction and wall dilation. *Phlebology*. 2008;23:85-98

9. Lim CS, Davies AH. Pathogenesis of primary varicose veins. *British Journal of Surgery*. 2009;96:1231-1242

10. Meissner MH, Eklof B, Smith PC, Dalsing MC, DePalma RG, Gloviczki P, Moneta G, Neglen P, T OD, Partsch H, Raju S. Secondary chronic venous disorders. *J Vasc Surg*. 2007;46 Suppl S:68S-83S

11. Gottlob R, May R, Geleff S. *Venous valves : Morphology, function, radiology, surgery*. Wien ; New York: Springer-Verlag; 1986.

12. Gohel MS, Davies AH. Pharmacological agents in the treatment of venous disease: An update of the available evidence. *Current vascular pharmacology*. 2009;7:303-308

13. Moore HM, Gohel MS, Davies AH. The forgotten burden of deep venous disease. *Phlebology*. 2010;25:53

14. Caggiati AC, L. Surgery of venous valve. *Reviews in vascular medicine*. 2013;1:15-23

15. Perrin M. [surgery for deep venous reflux in the lower limb]. *Journal des maladies vasculaires*. 2004;29:73-87

16. Neglen P, Raju S. Venous reflux repair with cryopreserved vein valves. *J Vasc Surg*. 2003;37:552-557

17. Kistner RL. Surgical repair of the incompetent femoral vein valve. *Arch Surg*. 1975;110:1336-1342

18. Teebken O, Puschmann C, Breitenbach I, Rohde B, Burgwitz K, Haverich A. Preclinical development of tissue-engineered vein valves and venous substitutes using re-endothelialised human vein matrix. *European Journal of Vascular and Endovascular Surgery*. 2009;37:92-102

19. Rosales A, Jørgensen JJ, Slagsvold CE, Stranden E, Risum Ø, Kroese AJ. Venous valve reconstruction in patients with secondary chronic venous insufficiency. *European Journal of Vascular and Endovascular Surgery*. 2008;36:466-472

20. Czarniawska-Grzesinska. Development of valves in the great saphenous vein of human fetuses. *Folia Morphol*. 2001;60:118

21. Kokova.J HM, Horakova.MA. L'evolution des veines pre-et post-natales. *Phlebologie*. 1993;46:241-252

22. Kampmeier.OF LFBC. The origin and development of the venous valves, with particular reference to the saphenous district. *American Journal of Anatomy*. 1927;38:451-499

23. Czarniawska-Grzesinska. Development of valves in the small saphenous vein in human fetuses. *Folia Morphol*. 2002;61:37-42

24. Rickenbacher.J. Zur entwicklung der venen der untern extremitat [on the development of the veins of the lower extremity]. *Zentralbl Phlebol*. 1966 15:6-14

25. Jager.O. Die entwinklung der venenklappen. *Morph. Jahrbuch.* 1926;56:25x

26. Franklin.KJ. Valves in veins: An historical survey. *J.Anat*. 1929;64:67

27. Amoroso EC, Edholm.,O.G, Rewell,R.E. Venous valves in the giraffe, okapi, camel and ostrich. *Proceedings of the zoological society of london*. 1947;117:435-440

28. Franklin KJ. Valves in veins: Further observations. *Journal of anatomy*. 1929;64:67-69

29. Hossler.FE WR. Venous valve anatomy and morphometry: Studies on the duckling using vascular corrosion casting. *Am J Anat*. 1988;181:425-432

30. Takase S, Pascarella L, Lerond L, Bergan JJ, Schmid-Schonbein GW. Venous hypertension, inflammation and valve remodeling. *Eur J Vasc Endovasc Surg*. 2004;28:484-493

31. Caggiati A, Phillips M, Lametschwandtner A, Allegra C. Valves in small veins and venules. *European Journal of Vascular and Endovascular Surgery*. 2006;32:447-452

32. Van Bemellen SP. *Venous valvular incompetence*. Amsterdam: Fa. Lameris; 1984.

33. Hossler FE, West RF. Venous valve anatomy and morphometry: Studies on the duckling using vascular corrosion casting. *Am J Anat*. 1988;181:425-432

34. Sabin.F. On the origin of the lymphatic system from the veins and the development of the lymph hearts and thoracic duct in the pig. *American Jorunal of Anatomy*. 1902;1:367-389

35. Wigle JT, Oliver G. Prox1 function is required for the development of the murine lymphatic system. *Cell*. 1999;98:769-778

36. François M, Caprini A, Hosking B, Orsenigo F, Wilhelm D, Browne C, Paavonen K, Karnezis T, Shayan R, Downes M, Davidson T, Tutt D, Cheah KSE, Stacker SA, Muscat GEO, Achen MG, Dejana E, Koopman P. Sox18 induces development of the lymphatic vasculature in mice. *Nature*. 2008;456:643-647

37. Hagerling R, Pollmann C, Andreas M, Schmidt C, Nurmi H, Adams RH, Alitalo K, Andresen V, Schulte-Merker S, Kiefer F. A novel multistep mechanism for initial lymphangiogenesis in mouse embryos based on ultramicroscopy. *The EMBO journal*. 2013;32:629-644

38. Tammela T, Alitalo K. Lymphangiogenesis: Molecular mechanisms and future promise. *Cell*. 2010;140:460-476

39. Norrmen C, Ivanov KI, Cheng J, Zangger N, Delorenzi M, Jaquet M, Miura N, Puolakkainen P, Horsley V, Hu J, Augustin HG, Yla-Herttuala S, Alitalo K, Petrova TV. Foxc2 controls formation and maturation of lymphatic collecting vessels through cooperation with nfatc1. *The Journal of Cell Biology*. 2009;185:439-457

40. Petrova TV, Karpanen T, Norrmén C, Mellor R, Tamakoshi T, Finegold D, Ferrell R, Kerjaschki D, Mortimer P, Ylä-Herttuala S, Miura N, Alitalo K. Defective valves and abnormal mural cell recruitment underlie lymphatic vascular failure in lymphedema distichiasis. *Nature Medicine*. 2004;10:974-981

41. Kampmeier.O.F. The genetic history of the valves in the lymphatic system of man. *Am J Anat*. 1928;40:413-457

42. Sabine A, Agalarov Y, Maby-El Hajjami H, Jaquet M, Hagerling R, Pollmann C, Bebber D, Pfenniger A, Miura N, Dormond O, Calmes JM, Adams RH, Makinen T, Kiefer F, Kwak BR, Petrova TV. Mechanotransduction, prox1, and foxc2 cooperate to control connexin37 and calcineurin during lymphatic-valve formation. *Dev Cell*. 2012

43. Bazigou E, Xie S, Chen C, Weston A, Miura N, Sorokin L, Adams R, Muro AF, Sheppard D, Makinen T. Integrin-α9 is required for fibronectin matrix assembly during lymphatic valve morphogenesis. *Developmental Cell*. 2009;17:175-186

44. Bazigou E, Lyons OT, Smith A, Venn GE, Cope C, Brown NA, Makinen T. Genes regulating lymphangiogenesis control venous valve formation and maintenance in mice. *J Clin Invest*. 2011;121:2984-2992

45. Levet S, Ciais D, Merdzhanova G, Mallet C, Zimmers TA, Lee SJ, Navarro FP, Texier I, Feige JJ, Bailly S, Vittet D. Bone morphogenetic protein 9 (bmp9) controls lymphatic vessel maturation and valve formation. *Blood*. 2013;122:598-607

46. Connell F, Brice G, Jeffery S, Keeley V, Mortimer P, Mansour S. A new classification system for primary lymphatic dysplasias based on phenotype. *Clinical Genetics*. 2010;77:438-452

47. Fang J, Dagenais SL, Erickson RP, Arlt MF, Glynn MW, Gorski JL, Seaver LH, Glover TW. Mutations in foxc2 (mfh-1), a forkhead family transcription factor, are responsible for the hereditary lymphedema-distichiasis syndrome. *Am J Hum Genet*. 2000;67:1382-1388

48. Mellor RH, Hubert CE, Stanton AWB, Tate N, Akhras V, Smith A, Burnand KG, Jeffery S, Mäkinen T, Levick JR, Mortimer PS. Lymphatic dysfunction, not aplasia, underlies milroy disease. *Microcirculation*. 2010;17:281-296

49. Brice G. Analysis of the phenotypic abnormalities in lymphoedema-distichiasis syndrome in 74 patients with foxc2 mutations or linkage to 16q24. *Journal of Medical Genetics*. 2002;39:478-483

50. Mellor RH, Brice G, Stanton AWB, French J, Smith A, Jeffery S, Levick JR, Burnand KG, Mortimer PS. Mutations in foxc2 are strongly associated with primary valve failure in veins of the lower limb. *Circulation*. 2007;115:1912-1920

51. Ferrell RE, Levinson KL, Esman JH, Kimak MA, Lawrence EC, Barmada MM, Finegold DN. Hereditary lymphedema: Evidence for linkage and genetic heterogeneity. *Hum Mol Genet*. 1998;7:2073-2078

52. Evans AL, Brice G, Sotirova V, Mortimer P, Beninson J, Burnand K, Rosbotham J, Child A, Sarfarazi M. Mapping of primary congenital lymphedema to the 5q35.3 region. *Am J Hum Genet*. 1999;64:547-555

53. Brice G. Milroy disease and the vegfr-3 mutation phenotype. *Journal of Medical Genetics*. 2005;42:98-102

54. Gordon K, Schulte D, Brice G, Simpson MA, Roukens MG, van Impel A, Connell F, Kalidas K, Jeffery S, Mortimer PS, Mansour S, Schulte-Merker S, Ostergaard P. Mutation in vascular endothelial growth factor-c, a ligand for vascular endothelial growth factor receptor-3, is associated with autosomal dominant milroy-like primary lymphedema. *Circ Res*. 2013;112:956-960

55. Balboa-Beltran E F-SM, Pérez-Muñuzuri A, Lago R, García-Magán C, Couce ML, Sobrino B, Amigo J, Carracedo A, Barros F. A novel stop mutation in the vascular endothelial growth factor-c gene (vegfc) results in milroy-like disease. *J Med Genet*. 2014

56. Laird DW. Syndromic and non-syndromic disease-linked cx43 mutations. *FEBS Lett*. 2014;588:1339-1348

57. Brice G, Ostergaard P, Jeffery S, Gordon K, Mortimer P, Mansour S. A novel mutation in gja1 causing oculodentodigital syndrome and primary lymphoedema in a three generation family. *Clin Genet*. 2013

58. Ostergaard P, Simpson MA, Brice G, Mansour S, Connell FC, Onoufriadis A, Child AH, Hwang J, Kalidas K, Mortimer PS, Trembath R, Jeffery S. Rapid identification of mutations in gjc2 in primary lymphoedema using whole exome sequencing combined with linkage analysis with delineation of the phenotype. *J Med Genet*. 2011;48:251-255

59. Orthmann-Murphy JL, Enriquez AD, Abrams CK, Scherer SS. Loss-of-function gja12/connexin47 mutations cause pelizaeus-merzbacher-like disease. *Molecular and cellular neurosciences*. 2007;34:629-641

60. Diekmann S, Henneke M, Burckhardt BC, Gartner J. Pelizaeus-merzbacher-like disease is caused not only by a loss of connexin47 function but also by a hemichannel dysfunction. *Eur J Hum Genet*. 2010;18:985-992

61. Odermatt B, Wellershaus K, Wallraff A, Seifert G, Degen J, Euwens C, Fuss B, Bussow H, Schilling K, Steinhauser C, Willecke K. Connexin 47 (cx47)-deficient mice with enhanced green fluorescent protein reporter gene reveal predominant oligodendrocytic expression of cx47 and display vacuolized myelin in the cns. *The Journal of neuroscience : the official journal of the Society for Neuroscience*. 2003;23:4549-4559

62. Gupta SK, Vlahakis NE. Integrin alpha9beta1: Unique signaling pathways reveal diverse biological roles. *Cell adhesion & migration*. 2010;4:194-198

63. Hoye AM, Couchman JR, Wewer UM, Fukami K, Yoneda A. The newcomer in the integrin family: Integrin alpha9 in biology and cancer. *Advances in biological regulation*. 2012;52:326-339

64. Palmer EL, Ruegg C, Ferrando R, Pytela R, Sheppard D. Sequence and tissue distribution of the integrin alpha 9 subunit, a novel partner of beta 1 that is widely distributed in epithelia and muscle. *J Cell Biol*. 1993;123:1289-1297

65. Huang XZ, Wu JF, Ferrando R, Lee JH, Wang YL, Farese RV, Jr., Sheppard D. Fatal bilateral chylothorax in mice lacking the integrin alpha9beta1. *Molecular and cellular biology*. 2000;20:5208-5215

66. Ma GC, Liu CS, Chang SP, Yeh KT, Ke YY, Chen TH, Wang BB, Kuo SJ, Shih JC, Chen M. A recurrent itga9 missense mutation in human fetuses with severe chylothorax: Possible correlation with poor response to fetal therapy. *Prenat Diagn*. 2008;28:1057-1063

67. Yang YS, Ma GC, Shih JC, Chen CP, Chou CH, Yeh KT, Kuo SJ, Chen TH, Hwu WL, Lee TH, Chen M. Experimental treatment of bilateral fetal chylothorax using in-utero pleurodesis. *Ultrasound Obstet Gynecol*. 2012;39:56-62

68. Danussi C, Spessotto P, Petrucco A, Wassermann B, Sabatelli P, Montesi M, Doliana R, Bressan GM, Colombatti A. Emilin1 deficiency causes structural and functional defects of lymphatic vasculature. *Molecular and cellular biology*. 2008;28:4026-4039

69. Wiester.LM GC. Expression and function of the integrin alpha9beta1 in bovine aortic valve interstitial cells. *Journal of Heart Valve Disease*. 2003;12:605-616

70. Kullander K, Klein R. Mechanisms and functions of eph and ephrin signalling. *Nature reviews. Molecular cell biology*. 2002;3:475-486

71. Cowan CA, Yokoyama N, Saxena A, Chumley MJ, Silvany RE, Baker LA, Srivastava D, Henkemeyer M. Ephrin-b2 reverse signaling is required for axon pathfinding and cardiac valve formation but not early vascular development. *Developmental Biology*. 2004;271:263-271

72. Pitulescu ME, Adams RH. Eph/ephrin molecules--a hub for signaling and endocytosis. *Genes Dev*. 2010;24:2480-2492

73. Makinen T, Adams RH, Bailey J, Lu Q, Ziemiecki A, Alitalo K, Klein R, Wilkinson GA. Pdz interaction site in ephrinb2 is required for the remodeling of lymphatic vasculature. *Genes Dev*. 2005;19:397-410

74. Jackson BC, Carpenter C, Nebert DW, Vasiliou V. Update of human and mouse forkhead box (fox) gene families. *Human genomics*. 2010;4:345-352

75. Kaestner KH, Lee KH, Schlondorff J, Hiemisch H, Monaghan AP, Schutz G. Six members of the mouse forkhead gene family are developmentally regulated. *Proc Natl Acad Sci U S A*. 1993;90:7628-7631

76. Seo S, Fujita H, Nakano A, Kang M, Duarte A, Kume T. The forkhead transcription factors, foxc1 and foxc2, are required for arterial

specification and lymphatic sprouting during vascular development. *Developmental Biology*. 2006;294:458-470

77. <fang j am j hum genet 2000 mutations in foxc2 (mfh-1), a forkhead family transcription factor, are responsible for the hereditary lymphedema-distichiasis syndrome..Pdf>.

78. Finegold DN, Kimak MA, Lawrence EC, Levinson KL, Cherniske EM, Pober BR, Dunlap JW, Ferrell RE. Truncating mutations in foxc2 cause multiple lymphedema syndromes. *Hum Mol Genet*. 2001;10:1185-1189

79. Tumer Z, Bach-Holm D. Axenfeld-rieger syndrome and spectrum of pitx2 and foxc1 mutations. *Eur J Hum Genet*. 2009;17:1527-1539

80. Winnier GE, Kume T, Deng K, Rogers R, Bundy J, Raines C, Walter MA, Hogan BL, Conway SJ. Roles for the winged helix transcription factors mf1 and mfh1 in cardiovascular development revealed by nonallelic noncomplementation of null alleles. *Dev Biol*. 1999;213:418-431

81. Topczewska JM, Topczewski J, Shostak A, Kume T, Solnica-Krezel L, Hogan BL. The winged helix transcription factor foxc1a is essential for somitogenesis in zebrafish. *Genes Dev*. 2001;15:2483-2493

82. Kume T. The murine winged helix transcription factors, foxc1 and foxc2, are both required for cardiovascular development and somitogenesis. *Genes & Development*. 2001;15:2470-2482

83. Kidson SH, Kume T, Deng K, Winfrey V, Hogan BL. The forkhead/winged-helix gene, mf1, is necessary for the normal development of the cornea and formation of the anterior chamber in the mouse eye. *Dev Biol*. 1999;211:306-322

84. Kume T, Deng KY, Winfrey V, Gould DB, Walter MA, Hogan BL. The forkhead/winged helix gene mf1 is disrupted in the pleiotropic mouse mutation congenital hydrocephalus. *Cell*. 1998;93:985-996

85. Alitalo K. The lymphatic vasculature in disease. *Nat Med*. 2011;17:1371-1380

86. Bouvree K, Brunet I, Del Toro R, Gordon E, Prahst C, Cristofaro B, Mathivet T, Xu Y, Soueid J, Fortuna V, Miura N, Aigrot MS, Maden CH, Ruhrberg C, Thomas JL, Eichmann A. Semaphorin3a, neuropilin-1, and plexina1 are required for lymphatic valve formation. *Circ Res*. 2012;111:437-445

87. Hayashi H, Sano H, Seo S, Kume T. The foxc2 transcription factor regulates angiogenesis via induction of integrin 3 expression. *Journal of Biological Chemistry*. 2008;283:23791-23800

88. Kume T. Foxc2 transcription factor: A newly described regulator of angiogenesis. *Trends in Cardiovascular Medicine*. 2008;18:224-228

89. Garg V, Muth AN, Ransom JF, Schluterman MK, Barnes R, King IN, Grossfeld PD, Srivastava D. Mutations in notch1 cause aortic valve disease. *Nature*. 2005;437:270-274

90. Murtomaki A, Uh MK, Kitajewski C, Zhao J, Nagasaki T, Shawber CJ, Kitajewski J. Notch signaling functions in lymphatic valve formation. *Development*. 2014;141:2446-2451

91. Hogan PG, Chen L, Nardone J, Rao A. Transcriptional regulation by calcium, calcineurin, and nfat. *Genes Dev*. 2003;17:2205-2232

92. Crabtree GR, Olson EN. Nfat signaling: Choreographing the social lives of cells. *Cell*. 2002;109 Suppl:S67-79

93. Kumai M, Nishii K, Nakamura K, Takeda N, Suzuki M, Shibata Y. Loss of connexin45 causes a cushion defect in early cardiogenesis. *Development*. 2000;127:3501-3512

94. Sabine A, Petrova TV. Interplay of mechanotransduction, foxc2, connexins, and calcineurin signaling in lymphatic valve formation. *Advances in anatomy, embryology, and cell biology*. 2014;214:67-80

95. Graef IA, Chen F, Chen L, Kuo A, Crabtree GR. Signals transduced by ca(2+)/calcineurin and nfatc3/c4 pattern the developing vasculature. *Cell*. 2001;105:863-875

96. Chang C-P, Neilson JR, Bayle JH, Gestwicki JE, Kuo A, Stankunas K, Graef IA, Crabtree GR. A field of myocardial-endocardial nfat signaling underlies heart valve morphogenesis. *Cell*. 2004;118:649-663

97. Arron JR, Winslow MM, Polleri A, Chang CP, Wu H, Gao X, Neilson JR, Chen L, Heit JJ, Kim SK, Yamasaki N, Miyakawa T, Francke U, Graef IA, Crabtree GR. Nfat dysregulation by increased dosage of dscr1 and dyrk1a on chromosome 21. *Nature*. 2006;441:595-600

98. Abdul-Sater Z, Yehya A, Beresian J, Salem E, Kamar A, Baydoun S, Shibbani K, Soubra A, Bitar F, Nemer G. Two heterozygous mutations in nfatc1 in a patient with tricuspid atresia. *PLoS One*. 2012;7:e49532

99. Zhou BP, Deng J, Xia W, Xu J, Li YM, Gunduz M, Hung MC. Dual regulation of snail by gsk-3beta-mediated phosphorylation in control of epithelial-mesenchymal transition. *Nat Cell Biol*. 2004;6:931-940

100. Ranger AM, Grusby MJ, Hodge MR, Gravallese EM, de la Brousse FC, Hoey T, Mickanin C, Baldwin HS, Glimcher LH. The transcription factor nf-atc is essential for cardiac valve formation. *Nature*. 1998;392:186-190

101. de la Pompa JL, Timmerman LA, Takimoto H, Yoshida H, Elia AJ, Samper E, Potter J, Wakeham A, Marengere L, Langille BL, Crabtree GR, Mak TW. Role of the nf-atc transcription factor in morphogenesis of cardiac valves and septum. *Nature*. 1998;392:182-186

102. Schulz RA, Yutzey KE. Calcineurin signaling and nfat activation in cardiovascular and skeletal muscle development. *Dev Biol*. 2004;266:1-16

103. Kulkarni RM, Greenberg JM, Akeson AL. Nfatc1 regulates lymphatic endothelial development. *Mechanisms of Development*. 2009;126:350-365

104. Sohl G, Willecke K. Gap junctions and the connexin protein family. *Cardiovasc Res*. 2004;62:228-232

105. Goodenough DA, Paul DL. Gap junctions. *Cold Spring Harbor perspectives in biology*. 2009;1:a002576

106. Meens MJ, Sabine A, Petrova TV, Kwak BR. Connexins in lymphatic vessel physiology and disease. *FEBS Lett*. 2014;588:1271-1277

107. Solan JL, Lampe PD. Connexin43 phosphorylation: Structural changes and biological effects. *Biochem J*. 2009;419:261-272

108. Laird DW. Life cycle of connexins in health and disease. *Biochem J*. 2006;394:527-543

109. Kanady JD, Dellinger MT, Munger SJ, Witte MH, Simon AM. Connexin37 and connexin43 deficiencies in mice disrupt lymphatic valve development and result in lymphatic disorders including lymphedema and chylothorax. *Dev Biol*. 2011;354:253-266

110. Kanady JD, Simon AM. Lymphatic communication: Connexin junction, what's your function? *Lymphology*. 2011;44:95-102

111. Munger SJ, Kanady JD, Simon AM. Absence of venous valves in mice lacking connexin37. *Dev Biol*. 2013;373:338-348

112. Fang JS, Angelov SN, Simon AM, Burt JM. Cx40 is required for, and cx37 limits, postischemic hindlimb perfusion, survival and recovery. *J Vasc Res*. 2012;49:2-12

113. Yamada Y, Izawa H, Ichihara S, Takatsu F, Ishihara H, Hirayama H, Sone T, Tanaka M, Yokota M. Prediction of the risk of myocardial infarction from polymorphisms in candidate genes. *N Engl J Med*. 2002;347:1916-1923

114. Kwak BR, Mulhaupt F, Veillard N, Gros DB, Mach F. Altered pattern of vascular connexin expression in atherosclerotic plaques. *Arterioscler Thromb Vasc Biol*. 2002;22:225-230

115. Francis R, Xu X, Park H, Wei CJ, Chang S, Chatterjee B, Lo C. Connexin43 modulates cell polarity and directional cell migration by regulating microtubule dynamics. *PLoS One*. 2011;6:e26379

116. Rhee DY, Zhao XQ, Francis RJ, Huang GY, Mably JD, Lo CW. Connexin 43 regulates epicardial cell polarity and migration in coronary vascular development. *Development*. 2009;136:3185-3193

117. Reaume AG, de Sousa PA, Kulkarni S, Langille BL, Zhu D, Davies TC, Juneja SC, Kidder GM, Rossant J. Cardiac malformation in neonatal mice lacking connexin43. *Science*. 1995;267:1831-1834

118. Olsson AK, Dimberg A, Kreuger J, Claesson-Welsh L. Vegf receptor signalling - in control of vascular function. *Nature reviews. Molecular cell biology*. 2006;7:359-371

119. Sawamiphak S, Seidel S, Essmann CL, Wilkinson GA, Pitulescu ME, Acker T, Acker-Palmer A. Ephrin-b2 regulates vegfr2 function in developmental and tumour angiogenesis. *Nature*. 2010;465:487-491

120. Blanco R, Gerhardt H. Vegf and notch in tip and stalk cell selection. *Cold Spring Harbor perspectives in medicine*. 2013;3:a006569

121. Makinen T, Veikkola T, Mustjoki S, Karpanen T, Catimel B, Nice EC, Wise L, Mercer A, Kowalski H, Kerjaschki D, Stacker SA, Achen MG, Alitalo K. Isolated lymphatic endothelial cells transduce growth, survival and migratory signals via the vegf-c/d receptor vegfr-3. *The EMBO journal*. 2001;20:4762-4773

122. Dumont DJ, Jussila L, Taipale J, Lymboussaki A, Mustonen T, Pajusola K, Breitman M, Alitalo K. Cardiovascular failure in mouse embryos deficient in vegf receptor-3. *Science*. 1998;282:946-949

123. Tammela T, Zarkada G, Nurmi H, Jakobsson L, Heinolainen K, Tvorogov D, Zheng W, Franco CA, Murtomaki A, Aranda E, Miura N, Yla-Herttuala S, Fruttiger M, Makinen T, Eichmann A, Pollard JW, Gerhardt H, Alitalo K. Vegfr-3 controls tip to stalk conversion at vessel fusion sites by reinforcing notch signalling. *Nat Cell Biol*. 2011;13:1202-1213

124. Benedito R, Rocha SF, Woeste M, Zamykal M, Radtke F, Casanovas O, Duarte A, Pytowski B, Adams RH. Notch-dependent vegfr3 upregulation allows angiogenesis without vegf-vegfr2 signalling. *Nature*. 2012;484:110-114

125. Makinen T, Jussila L, Veikkola T, Karpanen T, Kettunen MI, Pulkkanen KJ, Kauppinen R, Jackson DG, Kubo H, Nishikawa S, Yla-Herttuala S, Alitalo K. Inhibition of lymphangiogenesis with resulting lymphedema in transgenic mice expressing soluble vegf receptor-3. *Nat Med*. 2001;7:199-205

126. Haiko P, Makinen T, Keskitalo S, Taipale J, Karkkainen MJ, Baldwin ME, Stacker SA, Achen MG, Alitalo K. Deletion of vascular endothelial growth factor c (vegf-c) and vegf-d is not equivalent to vegf receptor 3

deletion in mouse embryos. *Molecular and cellular biology*. 2008;28:4843-4850

127. Tammela T, Zarkada G, Wallgard E, Murtomaki A, Suchting S, Wirzenius M, Waltari M, Hellstrom M, Schomber T, Peltonen R, Freitas C, Duarte A, Isoniemi H, Laakkonen P, Christofori G, Yla-Herttuala S, Shibuya M, Pytowski B, Eichmann A, Betsholtz C, Alitalo K. Blocking vegfr-3 suppresses angiogenic sprouting and vascular network formation. *Nature*. 2008;454:656-660

128. Gordon K, Spiden SL, Connell FC, Brice G, Cottrell S, Short J, Taylor R, Jeffery S, Mortimer PS, Mansour S, Ostergaard P. Flt4/vegfr3 and milroy disease: Novel mutations, a review of published variants and database update. *Hum Mutat*. 2013;34:23-31

129. Karkkainen MJ, Ferrell RE, Lawrence EC, Kimak MA, Levinson KL, McTigue MA, Alitalo K, Finegold DN. Missense mutations interfere with vegfr-3 signalling in primary lymphoedema. *Nat Genet*. 2000;25:153-159

130. Karkkainen MJ, Saaristo A, Jussila L, Karila KA, Lawrence EC, Pajusola K, Bueler H, Eichmann A, Kauppinen R, Kettunen MI, Yla-Herttuala S, Finegold DN, Ferrell RE, Alitalo K. A model for gene therapy of human hereditary lymphedema. *Proc Natl Acad Sci U S A*. 2001;98:12677-12682

131. Hove JR, Koster RW, Forouhar AS, Acevedo-Bolton G, Fraser SE, Gharib M. Intracardiac fluid forces are an essential epigenetic factor for embryonic cardiogenesis. *Nature*. 2003;421:172-177

132. Hogers B, DeRuiter MC, Gittenberger-de Groot AC, Poelmann RE. Extraembryonic venous obstructions lead to cardiovascular malformations and can be embryolethal. *Cardiovasc Res*. 1999;41:87-99

133. Vermot J, Forouhar AS, Liebling M, Wu D, Plummer D, Gharib M, Fraser SE. Reversing blood flows act through klf2a to ensure normal valvulogenesis in the developing heart. *PLoS Biol*. 2009;7:e1000246

134. Yashiro K, Shiratori H, Hamada H. Haemodynamics determined by a genetic programme govern asymmetric development of the aortic arch. *Nature*. 2007;450:285-288

135. Kwak BR, Silacci P, Stergiopulos N, Hayoz D, Meda P. Shear stress and cyclic circumferential stretch, but not pressure, alter connexin43 expression in endothelial cells. *Cell communication & adhesion*. 2005;12:261-270

136. Jong Lee H. Shear stress activates tie2 receptor tyrosine kinase in human endothelial cells. *Biochemical and Biophysical Research Communications*. 2003;304:399-404

137. Kume T, Deng K, Hogan BL. Murine forkhead/winged helix genes foxc1 (mf1) and foxc2 (mfh1) are required for the early organogenesis of the kidney and urinary tract. *Development*. 2000;127:1387-1395

138. Makinen T. Pdz interaction site in ephrinb2 is required for the remodeling of lymphatic vasculature. *Genes & Development*. 2005;19:397-410

139. Feil R, Wagner J, Metzger D, Chambon P. Regulation of cre recombinase activity by mutated estrogen receptor ligand-binding domains. *Biochem Biophys Res Commun*. 1997;237:752-757

140. Leone DP, Genoud S, Atanasoski S, Grausenburger R, Berger P, Metzger D, Macklin WB, Chambon P, Suter U. Tamoxifen-inducible glia-specific cre mice for somatic mutagenesis in oligodendrocytes and schwann cells. *Molecular and cellular neurosciences*. 2003;22:430-440

141. Nagy A. Cre recombinase: The universal reagent for genome tailoring. *Genesis*. 2000;26:99-109

142. Truett GE, Heeger P, Mynatt RL, Truett AA, Walker JA, Warman ML. Preparation of pcr-quality mouse genomic DNA with hot sodium hydroxide and tris (hotshot). *Biotechniques*. 2000;29:52, 54

143. Anderson RH, Webb S, Brown NA, Lamers W, Moorman A. Development of the heart: (3) formation of the ventricular outflow tracts, arterial valves, and intrapericardial arterial trunks. *Heart*. 2003;89:1110-1118

144. Schlaeger TM, Bartunkova S, Lawitts JA, Teichmann G, Risau W, Deutsch U, Sato TN. Uniform vascular-endothelial-cell-specific gene expression in both embryonic and adult transgenic mice. *Proc Natl Acad Sci U S A*. 1997;94:3058-3063

145. Coxam B, Sabine A, Bower NI, Smith KA, Pichol-Thievend C, Skoczylas R, Astin JW, Frampton E, Jaquet M, Crosier PS, Parton RG, Harvey NL, Petrova TV, Schulte-Merker S, Francois M, Hogan BM. Pkd1 regulates lymphatic vascular morphogenesis during development. *Cell reports*. 2014;7:623-633

146. Tatin F, Taddei A, Weston A, Fuchs E, Devenport D, Tissir F, Makinen T. Planar cell polarity protein celsr1 regulates endothelial adherens junctions and directed cell rearrangements during valve morphogenesis. *Dev Cell*. 2013;26:31-44

147. Hemmeryckx B, Emmerechts J, Bovill EG, Hoylaerts MF, Lijnen HR. Effect of ageing on the murine venous circulation. *Histochem Cell Biol*. 2012;137:537-546

148. Bazigou E, Makinen T. Flow control in our vessels: Vascular valves make sure there is no way back. *Cellular and molecular life sciences : CMLS*. 2013;70:1055-1066

149. Petrova TV, Makinen T, Makela TP, Saarela J, Virtanen I, Ferrell RE, Finegold DN, Kerjaschki D, Yla-Herttuala S, Alitalo K. Lymphatic endothelial reprogramming of vascular endothelial cells by the prox-1 homeobox transcription factor. *EMBO J*. 2002;21:4593-4599

150. Ostrowski MA, Huang NF, Walker TW, Verwijlen T, Poplawski C, Khoo AS, Cooke JP, Fuller GG, Dunn AR. Microvascular endothelial cells migrate upstream and align against the shear stress field created by impinging flow. *Biophysical journal*. 2014;106:366-374

151. Shen B, Shang Z, Wang B, Zhang L, Zhou F, Li T, Chu M, Jiang H, Wang Y, Qiao T, Zhang J, Sun W, Kong X, He Y. Genetic dissection of tie pathway in mouse lymphatic maturation and valve development. *Arterioscler Thromb Vasc Biol*. 2014;34:1221-1230

152. Singh P, Chen C, Pal-Ghosh S, Stepp MA, Sheppard D, Van De Water L. Loss of integrin alpha9beta1 results in defects in proliferation, causing poor re-epithelialization during cutaneous wound healing. *J Invest Dermatol*. 2009;129:217-228

153. Muzumdar MD, Tasic B, Miyamichi K, Li L, Luo L. A global double-fluorescent cre reporter mouse. *genesis*. 2007;45:593-605

154. Raffetto JD, Khalil RA. Mechanisms of varicose vein formation: Valve dysfunction and wall dilation. *Phlebology*. 2008;23:85-98

155. Davy A, Soriano P. Ephrin-b2 forward signaling regulates somite patterning and neural crest cell development. *Dev Biol*. 2007;304:182-193

156. Grunwald IC, Korte M, Adelmann G, Plueck A, Kullander K, Adams RH, Frotscher M, Bonhoeffer T, Klein R. Hippocampal plasticity requires postsynaptic ephrinbs. *Nature neuroscience*. 2004;7:33-40

157. Mellitzer G, Xu Q, Wilkinson DG. Eph receptors and ephrins restrict cell intermingling and communication. *Nature*. 1999;400:77-81

158. Oike Y, Ito Y, Hamada K, Zhang XQ, Miyata K, Arai F, Inada T, Araki K, Nakagata N, Takeya M, Kisanuki YY, Yanagisawa M, Gale NW, Suda T. Regulation of vasculogenesis and angiogenesis by ephb/ephrin-b2 signaling between endothelial cells and surrounding mesenchymal cells. *Blood*. 2002;100:1326-1333

159. Kawasaki J, Aegerter S, Fevurly RD, Mammoto A, Mammoto T, Sahin M, Mably JD, Fishman SJ, Chan J. Rasa1 functions in ephb4 signaling pathway to suppress endothelial mtorc1 activity. *J Clin Invest*. 2014;124:2774-2784

160. Hammill AM, Wentzel M, Gupta A, Nelson S, Lucky A, Elluru R, Dasgupta R, Azizkhan RG, Adams DM. Sirolimus for the treatment of complicated vascular anomalies in children. *Pediatric blood & cancer*. 2011;57:1018-1024

161. Kriederman BM. Foxc2 haploinsufficient mice are a model for human autosomal dominant lymphedema-distichiasis syndrome. *Human Molecular Genetics*. 2003;12:1179-1185

162. Iida K, Koseki H, Kakinuma H, Kato N, Mizutani-Koseki Y, Ohuchi H, Yoshioka H, Noji S, Kawamura K, Kataoka Y, Ueno F, Taniguchi M, Yoshida N, Sugiyama T, Miura N. Essential roles of the winged helix transcription factor mfh-1 in aortic arch patterning and skeletogenesis. *Development*. 1997;124:4627-4638

163. Sasman A, Nassano-Miller C, Shim KS, Koo HY, Liu T, Schultz KM, Millay M, Nanano A, Kang M, Suzuki T, Kume T. Generation of conditional alleles for foxc1 and foxc2 in mice. *genesis*. 2012;50:766-774

164. Schweisguth F, Hayashi H, Kume T. Foxc transcription factors directly regulate dll4 and hey2 expression by interacting with the vegf-notch signaling pathways in endothelial cells. *PLoS ONE*. 2008;3:e2401

165. Saiki S, Sakai K, Saiki M, Kitagawa Y, Umemori T, Murata K, Matsui M, Hirose G. Varicose veins associated with cadasil result from a novel mutation in the notch3 gene. *Neurology*. 2006;67:337-339

166. Zeng H, Chattarji S, Barbarosie M, Rondi-Reig L, Philpot BD, Miyakawa T, Bear MF, Tonegawa S. Forebrain-specific calcineurin knockout selectively impairs bidirectional synaptic plasticity and working/episodic-like memory. *Cell*. 2001;107:617-629

167. Johnson EN. Nfatc1 mediates vascular endothelial growth factor-induced proliferation of human pulmonary valve endothelial cells. *Journal of Biological Chemistry*. 2002;278:1686-1692

168. Musaro A, McCullagh KJ, Naya FJ, Olson EN, Rosenthal N. Igf-1 induces skeletal myocyte hypertrophy through calcineurin in association with gata-2 and nf-atc1. *Nature*. 1999;400:581-585

169. Ostergaard P, Simpson MA, Connell FC, Steward CG, Brice G, Woollard WJ, Dafou D, Kilo T, Smithson S, Lunt P, Murday VA, Hodgson S, Keenan R, Pilz DT, Martinez-Corral I, Makinen T, Mortimer PS, Jeffery S, Trembath RC, Mansour S. Mutations in gata2 cause primary lymphedema associated with a predisposition to acute myeloid leukemia (emberger syndrome). *Nat Genet*. 2011;43:929-931

170. Zhou B, Wu B, Tompkins KL, Boyer KL, Grindley JC, Baldwin HS. Characterization of nfatc1 regulation identifies an enhancer required for gene expression that is specific to pro-valve endocardial cells in the developing heart. *Development*. 2005;132:1137-1146

171. Simon AM, Goodenough DA, Li E, Paul DL. Female infertility in mice lacking connexin 37. *Nature*. 1997;385:525-529

172. Lohmann CH, Schwartz Z, Liu Y, Li Z, Simon BJ, Sylvia VL, Dean DD, Bonewald LF, Donahue HJ, Boyan BD. Pulsed electromagnetic fields affect phenotype and connexin 43 protein expression in mlo-y4 osteocyte-like cells and ros 17/2.8 osteoblast-like cells. *J Orthop Res*. 2003;21:326-334

173. Kirkin V, Thiele W, Baumann P, Mazitschek R, Rohde K, Fellbrich G, Weich H, Waltenberger J, Giannis A, Sleeman JP. Maz51, an indolinone that inhibits endothelial cell and tumor cell growth in vitro, suppresses tumor growth in vivo. *Int J Cancer*. 2004;112:986-993

174. Hu-Lowe DD, Zou HY, Grazzini ML, Hallin ME, Wickman GR, Amundson K, Chen JH, Rewolinski DA, Yamazaki S, Wu EY, McTigue MA, Murray BW, Kania RS, O'Connor P, Shalinsky DR, Bender SL. Nonclinical antiangiogenesis and antitumor activities of axitinib (ag-013736), an oral, potent, and selective inhibitor of vascular endothelial growth factor receptor tyrosine kinases 1, 2, 3. *Clin Cancer Res*. 2008;14:7272-7283

175. Evans CE, Grover SP, Humphries J, Saha P, Patel AP, Patel AS, Lyons OT, Waltham M, Modarai B, Smith A. Antiangiogenic therapy inhibits venous thrombus resolution. *Arterioscler Thromb Vasc Biol*. 2014;34:565-570

176. Srinivasan.RS OG. Prox1 dosage controls the number of lymphatic endothelial cell progenitors and the formation of the lymphovenous valves. *Genes Dev*. 2011;25:2187-2197

177. Persaud K, Tille JC, Liu M, Zhu Z, Jimenez X, Pereira DS, Miao HQ, Brennan LA, Witte L, Pepper MS, Pytowski B. Involvement of the vegf receptor 3 in tubular morphogenesis demonstrated with a human anti-human vegfr-3 monoclonal antibody that antagonizes receptor activation by vegf-c. *J Cell Sci*. 2004;117:2745-2756

178. Groenendijk BCW. Changes in shear stress-related gene expression after experimentally altered venous return in the chicken embryo. *Circulation Research*. 2005;96:1291-1298

179. Gotoh.H MY, Imamura.K. General anaesthesia of infant mice by isoflurane inhalation for medium-duration surgery. *Exp Anim*. 2004;53:63-65

180. Park.CM CK, Harvey-Clark.CJ, et al. . Improved techniques for successful neonatal rat surgery. *Lab Anim Sci*. 1992;5:508-514

181. Lurie F, Kistner RL. The relative position of paired valves at venous junctions suggests their role in modulating three-dimensional flow pattern in veins. *Eur J Vasc Endovasc Surg*. 2012;44:337-340

182. van Langevelde K, Sramek A, Rosendaal FR. The effect of aging on venous valves. *Arterioscler Thromb Vasc Biol*. 2010;30:2075-2080

183. Lane R, Graiche, JA, Cuzzilla, ML, Coroneos, JC. Incompetent venous valves: Ultrasound imaging and exo-stent repair. *Phlebolymphology*. 2007;14:105-115

184. Moore HM, Gohel M, Davies AH. Number and location of venous valves within the popliteal and femoral veins: A review of the literature. *Journal of anatomy*. 2011;219:439-443

185. Iimura A, Nakamura Y, Itoh M. Anatomical study of distribution of valves of the cutaneous veins of adult's limbs. *Annals of anatomy = Anatomischer Anzeiger : official organ of the Anatomische Gesellschaft*. 2003;185:91-95

186. Sano H, LeBoeuf JP, Novitskiy SV, Seo S, Zaja-Milatovic S, Dikov MM, Kume T. The foxc2 transcription factor regulates tumor angiogenesis. *Biochemical and Biophysical Research Communications*. 2010;392:201-206

187. Davy A, Bush JO, Soriano P. Inhibition of gap junction communication at ectopic eph/ephrin boundaries underlies craniofrontonasal syndrome. *PLoS Biol*. 2006;4:e315

188. Laemmli UK. Cleavage of structural proteins during the assembly of the head of bacteriophage t4. *Nature*. 1970;227:680-685

Appendix 1

Solutions and buffers

General solutions

PBS: Dulbecco's PBS (Sigma D5652)

PBST: 1x PBS and 0.3% Tritonx100, store at RT

Tyramide amplification

TNT wash buffer (these volumes are for the evaluation-size kit)

0.1M Tris-Hcl

0.15M NaCl

0.05% Tween 20

To make 5L wash buffer78.8g Tris Hcl and 43.83g of NaCl was dissolved in 4 litres of water, and 2.5ml Tween20 was added. The resulting solution was adjusted to pH 7.5 using 1M NaOH and the final volume was made up to 5L with water.

TNB blocking buffer (Perkin Elmer)

3g proprietary blocking reagent was gradually dissolved in 600ml TNT wash buffer and heated to 60^{o}c on a hit plate with continuous stirring. Cooled 50ml aliquots were frozen at -20oc in falcon tubes, and later thawed on the day of use.

Biotinyl tyramide amplification solution stock solution (Perkin Elmer)

Reconstitute amplification solution with 300μl DMSO.

Localisation of βgal in Tie2LacZ reporter

Fixative

5ml formaldehyde, 0.8ml glutaraldehyde, 200μl $MgCl_2$, 190mg EDTA made up to 100ml with Phosphate Buffered Saline (PBS)

Washing solution

200μl $MgCl_2$, 200μl NP40, 0.1g Na deoxycholate, made up to 100ml PBS

Staining solution

165mg $K_3Fe(CN)_6$, 211mg $K_4Fe(CN)_6.H_20$, 200µl $MgCl_2$, 10mg Na Deoxycholate, 20µl NP40 made up to 400ml PBS

Stock substrate

40mg/ml Xgal dissolved in dimethylformamide.

Final staining solution = stock substrate + staining solution 1:40.

Solutions for SEM at SGUL

Stock (2x) cacodylate buffer

Sodium cacodylate 10.7g, sodium chloride 7.1g, dissolved in 450ml dH_20 and adjusted to pH 7.4 and made up to 500ml. Store at +4^{o}c

SEM fix

50ml Stock cacodylate buffer, 8ml 25% electron microscopy grade glutaraldehyde, 2.5ml 38-40% formaldehyde, 39.5ml dH_20, made fresh on the day of use.

Solutions for SEM/TEM at KCL

Stock Solutions:

Part 1 0.2M di-sodium hydrogen orthophosphate dihydrate (Alkali solution)

Dissolve 35.6g of solid into 1 Litre of distilled water and store at RT.

Part 2 0.2M Sodium dihydrogen orthophosphate (Acid solution)

Dissolve 27.6g of solid into 1 Litre of distilled water and store at RT.

2.5% Glutaraldehyde fixative in phosphate buffer

77ml Part 1, 23ml of Part 2, 100ml $_{d}$H20, adjusted to pH 7.35. Withdraw 190ml and add to 10ml 50% Vacuum distilled glutaraldehyde. Store at +4^{o}c. Make fresh on day of use.

Glutaraldehyde Wash Solution

34.22g Sucrose, 50ml dH_20.

128ml Part 1, 38ml Part 2 adjusted to pH 7.3

Withdraw 62.5ml and make up to 250ml with dH_20, add 165ml phosphate solution and make up to 500ml. Store at +4^{o}c

General transmission electron microscopy

Fixation was performed as for scanning electron microscopy at KCL.

Immunofluorescence solutions

4% Paraformaldehyde

In a fume hood add 40g paraformaldehyde and 500ul 3M NaOH to 1L Dulbecco's PBS, heat to approximately 65^{o}c whilst stirring, until dissolved.

Once cooled adjust pH to 7.35 with HCl. Pass through a 0.22μm filter and freeze 30ml aliquots in 50ml falcon tubes at -20^{o}c. Thawed immediately before use. (Only freshly thawed solutions were used).

Wash Solution

Permeabilise and wash in PBST

Blocking solution

3% Foetal calf serum (Source Biosciences SBS10022) in PBST (above). Pass through a 0.22μm filter and freeze 200μl aliquots at -20^{o}c; thaw just before use.

Mowiol-based mounting solution (Courtesy of Dr Taija Makinen)

Mix: 36g glycerol, 14.4g Mowiol (Calbiochem 475904), 93ml dH_20.

Stir overnight at RT.

Add 14.4ml 1M Tris pH 8,5

Heat to 50°c for 10mins whilst stirring

Once Mowiol has dissolved, centrifuge at 5000xg for 15mins.

Aliquot (approx 200μl) and store at -20°c until required

(Prolong Gold (Invitrogen) was subsequently used as an alternative mounting medium).

HotSHOT DNA extraction for genotyping

These solutions were taken from Ref [142]

HotSHOT alkaline lysis reagent

25 mM NaOH, 0.2 mM disodium EDTA (pH12)

Neutralising reagent

40 mM Tris-HCl (pH5)

Appendix 2

Immunolocalisation of non-immune IgG in murine VV

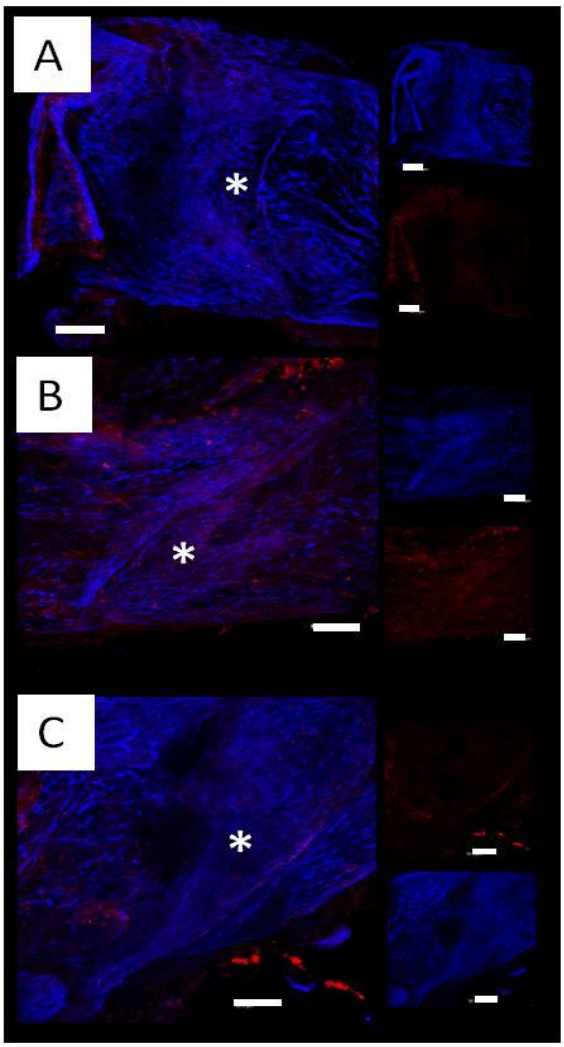

Figure 93 Non-immune IgG control imunostaining of Balb/c venous valves.
A) Goat IgG 10μg/ml with Donkey anti Goat-647

B) Rabbit IgG 10 μg/ml with Donkey anti Rabbit-647

C) Sheep IgG 10μg/ml with Donkey anti Sheep-647.

Red- IgG; Blue: PECAM1-550 (primary conjugate).

Adipose tissue caused significant autofluorescence and loss of signal at all ages, and prevented imaging beyond P8. * = venous valve. Scale bars 50μm.

Appendix 3

Antibodies and detection reagents

Table 10 Primary Antibodies

Target Protein	Target Species	Supplier	Catalogue	Concentration
Cx37	Mouse	Alpha diagnostics international	CX37A11-A	10μg/ml
Cx43	Mouse	Cell signalling	3512	5μg/ml
Cx43	Human	Invitrogen	71-0700	10μg/ml
Cx47	Human	Sigma-Aldrich	SAB2100924	10μg/ml
GFP	*Aequorea victoria*	Abcam	ab69313	2μg/ml
Integrin-α9	Human	Sigma	HPA030609	0.27μg/ml
Integrin-α9	Mouse	R&D	AF3827	2 μg/ml
α smooth muscle actin	Human, mouse	Sigma	C6198	7 μg/ml
FOXC2	Mouse	R&D	AF6989	7.5 μg/ml
GATA-2	Human	Sigma	HPA005633	2.3 μg/ml
NFATc1	Human	Santa Cruz	Sc-17834	2 μg/ml
NFATc1	Mouse	R&D	AF5640	10μg/ml
CD31/PECAM1	Mouse	Novus	NB600-1475G (Mec13.1)	2.5-5 μg/ml
Prox1	Mouse	Angiobio	11-002	10 μg/ml
Prox1	Human	R&D	Baf2727	2μg/ml
VEGFR2	Mouse	R&D	BAF644	5μg/ml
VEGFR3	Mouse	R&D	BAF743	5μg/ml

Table 11 Secondary antibodies

Target Species	Host Species	Conjugate	Supplier	Catalogue	Concentration
Goat	Donkey	Dylight-405	JIR	705-475-147	7.5 μg/ml
Goat	Donkey	Dylight-488	JIR	705-485-147	7.5 μg/ml
Goat	Donkey	Dylight-549	JIR	705-505-147	7.5 μg/ml
Goat	Donkey	Dylight-647	JIR	705-605-147	7.5 μg/ml
Rabbit	Donkey	Dylight-405	JIR	711-475-152	7.5 μg/ml
Rabbit	Donkey	Dylight-488	JIR	711-485-152	7.5 μg/ml
Rabbit	Donkey	Cy3	JIR	711-165-152	7.5 μg/ml
Rabbit	Donkey	Dylight-649	JIR	711-495-152	7.5 μg/ml
Rat	Donkey	Dylight-405	JIR	712-475-153	7.5 μg/ml
Sheep	Donkey	Dylight-649	JIR	713-495-147	7.5 μg/ml

Fluorophores were stored at -20^{o}c, aliquoted in 50% glycerol.

JIR = Jackson Immunoresearch

Labelled detecting agents

- Streptavidin-alexafluor-488 JIR 016-540-084 (1/200), Streptavidin-alexafluor-647 JIR 016-600-084 (1/500, 1.8μg/ml)
- Extravidin-ALP Sigma E2636 (1/200) 2.9μg/ml
- Polymer-HRP (Unknown host, anti-Rabbit/Mouse) Menarini Diagnostics, MP-XCP-PO25 (used neat as per manufacturer's instructions)

Appendix 4

PCR primer sequences and conditions

Itga9^{lx}

a9lxF (a9F1): 5'CCCTTACAGGGCTCTAGGAAAGGGG3'

a9lxR (a9R2): 5'AATAGTCATTGAGACTCTCCCTGG3'

EfnB2^{lx}

B2lx-F: 5'CTTCAGCAATATACACAGGATG3'

B2lx-R: 5'TGCTTGATTGAAACGAAGCCCGA3'

Foxc2^{lx}

c2-F2: 5'CTCCTTTGCGTTTCCAGTGA3'

C2-r2: 5'ATTGGTCCTTCGTCTTCGCT3'

Prox1CreERT2

Cre_F: 5'GCCTGCATTACCGGTCGATGCAACGA3'

Cre_R: 5'GTGGCAGATGGCGCGGCAACACCATT3'

Cx43^{lx}

Cx43lx-F: 5'CTTTGACTCTGATTACAGAGCTTAA3'

Cx43lx-R: 5'GTCTCACTGTTACTTAACAGCTTGA3'

Cx47GFP

Cx47-F: 5'CAGGATCAATGGAAGATTCTCGGTCCC3'

Cx47-R1: 5'GCCAAGCGGTGGACTGCATAGCCCAGG3'

Cx47-R2: 5'GACACGCTGAACTTGCCGTTTACG3'

Cx37

CX37-F: 5'GATCTCTCGTGGGATCATTG3'

CX37-R1: 5'TGCTAGACCAGGTCCAGGAAC3'

CX37-R2: 5'GTCCCTTCGTGCCTTTATCTC3'

Notch1^{lx}

Notch1-F: 5'CTGAGGCCTAGAGCCTTGAA3'

Notch1-R: 5'TGTGGGACCCAGAAGTTAGG3'

PPP3R1^{lx} (CnB1^{lx})

PPP3R1-F: 5'CAACACCAGAAACTCTGTCATG3'

PPP3R1-R: 5'GCACCACTATCATACTGGTCT3'

Allele	Taq activation		Denaturation		Annealing		Elongation		Total cycles	Final elongation	
Itga9lx	95	5min	95	30s	57	30s	72	90s	38	72	5min
EfnB2lx	95	5min	95	30s	62	30s	72	30s	35	72	5min
Foxc2lx	95	5min	95	30s	57	30s	72	90s	35	72	10min
Prox1CreERT2	95	5min	95	30s	63	30s	72	30s	35	72	5min
Cx43lx	94	2min	94	45s	60	30s	72	30s		72	10min
Cx47GFP	95	5min	95	30s	55	30s	72	110s	40	72	10min
Cx37	95	5min	94	30s	57	45s	72	120s	30	72	10min
Notch1lx	94	5min	94	30s	60	25s	72	30s	34	72	10min
PPP3R1lx	95	5min	94	30s	60	60s	72	60s	35	72	2min

The table shows the PCR conditions used for each allele. All temperatures are in ^{o}c. All programs ended with storage at 4^{o}c. 'Cycles' refers to denaturation-annealing-elongation.

Appendix 5

EfnB2GFP reporter analysis

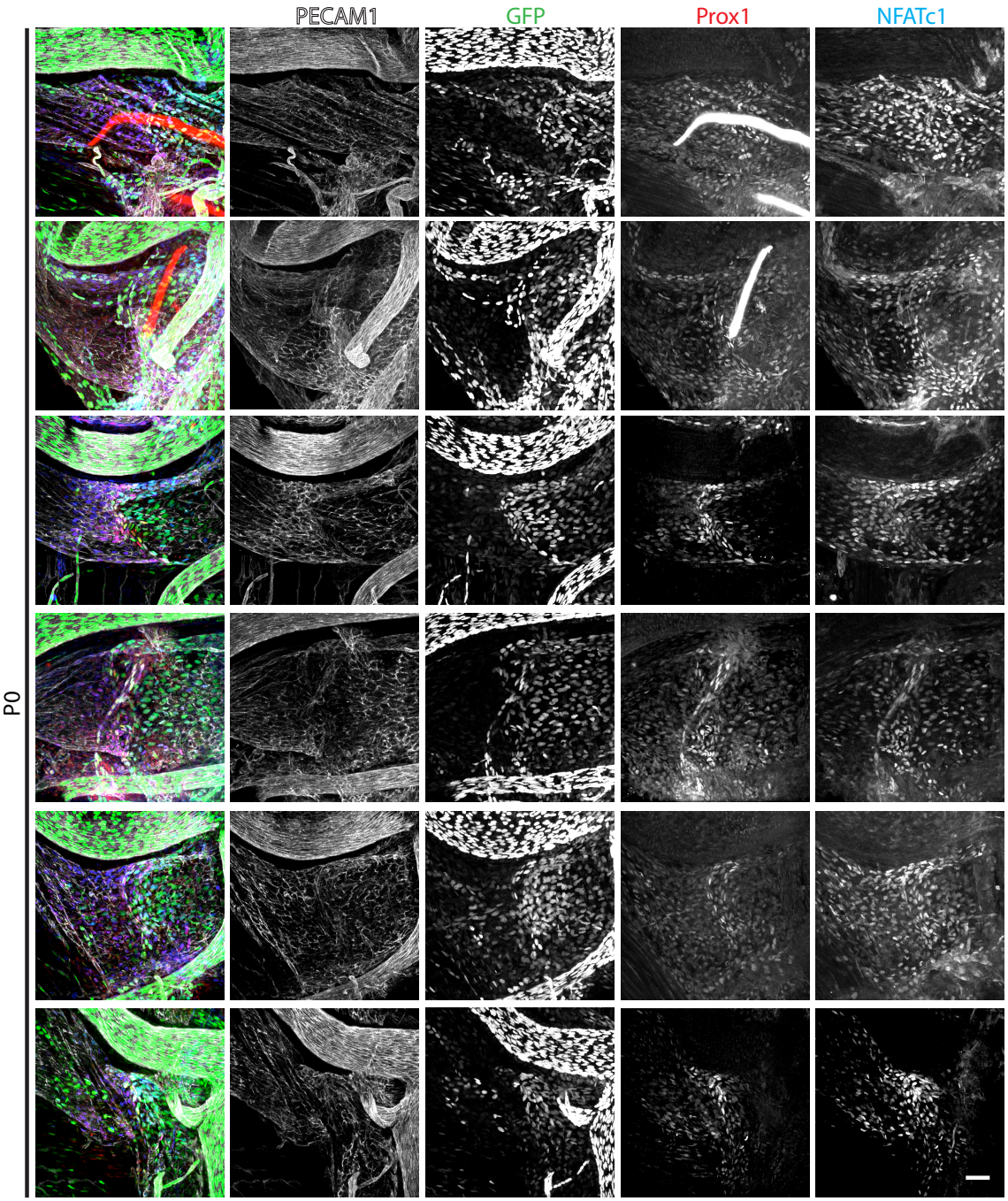

Figure 94 Analysis of EfnB2GFP reporter at P0
Images are 2D maximum projections of filtered confocal z stacks. EfnB2GFP, with immunolocalisation of PECAM1, Prox1, NFATc1. Reporter is heterozygous for ephrinB2. N = 6 at P0. Some images reflected so flow left to right in all images. Artifact from injection syringe material shows in top two rows in the Prox1 channel. Scale bar 50μm.

Appendix 6

Detection of Foxc1 by western blot

Aim

This experiment aimed to identify expression of Foxc1 (a nuclear transcription factor closely related to Foxc2) by western blotting of lysed human venous valve leaflets.

Methods

1. Human long saphenous veins were obtained from patients undergoing CABG as described in the General Methods Chapter. Veins were dissected under a microscope (Leica, UK) in PBS and valve leaflets removed and snap frozen in isopentane and stored at -80^{o}c. Sections of vein that did not contain a valve were similarly snap frozen and stored at -80^{o}c. HEK293 cell lysate (following Cx37 overexpression) was obtained from Novus Biologicals (NBL1-11088).

2. Tissue samples (pooled valve leaflets, or non-valved vein) were thawed on ice and homogenized in ice-cold radioimmunoprecipitation (RIPA) buffer (Thermo Fisher scientific, USA), supplemented with Halt protease inhibitors (Thermo Fisher Scientific, USA) using an pestle (Eppendorf) and then incubated on ice for 10mins.
3. Lysates were then cleared by centrifugation at 16,000xg for 15mins at 4°c and the resulting supernatant was transferred to a new microcentrifuge tube.
4. Total soluble protein concentration of tissue lysates were determined using the bicinchoninic acid (BCA) assay (Thermo Fisher Scientific, USA) as per the manufacturer's instructions.
5. Proteins were separated by sodium dodecyl sulphate polyacrylamide gel electrophoresis (SDS-PAGE).[188] Lysates were prepared by addition of LDS sample buffer (Invitrogen, UK) and heating for 5mins at 95°C.

6. Samples were loaded onto a 4-20% gradient gel (Biorad, UK) and electrophoresed in running buffer (25mM Tris, 192mM glycine, 0.1% (w/v) SDS) at 100V for 100mins.
7. Gels were equilibrated in transfer buffer (25mM Tris, 192mM glycine, 10% (v/v) methanol) for 5mins before being transferred to methanol activated polyvinylidene difluoride (PVDF) membranes (Amersham, UK) using a TransBlot Turbo (Biorad, UK).
8. Membranes were blocked in PBS supplemented with 5% low fat milk powder (Marvel, UK) for 1hr at room temperature, then washed for 6 x 5mins in PBS+0.05% Tween20 (PBST).
9. The primary antibody (monoclonal mouse anti-human Foxc1, R&D Systems MAB6329) was diluted to 1μg/ml in PBST+ 5% low fat milk powder. Membranes were incubated overnight at 4°C with agitation on the belly dancer.
10. Membranes were rinsed 3 times and washed 6 times for 5mins in PBST prior to incubation with secondary antibody (Goat anti-mouse HRP, Sigma AO168), diluted 1/80,000 in PBST + 5% low fat milk powder and incubated with the membranes for 1hr at room temperature.
11. Membranes were rinsed 3 times then washed 6 times for 5 minutes in PBST and incubated with a chemiluminescent substrate (KPL signalock HRP chemiwestern kit, 54-54-00). Luminescence was detected over 3 minutes using a ChemiDoc MP (Biorad, UK).
12. Molecular weight analysis was performed using Image Lab software (Biorad, UK).

Results

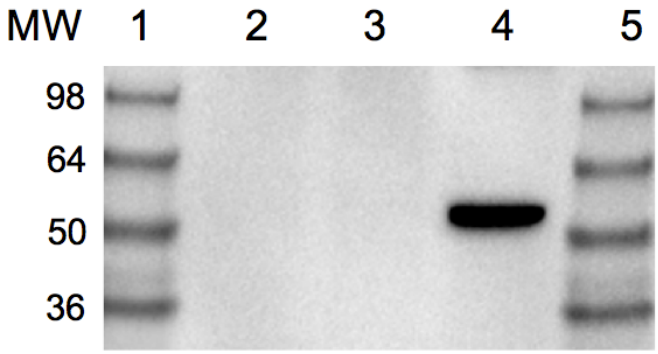

Figure 95 Western blot for Foxc1
This figure shows detection of a band of soluble protein at approximately 53.8 kDa in lysed human venous valve leaflet (Lane 4), using a monoclonal antibody against human Foxc1. No similar band was detected in whole lysed vein (lane 2) or HEK293 cell lysate (lane 3). The predicted molecular weight of Foxc1 is 57kDa (Uniprot), which is within 10% of the observed band. This result suggests expression of Foxc1 in human venous valve leaflets, but not the rest of the vein.

MW refers to weight in kDa, determined from markers in lanes 1 and 5.

Lane 1: MW marker (SeeBlue 2 plus, 10μl), as indicated in kDa

Lane 2: Whole lysed vein (30μg)

Lane 3: HEK293 cell lysate (15μg)

Lane 4: Lysed human VV leaflets (15μg). Major band calculated MW=53.8

Lane 5: MW Marker (10μl)

Appendix 7 Calcineurin-NFAT signalling

Effect of Ciclosporin on pup growth

Pups in two litters of 6 and 8 were randomly allocated to receive ciclosporin (N=7) or solvent control (N=7) bid as described in Chapter 7. Ciclosporin treatment was associated with a failure to survive and sub-normal weight gain.

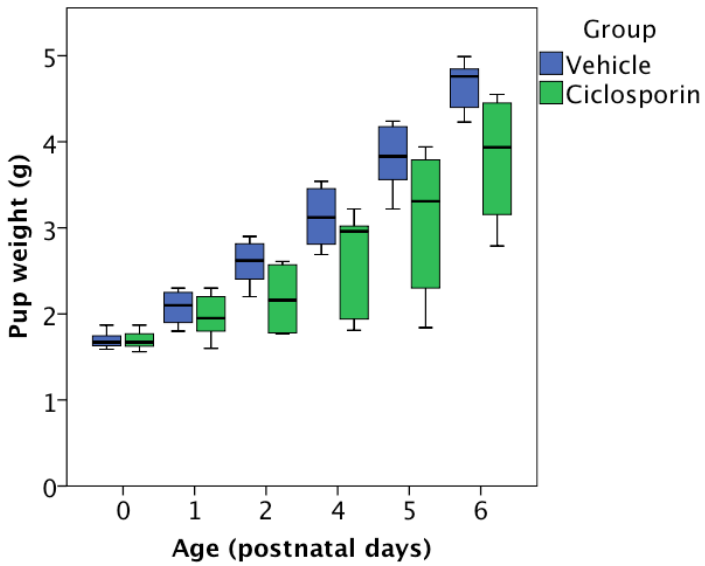

Figure 96 Growth (weight) of pups treated with ciclosporin
This graph shows that surviving ciclosporin-treated pups showed a failure to gain weight normally (P=0.015, ANOVA). Heavy line indicates median, box indicates inter-quartile range, and whiskers the range.

Template for measuring VV leaflet length

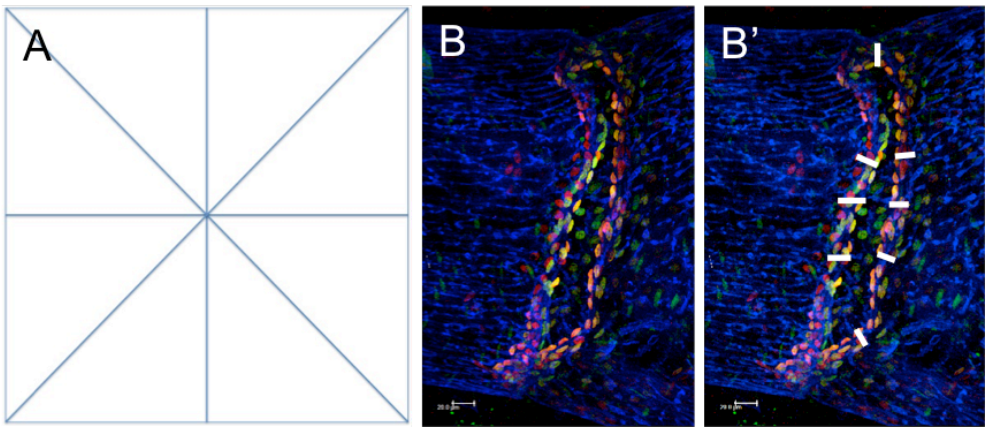

Figure 97 Template used for reference when measuring VV leaflets
The template shown on A was centered on the 2D projection of the confocal z-stack of the VV, and measurements of leaflet length (perpendicular to the free edge) were taken at each point where template lines bisected the free edges of the valve leaflets. An example valve is shown in B, with positions of measurements highlighted in B'. A mean of all 8 measurements was analysed for each valve. Scale bar 20μm.

Localisation of GATA2 in human VV

Immunolocalisation of the nuclear transcription factor GATA2 was performed as described in the General Methods chapter, using Polymer Amplification (Menarini) followed by Vector SG substrate to localise HRP activity. Human valves were obtained from clinically normal long saphenous veins as described in the General Methods chapter. Nuclear GATA2 expression was identified on both surfaces of the VV leaflet (* in Figure 98A).

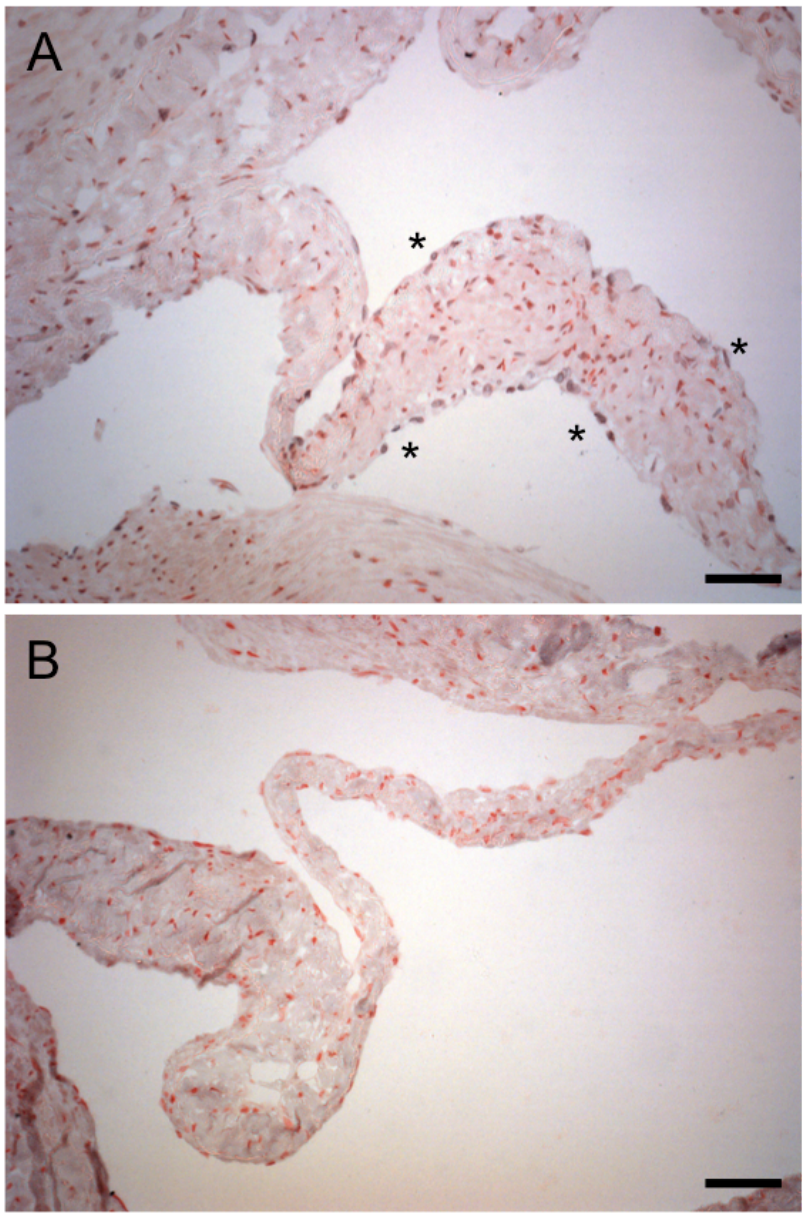

Figure 98 Localisation of GATA2 to adult human VV
A) GATA2 is expressed by endothelial cells on both surfaces of the human VV leaflet (dark blue nuclei marked by * in A). Some expression may be present in the interstitial cells of the leaflet. The non-immune IgG control is shown in B. Scale 50μm. Counterstain = nuclear fast red.

Appendix 8

Effect of axitinib treatment on survival and growth

Administration of the VEGFR tyrosine kinase inhibition with Axitinib was associated with failure to survive (Figure 99) but not failure to gain weight (P=ns, ANOVA) in survivors (Figure 100).

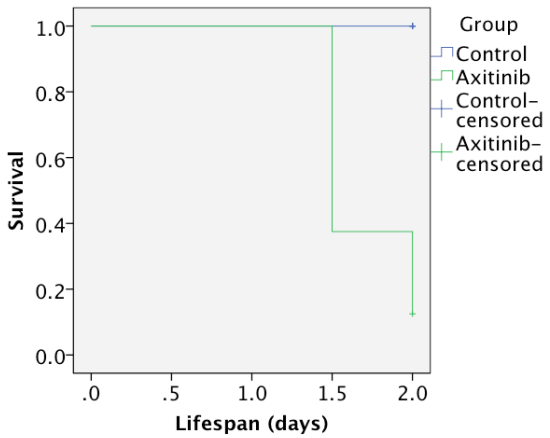

Figure 99 Kaplan-Meier plot of survival with postnatal axitinib
Survival in axitinib treated pups (n=8) compared with littermates treated with solvent only (n=7). Axitinib was associated with lethality from P1.5 onwards, whilst no deaths occurred in the control group.

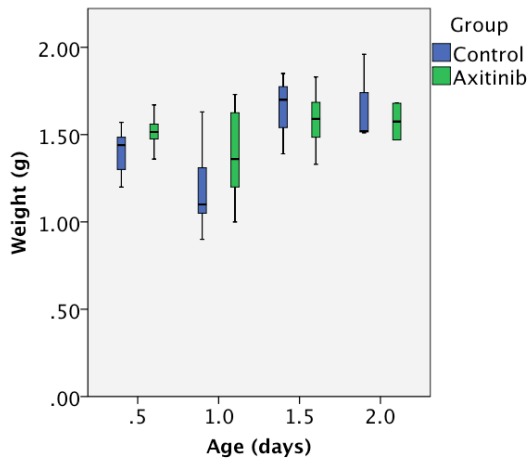

Figure 100 Effect of axitinib on postnatal weight gain
No difference was seen in weight gain in surviving axitinib treated pups (n=8) compared with littermates treated with vehicle only (n=7). P=ns (ANOVA) Heavy line indicates median, box the inter-quartile range, and whiskers the range.

Appendix 9

Analysis of P0 wildtype Prox1hi nuclear morphology

Because polarity could not be assigned to nuclei it was only possible to analyse the deviation of the axis of each nucleus away from the midline of the vessel. To appropriately convert angles from 0-360^{o} to the range 0-90^{o}, the angle derived from each length measurement was converted to radians, and the following function applied.

Converted angle = asin(sqrt(sin^2) of original angle

The results of this expression (using a dummy variables at 5^{o} intervals) are shown in Figure 101 in which it can be seen that nuclear angles are appropriately converted into angles between 0-90^{o}, reflecting the deviation of the axis of nuclear elongation away from the centreline of the vessel. These values were analysed as 'nuclear rotation' in all subsequent analyses of phenotypes associated with connexin deletion.

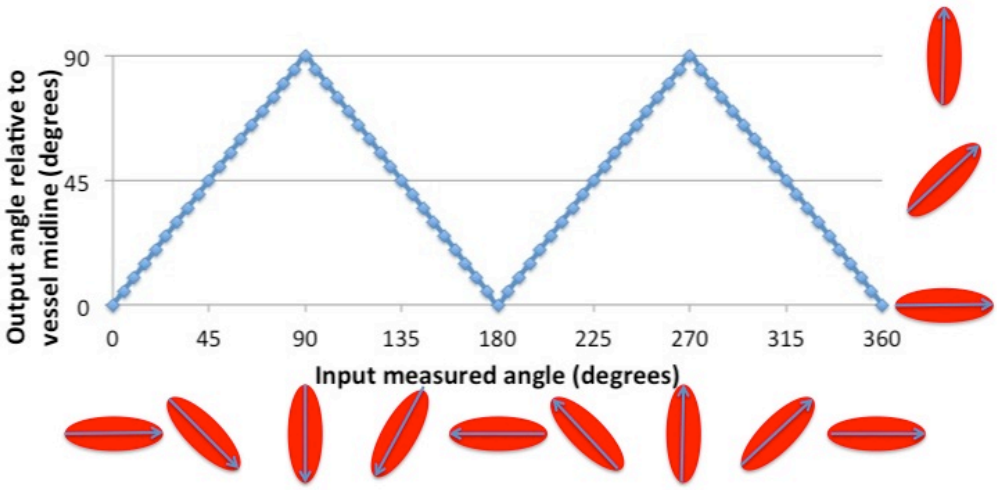

Figure 101 Conversion of rotation into deviation away from vessel midline
Nuclei below the graph demonstrate raw measurements taken from images, whilst those to the right reflect deviation away from the vessel midline. This figure relates to Figure 46 in the main text.

These data relate to the pooled analysis of Prox1^{hi} valve forming cell nuclei at P0 in the wildtype littermates analysed as part of the investigation of connexin 37/43/47 phenotypes.

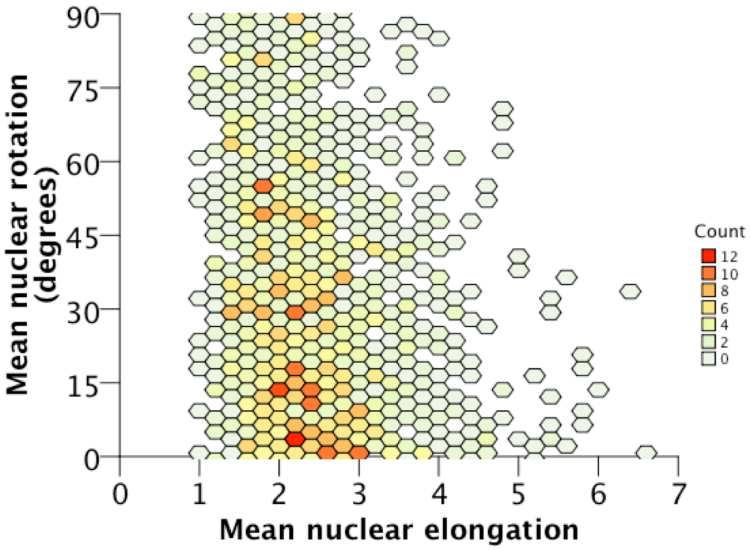

Figure 102 No correlation between Prox1^{hi} nuclear rotation and elongation
This graph shows the extremely weak correlation between nuclear rotation and elongation (Pearson's r=-0.153, P<0.0005) and so these parameters were subsequently analysed separately. A hex-binned scatter plot is shown in which colour represents the number (count) of measured Prox1^{hi} nuclei in each area. N=1388 nuclei.

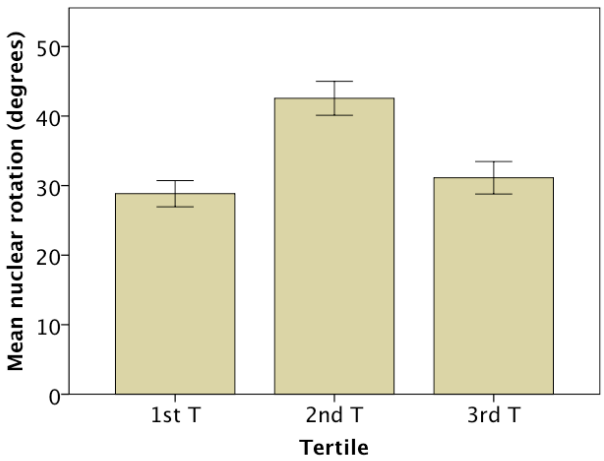

Figure 103 Mean nuclear rotation by tertile position across vein
This graph shows that in a pooled analysis of WT nuclei, each tertile showed a different mean nuclear rotation relative to the long axis of the vein. These three regions were subsequently analysed separately. Error bars represent 95% confidence intervals. N=1388 nuclei. A similar pattern was not seen for nuclear elongation, which was distributed relatively evenly across the vein (Figure 105). P<0.0005 (ANOVA) Bonferroni post-hoc tests showed no difference (P=ns) between tertiles 1 and 3, but both were significantly (P<0.005) less rotated that tertile 2.

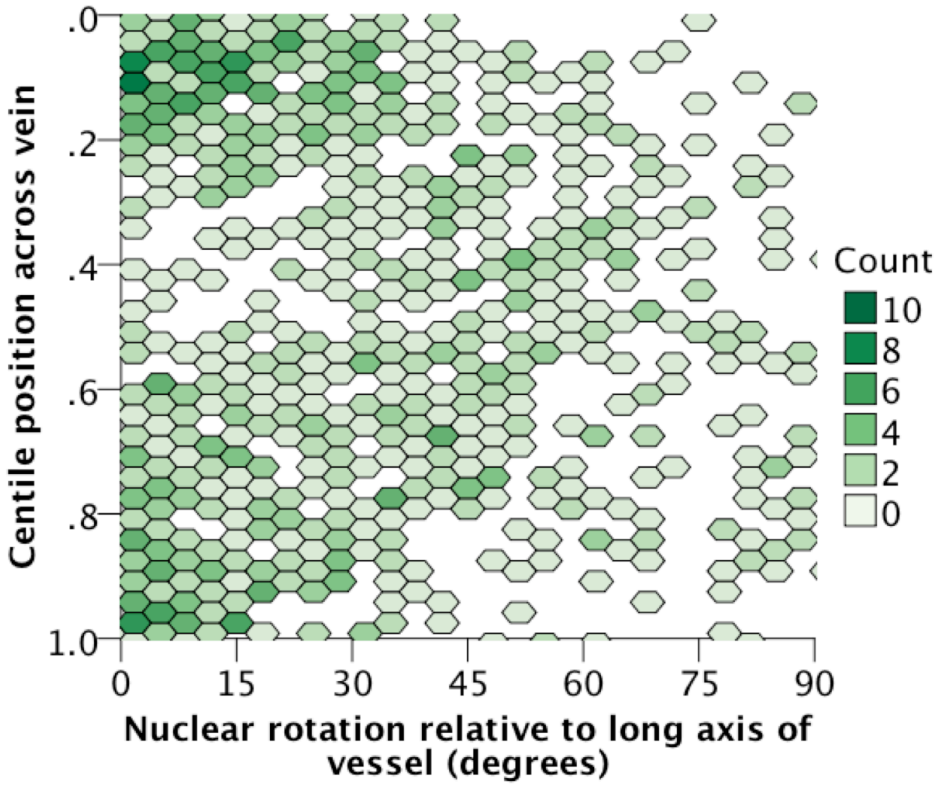

Figure 104 Normal variation in Prox1^{hi} nuclear rotation by position across the vein

This hex-binned scatter plot shows the variation in Prox1hi nuclear rotation with the position across the vein from superior to inferior. Colour indicates the number (count) f measured nuclei in each area. The graph shows two regions with a high number of nuclei with low rotation at the superior and inferior limits of the vessel, whilst the most rotated nuclei are found in the central region of the vessel (corresponding to the 2nd tertile). Statistical analysis of rotation in each tertile is given in Figure 103. Only nuclei elongated ≥2 are shown. N=953 nuclei.

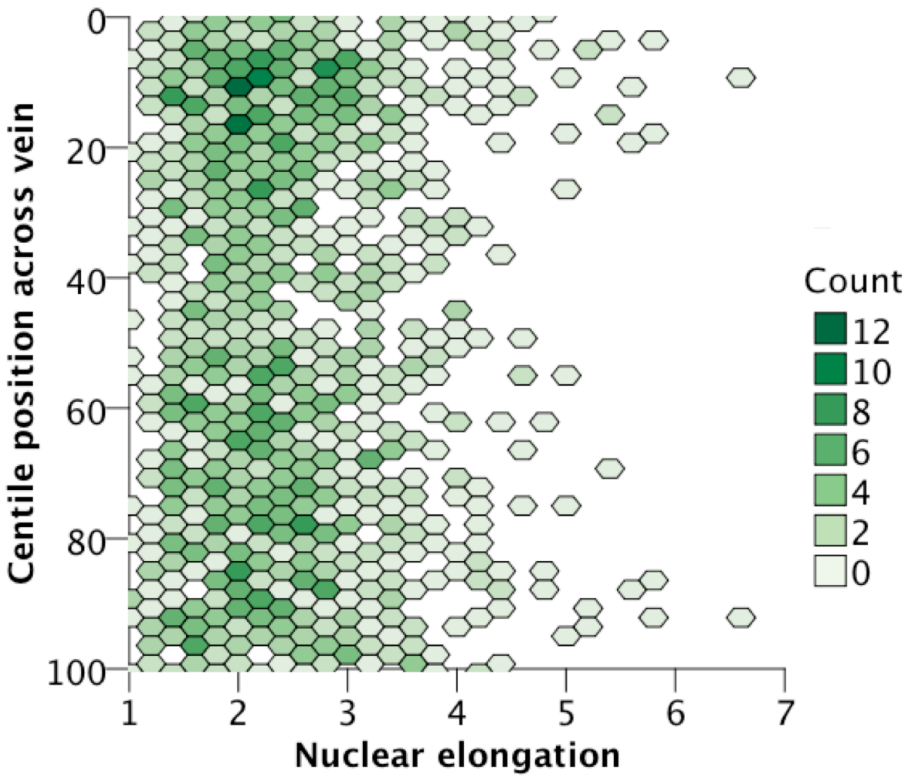

Figure 105 Normal variation in Prox1^{hi} nuclear elongation by position across the vein

This hex-binned scatter plot show the lack of significant variation in Prox1^{hi} nuclear elongation with the position across the vein from superior (0) to inferior (100). All measured wildtype nuclei are shown. N=1388 nuclei. Statistical analysis showed no difference (P=ns) in nuclear elongation between the three tertiles (ANOVA).

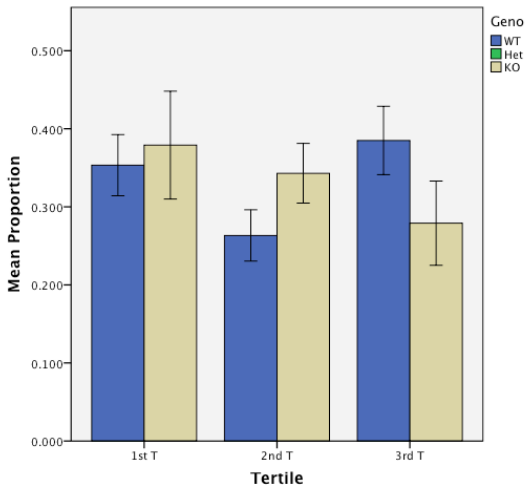

Figure 106 Proportion of analysed VFC's in each region at P0 following Cx43 deletion

This graph shows that there was no significant difference in the proportion of measured nuclei in each tertile, when comparing wildtype littermates and Cx43-deleted VV. Error bars represent 1 SEM. P=ns for all comparisons (t test).

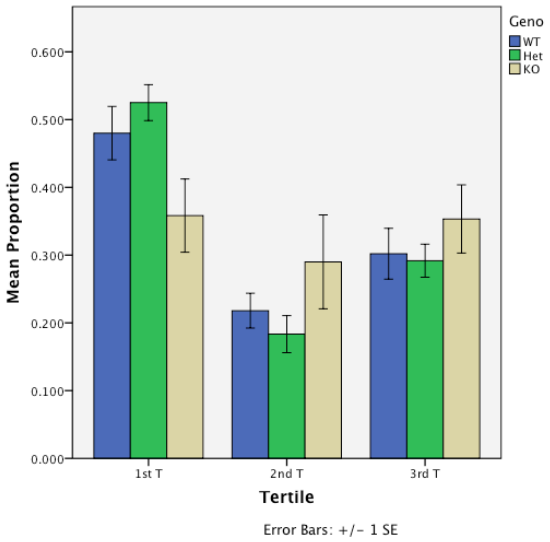

Figure 107 Proportion of analysed VFC's in each region at P0 following Cx47 knockout

This graph shows that there was no significant difference in the proportion of measured nuclei in each tertile, when comparing wildtype littermates and Cx47-deleted VV. Error bars represent 1 SEM. P=ns for all comparisons (t test).

Appendix 10

Reproducibility of valve identification in man

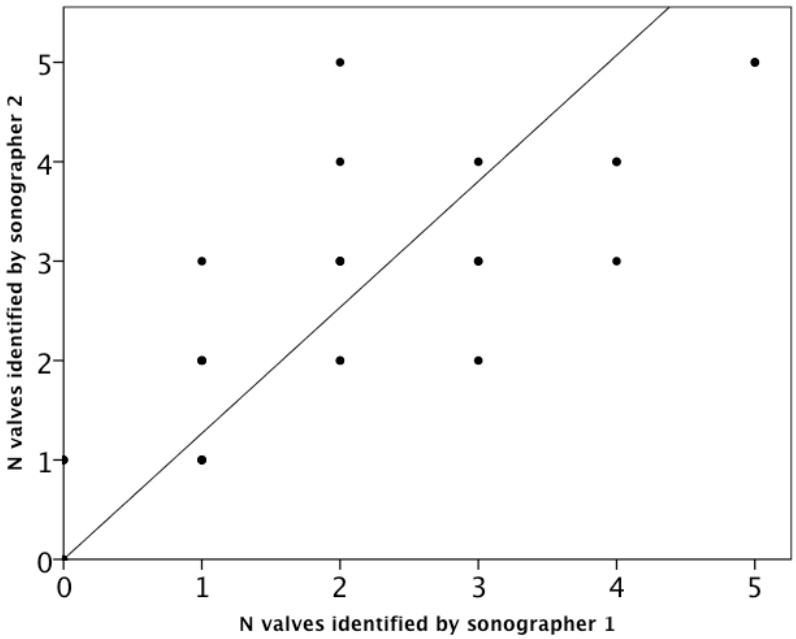

Figure 108 Reproducibility of detection of the number of valves in a vein
This graph shows a strong correlation between repeated measures of the number of valves in a vein by two different ultrasonographers. Intraclass correlation coefficient 0.896, P<0.0005. Overlapping integer values are concealed in the above graph but shown side by side in Figure 82 in the main text, which demonstrates all data points. A line of best fit through the origin is shown.

Appendix 11

Lack of evidence for the endothelial origin of interstitial cells after P1

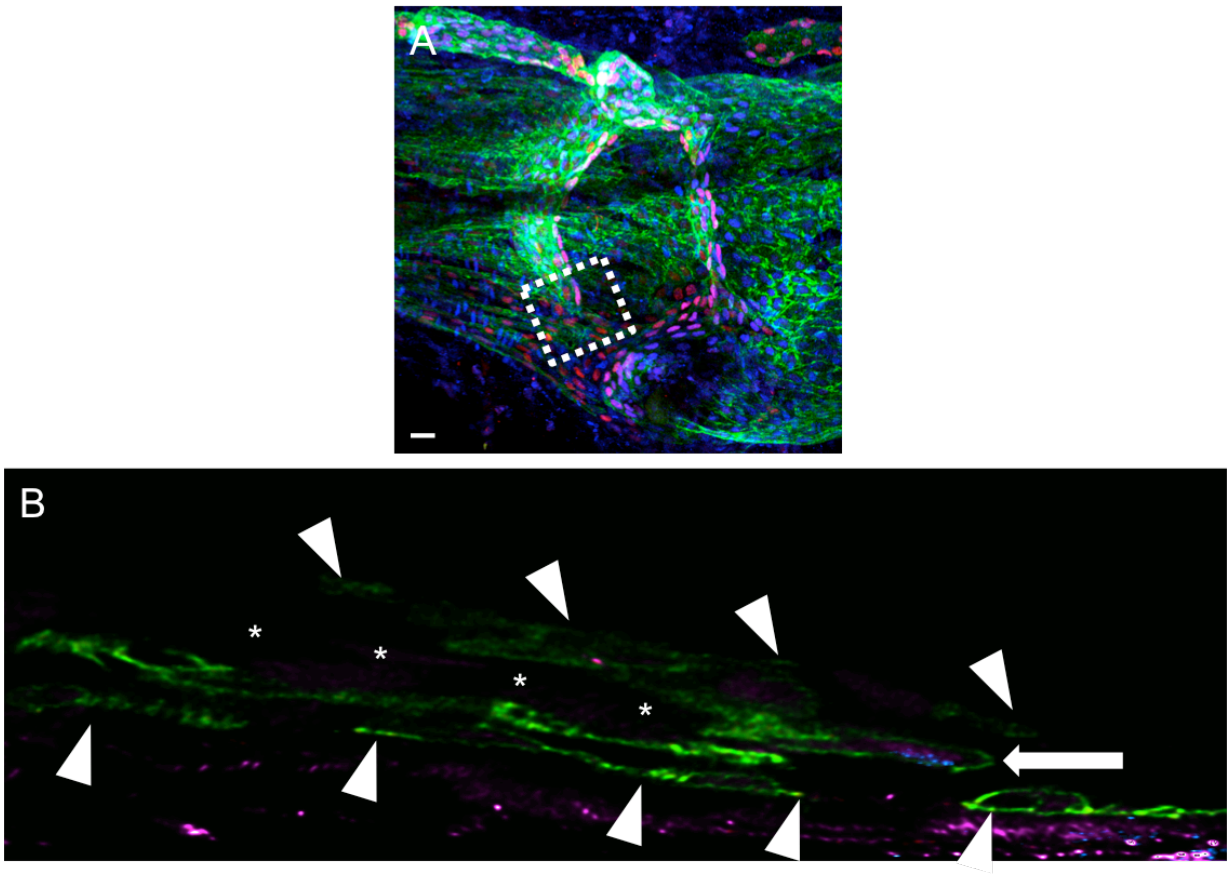

Figure 109 Lack of evidence for endothelial origin (after P1) of interstitial cells

A) A routine 2D projection of a confocal z-stack through VV in a mTmG;Prox1CreERT2 mouse, injected with 4OHT at P1+P2 and analysed at P6 is shown. Green=GFP, Blue=Foxc2, Red=Prox1 (tdTomato not scanned) Scale bar 20μm.

B) An XZ (side) projection of a deconvolved z-stack through the boxed region in A. Arrowheads indicate GFP expressing endothelial cells lining the vein. Arrowheads indicate immunolocalisation of Prox1 and Foxc2 within the nucleus of a free-edge cell. * = known positions of interstitial cells, which are GFP-ve indicating that endothelial to mesenchymal (interstitial cell) transition has not occurred after P1. Green=GFP signal (membrane targeted), magenta=Foxc2, cyan=Prox1 immunolocalisation. tdTomato signal (red) is not clearly visible. An mTmG;Prox1CreERT2 mouse was injected with 4OHT at P1+P2 and analysed at P6, with

immunolocalisation of Prox1, Foxc2 as well as tdtomato and GFP. Imaging was performed on a Leica SP5 confocal microscope using 63x lens, 2048x2048 resolution, 200Hz, frame averaging of 2, 125nm z-step (413 slices), 4 channels. Data were deconvolved in Huygens (SVI) using classic maximum likelihood estimation, with medium RI, SNR and quality threshold parameters optimized for sharp cell membranes in the GFP channel. Data were exported into NIH ImageJ and re-sliced to give XZ projections; an example slice is shown. Images are representative of N = 5 deconvolved stacks in 5 valve leaflets of 3 mice. Flow from left to right in A and B.

Appendix 12

Model of altered flow in VV development

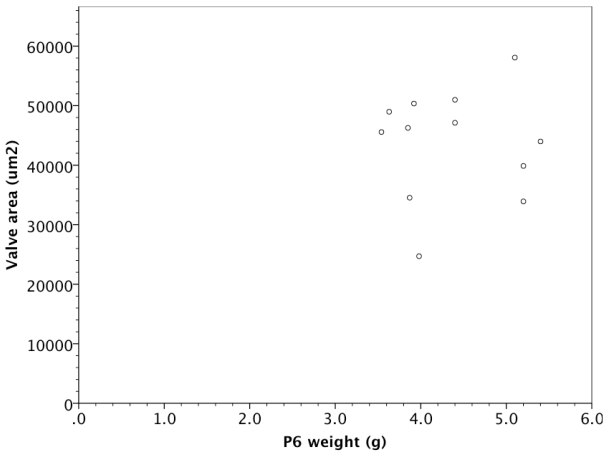

Figure 110 No correlation between weight at P6 and observed valve area.
Pearson correlation = 0.03, P=0.93. (A line of best fit was not drawn as the variables appear unrelated)

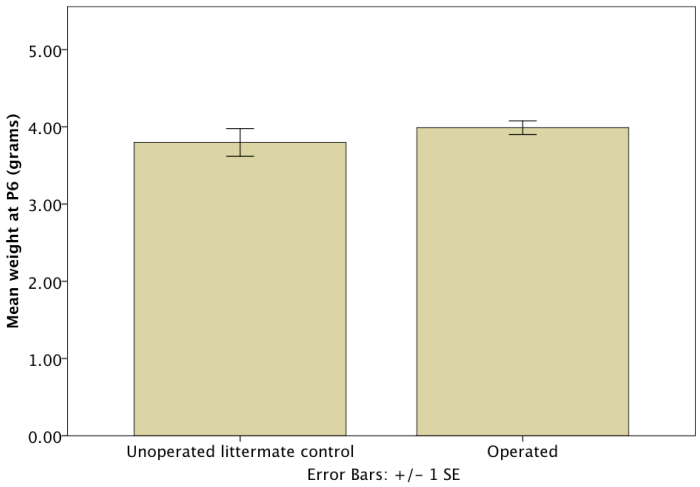

Figure 111 Operated pups gain weight normally.
Taking operated and unoperated pups from the same litters, the effects of surgery and anaesthesia did not alter weight gain at P6. N=10 littermate controls, 16 operated pups. P=0.355 (independent samples t test, unequal variance).